The Chronic Lymphocytic Leukaemia Lymph Node Microenvironment

by

Laura Cronin

A Thesis Submitted to

UNIVERSITY OF BIRMINGHAM

for the Degree of

DOCTOR of PHILOSPHY

College of L.E.S.
School of Biosciences
The University of Birmingham

September 2015

Abstract

The lymph node (LN) microenvironment in Chronic Lymphocytic Leukaemia (CLL) is the main site of disease progression and maintenance. Whilst isolated components of the LN niche have been studied *in vitro*, to date, no comprehensive architectural overview of the microenvironment has been attempted. A more holistic view is essential in order to fully understand this disease. LN CLL cells are likely to receive a complex array of survival signals from accessory cells which drive disease and protect against conventional therapeutics. This study has embarked upon establishing reliable combinations of primary and secondary antibodies that permit multicolour immunohistochemical (IHC) interrogation of the CLL LN in formalin fixed paraffin embedded samples (FFPE).

Analysis of cells in cell cycle using Ki-67 and morphological appraisal of tissues demonstrated a general lack of proliferation centre structures in the majority of CLL LN tissue samples. Independent of disease stage, all tissues showed a significant presence of both CLL cells ($PAX5^+$) and T cells ($CD3^+$), often in close proximity to each other. Whilst total numbers of T cells did not appear to relate to stage of disease, analysis of T-helper ($CD4^+$) and T-cytotoxic ($CD8^+$) subsets suggest a differential spatial distribution as disease progresses, in keeping with the understanding that the architecture of the CLL LN changes as disease progresses.

To further investigate the impact of T cell -CLL cell interactions in the LN, an *in vitro* assay was developed to co-culture CLL cells with normal donor allogeneic $CD4^+$ T cells. A mutual protective effect in survival was observed in both the CLL and T cell populations. However, despite increased ^3H-thymidine incorporation being observed in co-cultures there was no evidence of induced proliferation in either T cell or CLL subsets. Indeed the data suggest

that ^{3}H-thymidine incorporation observed upon co-culture of CLL cells with CD4^{+} T cells represents T cell supported CLL cell DNA repair. If true, this scenario would have substantial impact upon the therapeutic options provided to patients in the future and warrants further investigation.

The supportive role of monocyte-derived cells in CLL has been the focus of many *in vitro* studies in recent years, however very few studies have focused upon these cells *in situ*. Here, CLL LN tissues were stained for the presence of macrophages (CD68^{+}) and Nurse-like cells (CD163^{+}). The expression of CD68 was variable but the frequency of expression correlated with disease stage, where CD68^{+} cell frequency decreased as disease progressed. CD163^{+} cells were detected in normal spleen, stage A, B & C CLL LN tissue, although the presence of these cells was highly variable between CLL LN samples, unrelated to disease stage. These data highlight the complex role macrophage/monocyte cells may play in the CLL LN and the need for future studies to elucidate the impact of different subtypes of these cells.

This work demonstrates that the architecture of the CLL LN microenvironment is complex, dynamic and heterogeneous and highlights the advantages multicolour IHC can present to the field for understanding the therapeutic opportunities in this disease.

To my parents John & Mary

& my grandparents, for their faith & love

To Andy,

for being the best brother

&

To Andy,

for loving me despite the Ph.D. induced madness

"We should emphasize that virtually nothing comes out right the first time. Failures, repeated failures, are finger posts on the road to achievement. The only time you don't fail is the last time you try something, and it works. ***One fails forward toward success****."*

Charles F. Kettering

The phrase *"A smooth sea never made a skilled sailor"* seems especially apt for a Ph.D. journey and mine has been no exception. There have been ups and downs that I couldn't have foreseen, but each has helped shape me as a person and I'm grateful for them all. I am so pleased and proud to be at the stage where I have achieved my goal and can express my gratitude towards the people who helped me do this.

First and foremost, I must thank my excellent supervisors, a dream team without whom I would have had a lesser experience during this Ph.D. Thank you to Professor Chris Bunce for the opportunity, continued faith, encouragement and the amazing out-of-left-field nuggets of wisdom. I always appreciated our great Friday discussions and your endless enthusiasm for my project, the data I produced and the plans I had made. You could always see the bigger picture and your support then and now is invaluable. Thank you to Dr Rachel Hayden, a.k.a. Dr CLL, a wonderful person and supervisor. Thank you for your constant support, guidance, wisdom and amazing/uncanny psychic connection to the Calibur…! I'll be eternally grateful for your ability to see where I was trying to get to with an idea and helping me figure out how to do it, without controlling or taking over and for your never-ending patience with my moaning and grumbling about all things project and non-project. I am so thankful for your commitment and the sacrifices you made to help me on my way. I'm also grateful for your killer chocolate orange brownies and ability to make me smile regardless of just how bad the lab had been that day. Chris & Rach, I feel extremely lucky that you took me on as a Ph.D. student (despite the fact you'd already endured me as an undergraduate!) and so happy that I could produce a piece of work to show that your faith and trust paid off.

I'd also like to thank my friends and colleagues in the lab for making my day-to-day Ph.D. life enjoyable. In particular Andy, Nikos, Kasia, Josh, Julia, Jane & Nick, your advice, support and friendship has been wonderful – thank you. To my talented partner in crime Beccy, my 4th floor buddy Alex and the lovely Laura – I'm so glad I had you around to give me a heads up on the year ahead, thank you for being excellent friends and not rolling your eyes when I worried/complained about the "easy" stages you'd already made it past! A big thank you too to all the 4th and 8th floor peoples – you were wonderful and made me feel like a part of the gang very quickly.

Thank you to Dr Guy Pratt and Dr Helen Parry for constant provision of the patient samples I required to complete this work, not to mention the patients themselves for supporting this research and a thank you to the willing volunteer donors who allowed me to stab them in the name of research! Thank you also to Professor Mark Drayson and Dr Claudia Roberts – your intellectual input and personal support were fantastic, I feel lucky to have had such great people to work and collaborate with. A big thank you to all the lovely people in our Birmingham CLL group too.

Of course I owe a huge amount to my bestie Sarah and you too Robin; you supplied me with food, wine and great times to get me through and always asked how it was going, despite

the usual response being a complaint of some sort. You're wonderful people whom I love – thanks so much.

I'd like to say thank you to my wonderful family, especially my fantastic parents for being so supportive and caring and always encouraging me and my brother to follow our interests. Speaking of, thanks to my brother Andy for always making me feel like a superstar nerd, even when I was feeling rubbish. A big thank you to my "other" family – the Murch gang; Aileen, David, Nicquii, Rosstopher, Jeni, Damo & Stirling for caring about me and my work and always having the time to make me a gin/find me some wine, making me laugh and smile and forget about the lab for a while.

Last but by no means least, the biggest thank you to Andy, the person who moved cities so I could do this work, who stood by me through the (many) major tantrums, tears and madness, who always told me to focus on what I'd already achieved as much as where I was aiming and who always makes me laugh and smile and feel loved. You're amazing and I'm very grateful to you, A, A&F!

I'm going to sign off with one more quote (why not?!);

"There's nothing like biting off more than you can chew, and then chewing anyway"

Mark Burnett

^{3}H	tritiated
Ab	antibody
Ag	antigen
AID	activation induced deaminase
APC	antigen presenting cell
ATM	ataxia telangiectasia mutated
AV	Annexin V
B cell	B lymphocyte
BCR	B cell receptor
BM	bone marrow
BTK	Bruton's tyrosine kinase
CD40L	cluster of differentiation 40 Ligand
CLB	Chlorambucil
CLL	chronic lymphocytic leukaemia
CLP	common lymphocyte progenitor
CPM	counts per minute
DNA	deoxyribonucleic acid
DPBS	Dulbecco's phosphate buffered saline
FBS	foetal bovine serum
FDC	follicular dendritic cell
FFPE	formalin fixed paraffin embedded
FSC	forward scatter
GC	germinal centre
GEP	gene expression profile
hdaCD4^{+}	healthy donor allogeneic CD4^{+} T cells
HSC	haematopoietic stem cells
Ig	immunoglobulin
IgH	heavy chain
IgL	light chain
IgVH	immunoglobulin heavy chain variable
IHC	Immunohistochemisty
ITAM	immunoreceptor tyrosine-based activation motifs

LN	lymph node
M2	macrophage type II
MBL	monoclonal B cell lymphocytosis
M-CLL	CLL with mutated IgVH
MNC	mononuclear cell
NK cell	natural killer cell
NLC	nurse-like cells
OS	Overall survival
PB	peripheral blood
PI3K	phosphoinositide-3-kinase
Pre-B cell	precursor B cell
Pro-B cell	progenitor B cell
RAG1/RAG2	recombination activating genes 1 and 2
RS	Richters syndrome
SHM	somatic hypermutation
SSC	side scatter
TAM	tumour associated macrophage
T_{cyt}	T cytotoxic cell
T_{fh}	T follicular helper cell
T_h	T helper cell
TP53	tumour protein P53
U-CLL	CLL with unmutated IgVH
ZAP-70	70kDa ζ- (Zeta) activating protein

1 GENERAL INTRODUCTION

1.1 B cells

B cells in humans and other mammals form an integral part of the adaptive immune system and provide humoral immunity against invading pathogens (LeBien & Tedder 2008; LeBien 2000; Raff 1973). B cells are capable of raising specific immune responses against a vast array (~10^{13}) different antigens (Ag) (Janeway et al. 2001; Reddy & Georgiou 2011). B cells are also important antigen presenting cells (APC) which activate other cells in the immune system (LeBien & Tedder 2008; Pieper et al. 2013). B cell immunity is highly important; in addition to poor immune responses against infections, many autoimmune diseases are caused by defects in B cell development, function or regulation (LeBien & Tedder 2008; Pieper et al. 2013; Goodnow et al. 1990). In addition, a large number of phenotypically distinct tumours may arise from B cells whose characteristics depend upon the stage of development of the initiating oncogenic B cell. The B cell leukaemia Chronic Lymphocytic Leukaemia (CLL) is the focus of this project and the healthy development of B cells and their normal function will be initially discussed to provide context.

1.1.1 B cell Development

In adults, B cells (B lymphocytes) develop from common lymphocyte progenitor (CLP) cells within the bone marrow (BM). Commitment to B lymphopoiesis is followed by CLP maturation into progenitor B cells (pro-B cell) and subsequently precursor B cells (pre-B cell). The ensuing development of functional and mature B cells depends upon the sequential rearrangement of several elements within the immunoglobulin (Ig) gene locus to encode a B cell receptor (BCR) which is then expressed on the B cell surface. Until this point B cell development occurs without the engagement of antigen. Once the putative BCR is expressed it becomes crucial for the cells survival as well as for the functional capacity of the resultant

mature B cell (LeBien & Tedder 2008). Successive development of the B cell depends upon the cell's experience of Ag.

1.1.1.1 The BCR structure

The BCR complex consists of a membrane bound antigen-specific immunoglobulin (Ig) flanked by two non-covalently associated proteins, Ig alpha (Igα) and Ig beta (Igβ) (CD79A and CD79B). These proteins are necessary for the correct expression and function of the BCR (Minegishi et al. 1999; Ferrari et al. 2007). The key functional element of the BCR complex is the antigen-binding Ig which, when bound by its cognate antigen, elicits B cell activation (Pieper et al. 2013). The Ig is constructed from two heavy and two light chain proteins that are separately encoded. The locus for heavy chains (IgH) is found on chromosome 14 (14q32.33) and there are two loci that encode Ig light chains (IgL), which may be kappa (κ) or lambda (λ). The λ light chain locus is on chromosome 22 (22q11.2) whilst the κ locus is found on chromosome 2 (2p11.2) (Lefranc 2014). Both heavy and light chain proteins are encoded by gene sequences that have to be somatically recombined in each B cell prior to their expression. The functional IgH and IgL both consist of a constant region encoded by the Constant (C) gene region and a variable region encoded by the combination of Variable (V), Joining (J) and Diversity (D) (IgH only) gene regions (figure 1).

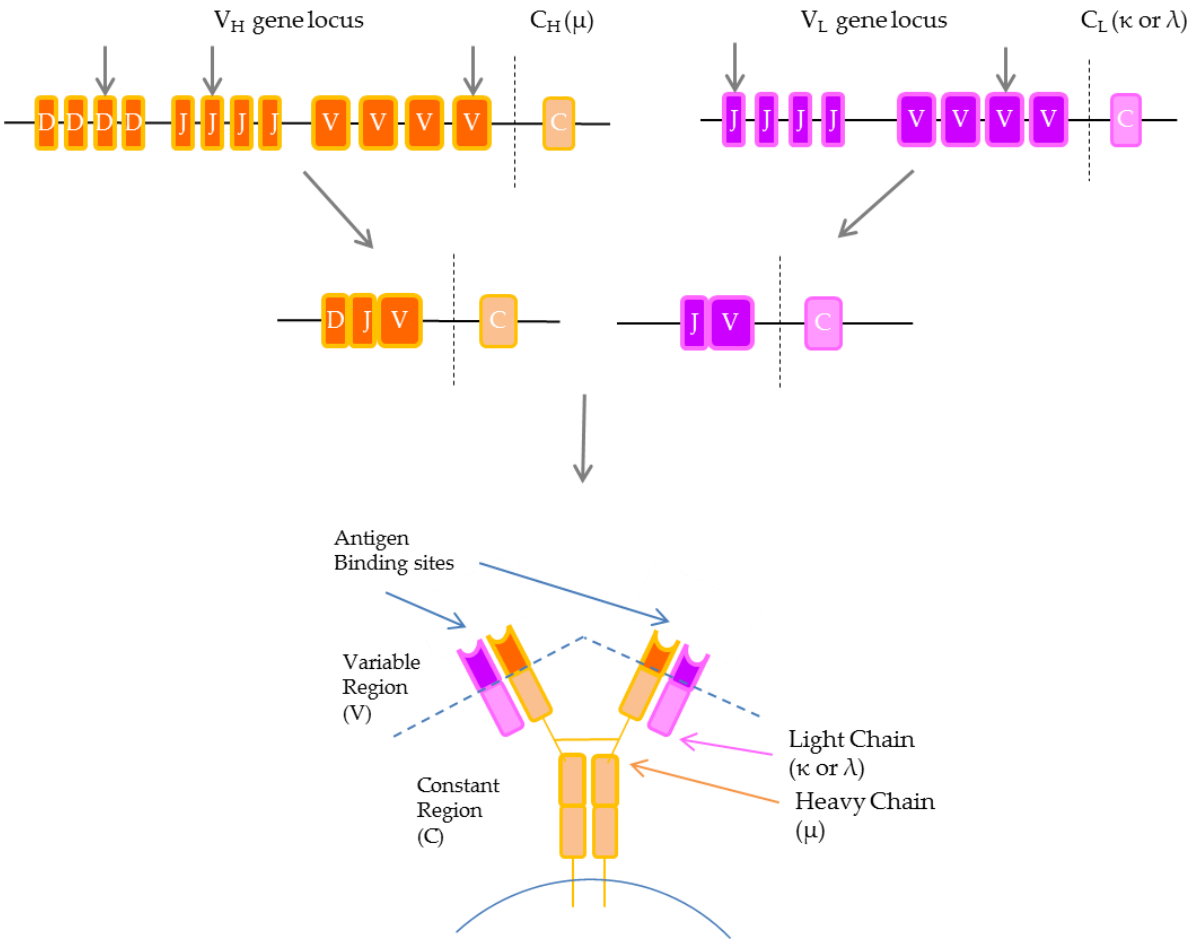

Figure 1. B cell receptor structure.

The B Cell Receptor (BCR) is comprised of 2 heavy and 2 light immunoglobulin chains (Ig), each with a constant and a variable region. Variable regions are encoded through combination of multiple gene loci; the heavy chain variable region by one each of Variable, Diversity and Joining regions, the light chain variable region by Variable and Joining regions only. The heavy chain constant region is encoded by Ig μ whilst the light chain constant region is encoded by κ or λ. These variable and constant regions are transcribed to produce a membrane bound IgM which in combination with Igα and Igβ form the functional BCR. The rearrangements of V,D and J gene regions generate diversity in the BCR antigenic repertoire.

1.1.1.2 Ig gene recombination

The recombination of Ig genes is driven by the activity of the Recombination Activating Genes 1 and 2 (RAG1/RAG2) (Schatz et al. 1992; Oettinger et al. 1990) which are essential for the recombination process. RAG1 and RAG2 are closely located to one another on chromosome 11p13 (Sherrington et al. 1992) and have little homology between the two sequences, although as a pair are highly conserved across many species. RAG1 and RAG2 are expressed exclusively in lymphoid lineage cells and their transduction into non lymphoid cells (such as fibroblasts) is sufficient to induce gene rearrangements (Schatz et al. 1992). The expression of RAG1 & RAG2 is downregulated in mature B cells which is thought to protect the cell from erroneous recombination of DNA as this may lead to translocations with oncogenic implications (Hiom et al. 1998).

RAG1 and RAG2 induce double stand breaks in the DNA within the recombination signal sequence (RSS) to allow recombination of the V (D) J gene regions. Production of the IgH chain of the BCR occurs first during development, with the RAG genes initiating a D to J gene rearrangement followed by a V to DJ gene rearrangement. The initial constant (C) region of the IgH is mu (μ), however, during class switching later in development, another C region may be selected to replace μ. Each of these C regions (μ, mu; δ, delta; ɣ, gamma; α, alpha; ε, epsilon) endows the functional Ig molecule with different capabilities. Examples of these properties include that IgG (ɣ) has been shown to improve phagocytosis of antigens whilst IgE (ε) can induce the activation of mast cells and basophils initiating their degranulation, important in the response against helminths (Woof & Ken 2006; Wu & Zarrin 2014; Nimmerjahn & Ravetch 2008). Indeed, some C regions also contain sub-isotypes and these in turn have altered functional impact upon the antibody (Ab) produced by the B cell. This has been demonstrated by several groups, including observation of differential

responses seen from murine IgG1, IgG2α and IgG2β Ab against a capsular polysaccharide of *Cryptococcus neoformans* despite identical Ig variable regions (Torres et al. 2007). In this way the same B cell may produce antibodies with different functional capacities whilst maintaining specificity by retention of the Ig V binding region.

Following IgH chain transcription and translation, rearrangement of the V and J regions of the IgL variable region occurs, whilst either κ or λ C genes are selected as the IgL C region. The combination of two IgH chains and two IgL chains form a putative BCR which is then expressed on the B cell surface.

The expression of the master B cell regulator PAX5 is also important for the proper formation and expression of the BCR and development of B cells (Cobaleda et al. 2007). PAX5 is a transcription factor with a large range of important roles necessary for B cell development including the recruitment of RAG1 and RAG2 to the human IgVH genes (Zhang et al. 2006; Fuxa et al. 2004).

1.1.1.3 The Immature B cell

With a BCR expressed on its cell surface, the B cell becomes an immature B cell and leaves the BM (figure 2). At this stage immature B cells are already capable of responding to the presence of a subset of pathogens known as Type I Ags. When activated in this manner the immature B cell clonally expands and differentiates into short lived plasma cells, which are capable of excreting non-membrane bound forms of the IgM they express as part of their BCR. These secreted Ig are called antibodies (Ab) and can be raised independent of assistance from other immune cells. Type I Ag that elicit these responses from immature B cells include common bacterial Ag such as lipopolysaccharides and free DNA (Kreig et al. 1995).

1.1.2 B cell Maturation

After the immature B cell migrates out of the BM, it circulates in the periphery until reaching secondary lymphoid tissues, such as a lymph node (LN) or lymphoid follicles within the spleen or gut-associated lymphoid tissues (GALT). Upon entry into the LN the immature B cell becomes a mature naïve B cell which may be activated through the binding of a cognate Ag to its BCR. This Ag may be free within the lymph inducing B cell differentiation into a short lived plasma cell, which secrete Ab. Alternatively, the Ag may be presented to the naïve B cell via an antigen presenting cell (APC) such as a T helper cell (T_h) or a follicular dendritic cell (FDC) leading to the formation of a germinal centre (GC) wherein the B cell will undergo rapid clonal expansion (figure 2) (LeBien & Tedder 2008; Pieper et al. 2013; Sagaert et al. 2007).

1.1.3 B cell Activation

The germinal centre in LN tissue is a region within which mature activated B cells proliferate profusely and undergo somatic hypermutation to create an amended BCR molecule with a greater affinity for the original antigen (Di Noia & Neuberger 2007). This process allows a robust immune response and secures a specific long-term protection to the host against this antigen.

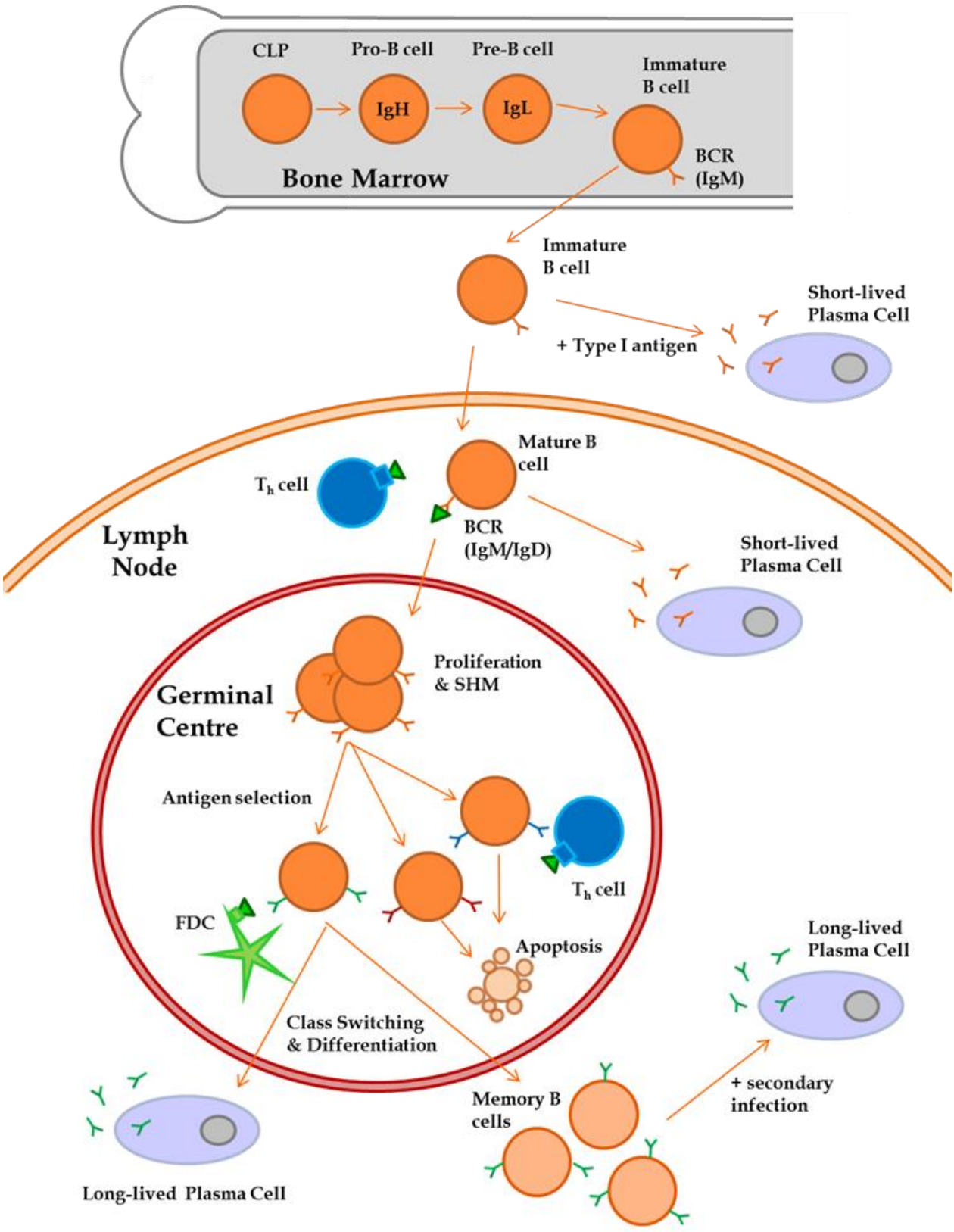

Figure 2. Healthy B cell development, maturation and activation.

Diagrammatical representation of healthy B cell development, maturation and activation as described in Chapter 1.1

Engagement of the BCR by its cognate antigen causes activation of the B cell through the release of calcium (Ca^{2+}) from intracellular stores. Activation requires the crosslinking of multiple BCR complexes on the B cell surface, leading to the phosphorylation of immunoreceptor tyrosine-based activation motifs (ITAM) found on the intracellular regions of the Igα and Igβ co-receptors. This induces the recruitment and activation of several downstream signalling molecules such as SYK and LYN kinases which, once activated, cause phosphorylation and activation of Bruton's tyrosine kinase (BTK). In addition, phosphatidylinositol- 4,5-bisphosphate-3-kinase (PI3K) is activated, and together these lead to phospholipase C-gamma-2 (PLCɣ2) and phosphoinositol-diphosphate (PIP_2) activation and eventual release of Ca^{2+}, activating the B cell (Guo et al. 2000; Dubravka & Scott 2000; Kuwahara et al. 1996).

1.1.4 Affinity Maturation

Within the GC an activated B cell will undergo a process of affinity maturation which involves both Somatic Hypermutation (SHM) and class switch recombination (CSR) of the genes encoding the BCR. Both of these processes fall under the control of the enzyme Activation Induced Deaminase (AID). AID is responsible for the rearrangement and hypermutation of the BCR Ig variable gene structures (Muramatsu et al. 2000; Revy et al. 2000). AID facilitates the deamination of cytosine residues within the DNA of the Ig gene regions creating a uracil residue, which is then point mutated during the repair process. These point mutations lead to random variations within both the variable and constant regions of the Ig locus. Mutations in the Ig variable region lead to the production of daughter B cells that express slightly different variable regions within the BCR molecules on the cell surface when compared to the parent cell (Di Noia et al. 2007; Di Noia & Neuberger 2007). These BCR molecules either possess a higher or lower affinity for the original

activating antigen and this process ultimately produces a daughter cell with a much higher affinity for the original antigen. The daughter cells produced by SHM undergo selection for their ability to bind the original antigen via interaction with T_h or FDC within the LN follicle. If a B cell is capable of strongly binding the Ag via its altered BCR it will progress to CSR and finally differentiation. If a B cell fails to sufficiently bind the presented antigen it will undergo apoptosis. Where AID induces mutation in the Ig C gene region, repair processes lead to the replacement of the chain with an α, δ, ɣ or ε chain instead in a process called CSR (Stavnezer 2008).

1.1.5 Terminal Differentiation

Following CSR, the high affinity mature B cell will proliferate and/or differentiate into one of two types of long lived high-affinity B cells; a memory B cell or a plasma cell (Pieper et al. 2013). Memory B cells reside within secondary lymphoid organs and will proliferate and terminally differentiate upon secondary expose to the same antigen to produce plasma cells (McHeyzer-Williams & McHeyzer-Williams 2005). Plasma cells are non-replicating long lived cells which can secrete high-affinity antibodies. These cells preferentially home to the BM microenvironment for stromal support necessary for long term survival (Underhill et al. 2012).

1.1.6 B cell tolerance and anergy

During the process of B cell development some cells will generate BCR molecules that will react against self-Ag. For a healthy immune system to develop, these self-reactive cells must be prevented from causing damage to the host. In cases where this does not occur, autoimmune disease arises. There are several mechanisms inbuilt within the immune system that protects the body against self-reactivity. When newly developed BCR are

initially presented in the BM they undergo testing for self-reactivity. Should a B cell be strongly self-reactive it will be destroyed and never enter the circulation (Goodnow et al. 1991; Hartley et al. 1991), a phenomenon that was initially demonstrated in mouse models (Goodnow et al. 1988). However, if a B cell has a low level of self-reactivity they may enter a state of anergy instead of being destroyed (Melamed & Nemazee 1997; Pieper et al. 2013). Within the periphery, should these anergic B cells bind a non-self-Ag with high affinity, they are brought out of their anergic state. During affinity maturation, the cells undergo SHM and their BCR structure is mutated. Those cells which lose self-reactivity and bind non-self-Ag with high affinity will progress and survive. This process of re-purposing self-reactive B cells provides a greater pool of B cells from which protection against infections can be raised (Heltemes-Harris et al. 2004). In this way the body is able to balance the need for a large repertoire of antigenic binding receptor structures with the risk of autoimmunity. However, the presence of anergic B cells provides the potential for their oncogenic transformation. Indeed it has been reported that some leukaemic cell types, including Chronic Lymphocytic Leukaemia cells (CLL), share many commonalities with anergic B cells such as low expression of IgM on the cell surface (Apollonio et al. 2013).

As described above the development, maturation and activation of B cells is a complex and tightly regulated process within which there are inherent dangers to cellular integrity. It is not surprising therefore that where elements of this machinery malfunction it can lead to tumorigenesis (Ramiro et al. 2006).

1.2 CLL Biology

Chronic Lymphocytic Leukaemia (CLL) is a disease of mature B cells, which accumulate as $CD5^+$ $CD19^+$ cells in the bloodstream. CLL usually affects older individuals, with a median age of 72 years at presentation (Oscier et al. 2012). Following publication of the International Workshop in Chronic Lymphocytic Leukemia (iwCLL) 2008 guidelines, a diagnosis of CLL requires the detection of an absolute peripheral blood $CD5^+$ $CD19^+$ B cell count $\geq 5x10^9$cells/litre (Hallek et al. 2008). Detection of a clonal population of B cells $\leq 5x10^9$cells/litre with a CLL phenotype is diagnosed as monoclonal B cell lymphocytosis (MBL). During the course of their disease, approximately 5% of CLL patients will have a transformation of their disease into a high grade lymphoma called Richters Syndrome (RS).

1.2.1 MBL

MBL is divided into two categories based upon the quantity of monoclonal B cells in the blood; low grade MBL ($\leq 0.5x10^9$cells/L) and high grade MBL ($\geq 0.5x10^9$cells/L – $\leq 5x10^9$cells/L) also known as clinical MBL. Whilst low grade MBL has a low risk for progression to CLL, approximately 1-2% of individuals with high grade MBL progress to stage A CLL classification per year (Strati & Shanafelt 2015). The mechanisms for this progression are as yet poorly understood and it is currently unclear as to whether there are driver mutations present or whether the microenvironmental signals play a larger role in CLL disease initiation (Ghia et al. 2012). The similar immunophenotypic markers and advancement of high grade MBL suggest that all cases of CLL have preceding clinical MBL but this requires confirmation. Stratification of these individuals is needed in the future to assist in ensuring therapy is appropriately provided.

1.2.2 Richters Syndrome

Between 5-10% of CLL patients have a transformation of their disease into a high grade B cell lymphoma, a process known as Richters Syndrome (RS). The most common form of lymphoma arising in RS is diffuse large B cell lymphoma (DLBCL), although in rare cases the transformation may lead instead to Hodgkins lymphoma (Parikh & Shanafelt 2014). RS may develop *de novo* or from a mutation within a sub-clone of the patient's CLL disease causing its rapid outgrowth. Prognosis for RS individuals is poor as disease is aggressive and often refractive to many therapies that have efficacy in CLL or DLBCL. Indeed, whilst great advances have been made in the management and treatment of CLL, these have not transferred to RS patients. The driving mutations leading to RS are as yet unconfirmed although it is reported that commonly mutated master genes such as MYC are affected. As untreated CLL patients have also been shown to develop RS it appears there is an inherent risk of transformation within the disease, although RS risk may also be affected by prior therapy (Chigrinova et al. 2014; Tsimberidou & Keating 2005). The genomic profile of RS shows a level of complexity in mutational events that sits between CLL and de-novo DLBCL (relatively low - high respectively) (Chigrinova et al. 2014). This indicates that RS is a related but distinct condition, likely with a need for its own distinct therapeutic strategies. Whilst the outlook for these patients is poor with conventional therapy (OS approximately 5–8 months after diagnosis) the use of new therapeutic combinations, such as Ibrutinib and Rituximab, may hold significant promise for these patients (Tsang et al. 2015).

1.3 CLL Stratification

The highly variable clinical course of individual CLL patients renders it important to stratify patients for their risk of progression and need for treatment. The Rai or Binet classification systems (figure 3) are used to separate patients based on lymphocyte count and lymphadenopathy (enlarged lymph nodes). In addition, molecular markers including the mutation status of the Ig variable heavy chain gene (IgVH) (Hamblin et al. 1999), CD38 (Damle et al. 1999) and zeta chain activated phosphatase 70 (ZAP-70) cell surface expression levels (Wiestner et al. 2003) have also been shown to correlate strongly to patient prognosis. Individuals who have a high expression of CD38, ZAP-70 or have unmutated IgV_H genes (U-CLL) (i.e. CLL B cells have not undergone SHM) tend to have a more rapidly advancing disease course, are considered "high risk" and more likely to require intensive therapy.

1.3.1 IgVH gene mutation status impacts survival

It has been suggested due to the striking survival differences between mutated and non-mutated IgVH gene diseases (M-CLL and U-CLL respectively) (figure 4) that CLL should be subdivided into two different diseases (Hamblin et al. 1999) and treated accordingly. This observation also initially suggested that CLL may arise from two different cell types, albeit that both cell types would be $CD5^+$ B cells from early development. The exact cellular origins of CLL remain as yet unconfirmed however, with supporting data published for both single cellular origin and two cell origin theories. Whilst survival differences between U-CLL v.s. M-CLL are greatly different, GEP of CLL cells revealed that the overall expression profiles of these subtypes show only minor differences, supporting the theory of a single cellular origin (Klein et al. 2001; Rosenwald et al. 2001). As such, the originating cell type

within this disease remains a controversial topic and different CLL subtypes have common features to memory B cells, naïve B cells and anergic B cells.

1.3.2 Common genetic aberrations in CLL

With the advent of new technologies, such as in-depth sequencing, there is now a plethora of information regarding genomic aberrations found in CLL. Due to the heterogeneic nature of the disease, some mutations are rarely applicable to the general patient population; however there are several mutations, commonly found in CLL, which bear the potential to be targeted as a treatment strategy (Strefford 2014).

1.3.2.1 13q deletion

The most commonly occurring mutation in CLL is 13q deletion (del(13q)) (60-80%) which has been shown be a favourable marker of overall survival (OS) in CLL when found in isolation (Döhner et al. 2000). Trisomy 12, another relatively common mutation (10-15%) has also been implicated in improved OS, although deaths within this patient cohort have also been typically linked to the development of a secondary tumour type or disease transformation to RS (Strati et al. 2015). In contrast, deletions in 11q (del(11q)) and 17p (del(17p)) have a strongly negative correlation with patient OS and the mechanisms for these are relatively well understood.

	Stage	Definition
Binet Staging System		
	A	Less than 3 enlarged lymphoid areas* **Hb ≥10g/dL and platelets ≥100,000/mm^3**
	B	3 or more enlarged lymphoid areas* **Hb ≥10g/dL and platelets ≥100,000/mm^3**
	C	Any number of enlarged lymphoid areas **Hb <10g/dL and/or platelets <100,000/mm^3**
		*(cervical, axillary, inguinal, spleen or liver each count as a single area)
Rai Staging System		
	0	Lymphocytosis only (BM and PB)
	I	Lymphocytosis with lymphadenopathy
	II	Lymphocytosis with splenomegaly and/or heptomegaly
	III	Lymphocytosis with anemia **(Hb <11g/dL)**
	IV	Lymphocytosis with thrombocytopenia **(platelets <100,000/mm^3)**

Figure 3. Prognostic staging systems.

Details for the Rai and Binet staging system criteria. Table information collated from Rai 1975, Binet 1980 and Hallek et al 2008

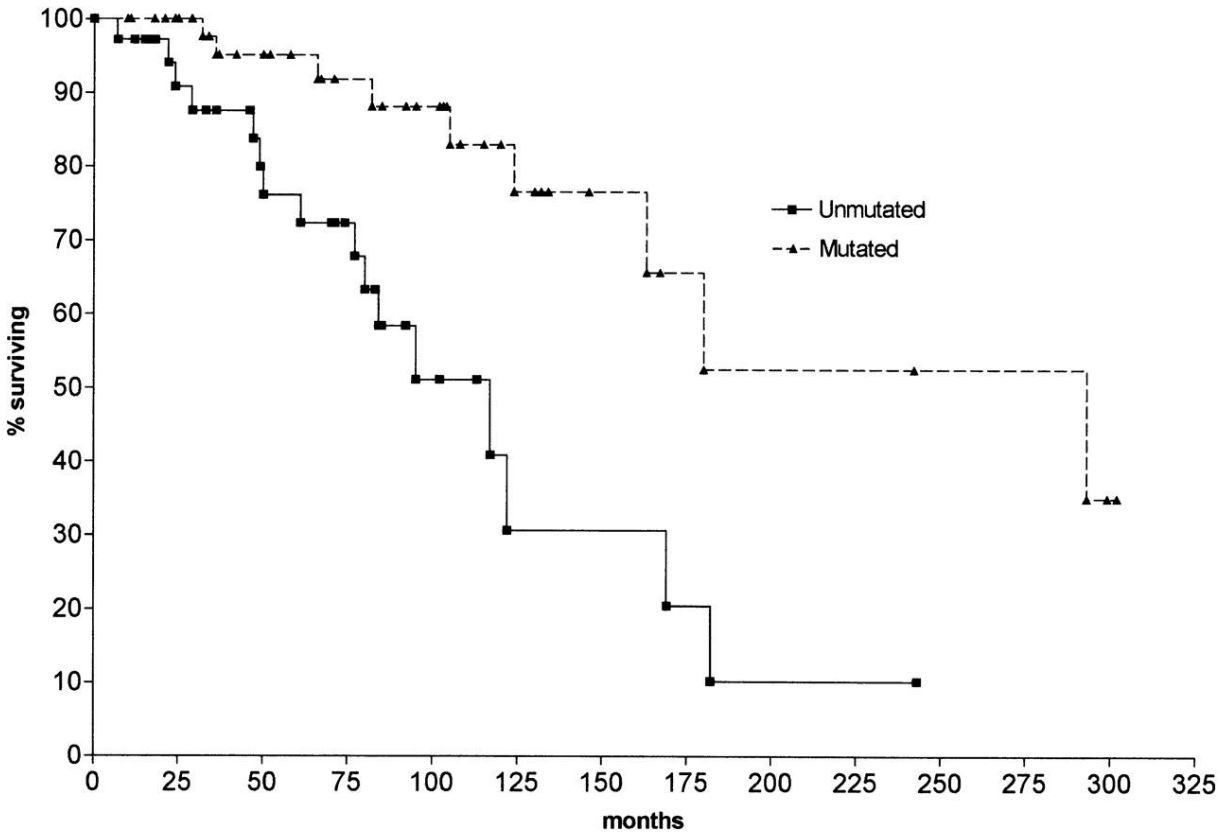

Figure 4 Overall survival curves from comparison of patients with unmutated (U-CLL) versus mutated (M-CLL) IgVH genes.

Image taken from (Hamblin et al. 1999).

1.3.2.2 11q deletion

Del(11q) impacts many genes, including most notably the ataxia telangiectasia mutated (ATM) gene (Austen et al. 2007; Stankovic et al. 1999; Rose-Zerilli et al. 2014). ATM has several roles including sensing double strand breaks in DNA and activating the DNA damage machinery. As such, its loss has grave consequences for maintaining genomic integrity (Stankovic et al. 1999; Rose-Zerilli et al. 2014) and is a distinct marker of poor outcome in CLL patients, also occurring independently of del(11q).

1.3.2.3 17p deletion

Del(17p) affects the TP53 gene, encoding the tumour suppressor gene p53 (Döhner et al. 2000). Whilst patients who are previously untreated rarely present with this mutation, greater than 50% of refractory patients possess this mutation. Outcome in these patients is only improved by therapy which has action independent of p53 i.e. non-chemotherapeutic agents such as monoclonal antibodies or small molecule therapies. This finding was highlighted by the poor outcome of del(17p) patients when treated with FCR therapy (Zenz et al. 2010; Hallek et al. 2010; Tam et al. 2008). More favourable outcomes have now been seen using new combinations of therapy and trials are ongoing to determine the optimal therapies for this subset of high risk CLL patients (Hillmen 2011; Stilgenbauer & Zenz 2010).

1.3.2.4 Clonal evolution

Due to the relatively low presence of del(17p) in initially presenting CLL patients compared to 50% of refractory patients, greater focus has been placed upon better understanding of the clonal evolution occurring in CLL patients over the course of disease. Whilst all CLL

patients will have a dominant CLL clone, there are also likely to be small numbers of other clones, known as sub-clones, within these patients. The presentation of del(17p) in many refractory patients reflects the fact that cells with this mutation are less susceptible to traditional therapies. As such, sub-clones possessing the del(17p) mutation are likely to survive initial therapies that otherwise eradicate the major clone. The del(17p) sub-clones in these patients then outgrow at later stages and form the major clone of the relapsed disease, ultimately making relapsed disease relatively more difficult to treat. The process of clonal evolution has been shown to occur via branching and linear progression and may be significantly affected by therapy choices (Schuh et al. 2012; Landau et al. 2013; Landau et al. 2014).

1.3.2.5 Additional mutations

Mutations in NOTCH1 and SF3B1 genes are also relatively common within CLL. NOTCH1 mutations in CLL induce the constitutive expression of a highly active and stable Notch protein (Rosati et al. 2009; Puente et al. 2011). Through whole genome sequencing it has been shown that mutations in the NOTCH1 gene are present in approximately 10-20% of patients and Notch signalling improves the ability of CLL cells to survive and resist chemotherapy *in vitro* when cultured on BM derived mesenchymal cells (Kamdje et al. 2012). This subclass of patients show a relatively poor OS, with the importance of this mutation on survival reflected by the promising results from therapies targeting the NOTCH pathway and protein (Lopez-Guerra 2015).

SF3B1 encodes the splicing factor 3b protein which has an important role in RNA splicing. Independent of ATM or TP53 gene mutation status, SF3B1 mutants have defects in the DNA

damage response pathway and typically harbour more DNA damage (Te Raa et al. 2014). Present in ~10-15% of CLL patients, sufferers in this cohort are considered high risk as they typically have shorter overall survival and a shorter time to first treatment (Sutton & Rosenquist 2015).

In addition to the discovery of these common mutations that can assist in the stratification of patients, the presence of shortened telomeres can identify asymptomatic patients who are likely to progress (Lin 2014). Furthermore, screening of patient samples for combinations of these aberrations is showing promise for future assistance in the stratification of patients (Cornet 2015).

Overall these advances are leading to a better understanding of patient prognosis, providing a more accurate stratification of individuals for therapies. Ultimately, a better understanding of these mutations in combination with disease biology will afford clinicians the best opportunity to provide personalised therapy that suits each patient.

1.4 Impact of antigen and the BCR in CLL

CLL cells have active, and in some cases constitutively active, BCR signalling which correlates to prognosis and disease progression in CLL (Stevenson & Caligaris-Cappio 2004; Stevenson et al. 2011). As in the normal immune response, activated BCR signalling primes the cell for proliferation and promotes survival.

In other B cell lymphomas this survival advantage is gained through mutational events in the BCR itself; leading to tonic constitutive signalling without the need for Ag binding and canonical activation (Davis et al. 2010), but this is not the case in CLL.

As the BCR structure itself is not mutated to induce constitutive activation in CLL, this supported the premise that the disease may be driven by Ag stimulation. Whilst no global common Ag has been indicated in CLL, there have been several cases of "stereotyped" BCR signatures found across patient cohorts (Agathangelidis et al. 2012). This refers to populations of CLL cells within separate patients possessing the same variable IgH sequence, specifically within the complementarity determining region of the receptor, indicating that these BCR will bind the same antigen (Messmer et al. 2004). This discovery was the first indication that CLL disease is driven by Ag and whilst there are commonalities between unrelated patient groups, there is still a great heterogeneity in Ag to which these stereotyped BCRs are raised and they include both self- and non-self Ag. As such, whilst there is an acknowledged role for BCR signalling in CLL, the initial cause of the increased signalling does not appear to be common across the disease, and because of this seems unlikely to be an initiating step in formation of CLL.

A subset of CLL patients with aggressive disease, U-CLL, have polyreactive BCRs that recognise multiple Ag epitopes (Hwang et al. 2014). In U-CLL BCRs are activated when

exposed to several different antigen epitopes, making these cells more likely to receive a pro-stimulatory and subsequent pro-survival response than a B cell with a specific BCR. This is likely due to the nature of their BCR, which has not undergone SHM and so does not possess a highly specific Ag epitope. This quality is likely to contribute to the aggressive nature of U-CLL.

The overall importance of BCR signalling in the proliferation and progression of CLL has been further displayed via the impact of trials of several new therapies targeting the BCR and its downstream signalling molecules as discussed below (Chapter 1.6) (Byrd et al. 2013; Maffei et al. 2015; Brown et al. 2014).

1.5 Microenvironments in CLL

CLL is a disease of multiple contrasting microenvironments; the peripheral blood (PB), the bone marrow (BM) and the lymph node (LN) compartments. Whilst CLL cells circulate through all these compartments, it is only the BM and LN that provide chemoprotection to tumour cells during drug treatment. This is thought to be provided via interaction with non-malignant accessory cells.

1.5.1 The Lymph Node, Bone Marrow and Peripheral Blood in CLL

CLL cells within the PB are in G_0/G_1 arrest in contrast to the cell cycle profile of CLL cells within the LN (Messmer et al. 2005; Rosenwald et al. 2001; Herishanu et al. 2011). Despite their quiescent status, it should be noted that CLL cells in the PB are metabolically active (Koczula et al. 2015) and are primed to circulate between compartments. PB cells can be categorised into those which have recently left the microenvironment and those which have been in the periphery for an extended time based upon their cell surface expression profile (Calissano et al. 2011). PB cells with $CD5^{High}CXCR4^{Low}$ have just egressed from the microenvironment whilst those homing to the niche present with a $CD5^{Low}CXCR4^{High}$ phenotype. High expression of CXCR4 (in addition to CXCR5) allows these cells to home to and enter LN and BM microenvironments where they receive support (Chiorazzi et al. 2005). Cells which home to the LN and BM microenvironments subsequently return to the PB and re-circulate cyclically between these environments.

Traditionally CLL LN tissues and to a lesser extent, BM, have been reported to contain areas of highly proliferative tumour cells known as proliferation centres or psuedofollicles (Schmid & Isaacson 1994; Bonato et al. 1998; Ponzoni et al. 2011). These proliferation centres (PC) are thought to be the regions within the LN environment where CLL cells interact with

non-malignant supportive cell types and proliferate (Ciccone et al. 2012; Plander et al. 2009; Patten et al. 2008; Vandewoestyne et al. 2011).

1.5.2 Cellular support in the LN

A multitude of cells are thought to interact with CLL cells in both the LN and BM, and these accessory cells are either activated or suppressed to the benefit of tumour growth. These cells include but are not limited to T cells, Natural Killer cells (NK cells), Nurse-like cells (NLC) and mesenchymal stromal cells (MSC). The investigation of the role of these cell types to date has been guided by the normal interactions of healthy B cells as well as observations of *in vitro* work, particularly with co-culture and mouse experimental models of CLL, in addition to observations during routine histopathology and diagnosis of CLL.

1.5.3 T cells

Collectively T cells have multifunctional relationships with other host cells in both normal homeostasis (health) and disease. They are able to nurture and promote APC induced immune responses, as well as destroy aberrant host cells when presented with the correct stimulatory signals. However, CLL cells are effective at dampening the natural aggressive anti-tumour response of T cells and equally preserve, promote and manipulate the nurturing interactions T cells have with their normal B cell counterparts, thus promoting immune-evasion, pro-survival and pro-proliferative environments for the tumour cells (Riches et al. 2010). Indeed, CLL cells stimulated with T cell derived markers such as CD3 and CD28 became activated and immunosuppressive (Hock et al. 2014). These alterations in T cell responses can be broken down into distinct categories of adaptation.

1.5.3.1 $CD4^+$ vs. $CD8^+$ cell balance

In CLL there is a skewing of the regular balance of T_h ($CD4^+$) to T_{cyt} ($CD8^+$) cells, with many more T_{cyt} cells present in the PB of patients (Nunes et al. 2012; Gonzalez-Rodriguez et al. 2010). Despite the large relative number of T_{cyt} cells in CLL the anti-tumour immune response of these cells is ineffective. CLL T_{cyt} cells are ineffective at forming functional immune synapses (IS) with CLL cells, due to a disrupted cytoskeleton and ineffective packaging and release of cytolytic enzymes. CLL cells have been shown to negatively affect actin polymerisation in T_{cyt}, which is necessary for cell membrane movements, via their expression of multiple inhibitory ligands such as CD200 and CD274 (PD-L1) (Ramsay et al. 2012). In addition, the polarised release of granzyme from T_{cyt} is important for its successful induction of target cell death (Riches et al. 2010; Ramsay et al. 2008). Recent work has highlighted that these CLL-induced impediments are due to induction of a T cell exhaustion phenotype as discussed below.

1.5.3.2 T cell exhaustion

CLL patient T cells have been shown to express the markers of chronic activation and GEP has indicated a pseudo-exhaustion phenotype (Görgün et al. 2005; McClanahan et al. 2015). This is due to the dampened ability of these T cells to mount an immune response despite their continued expression of IFNɣ, TNFα and IL-2, all pro-stimulatory signals which are atypical secretions for exhausted cells. This combination of factors simultaneously dampens the immune response against CLL whilst supporting the tumour survival and proliferation (Görgün et al. 2005; Davis & Ritchie 2014). This effect is mediated by the expression of exhaustion-inducing ligands by CLL cells such as CD200, PD-L1, CD276 (B7-H3) and CD270 and their knockdown improves IS formation (Ramsay et al. 2012). It has been recently demonstrated that the expression of PD-1L on the surface of CLL cells is a large contributor

to the suppression and pseudo-exhaustion of T cells in CLL (Riches et al. 2013). Indeed a clinical trial testing the efficacy of an anti-PD1 antibody is currently underway and preliminary data gathered from testing in the TCL-1 mouse model of CLL has shown promising efficacy in reversing the T cell deficiency (McClanahan et al. 2015). In this way physiologically relevant mechanisms which are present to protect the host against damaging self-reactive responses are manipulated in CLL for the benefit of tumour immune evasion and progression.

1.5.3.3 $CD4^+$ T cell compartment

In addition to its suppression of the $CD8^+$ T_{cyt} compartment, CLL also significantly impacts the $CD4^+$ T_h cell compartment. $CD4^+$ T cells have a crucial role in the activation and suppression of immune responses through their own interaction and activation via APC cells in healthy individuals. It has been shown that CLL cells are capable of recruiting $CD4^+$ $CD40L^+$ T cells via the secretion of chemokines such as CCL22 (Ghia et al. 2002) and subsequently suppressing their immune response through the induction of IL-10 secretion by T cells. Whilst CLL $CD4^+$ T cells provide pro-stimulatory signals such as CD40L, IL-4 and IL-21 which promotes CLL cell survival and proliferation (Pascutti et al. 2013; Girbl et al. 2013), the secretion of TNF family member signals such as BAFF and APRIL by T cells and CLL cells themselves lead to the activation of several receptors including TACI (Haiat et al. 2006). Downstream signalling from TACI induces the secretion of the immunosuppressive cytokine IL-10 (Saulep-Easton et al. 2015), leading to a protective, pro-proliferative environment for CLL cells with dampened T cell immune responses.

Whilst T cells are known to be heavily involved and impactful in CLL, full details of these processes have yet to be confirmed. The presence and interaction between various T cell

subsets and CLL cells in the LN microenvironment need to be carefully studied to allow a better understanding to shape drug use in this disease.

1.5.4 Natural Killer Cells

NK cell responses are also heavily dampened in in CLL; they have ineffective IS formation, similar to the impact upon the CLL T_{cyt} cell compartment (Kay & Zarling 1987). Recently further details into the mechanisms of suppression have been highlighted including secretion of inhibitory ligands by CLL cells (Reiners et al. 2013). The suppressive effects of CLL cells upon NK cells has been shown to be reversible *in vitro* by addition of cytokines, or the use of the immunomodulatory drug Lenalidomide (Acebes-Huerta et al. 2014; Lagrue et al. 2015; Huergo-Zapico et al. 2014).

1.5.5 Macrophages and Nurse-like cells

Monocyte-macrophages lineage cells are the chameleons within the haematopoietic system, capable of developing in to a multitude of tissue-specific cell types such as Kupffer cells or Langerhans cells (Lewis & Pollard 2006; Ross & Auger 1993). In CLL, it has been demonstrated through immunohistochemistry and co-culture experiments that a novel cell type of monocyte origin are present in the microenvironments which support the survival and progression of CLL cells. These cells are known as Nurse-like cells (NLC) and develop in high-density *in vitro* cultures of CLL cells (greater than $1x10^7$cells/mL) after 7-14 days (Burger et al. 2000). These cells were initially identified by the long term culture of CLL peripheral mononuclear blood cells (PMBC) but have since been indicated as present in the CLL LN. Prior to their identification within the LN, it was shown that these cells were likely to have a role in this important environment as GEP profiling of CLL cells in NLC co-

cultures displayed similarities to profiles seen from LN residing CLL cells (Burger et al. 2009).

In vitro studies have shown that, much like $CD4^+$ T cells, CLL cells actively recruit monocytes to the microenvironment via expression of a variety of chemokines (CCL3, CCL4, CCL5, CXCL10, IL-10) and induce a phenotypic change of these cells into an immunosuppressive NLC subtype (Giannoni et al. 2014; Bhattacharya et al. 2011; Filip et al. 2013; Ysebaert & Fournié 2011). Indeed the development of a NLC phenotype appears to be driven by the microenvironment and proximity to CLL cells, as healthy donor monocytes can be subverted to produce pseudo-NLC by co-culture with NLC (Bhattacharya et al. 2011; Ysebaert & Fournié 2011; Tsukada et al. 2002). GEP profiling of NLC have shown their similarity to immunosuppressive M2 macrophages which are anti-inflammatory and dampen immune responses. It has recently been indicated that this subversion of monocyte/macrophage cells to the NLC/M2 phenotype may be driven by secretion of nicotinamide phosphoribosyltransferase (NAMPT) by CLL cells (Audrito et al. 2015). In addition to immunosuppression, CLL cell survival is improved *in vitro* via co-culture with NLC. This is thought to be due in part to the secretion of TNF family members BAFF and APRIL which up regulate BCR signalling and NFκB expression (Nishio et al. 2005). NLC are also attributed a role in CLL cell homing to the LN microenvironment due to the secretion of the chemokines CXCL12 and CXCL13 (Burger & Kipps 2006). CLL cells home towards these signals moving up the concentration gradient, due to their expression of the respective receptors CXCR4 and CXCR5 on their cell surface. Targeting this cell type within CLL has shown promise *in vitro* as an emerging CLL therapy (Stamatopoulos et al. 2012).

The concept of a monocyte derived macrophage-like cell providing support to tumour cells is not novel. NLC have their equivalents in Lymphoma Associated Macrophages and

Tumour Associated Macrophages in solid tumours (Lewis & Pollard 2006). The presence of these cells, in many cases, have been linked to poorer prognosis, shorter progression free survival (PFS) and a more aggressive disease course (Lewis & Pollard 2006; Colvin 2014; Qian & Pollard 2010; Farinha et al. 2005; Lissbrant et al. 2000).

1.5.6 Mesenchymal Stromal cells

MSCs are found in both the BM and LN microenvironment. Under normal physiological conditions, MSCs are important in B cell development (BM) and for the structure and organisation of GCs (LN). MSCs have been shown to attract and activate CLL cells, observed through studies of *in vitro* co-culture experiments. The presence of BM-derived Stromal Cells (BMSC) *in vitro* has been shown to elicit protective and pro-survival effects upon CLL cells isolated from patient PB. These effects were stimulated via a mixture of contact dependent and secreted support, during which the BMSC were also activated.

1.6 Therapy

The scope of treatments available for patients with CLL has dramatically changed over the last decade bringing improvements in remission rates and overall survival (Jain et al. 2015). This is in large part due to the growing appreciation for the significance of the microenvironment in CLL disease relapse and protection from therapy. Many groups have called for new therapies to be developed targeting multiple important interactions believed to reside in these environments, acknowledging that without microenvironmental impact, a curative treatment is unlikely to be found (Burger 2011; Fecteau & Kipps 2012; Hayden et al. 2011; Hillmen 2011; Ponzoni et al. 2011). In recent years there has been progress towards this end, with the advent of new therapies targeting the BCR. Some of these are now in late stage clinical trials, including idelalisib (a PI3Kδ inhibitor) and Ibrutinib (a BTK inhibitor).

1.6.1 Idelalisib

Idelalisib is a selective phosphoinositol-3-kinase-delta (PI3Kδ) inhibitor. PI3Kδ is involved in propagating downstream signalling from multiple crucial receptors in CLL, including the BCR and CD40, promoting survival and proliferation. For the initial few weeks of treatment, patients show rapid LN shrinkage coupled with lymphocytosis (Hoellenriegel et al. 2011; Lannutti et al. 2011). Testing *in vitro* has shown Idelalisib inhibits CLL cell chemotaxis by reducing the levels of CXCR12 and CXCR13 expression by BMSC and NLC; signals crucial for homing of CLL cells to the microenvironments. Idelalisib has also been shown to reduce the levels of survival signals CLL cells receive from BCR signalling, as well as reducing pro-survival stromal cell interactions (Hoellenriegel et al. 2011; Lannutti et al. 2011; Maffei et al. 2015). In this way, Idelalisib reduces the protective crosstalk and retention of CLL cells in the LN, causing blasts to enter the PB. It is thought that this type of exclusion from the LN starves some of the blasts from the survival signals they require, causing the apoptosis of a

proportion of the circulating cells (Messmer et al. 2005; Chiorazzi et al. 2005; Damle et al. 2011). In addition, CCL3 and CCL4 signalling of CLL cells is reduced, which may reduce their ability to recruit protective T cells to the niche.

1.6.2 Ibrutinib

Ibrutinib is a Bruton's Tyrosine Kinase (BTK) inhibitor (Byrd et al. 2013). BTK is an important component of the BCR downstream signalling cascade and requires phosphorylation and binding of phosphatidylinositol-triphosphate (PIP3) to be activated (Byrd et al. 2013; Pieper et al. 2013). Once active, BTK translocates to the plasma membrane and its signalling cascade ultimately leads to calcium mobilisation, NFκB and PLCγ activation. Ibrutinib binds irreversibly to BTK stabilising it in an inactive state and treatment shows rapid lymphocytosis of CLL cells, with a reduction in BCR signalling and NFκB activation *in vivo* (Herman et al. 2014). Despite seeing an overall reduction in cell number, clinical studies show low rates of remission (2% in previously treated patients, 13% in treatment naïve patients (Hutchinson & Dyer 2014)).

With both Ibrutinib and Idelalisib, cessation of treatment sees a rapid reversal of lymphocytosis and down-regulated signalling. Consequently patients are likely to need lifelong treatment which may prove to be challenging. Due to this, toxicity profiles, whilst relatively manageable in early treatment, may pose problems in the longer term (Hutchinson & Dyer 2014). Resistance to therapy has already been reported in clinical trials (Hutchinson & Dyer 2014; Woyach & Johnson 2015) and the growing number of cases of primary and secondary resistance demand further investigation and careful consideration of follow-up therapy options. In addition, cost of treatment is of major concern which may be a limiting factor (Shanafelt et al. 2015) If these issues can be addressed, these targeted therapies hold

great promise for CLL patients over the long term. The lymphocytosis effects induced by Idelalisib or Ibrutinib are likely to be best utilised in combination therapies with monoclonal antibodies (mAb).

1.6.3 Traditional course of therapy

Most patients (70-80%) are typically diagnosed with CLL following a routine blood test (Oscier et al. 2012) and as such tend to have early stage disease (e.g. Binet stage A). Following the iwCLL guidelines for treatment (Hallek et al. 2008) most individuals will be assigned to observation rather than therapy until their disease progresses. This clinical strategy may be altered in the near future due to the ability to stratify patients for risk of progression and the advent of new therapies which hold lower toxicity profiles than traditional treatments. An example of this is the CLL12 trial (Langerbeins et al. 2015) which compares Ibrutinib monotherapy to the traditional "watch and wait" approach. High risk stage A patients are identified in this study using a combination of risk factors including sex, age and IgVH gene mutation status as well as cytogenetic features. The results of this study are as yet unconfirmed, but may initiate a revolutionary way to treat subsets of CLL patients in the future.

Once patients are showing signs of progressive disease and require treatment, the type of therapy that is offered will depend upon their individual circumstances, including the presence of any other comorbidities (figure 5). As the average age for CLL patients at diagnosis is 72, the presence of several comorbidities at time of therapy is not uncommon (Oscier et al. 2012). The identification of differential patient cohorts within CLL has proved invaluable in ensuring that individuals receive the most appropriate course of treatment for their disease. As previously discussed, CLL is highly heterogeneous and patients are

stratified into risk groups before treatment decisions are made (Oscier et al. 2012; Hallek et al. 2008). Routinely patients will be tested for the presence of TP53 mutations after diagnosis as this indicates a separate subgroup of typically high-risk patients who respond poorly to the traditional use of DNA-damaging therapies and so require alternative treatments (Stilgenbauer & Zenz 2010; Zenz et al. 2010).

1.6.4 "High Risk" patients (TP53 mutations)

Individuals with TP53 mutations are treated using combinations of non-DNA damage inducing therapies. Traditionally this may have been Alemtuzumab (a mAb targeting CD52 expression) or another mAb in combination with steroids (to boost the patient immune response) but recent studies have shown great efficacy in treating this high-risk category with the new class of BCR pathway targeting drugs Ibrutinib and Idelalisib alone or in combination with mAb therapy (Farooqui et al. 2015; Chavez et al. 2013; Byrd et al. 2013)).

New guidelines for the clinical treatment of CLL are continually updated to ensure the levels of patient care advances with the understanding of available therapies and it is currently recommended that, if eligible, patients should consider entry into clinical trials for new drug combinations. Where ineligible for these trials, the front line therapy offered to each patient is dependent upon their individual circumstances.

1.6.5 "Fit" Patients

For those patients considered fit enough to withstand the related toxicities, Fludarabine, Cyclophosphamide and Rituximab (FCR) therapy is first choice. FCR combines two chemotherapies with an immunotherapy; the purine analogue Fludarabine, the alkylating agent Cyclophosphamide and the mAb Rituximab.

<table>
<tr><td>Early Stage</td><td>No therapy</td><td colspan="3">Observation only
“Watch & Wait”</td></tr>
<tr><td rowspan="3">Progressive Disease</td><td>1st Line Therapy;
Clinical Trial Eligible</td><td colspan="2">Fit

FLAIR

Ibrutinib + Rituximab
vs
FCR</td><td>Unfit

RIALTO
Ofatumumab + CLB
+/- Idelalisib
-or-
Ofatumumab + Bendamustine
+/- Idelalisib</td></tr>
<tr><td>1st Line Therapy;
Clinical Trial
Ineligible</td><td>Fit

6 cycles of FCR
-or-
6 cycles of BR</td><td>Less Fit

CLB +
Obinutuzumab/
Ofatumumab
-or-
CLB + Rituximab</td><td>Frail

CLB
-or-
mAb
monotherapy</td></tr>
<tr><td>1st Line Therapy
TP53 patients</td><td colspan="3">Options include
Idelalisib + mAb or Ibrutinib + mAb
Alemtuzumab +/- steroids
Depending upon Pt disease and availability</td></tr>
<tr><td>Relapse
/Refractory</td><td>2nd+ Line Therapy</td><td colspan="3">Retest for TP53 mutation status. Therapy dependent upon Pt response in previous round(s) and “fitness” at time of requiring therapy</td></tr>
</table>

Figure 5. Representation of the current therapy options for CLL patients.

Therapy options available to CLL patients in the UK, table adapted from the Interim statement from the BCSH CLL Guidelines Panel 2015 (Follows et al. 2015; Oscier et al. 2012) Key. FCR; Fludarabine +Cyclophosphamide + Rituximab CLB; Chlorambucil, BR; Bendamustine + Rituximab, mAb; monoclonal Antibody therapy, Pt; Patient

Fludarabine interferes with DNA replication and repair whilst Cyclophosphamide causes inter- and intra- DNA strand crosslinks. Rituximab is a chimeric (human/mouse) monoclonal antibody which targets CD20, a cell surface marker found on all malignant and non-malignant B cells. Rituximab induces antibody dependent cytotoxic cell killing (ADCC) by NK cells, complement driven cytotoxicity, or direct apoptosis of the target cell. As a result Rituximab clears the body of both healthy B cells and CLL cells (James & Kipps 2011; Keating et al. 2005). Although Rituximab effectively clears the peripheral tumour burden in CLL, allowing patients to enter remission, relapse appears inevitable in most if not all patients.

Whilst being first choice for this patient group, FCR does present significant toxicities (for example therapy related pneumonia or neutropenia) and due to its immunosuppressive nature, leads to a higher risk of secondary complications such as infection (Riches et al., 2012). Nevertheless FCR replaced FC as the treatment of choice for these patients, achieving CR rates of 72% compared to 20-30% for FC alone (James and Kipps, 2011, Keating et al., 2005, Hillmen, 2011, Masood et al., 2011).

1.6.6 "Less Fit" Patients

Less fit patients ineligible for FCR will typically be treated with an alternative alkylating agent, Chlorambucil (CLB) in combination with a mAb therapy such as obinutuzumab, ofatumumab or rituximab as these combinations have been shown to be more effective than CLB alone (Goede et al. 2015; Hillmen et al. 2015; Hillmen et al. 2014). Obinutuzumab is a humanized anti-CD20 monoclonal antibody which has an engineered Fc region, improving its affinity to the FcγRIII on effector cells, improving ADCC and phagocytosis in addition to direct non-apoptotic tumour cell death. Obinutuzumab in combination with CLB has been

shown have superior levels of PFS compared to Rituximab (Goede, et al. 2015). Ofatumumab is also capable of improved ADCC compared to Rituximab (Bologna et al. 2012). Individuals who are considered too fragile to undertake CLB with mAb may be offered a mAb monotherapy or even CLB monotherapy which can help manage the disease but achieves low CR rates and as such could be considered palliative care (figure 5).

It is widely accepted that FCR is less efficient at targeting CLL cells within the LN or BM microenvironments and so successful therapy with these agents will leave behind a small reservoir of tumour cells from which relapse occurs (Bottcher et al. 2012). This inevitable relapse of patients having achieved a CR following chemoimmunotherapy is powerful evidence that that the current definition of CR does not represent eradication of all CLL cells but rather a reduction in CLL cell numbers to very low levels. The role of the microenvironment has therefore become a focus in CLL research, both to understand the biology of the disease and to develop targeted treatments to disrupt the supportive interactions within these niches.

1.6.7 Alternative Therapies

There are also alternative therapies available which focus upon rebalancing the immune system and target the microenvironment such as Lenalidomide. Lenalidomide is an immunomodulatory agent which has been shown to have multiple effects upon non-CLL cells in patients in addition to recent reports of direct anti-proliferative action upon CLL cells themselves (Fecteau et al. 2014; Acebes-Huerta et al. 2014). These effects can be broadly divided into improving natural anti-tumour immune responses, reducing supportive microenvironmental signals and reducing homing signals to the LN. Improvements in anti-tumour immune responses include reinstatement of T_{cyt} cells ability to form an effective

Immune Synapse (Ramsay et al. 2008) and in multiple myeloma has been shown to reduce the threshold for NK cell activation (Lagrue et al. 2015). In addition, Lenalidomide has been shown to suppress the supportive effect NLC cells provide to CLL cells, with GEP profiling indicating a reversion of NLC to a more M1 like phenotype (Fiorcari et al. 2014) and a relatively lower expression of CXCR12 (Fiorcari et al. 2014; Schulz et al. 2013). Showing efficacy in relapsed patients and those with del(17p), Lenalidomide provides an alternative therapy option for these high risk patient cohorts (Sylvan et al. 2012), although it has also been reported to induce significant adverse effects in CLL patients. These include tumour lysis syndrome, which is induced following the lysis of high numbers of CLL cells in a relatively short timeframe, leading to a storm of cytokines and intracellular metabolites being released into the blood (Coiffier et al. 2008). In addition, patients may experience a tumour flare reaction where the LN become inflamed and patients may experience fever (Badoux et al. 2011). Lenalidomide therapy requires careful management to protect patients from these effects, nevertheless its use shows promise, as a single agent and in combination.

It should be noted that until relatively recently effective treatments for CLL have been associated with significant toxicities that carry a particularly high risk to the older group of CLL patients and benefits seen in trials of younger patients do not transfer to the wider elder cohort (Eichhorst et al. 2013) who are frequently excluded from trials due to underlying comorbidities. As such this cohort of patients require careful management (Lamanna 2012; Goede & Hallek 2015; Tadmor & Polliack 2012; Ysebaert et al. 2015) and these advances in targeting the microenvironment with new non-chemotoxic therapies, as discussed above, have shown important promise particularly in the treatment of relapsed and refractory disease in the elderly and P53 cohorts of patients.

1.7 Modelling CLL

For the successful development of new therapies which target CLL cells in the microenvironment it is essential to be able to model CLL disease *in vitro*. Traditional models have been typically based upon the understanding of CLL from PB and BM samples, and have led to a wide variety of disease models being developed and routinely used in studies. Ultimately, a robust representation of the protective LN and BM environments is likely to best help in the development of effective, low toxicity therapies in CLL. It should be noted that whilst strides are made in the understanding of these disease niches *in vitro* utilising PB samples, these findings should be reconfirmed *in situ* wherever possible to ensure that a real-world view of the LN is being created.

1.7.1 In Vitro culture models

The culture of CLL cells *in vitro* commonly uses supportive stromal cells in combination with cytokine support (Hamilton et al. 2012; Hayden et al. 2011). These assay systems attempt to provide the CLL cells with specific signals thought or known to be required for survival and proliferation. This is with the purpose of replicating the microenvironment in CLL where cells are actively proliferating and protected from apoptosis. This allows screening of therapies aimed at targeting microenvironment residing CLL cells.

1.7.1.1 BM stromal cells

These systems investigate the important cellular and supernatant derived interactions found within the BM and these cultures have been reported to protect CLL cells during drug treatment. Through these models much information has been derived regarding CLL cell homing to the BM and how they are supported within them (Panayiotidis et al. 1996; Brachtl et al. 2011; Purroy et al. 2014; Lagneaux et al. 1998; Plander et al. 2009).

1.7.1.2 NLC

NLC cultures have been widely studied since their initial observation in CLL cultures (Burger et al. 2000; Tsukada et al. 2002; Burger et al. 2013; Filip, Ciseł & Wasik-Szczepanek 2013; Nishio et al. 2005) and research has shown their capabilities in supporting CLL cell survival, protection from drug-induced apoptosis, induction to proliferate and secretion of chemokine homing signals for CLL cells and for T cells.

1.7.1.3 CD40L stroma

CD40L, IL4 and IL-21 all represent important T cell derived signals which have been shown to be particularly important in CLL cell survival and proliferation (Bhattacharya et al. 2014; Ferrer et al. 2014; Pascutti et al. 2013; Hayden et al. 2011; Ahearne et al. 2013). Systems which provide these signals allow the culture of CLL cells *in vitro* without need for laborious purification of BMSC or NLC outgrowth prior to CLL cell co-culture. The CD40L and IL-4 system has been shown to induce GEP profiles in the CLL cells similar to those in LN residing cells, currently indicating this system as one of the best for drug screening to target protected LN residing CLL cells (Hayden, data unpublished).

1.7.1.4 Autologous T cells

Several labs have reported the use of artificially stimulated autologous T cells for the culture and study of CLL cells. In many cases a combinations of CD3, CD28, IL-2 and other compounds are used to stimulate isolated autologous T cells from patient samples, which are then co-cultured with cognate CLL cells (Asslaber et al. 2012; Pascutti et al. 2013). T cells in CLL are heavily deregulated and whilst these assays are informative, pre-stimulated T cells are unlikely to fully recapitulate the response of T cells within the CLL microenvironment.

1.7.1.5 Allogeneic T cells

The use of healthy donor allogeneic T cells has been previously reported, whereby the APC capabilities of T cells have been considered and showed a reduced capability to form functional immune synapse with CLL cells (Ramsay et al. 2008; Ramsay et al. 2012). Additionally, the use of whole PBMC samples artificially stimulated with CD3 and CD28 (Hock et al. 2014; Asslaber et al. 2012) have induced activation of CLL cells and their subsequent suppression of PMBC activation. These models allow the consideration of the immunosuppressive effects that CLL cells have upon their microenvironment and particularly upon T cells.

1.7.2 In Vivo Mouse Models

Mouse models of CLL have proven difficult to develop, likely due to the complex nature of the microenvironment that supports the disease *in situ,* but there are now several models widely accepted as useful for the study of CLL and investigation of potential new drug treatments.

1.7.2.1 Eμ TCL-1 mouse

The Eμ TCL-1 mouse is one of the most widely used models of CLL, where the TCL-1 gene (T cell leukemia-1) is induced to express in both mature and immature B cells by being placed under the control of an IgVH promotor and Eμ enhancer. In this model, TCL-1 expression in B cells causes a CLL-like disease to develop in mice over time with accumulation of IgM^+ $CD5^+$ lymphocytes. These cells are quiescent (G_0/G_1) and mice progress to develop lymphadenopathy (Bichi et al. 2002). Engraftment of CLL cells in mouse models have been improved via addition of other cell types such as T cells (Bagnara et al. 2011) highlighting the importance of microenvironmental interactions in the establishment

and maintenance of this disease. The Eμ TCL-1 mouse model has also proved a useful tool for drug response predictions; when treated with fludarabine, murine disease mimics the patient reaction, where an initial response develops into resistance and relapse (Johnson et al. 2006).

1.7.2.2 Alternative Mouse Models

The development of mouse models has been difficult but informative for the CLL community; for example different pathogenic pathways have been highlighted by their relative importance in producing a CLL-like disease. Whilst Eμ TCL-1 mice develop CLL-like disease, models impacting the cell death regulator BCL-2 or APRIL (a pro-proliferative signalling TNF family member) show an increase in B cell count but do not develop malignancy (Planelles et al. 2004; Lascano et al. 2013; Katsumata et al. 1992). In addition, utilisation of mouse models have highlighted that CLL patients' HSC have a propensity to produce clonal B cell populations. NOD/SCID/IL-2^{null} mice transplanted with HSC from CLL patients proceeded to develop multiple monoclonal B cell populations, in a manner similar to MBL disease (Kikushige et al. 2011). This work suggests that there may be a propensity to develop CLL disease from an early stage in B cell development.

Despite these insights garnered from the use of mouse models, the cellular support within murine tissues is unlikely to fully recapitulate the human LN or BM microenvironments and as such, these models need to be used in conjunction with ongoing *in situ* observation of human tissues and *in vitro* modelling. Only by using multiple approaches is it likely that a full understanding of this disease will come to fruition.

1.8 Dissecting the LN microenvironment

Whilst the CLL LN microenvironment is thought to be of paramount importance to the survival and proliferation of the tumour cells, the direct study of such tissues has inherent difficulties.

CLL LN tissue samples are no longer collected routinely as diagnosis is obtained through the flow cytometric analysis of patient PB. As such, supplies of LN material are relatively scarce compared to potential access to patient blood samples. The tissues that are available are typically archived samples from historic cases of CLL and as such are formalin fixed paraffin embedded samples (FFPE). FFPE tissue presents its own inherent challenges for interrogation as whilst Immunohistochemisty (IHC) is routinely performed by histopathogists, these analyses are single colour one-dimensional studies of tissue sections. In order to build an insight into the presence, proximities and potential interactions of cell types in the LN, multicolour analysis would be a better method. However, commercially available antibodies for IHC staining of FFPE tissue are typically unsuitable for multiplexing as they are raised in the same species (typically mouse) and as such are likely to cross react and induce false positive signalling.

Despite these challenges the study presented here utilised multicolour immunofluorescent staining and confocal microscopy to interrogate archived FFPE CLL LN tissue samples from seven CLL patients with the aim of gaining novel insight into the cell types and signals present within this tissue. Complimentary to this work, *in vitro* co-cultures of CLL PB cells with allogeneic T cells were investigated to consider the interactions of T cells and CLL cells within the microenvironment.

Study Aims;

Overall this study looked to confirm the presence of specific cell types and signals in the LN microenvironment and provide a deeper understanding of this important niche. In order to carry this out the following specific aims are highlighted:

- To identify commercially available antibodies which sufficiently allow the interrogation of FFPE CLL LN material; initially as single stains and subsequently as panels of up to three antibodies, to highlight the complexity of the disease and the untapped potential of such tissues. These antibody panels will initially focus upon investigating T cell subtypes and distribution within the CLL LN before considering the balance of proliferation and apoptosis within this important microenvironment.

- To use the data from initial above described studies in the CLL LN to establish a more informed *in vitro* assay utilising T and CLL cells, to allow further interrogation of their interactions.

- To broaden current knowledge about CLL LN complexity by more fully investigating the presence and role of additional accessory cells to T cells, including but not limited to macrophages and Nurse-like cells which have not been widely studied *in situ* to date.

2 MATERIALS & METHODS

2.1 Patient and healthy donor blood samples

Consented CLL patient blood samples were collected during routine appointments at the University Hospital Birmingham and Heartland Hospital West Midlands under an ethically approved study [Dr G. Pratt (10/H1206/58)]. All CLL patient MNC samples used had ≥75% $CD19^+$ cell presence and a lymphocyte count ≥ $1x10^7$cells/mL whole blood. Healthy donor blood samples were collected from volunteers following the ethically approved protocol for this project (15/NE/0045). All samples were handled individually and not pooled.

2.2 Blood Sample Preparation

All centrifugation steps were performed in a Falcon 6/300 centrifuge unless otherwise stated and were performed as follows.

2.2.1 Mononuclear Cell Isolation

Mononuclear cells (MNC) were isolated from whole blood samples through the use of density centrifugation media which allows the separation of different blood cell components into fractions based on their density. Blood was diluted in a 1:1 ratio with wash media (RMPI1640 supplemented with 100µg/mL streptomycin and 100U/mL penicillin) and carefully layered onto 15mL density centrifugation media (Ficoll Paque Plus, GE Healthcare, Buckinghamshire UK) in a 50mL tube (BD Falcon, Oxford, UK). Samples were centrifuged at 395 x *g*, 40 min, room temp (rt), centrifuge braking system turned off, to separate the blood into fractions. The upper fraction (plasma) was discarded and the MNC layer beneath carefully removed, diluted in 20mL wash media in a universal tube (Sterilin, Newport, UK) and centrifuged at 511 x *g*, 10 min, rt. The remaining fractions from the whole blood

preparation were discarded. The MNC layer underwent two further wash steps by diluting the cell pellet in 20mL wash media and centrifuging at 225 x *g*, 10 min, rt, to pellet the cells, then the wash media was removed and discarded.

2.2.2 Maintaining CLL samples in culture

Prepared MNC were counted and the suspension diluted to $5x10^6$cells/mL in ITS^+ media (RPMI1640 media (Gibco, Life Technologies, Paisley, UK) supplemented with 1% ITS^+ Premix (Corning, Amsterdam, The Netherlands) 100µg/mL streptomycin and 100U/mL penicillin (Gibco)). Cell suspensions were seeded into vented tissue culture flasks (Corning) and placed into a humidified incubator at 37°C, 5% CO_2 until use.

2.2.3 CLL Cell Purification

Where stated in Chapter 3, CLL samples were purified in order to remove all non-B cells. CLL MNC samples were purified using one of two types of commercially available isolation kits; either cells were purified by negative isolation where all other cell types are removed from the suspension (B-CLL cell isolation kit, human, Miltenyi Biotech, Surrey, UK), or through positive isolation where CLL cells are selected via their cell surface expression of CD19 (Dynabeads® $CD19^+$ Pan B cell isolation and DETACHaBEAD® CD19 kit, both Invitrogen, Life Technologies). It should be noted that trials of different commercially available isolation kits highlighted that some B cell isolation kits are ineffective for CLL cell isolation. This is due to the inclusion of CD43 in the antibody cocktail, which is not expressed on healthy B cells but is expressed on CLL cells, leading to the loss of CLL cells during the purification process. As such, caution is recommended when selecting an isolation kit for use with CLL cells. For this project, both positive and negative isolation kits

selected were used followed manufacturer's instructions and these methods are described briefly below.

Following isolation as described above (2.2.1) CLL MNC samples were counted to determine cell number and the cell suspension centrifuged at 300 x *g*, 10 min, rt.

2.2.3.1 Negative Isolation

The supernatant was aspirated and the cell pellet resuspended in 40µL MACS buffer (see Appendix I) per 10^7 total cells. 10µL Biotin-antibody cocktail (containing anti-human CD2 [T cells, NK cells], CD3 [T cells], CD4 [T cells, monocytes, macrophages, dendritic cells], CD14 [macrophages], CD15 [neutrophils, monocytes], CD16 [NK cells], CD34 [megakaryocytes], CD56 [NK cells], CD61 [thrombocytes], CD235a (Glycophorin A) [erythrocytes] and FceRIa [mast cells and basophils], targeting non-CLL cells within the MNC, was added per 10^7 cells and incubated (4°C, 10 min). Cells were subsequently washed by addition of 2mL MACS buffer and the cell suspension was centrifuged at 300 x *g*, 10 min, rt. The supernatant was discarded and the pellet resuspended in 80µL buffer per 10^7 cells. 20µL anti-Biotin microbeads were added per 10^7 cells and the cell suspension-bead mix was incubated (4°C, 15 min). The cell suspension was then applied to a prepared "LS" MACS column to which the non-CLL cell-bead complexes adhered. The untouched CLL cells within the eluent were collected in a fresh universal tube, counted and resuspended at $5x10^6$ cells/mL in ITS^+ media ready for use.

2.2.3.2 Positive Isolation

The supernatant was aspirated and the cell pellet resuspended to $2.5x10^7$ cells/mL in MACS buffer within a 15mL tube (BD Falcon). The CD19 Pan B Dynabeads, which bind to CD19

expressing CLL cells and B cells only, were mixed thoroughly and 25µL beads were added to the cell suspension per $2.5x10^7$ cells. The cell-bead mixture was incubated (4°C, 20 min) with gentle mixing to allow binding of the Dynabeads to the CLL cells. The mixture was subsequently placed on a Dynamag-15™ magnet (2 min) and whilst still on the magnet, the supernatant containing the non-$CD19^+$ cells was removed and discarded. To wash the $CD19^+$ cell-bead pellet, the tube was removed from the magnet and 1mL fresh MACS buffer added, gently mixed and the solution replaced on the magnet. The supernatant was removed and discarded and this wash step was repeated. After washing, the $CD19^+$ cell-bead pellet was resuspended in 250µL ITS^+ media per $2.5x10^7$ cells (from original cell count). 10µL DETACHaBEAD® solution was added per 250µL cell-bead suspension to cleave the magnetic beads from the $CD19^+$ cells. This mixture was incubated (45 min, rt) with gentle mixing. The suspension was placed onto the magnet (2 min) and the supernatant containing the cleaved $CD19^+$ cells was collected into a fresh universal tube. This cell suspension was counted, washed with 5mL fresh ITS^+ media and centrifuged at 300 x *g*, 10 min, rt. The cell pellet was resuspended in ITS^+ media at $5x10^6$ cells/mL ready for use as described below.

2.2.4 CLL Sample Irradiation

Where required, CLL samples were irradiated (10 min) using a sub-lethal dose of gamma rays (2.38 Greys/min) (Button et al. 1981; Finney et al. 1996) to prevent their proliferation when stimulated *in vitro*. These irradiated CLL cells were used during co-culture assays with $CD4^+$ T cells or alone as control as described in Chapter 3.

2.2.5 CD4⁺ T cell Purification

$CD4^+$ T cells were purified from healthy donor MNC samples by negative selection using a commercially available isolation kit ($CD4^+$ T cell Isolation kit, human, Miltenyi Biotech) following manufacturer's instructions. Samples were only utilised in co-culture assays providing they had ≥95% purity by flow cytometry analysis following purification. Briefly the supernatant from the MNC pellet was aspirated and the cell pellet resuspended in 40µL MACS buffer (see Appendix I) per 10^7 total cells. 10µL Biotin-antibody cocktail, targeting non-$CD4^+$ cells within the MNC, was added per 10^7 cells and incubated (4°C, 5 min). 30µL buffer per 10^7 cells was added to the cell suspension-antibody mix followed by 20µL anti-Biotin microbeads per 10^7 cells. The suspension was gently mixed and incubated (4°C, 10 min). The suspension was then applied to a prepared "LS" MACS column to which the non-$CD4^+$ cell-bead complexes adhered. The untouched $CD4^+$ T cells within the eluent were collected in a fresh universal tube, counted and resuspended at $5x10^6$ cells/mL in ITS^+ media ready for use.

2.2.6 CellTrace™ CFSE and CellTrace™ Far Red labelling of cell populations

CellTrace™ Carboxyfluorescein succinimidyl ester (CFSE) and CellTrace™ Far Red labelling was employed to allow monitoring of cellular proliferation in assay using flow cytometry analysis. These dyes can cross the cell plasma membrane and bind covalently within cells to free amines. As cells divide, their fluorescence intensity reduces and this can be monitored over time as a marker of proliferation.

The MNC, purified CLL cells or $CD4^+$ T cells were counted following their isolation and cell suspensions were washed twice by addition of 10mL warm Dulbecco's phosphate buffered

saline (DPBS) (GE Healthcare) and centrifuged at 511 x *g*, 10 min, rt. Subsequently cells were resuspended in 1mL warm DPBS and incubated with either 5µL 1mM CellTrace™ CFSE or CellTrace™ Far Red label (both Life Technologies) per $1x10^7$cells. Cells were incubated in the dark (10 min, rt), with occasional swirling of the cell suspension to ensure even labelling. Excess CellTrace™ label was washed away by the addition of 20mL 10% media (RPMI1640 supplemented with 5% foetal bovine serum (FBS) (Invitrogen) 100µg/mL streptomycin and 100U/mL penicillin) and centrifuged at 511 x *g*, 10 min , rt. This wash step was repeated and subsequently cells were resuspended in ITS^+ media at $5x10^6$ cells/mL.

2.3 Stromal Cell Preparation

2.3.1 Stromal Cell Initiation

Stably transfected murine L-cells expressing CD40L (L-40) and control L-cells (L-cont) [both a gift from Professor Gordon, University of Birmingham] were initiated in 10mL warm 10% media and cultured to confluence. Stromal cells were routinely tested each month to check for maintenance of CD40L expression by flow cytometry.

2.3.2 Stromal Cell Maintenance

To maintain cells in a proliferative state, confluent flasks were washed once, by removal of the 10% media within the flask and the addition of 10mL DPBS to rinse off any remaining FBS containing media from the cells (as this would impede the action of the subsequent dissociation step). The DPBS was discarded and cells were incubated with 3mL trypsin EDTA (GE Healthcare) (5 min) at 37°C 5% CO_2 to allow dissociation of the cell monolayer.

Complete dissociation of the monolayer was confirmed via microscopy, and subsequently 7mL 10% media was added to each flask. The cell suspension was gently mixed and centrifuged at 511 x *g*, 10 min, rt. The supernatant was discarded, the pellet agitated and resuspended in 10mL fresh 10% media and used to seed up to five fresh flasks.

2.3.3 Mitomycin C Treatment of stromal cells to prevent growth

Confluent large flasks were treated with 0.02M Mitomycin C (Sigma-Aldrich, Dorset, UK) for 3 hours to prevent cell proliferation. Flasks were subsequently washed three times with DPBS and cells were harvested as previously described using trypsin EDTA. Cell suspensions were frozen (see below) and stored at -80^{o}C prior to use.

2.3.4 Stromal Cell Stock Freezing

Cell suspensions were centrifuged at 511 x *g*, 10 min, rt, the supernatant discarded and cells were resuspended to 1x10^{7}cells/mL in freezing media (90% FBS (Invitrogen) 10% DMSO (Sigma)) and wrapped in cotton wool to slow freezing. 1mL aliquots were initially frozen at -80^{o}C overnight, with longer term storage in liquid nitrogen until required.

2.3.5 Creation of stromal control plates for assay cultures

Mitomycin C treated L-40 and L-cont were initially brought up from freeze by addition to 20mL 10% media, counted, and then made up to a density of 1x10^{5}cells/mL in fresh 10% media. Cells were seeded into 96 well plates at 1x10^{4}cells/well. Plates were placed into a humidified incubator for a minimum of 24 hours at 37^{o}C, 5% CO_2 to allow stromal cell attachment prior to their use in co-culture experiments.

2.4 Co-culture assay

CLL MNC (or purified CLL cells) and $CD4^+$ T cells were each seeded into clean 96 well plates at $2.5x10^5$ cells/well in a final volume of 200µL media per well. As a control, CLL MNC (or purified CLL cells) were seeded onto Mitomycin C treated L-40 and L-cont stroma plates (as described above, Chapter 2.3.5) at $2.5x10^5$ cells/well, in a final volume of 200µL media per well. All conditions at each time point were set in triplicate. Cells were cultured for 3-7 days at 37°C, 5% CO_2. Where stated, media was supplemented with recombinant human IL-21 (eBiosciences, Hatfield, UK) and/or recombinant IL-4 (R&D) at 25ng/mL and 1ng/mL respectively.

2.5 Co-culture analysis

All flow cytometry analysis was performed on a FACS Calibur (BD Biosciences) which was calibrated for each analysis assay run for this project. This involved manual compensation to create new settings for each fluorophore panel combination.

2.5.1 ^{3}H-Thymidine incorporation analysis

24 hours prior to readout, appropriate triplicate wells were pulsed using 20µci/mL ^{3}H-thymidine (GE Healthcare). Following the incubation period, the wells were transferred into a fresh plate and frozen at -20°C overnight. To analyse, plates were defrosted and harvested onto a glass fibre filter mat (Thermo Fischer Scientific, Loughborough, UK) using a Skatron cell harvester (Skatron Instruments) which uses vacuum pressure to transfer cells from plates to the filter mats. Filter mats were air dried and subsequently analysed using a Beta-Plate Scintillation counter (Skatron Instruments).

2.5.2 Bromodeoxyuridine (BrdU) incorporation analysis

During co-culture set up required triplicate wells were supplemented with BrdU-containing ITS+ media (200µM/well) for the course of the experiment. At readout, triplicate wells from 96 well assay plates were pooled and analysed for incorporation of BrdU by immunfluorescent staining of cell cytospins (below).

2.5.2.1 Making Cytospins

Triplicate wells from 96 well assay plates were pooled and 100µL of the homogenous cell suspension centrifuged onto slides using a Shandon CytoSpin III Cytocentrifuge at 28.23 x *g*, 3 min, rt. Cytospins were air dried before being fixed by immersion in ice cold acetone (10 min). Slides were allowed to air dry completely before commencing immunfluorescent staining.

2.5.2.2 Immunofluorescent Staining of Cytospins

All wash steps for cytospins staining refer to the immersion of slides in 1x Wash Buffer (Dako, Cambridgeshire, UK) twice (2 x 3 min) and all steps were performed at rt protected from light unless otherwise stated.

Sample cytospins were immunofluorescently stained for the incorporation of BrdU. The cell spots were encircled by a hydrophobic pen (Dako) to create a waterproof barrier around the cells. Slides were washed and incubated with 50µL Reagent A (Fix and Perm®, Life Technologies) (15 min). Slides were washed and incubated with 50µL Reagent B (Fix and Perm®, Life Technologies) (20 min) followed by washing and incubation with FcR blocking solution (Innovex Biosciences, Wako, Germany) (10 min). To unmask the epitope for the Anti-BrdU antibody, slides were washed and incubated with 305.6µg/mL DNAse I solution

(Sigma-Aldrich) (1 hour, 37°C). This was followed by washing and incubation with the primary antibody: Anti-BrdU-FITC (BD Biosciences, Oxford, UK) (30 min). Slides were washed and then incubated with the secondary antibody: anti-fluorescein/Oregon green Goat IgG Alexa488 (Invitrogen) (30 min). Finally, slides were washed and immersed in Hoescht solution (20µg/mL) (Invitrogen) (1 min), immersed in dH_20 (1 min) and then mounted with a coverslip using ProLong® Gold Anti-fade reagent with DAPI (Life Technologies). Slides were allowed to cure overnight before being viewed on a Nikon A1 confocal microscope (BALM).

2.5.3 CellTrace™ CFSE and CellTrace™ Far Red Analysis

Triplicate wells were pooled and washed with 2mL DPBS, centrifuged at 511 x *g*, 5min, rt, the supernatant discarded and the pellets agitated. 200µL FACS Fix solution (see Appendix I) was added per sample and tubes were stored at 4°C until analysed by flow cytometry (within one week).

2.5.4 Cell Cycle Analysis

Triplicate wells from 96 well assay plates were pooled and washed with 2mL DPBS, centrifuged at 511 x *g*, 5 min, rt the supernatant discarded and pellets agitated. 500µL cell cycle buffer (see Appendix I) was added per sample tube and tubes were stored at 4°C for 24 hours before being analysed by flow cytometry.

2.5.5 Analysis of Immunophenotype

Samples were stained for the presence of several extracellular markers to check the immunophenotype of the cells within samples (see table 1 for full details). Triplicate wells

from 96 well assay plates were pooled and stained using 2µL of each required antibody or relevant isotype control (BD Biosciences) per sample. Samples were incubated in the dark (15 min, RT), and then washed with 3mL DPBS, centrifuged at 511 x *g*, 5 min, rt and the supernatant discarded. Cell pellets were agitated, resuspended in 200µL FACS Fix and stored at 4°C until analysis by flow cytometry (within one week).

Antibody	Fluorophore	Manufacturer
Anti-CD3	FITC	BD Biosciences
Anti-CD4	PeCy7	BD Biosciences
Anti CD19	APC	BD Biosciences

Table 1. Antibodies used for routine immunophenotyping of CLL samples by flow cytometry.

2.5.6 Analysis of cell viability

Samples were analysed for their viability using an AnnexinV/ Propidium Iodide flow cytometry assay. Propidium iodide (PI) is commonly used as a converse marker of viability; healthy cells take up PI but simultaneously re-export PI via efflux pumps. In contrast, dying cells lose membrane integrity and this allows PI to enter the cell and intercalate irreversibly with DNA. Once intercalated, PI fluoresces and can be detected by flow cytometry. Triplicate wells from 96 well assay plates were pooled and washed with 3mL DPBS, centrifuged at 511 x *g*, 5 min, rt) and the supernatant discarded. Cell pellets were agitated and resuspended in 200µL 1 x AV binding buffer with 5µL AnnexinV-FITC (BD Biosciences) and/or 5µL Propidium Iodide (BD Biosciences). Samples were incubated (15 min, rt) and subsequently analysed by flow cytometry (within 1 hour).

2.6 CLL patient lymph node and healthy donor spleen Formalin Fixed Paraffin Embedded tissue samples

Healthy donor spleen tissue samples and CLL patient lymph node tissue samples were accessed via the Human Biomaterials Resource Centre (HBRC) at the University of Birmingham under ethical approval for the centre and this project (09/H1010/75 and 15/NE/0045 respectively).

2.7 Staining of FFPE tissue samples

2.7.1 Dewaxing and Antigen Retrieval

Paraffin embedded tissue sections on glass slides were baked (30-60 min, 60°C) in a drying oven prior to processing, to ensure sections were well adhered to the slides. Tissue sections were dewaxed and antigen retrieved using the commercially available citrate buffers and the automated Dako PT Link Module (Dako). Whilst the tissue sections were baked, the retrieval buffers were warmed to 84°C within the PT Link Module. Either pH6 (EnVision™ Flex Target Retrieval Solution, low pH, Dako) or pH9 (EnVision™ Flex Target Retrieval Solution, high pH, Dako) buffers were used for antigen retrieval. Sections were immersed in the buffers and the buffers heated to 97°C and held at this temperature for 17 min (high pH) or 20 min (low pH) before being cooled to 65°C. Tissue sections were subsequently allowed to rest in the cooled buffers (5 min) before being transferred to wash buffer (EnVision™ Flex Wash Buffer, Dako) to cool (5 min).

2.7.2 Chromogenic Staining

All wash steps for chromogenic staining refer to the immersion of slides in 1x Wash Buffer (Dako) twice (2 x 3 min) and all steps were performed at rt protected from light unless otherwise stated.

Sections were blotted to remove excess wash buffer and a hydrophobic pen was used to encircle the tissue to form a waterproof barrier. Sections were incubated with 150µL of Fc Receptor block (Innovex Biosciences) (10min), washed and incubated with the relevant primary antibody (30 min) (see table 2 for a list of primary antibodies). Sections were washed and then incubated with a horseradish peroxidase-conjugated (HRP) secondary antibody (Dako) (30 min). Chromogenic developer solution was prepared by a diluting 20µL Diaminobenzidine substrate (Dako REAL™ DAB+ Chromogen, (x50) (Dako)) in 1mL Dako REAL™ Substrate Buffer (Dako). Sections were washed and incubated with chromogenic developer solution (1-10 min) to allow staining to develop. Once a sufficient depth of stain had developed sections were briefly rinsed in DPBS. Sections were counterstained with haematoxylin (Envision™ FLEX Hematoxylin (Link), Dako) and subsequently dehydrated using increasing concentrations of alcohol solution: sections were immersed twice in fresh 50% ethanol solution (5 sec), twice in fresh 70% ethanol solution (5 sec) and incubated in 96% ethanol (3 min). Sections were then incubated in fresh 96% ethanol solution (2 min), 98% ethanol solution (2 min) and 100% ethanol (2 min) before being allowed to air dry completely. Once dry, sections were mounted using dibutyl phthalate xylene (DepeX Mountant, Sigma-Aldrich). Sections were viewed on an Olympus BX40 microscope once the mountant had fully cured (approx. 12 hours).

2.7.3 Haematoxylin and Eosin Staining

All steps for haematoxylin and eosin staining (H&E staining) were performed at rt.

Sections were blotted to remove excess wash buffer and a hydrophobic pen was used to encircle the tissue to form a waterproof barrier. Sections were immersed in haematoxylin stain (Pioneer Research Chemicals Ltd, Essex, UK) (2 min) and subsequently rinsed under cold running tap water (2 mins). Sections were subsequently immersed in 1% Acid Alcohol solution (Pioneer Research Chemicals Ltd) (30 sec) followed by immersion in Scott's tap water substitute (Pioneer Research Chemicals Ltd) (2 mins). Sections were counterstained by immersion in Eosin stain (Pioneer Research Chemicals Ltd) (2min) and subsequently rinsed under cold running tap water (2mins). Sections were dehydrated by immersion in fresh 96% ethanol (1 min) followed by immersion in 100% ethanol (1 min) before being allowed to air dry completely. Once dry, sections were mounted using dibutyl phthalate xylene (DepeX Mountant, Sigma-Aldrich). Sections were viewed and images collected on a Zeiss AxioScan microscope (MISBU) once the mountant had fully cured (approx. 12 hours).

2.7.4 Immunofluorescent Staining

All wash steps for immunofluorescent staining refer to the immersion of slides in 1x Wash Buffer (Dako) twice (2 x 3 min) and all steps were performed at rt protected from light unless otherwise stated.

Sections were blotted to remove excess wash buffer and a hydrophobic pen was used to encircle the tissue to form a waterproof barrier. Sections were blocked by incubation with 60µg/mL Donkey Serum (Jackson ImmunoResearch, Suffolk, UK) (10 min). Sections were washed and incubated with the relevant primary antibody (30 min) (see table 2 for a list of

primary antibodies). Sections were washed and incubated with the appropriate fluorochrome-conjugated secondary antibody (30 min) (see table 2 for a list of secondary antibodies used). To achieve multicolour immunofluorescent staining and reduce cross-reactivity of antibodies, when more than one epitope was being targeted on the same section, each epitope would be stained for separately. In these cases, after the first primary antibody and secondary antibody staining steps had been completed, sections were washed and incubated again with Donkey Serum (10min) as a blocking step to reduce cross reactivity. The staining process was repeated as described above for each epitope. Once all targets had been stained for, sections were washed and counterstained for nuclei using 20µg/mL Hoechst 3334 (1 min). Finally, sections were mounted using ProLong Gold ™ Anti-fade mountant and cured overnight in the dark. Sections were stored long term at 4^{o}C protected from light until viewed on a Zeiss Zen 780 Confocal Microscope (MISBU) (within 14 days).

Primary Antibodies			
Mouse Antibodies			
Target	**Catalogue Number**	**Manufacturer**	**Dilution**
CD3	M7254	Dako	1:100
Ki-67	M7240	Dako	1:50
CD163	NCL-CD163-S	Novocastra	1:200
CD4	M731029-2	Dako	1:10
CD68	M0814	Dako	1:150
NAMPT	AG-20A-0034-C100	Adipogen	1:200
Goat Antibodies			
Target	**Catalogue Number**	**Manufacturer**	**Dilution**
Pax5	AF3487	R&D Systems	1:20
CD3	sc1128	Santa Cruz	1:10
Rabbit Antibodies			
Target	**Catalogue Number**	**Manufacturer**	**Dilution**
Ki-67	HPA000451	Atlas Antibodies	1:100
CD68	HPA048982	Atlas Antibodies	1:200
CD8a	HPA037756	Atlas Antibodies	1:10
CD3	IS503	Dako	neat (prediluted)
Cleaved Caspase 3	9661S	Cell Signaling	1:300
Isotype Controls			
Target	**Catalogue Number**	**Manufacturer**	
Mouse IgG	10R-I169A-FIT	Fitzgerald	
Rabbit IgG	AB-105-C	R&D Systems	
Goat IgG	AB-108-C	R&D Systems	
Secondary Antibodies			
Target	**Catalogue Number**	**Manufacturer**	**Dilution**
Anti-Mouse Alexa488	715-545-151-JIR	Jackson Immunoresearch	1:100
Anti-Rabbit Alexa647	711-605-152-JIR	Jackson Immunoresearch	1:100
Anti-Goat Alexa568	A11057	Life Technologies	1:100

Table 2: Details of primary and secondary antibodies used in chromogenic and immunofluorescent staining of FFPE tissue samples.

2.8 Image Analysis

For quantitative analysis of immunofluorescently stained CLL LN and healthy donor spleen tissues, three images were obtained per tissue sample for each stained and isotype section. These images were analysed and edited using the open source Fiji Image J software (Schindelin et al. 2012). Images were adjusted for their brightness and contrast as well as reducing background as appropriate for each staining panel when compared to the isotype tissue. Images were counted for positivity using Analyze Particles plug-in within Fiji, which uses an algorithm to detect boundaries of high and low fluorescence intensity and requires user input of size limits for "events" to be counted within each image. Numerical data from these analyses were collected in Microsoft Excel for further processing and analysis. As red blood cells autofluoresce across a large spectrum of fluorescence, their presence in images posed an issue to create false positive events during quantification. To prevent this, the fluorescence channel of interest was overlaid onto the nuclear channel reading from which these red blood cells could be easily identified by their high fluorescence intensity across both channels. This allowed their subtraction from the final quantification analysis. Automation of quantification was utilised where possible to ensure consistency of analysis. This was achieved by designing macro instructions for the Fiji Software. Example images from this analysis process can be found within Appendix I.

2.9 Statistical Analysis

Unless otherwise indicated in Chapter 4, all non-parametric co-culture data was routinely analysed using the Wilcoxon signed rank test, as these experiments used paired primary samples. Where appropriate, the Student's paired t-test was used and this is noted within the text in Chapter 4. Statistical significance was considered to be reached where $p \leq 0.05$

except in instances where the control samples were used as a comparison for multiple samples. In these cases, to guard against multiplicity the Bonferroni correction was applied, where the required p value for significance (usually ≤0.05) was divided by the number of samples being tested against the same control to give the new p value for significance. For example, where 2 test samples were checked against a common control, significance was considered reached where $p \leq 0.025$.

3 T CELLS & CLL CELLS IN THE LN MICROENVIRONMENT

3.1 Introduction

As discussed in Chapter 1, the CLL LN microenvironment is known to be the major site of disease progression and maintenance and whilst there are many *in vitro* and *in vivo* models of CLL, most do not fully represent this important niche. A fuller understanding of the LN would allow the development of targeted therapies which could bring about longer remissions and the potential for curative therapy.

Aside from the relative scarcity of fresh CLL LN material available, current routine practices for the interrogation of such tissues involve single colour immunohistochemistry (IHC). Whilst this may be adequate for histopathological diagnosis, single colour staining does not provide insight into the proportions, proximities or interactions occurring in this environment. As such this study investigated the potential of utilising commercially available antibodies against a range of different cell markers to allow a real-world view of the CLL LN, highlighting not only the different cell types present but also their relationship to one-another. The use of robust fluorophores and confocal microscopy allowed the capture of high resolution, high quality images, in turn permitting robust quantitative analysis. The development of these approaches for use with formalin fixed paraffin embedded (FFPE) tissue also allowed a greater opportunity to access architecturally preserved high quality tissue (figure 6).

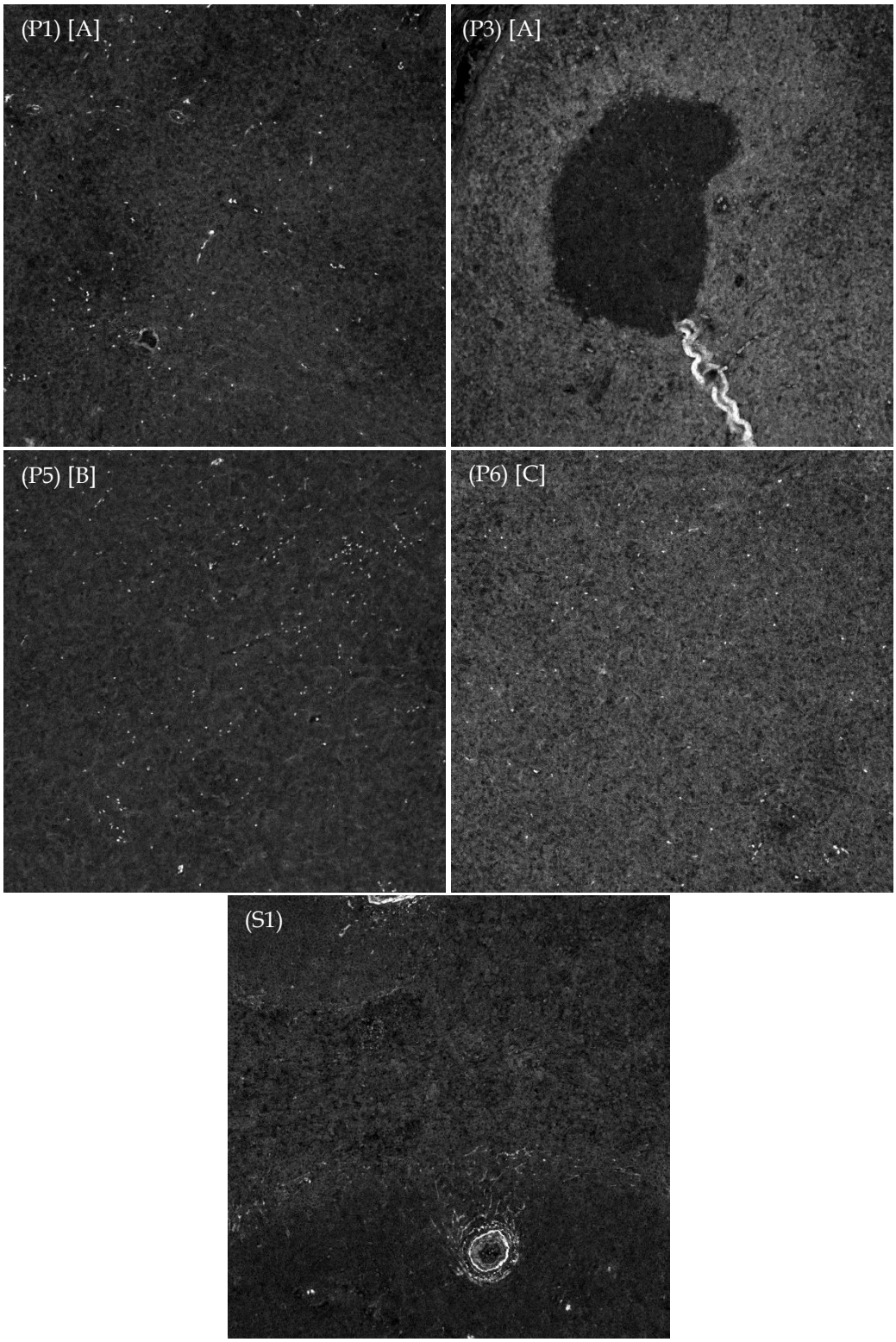

Figure 6. Cellular architecture is well preserved in FFPE tissue.

5µm thick sections of FFPE tissues were counterstained for nuclei using Hoescht 33343. Data shows representative images of CLL LN tissue from patient samples (n=4) with [stage of disease] in addition to healthy spleen tissue (n=1).

This study used FFPE primary LN tissue samples from seven CLL patients and FFPE healthy spleen tissue samples as control. The list of patient details can be found in table 3. Each patient sample, with the exception of tissue sections from Patient 3 (P3), was imaged in three different areas for each panel of markers being studied. Three discrete areas were selected in an effort to provide a balanced insight into the cellular contents of each sample whilst reducing potential sampling bias which may occur with a single image. Every effort was made to record images from the same three areas on serial sections stained with differing marker combinations. This was facilitated by noting the shape of each tissue and seeking specific "landmarks" within the same regions of sequential sections such as blood vessels. Sample P3 had three areas collected from each of two different zones within the tissue (hereafter referred to as Zone 1 and Zone 2 or Z1 and Z2 respectively). An exception was made for sample P3 in this way due to the striking differences seen in the architecture and proliferative activity (Ki-67 positivity and distribution) of the two zones within P3 tissue sections as described within this chapter (3.3.1).

Sample	Stage	Sex	Age	Lymph Node Size	Treatment	Additional malignancies	Death	Notes
P1	A	F	59	28x24x10mm	N	N	N	
P2	A	M	75	20x13x6mm	N	Previous Squamous Cell Carcinoma (Rx) Basal Cell Carcinomas	Y (5y PD)	Pt admitted with chest infection prior to death
P3	A	F	68	10x11x8mm	N	N	N	Pt had flow cytometry performed on BM (2010) which was consistent with B-CLL. However, serum free-kappa (κ) & free-lambda (λ) and κ/λ ratio normal (Oct 14)
P4	A	M	85	Up to 21mm	N	Metastatic Squamous Cell Carcinoma (Rx)	Y (5y PD)	Pt breathlessness reported prior to death
P5	B	M	57	20x20x20mm	Y 6x cycles FCR	N	N	
P6	C	F	77	35x20x10mm	Y FC therapy	N	Y (5y PD)	Queried Richter's transformation 2 days prior to death
P7	C	M	76	Largest 70mm	N	Synchronous Transitional Cell Carcinoma	Y (5y PD)	In addition to CLL and TCC, Pt also had metatstatic oesophogeal cancer

Table 3. Patient information for 7 FFPE CLL LN samples used in this study.

Patients had a mean age of 71 years at diagnosis and 4 out of 7 patients died 5 years after diagnosis. Key; Rx radiotherapy, PD post diagnosis, P/Pt patient.

3.2 Chromogenic staining methods can be successfully optimised to produce high quality multicolour immunofluorescent images of FFPE tissue

In order to develop a multicolour immunofluorescent staining protocol for use on FFPE CLL LN tissue, single colour chromogenic staining of FFPE healthy spleen tissue was first utilised to (i) validate antibodies being used and (ii) test the antigen retrieval and dewaxing techniques to be employed. Having established these parameters single colour immunofluorescent stains were trialled on spleen tissue followed by combining stains into three-way multicolour panels for interrogation of CLL LN. This process is outlined in Figures 7 and 8.

Figure 7 shows representative images of chromogenic stained sections of FFPE healthy spleen tissue stained for the cell cycle activation marker Ki-67 and the T cell marker CD3. Following confirmation of the suitability of these antibodies and retrieval techniques, the methods were adapted to allow immunofluorescent staining of these markers and finally three-way staining of CLL LN. As an example figure 8 shows a representative image of a multicolour stain on FFPE CLL LN tissue using the B cell marker PAX5, in combination with CD3 and Ki-67. Additional staining panels were constructed based on this approach and images were subsequently quantitatively analysed using Fiji Image J Open Source software (see Appendix I for further details).

In multicolour immunofluorescent staining, the order of staining was determined based upon the resilience of the fluorochrome-conjugated secondary antibody to light. Primary antibodies for which the secondary antibody was Alexa 488-conjugated were stained for first as it is the most resilient to degradation, followed by Alexa 647 and finally Alexa 568. Details of the antibodies used to target the different cell types are listed in table 4 below.

Target	Cell Type/Marker
CD3	T cell
CD4	T_h cells
CD8a	T_{cyt} cells
CD68	Macrophage
CD163	Nurse-like cells/M2 cells
Pax5	CLL/B cells
Ki-67	Proliferation (Cell cycle activation)
Cleaved Caspase 3	Apoptosis (activation of the caspase pathway)
NAMPT	Nicotinamide phophoribosyl transferase enzyme

Table 4: Details of primary antibodies used in chromogenic and immunofluorescent staining of FFPE tissue samples and the cell types or markers they represent.

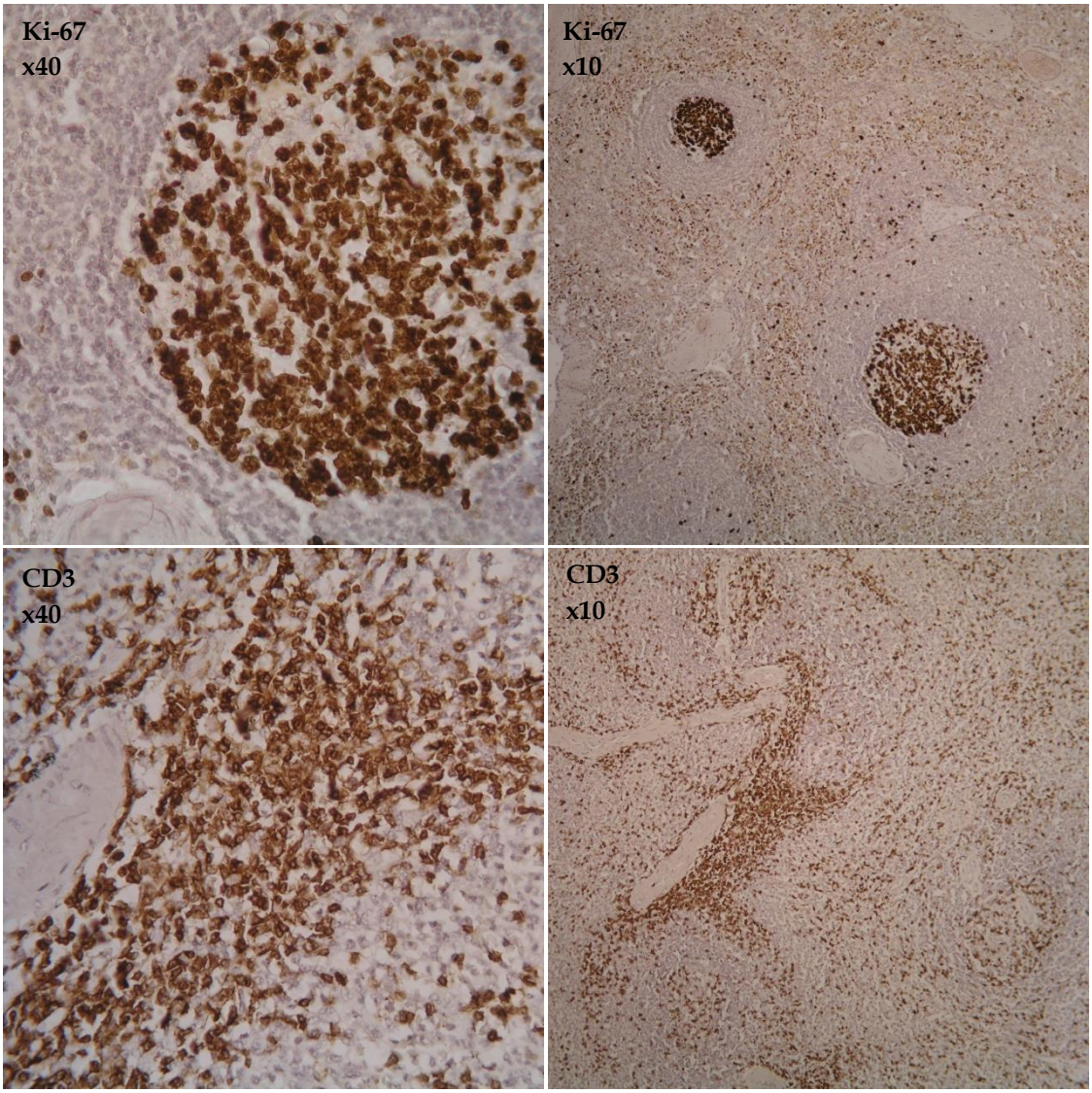

Figure 7. Chromogenic staining of FFPE healthy spleen tissue is informative but requires antibody optimisation.

FFPE healthy spleen tissue was chromogenically stained using Horse-radish peroxidase (HRP) chromogen for the presence of different cell markers. Data shows representative images of Ki-67 and CD3 staining taken using x40 and x10 objective lenses on an Olympus BX40 light microscope.

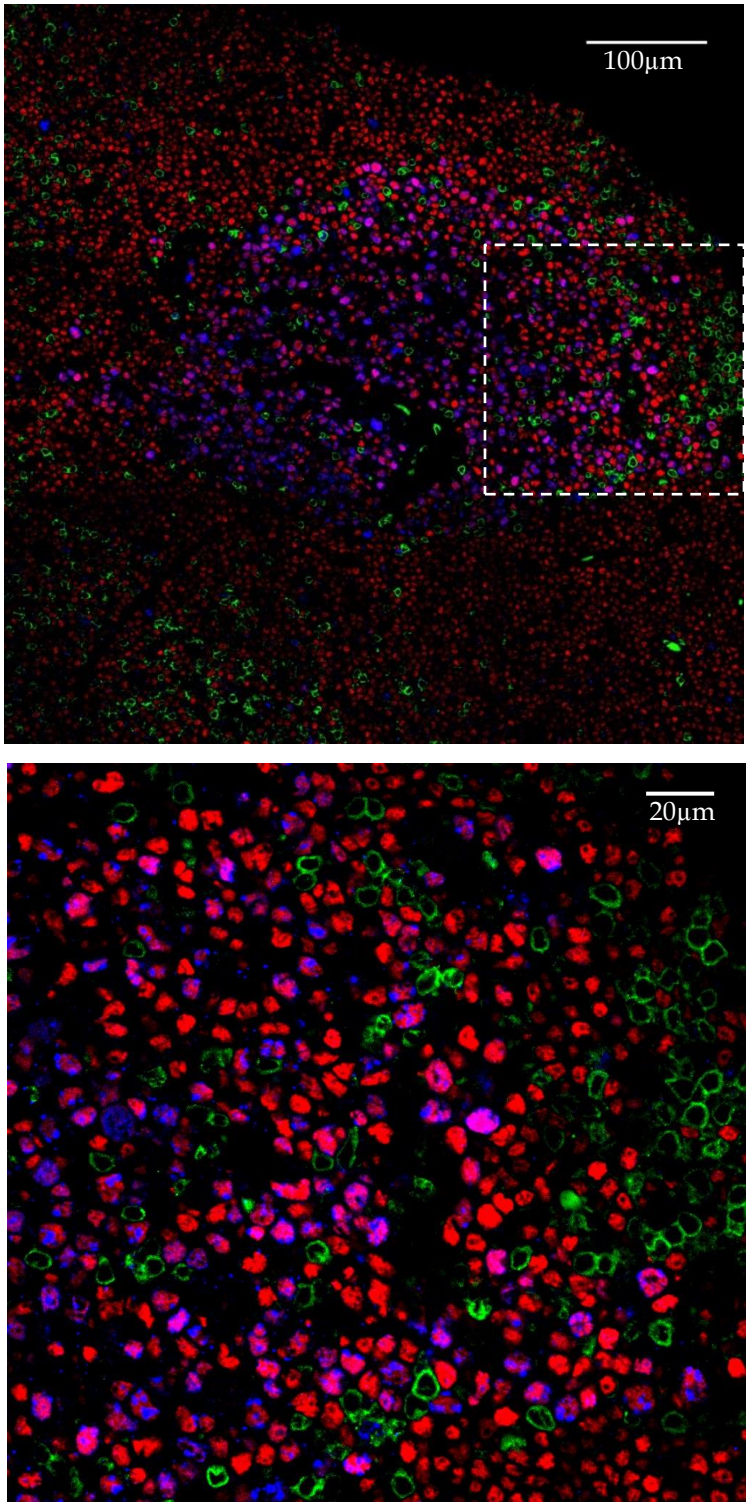

Figure 8. Multicolour immunofluorescent staining of FFPE CLL LN tissue shows novel insight above the capabilities of chromogenic staining.

CLL LN tissue sections were stained for the expression of CD3 (green), PAX5 (red) and Ki67 (blue). A representative sample (n=1) is shown. TOP: 9 images were collated using Zeiss Zen Black software to show a proliferative zone. BOTTOM: Larger view of the image within the dashed line on the top panel. Images collected using x40 objective on a Zeiss Zen780 confocal microscope.

3.3 T cells and CLL cells in the proliferative CLL LN microenvironment

As discussed in Chapter 1.4.1 a large literature has amassed on the many and varied potential roles of different subsets of T cells in the CLL environment and it has been shown that the T cell compartment in CLL is highly affected in this disease. Consequently this project initially focused on the presence of T cells in the CLL LN, their relationship with CLL cells and the proliferative and apoptotic signature of the LN microenvironment across different stages of disease. In addition, this project also investigated the balance of proliferation and apoptosis in the CLL LN tissue, which is markedly skewed in many cancers (Evan & Vousden 2001; Hanahan & Weinberg 2000). This was achieved by utilising Ki-67 and cleaved caspase 3 as markers of proliferation and early apoptosis respectively.

Initially tissue samples were stained with haematoxylin and eosin dyes (H&E staining) to consider their morphology and to determine the presence of proliferation centres in these CLL LN samples. This staining was then considered in the context of Ki-67 distribution within these tissues.

3.3.1 Ki-67 profiles of CLL LN are highly variable and evidence of "traditional" proliferation centres as observed by H&E are not always apparent

Sections from seven CLL LN tissue samples and one healthy spleen tissue sample were H&E stained (method as described in chapter 2.7.3) to determine the presence of classical proliferation centres (figure 9). These data demonstrated that all CLL LN tissues in this study appear to contain proliferation centres, as seen in low magnification images by observation of paler circular areas of tissue (figure 9). The numbers of these centres vary across the CLL LN samples and appear strikingly different in sample P3 compared to the other tissues. Subsequently, sections from the same seven CLL LN tissue samples and one healthy spleen tissue sample were then immunofluorescently stained for their expression of Ki-67 as a marker of active cell cycle. There was a variation in expression of Ki-67 across the samples, with most showing a diffuse spread of Ki-67$^+$ cells. The exception to this observation was sample P3, within which there were two strikingly different types of proliferative architecture; pockets of highly Ki-67$^+$ "proliferative" cells, denoted as Zone 1 (Z1) and areas of low, diffuse proliferation denoted as Zone 2 (Z2) (representative images seen in figure 10A & B).

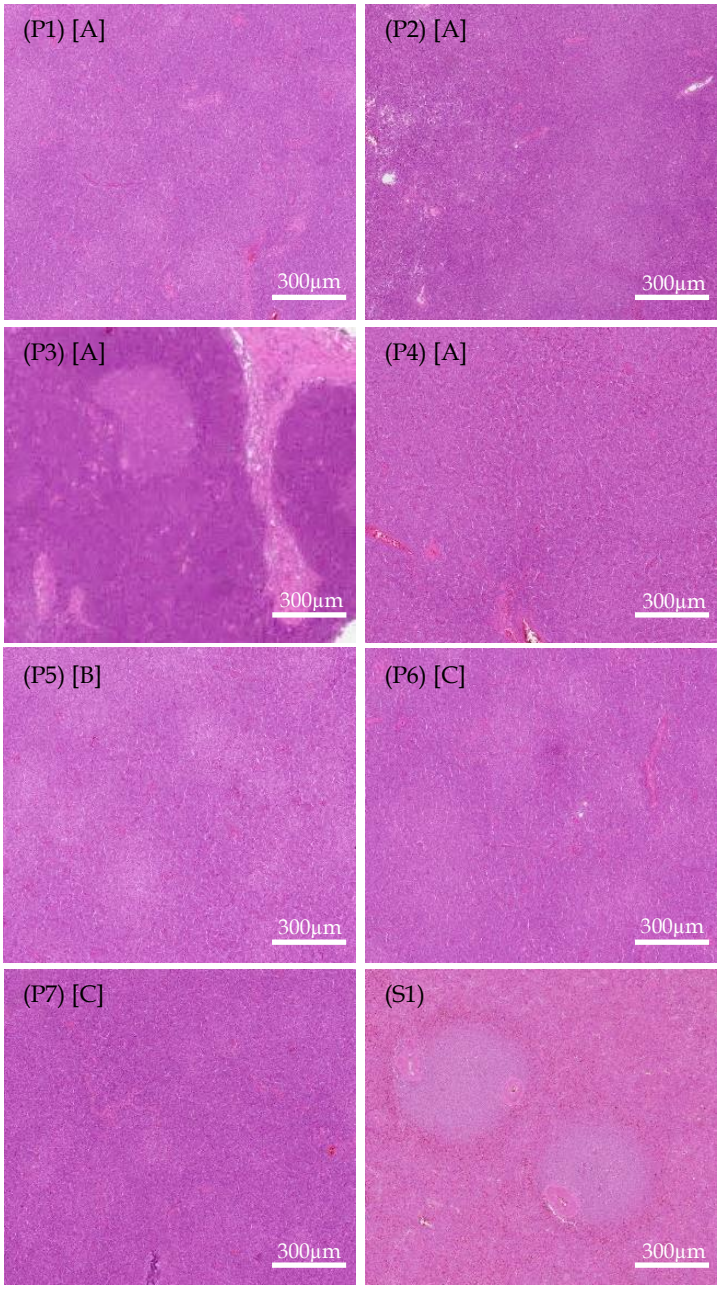

Figure 9. H&E staining of CLL LN demonstrate varying presence of traditional proliferation centres.

Sections from seven CLL LN and one healthy spleen tissue sample were stained with haematoxylin and eosin to investigate their morphology. Representative images are shown for each sample, labelled with patient code and [stage of disease].

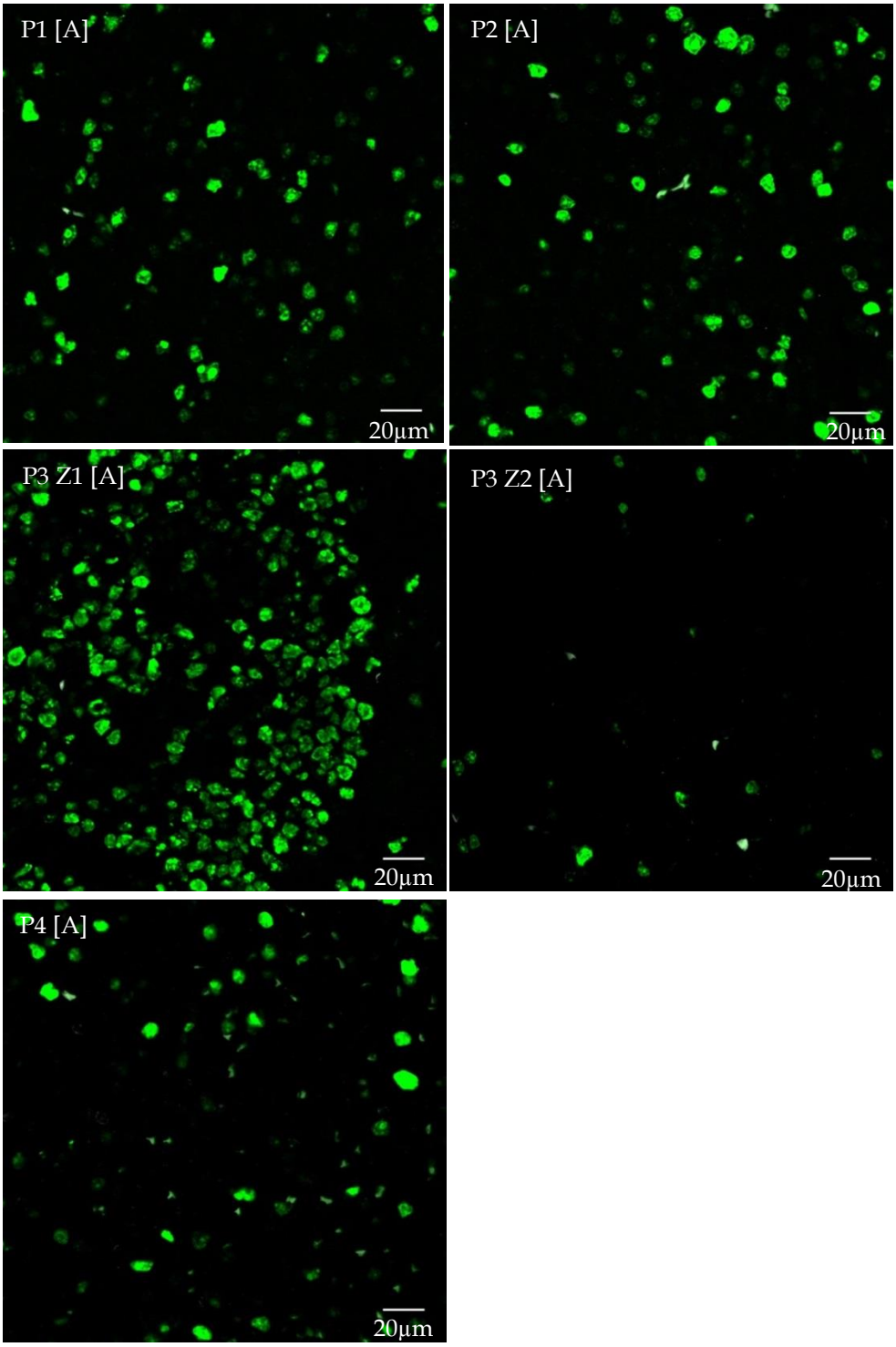

Figure 10A. CLL LN & healthy spleen show varying Ki-67 positivity.

CLL LN and healthy spleen tissue sections were stained for the expression of Ki-67 (green). Representative images (x40 objective) are shown for stage A patient samples (n=4) with two images shown from sample P3, referred to as Zone 1 (Z1) and Zone 2 (Z2). Samples labelled with patient code and [stage of disease]. Further images for later stage disease and healthy spleen tissue shown below.

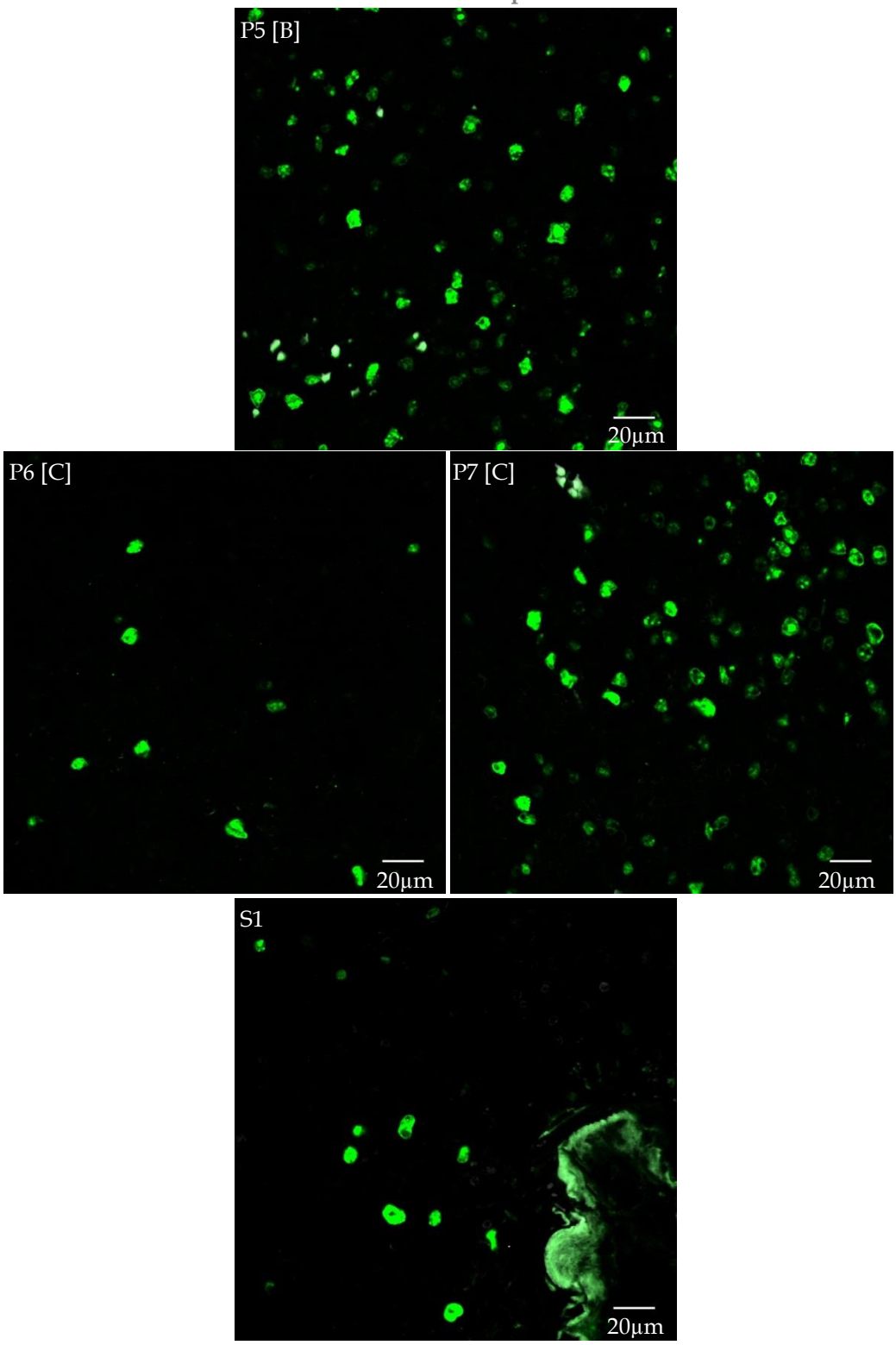

Figure 10B. CLL LN & healthy spleen show varying Ki-67 positivity.

CLL LN and healthy spleen tissue sections were stained for the expression of Ki-67 (green). Continued from figure 9A; Representative images (x40 objective) showing Ki-67 immunofluorescent staining of stage B (n=1) & C (n=2) patient samples and healthy spleen tissue (n=1). Samples labelled with patient code and [stage of disease].

Interestingly the Ki-67 distribution of these samples did not align with the presence of proliferation centres as seen by H&E staining, with the exception of sample P3. Instead of dense areas of proliferation, the majority of these samples had a diffuse Ki-67 staining pattern (as seen in figure 10A&B). This is perhaps unexpected as many groups discuss high prevalence of PC within the CLL LN and to a lesser extent the BM (Chapter 1.5.1) (Schmid & Isaacson 1994; Bonato et al. 1998; Ciccone et al. 2012; Plander et al. 2009). The data shown here may highlight that these proliferation centres may be a misnomer.

Based on these data, the Z1 areas seen within sample P3 may represent very early stage A disease, where the germinal centre (GC) architecture of the previously healthy LN has not yet been fully disrupted by the CLL tumour clone. In this scenario, rather than being a marker of CLL disease, the GC (potentially subsequently labelled a putative PC) actually represents the remnants of the healthy tissue and architecture.

Overall the Ki-67 expression of the seven CLL LN samples varied greatly and did not appear to correlate to disease stage (figure 11).

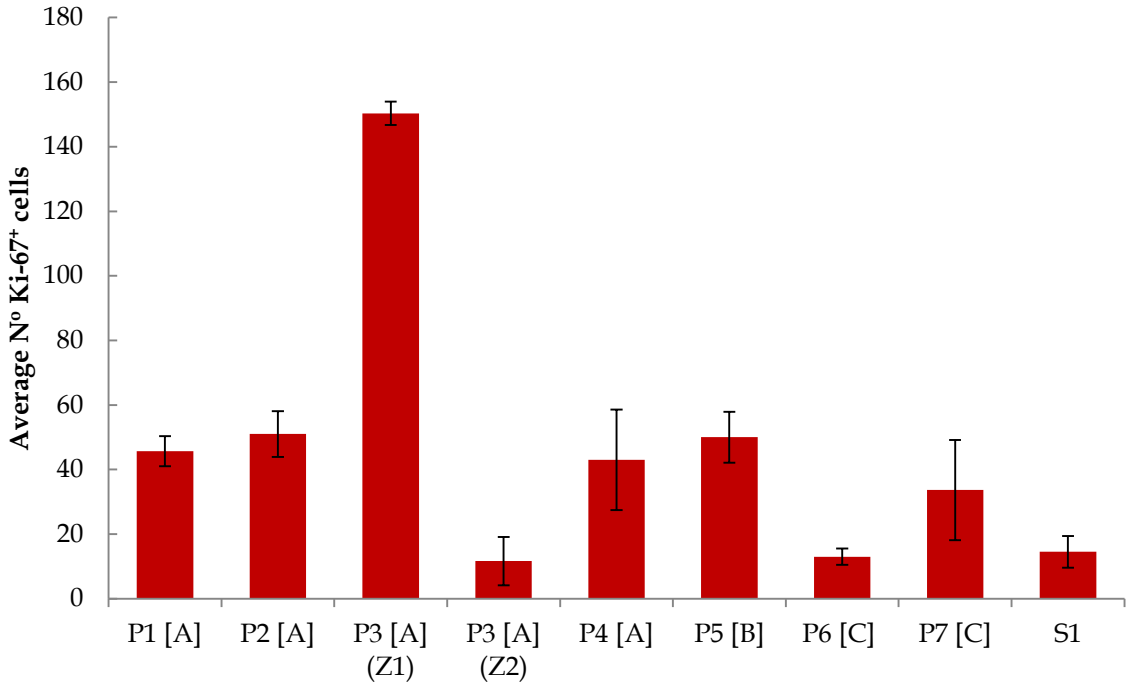

Figure 11. Ki-67 positivity in CLL LN and healthy spleen is diverse and not related to stage of disease.

Sections of seven CLL LN tissue samples and one healthy spleen sample were immunofluorescently stained for the expression of Ki-67. Three areas from each tissue were imaged (with the exception of sample P3, which had 3 areas images from each of Z1 and Z2) and these images were quantitatively analysed for Ki67 positivity using Fiji Image J analysis software. Numbers of positive cells were averaged across the three images collected for each sample and mean data is plotted with S.E.M. Samples are labelled with [stage of disease] along the x-axis.

3.3.2 PAX5 expression and PAX5$^+$Ki67$^+$ cells within the CLL LN decrease associated with stage of disease

In conjunction with the Ki-67 observations described above, sections were stained for the presence of CLL cells using the pan-B cell marker PAX5 (figure 11A & B). As described in Chapter 1.1.1 PAX5 is an important B cell transcription factor responsible for the correct development of B cells (Cobaleda et al. 2007) and has been used routinely as a marker of CLL cells and in the diagnosis of B cell lymphomas (Torlakovic et al. 2002). Two significant findings were noted from interrogation of these tissues with the combination of PAX5 and Ki-67.

Firstly, it was noted that the presence of PAX5$^+$ cells within the CLL LN decreases in correlation to stage of disease (figures 13 & 14). Initially this suggested that the numbers or density of tumour cells within the LN reduce as disease progresses. However this is questionable and the data more likely indicates that expression of PAX5 reduces as disease progresses. This may have important implications for the understanding of CLL biology.

Furthermore, there was also a marked decrease in PAX5$^+$Ki-67$^+$ cells in the CLL LN correlated to disease stage (figures 13 & 14). This was more than the general decrease seen in PAX5 expression as described above and so cannot be explained by this observation alone. As such, these data may indicate that there is a relative decrease in the number of Ki-67$^+$ CLL cells in the CLL LN or, more feasibly, that the expression of PAX5 in proliferating tumour cells significantly decreases as in later stage disease. Although the numbers of tissues are small, these observations indicate the changing biology of CLL cells *in situ* during disease progression.

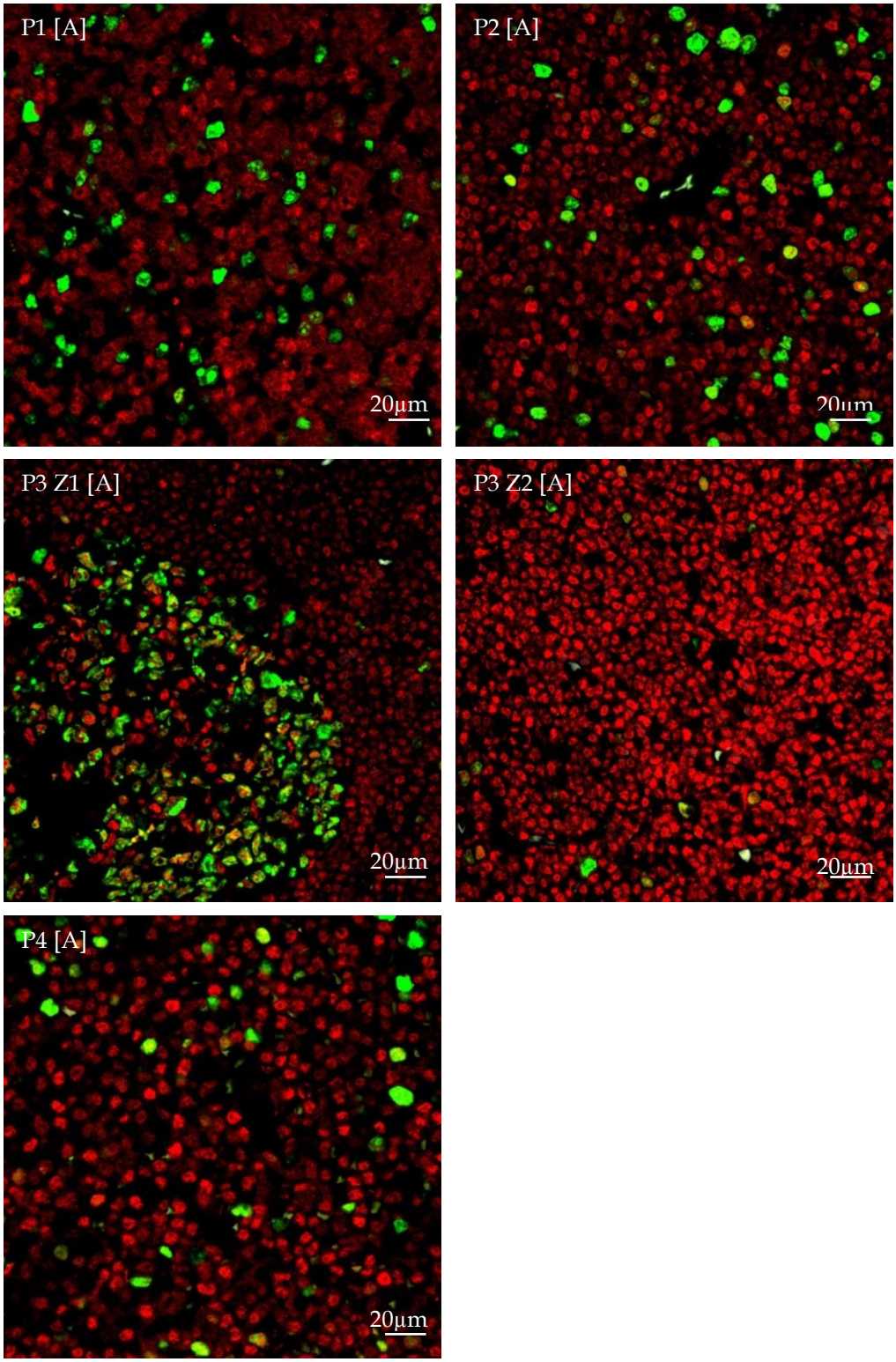

Figure 12A. CLL cells in the LN and B cells in healthy spleen are PAX5⁺ and dual staining of PAX5⁺Ki-67⁺ cells can be determined.

CLL LN and healthy spleen tissue sections were stained for the expression of PAX5 (red) and Ki-67 (green). Representative images (x40 objective) are shown for stage A patient samples (n=4). Samples labelled with patient code and [stage of disease]. Further images for later stage disease and healthy spleen tissue shown below.

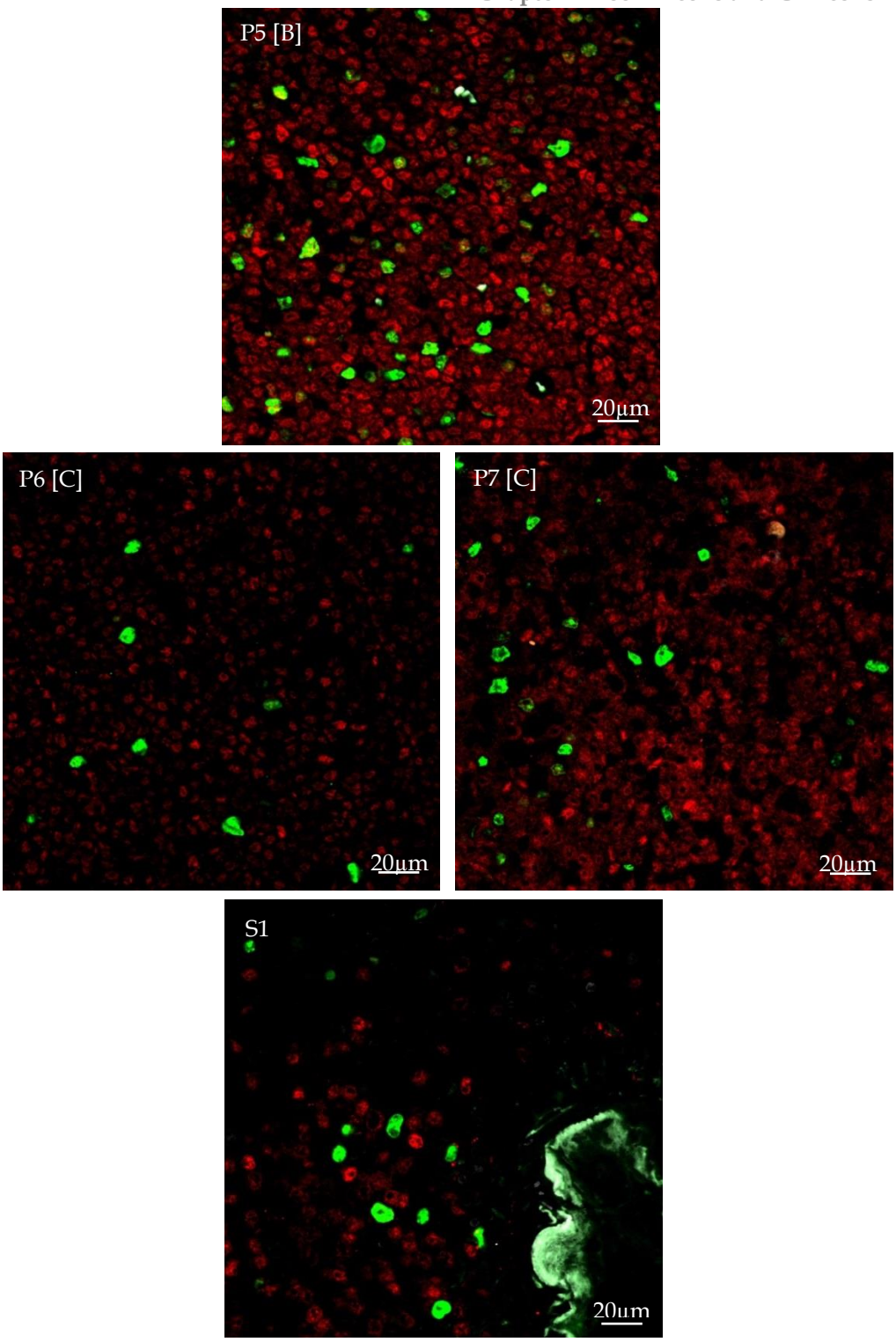

Figure 12B. CLL cells in the LN and B cells in healthy spleen are Pax5⁺ and dual staining of Pax5⁺Ki-67⁺ cells can be determined.

CLL LN and healthy spleen tissue sections were stained for the expression of PAX5 (red) and Ki-67 (green). Continued from figure 12A; Representative images (x40 objective) are shown for stage B (n=1) & C (n=2) patient samples and healthy spleen tissue (n=1). Samples labelled with patient code and [stage of disease].

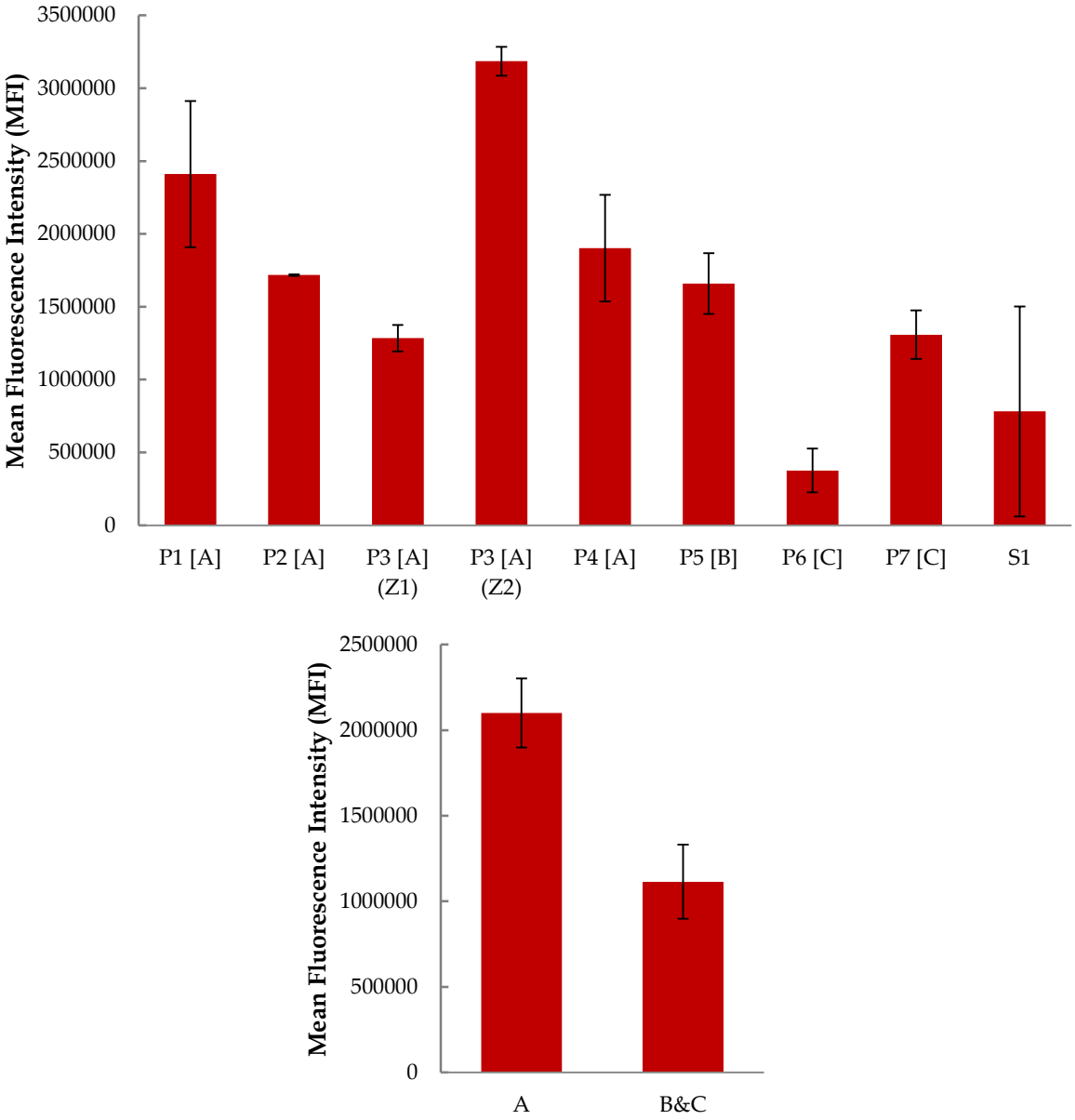

Figure 13. PAX5⁺expression is variable but decreases as disease progresses.

Sections of seven CLL LN tissue samples and one healthy spleen sample were immunofluorescently stained for expression of PAX5. Three areas from each tissue or zone were imaged and quantitatively analysed for PAX5 positivity using Fiji Image J analysis software. **Upper graph;** Mean Fluorescence Intensity values were averaged across the three images and mean data are plotted ±S.E.M. Samples labelled with [stage of disease] along the x-axis. **Lower graph;** Mean Fluorescence Intensity values for early (stage A (n=4)) and late (stage B & C (n=3)) samples were collated and mean data plotted ±S.E.M.

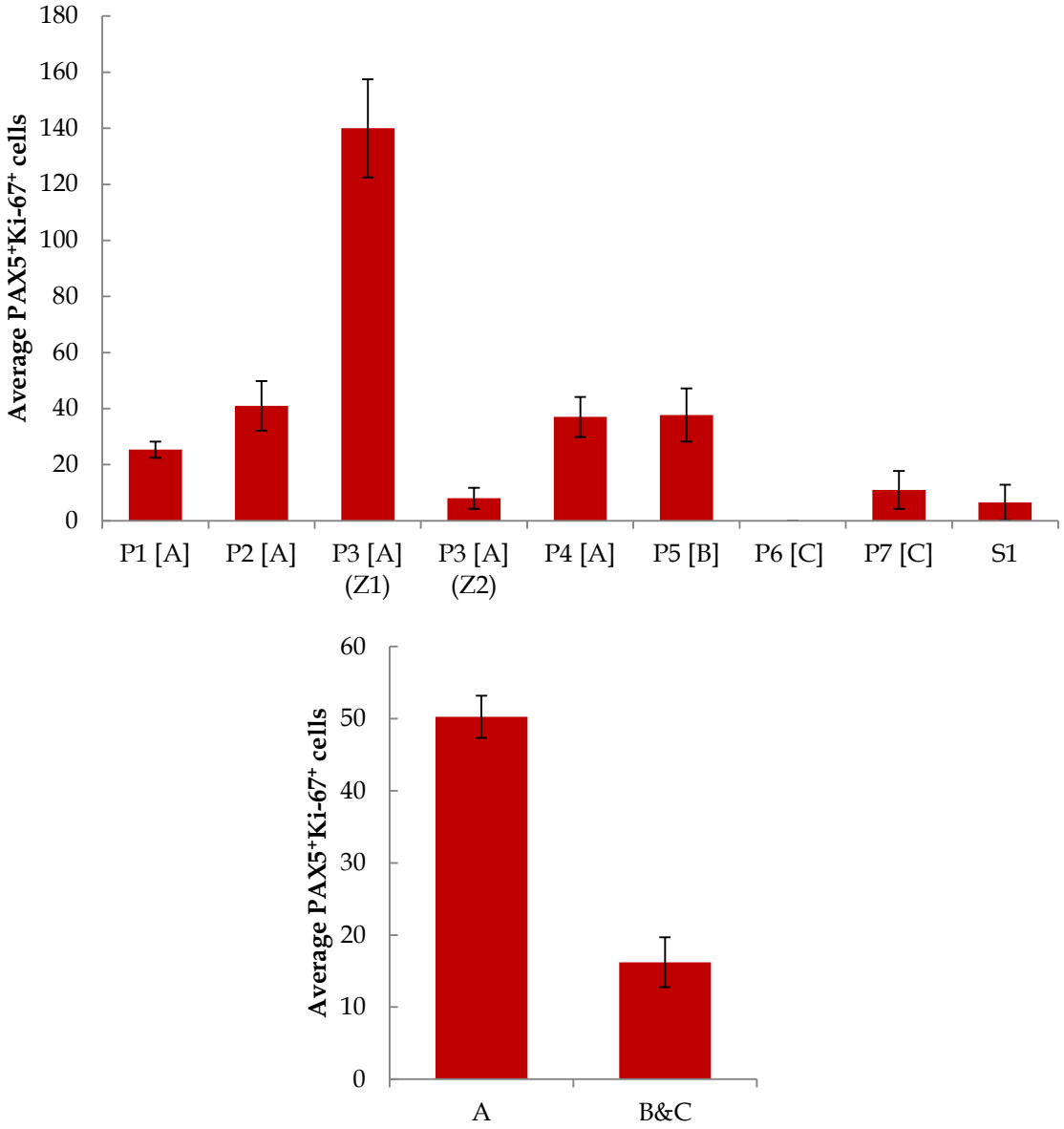

Figure 14. PAX5⁺ Ki67⁺ expression is variable but decreases as disease progresses.

Sections of seven CLL LN tissue samples and one healthy spleen sample were immunofluorescently stained for expression of PAX5 (pan-B cell) and Ki-67(active cell cycle). Three areas from each tissue or zone were imaged and quantitatively analysed for dual positivity for PAX5 and Ki-67 using Fiji Image J analysis software. **Upper graph;** numbers of dual positive cells were averages across the three images and mean data are plotted ±S.E.M. Samples labelled with [stage of disease] along the x-axis. **Lower graph;** numbers of dual positive cells for early (stage A (n=4)) and late (stage B & C (n=3)) samples were collated and mean data plotted ±S.E.M.

3.3.3 T cells are dispersed within the CLL LN at all stages of disease and proliferating CLL cells frequently appear to be localised close to T cells

Following the observations of PAX5 and Ki-67 positivity in the LN, CLL tissue sections were stained with these markers in combination with the pan-T cell marker CD3 to observe the proportions and distribution of T cells in the niche in relation to proliferative CLL cells (figure 15A & B).

As may be expected these data indicate that T cells are present in the CLL LN at all stages of disease, although when quantitated it was noted that there was a high level of variability in CD3 expression across the samples (figure 16). This variability is particularly striking in early stage disease samples. When considering the distribution of CD3 cells within these tissues, the variability seen from quantification likely reflects the presence of T cell rich and T cell poor areas within the tissues. This, particularly in early stage disease, may reflect the remnants of the healthy LN architecture, where distinct T cell and B cell zones are found within the tissues (figure 17). In particular, consideration of the variability seen within the sample P3 in combination with previous Ki-67 distribution data further supports the concept that this sample is a very early stage CLL, which has distinct T and B cells zones remaining in the LN tissue.

Despite the variability, it was observed from these multicolour images that Ki-67$^+$ positive CLL cells were frequently adjacent to T cells (figure 18) supporting the *in vitro* literature indicating that T cells can provide pro-survival and pro-proliferative signals to CLL cells.

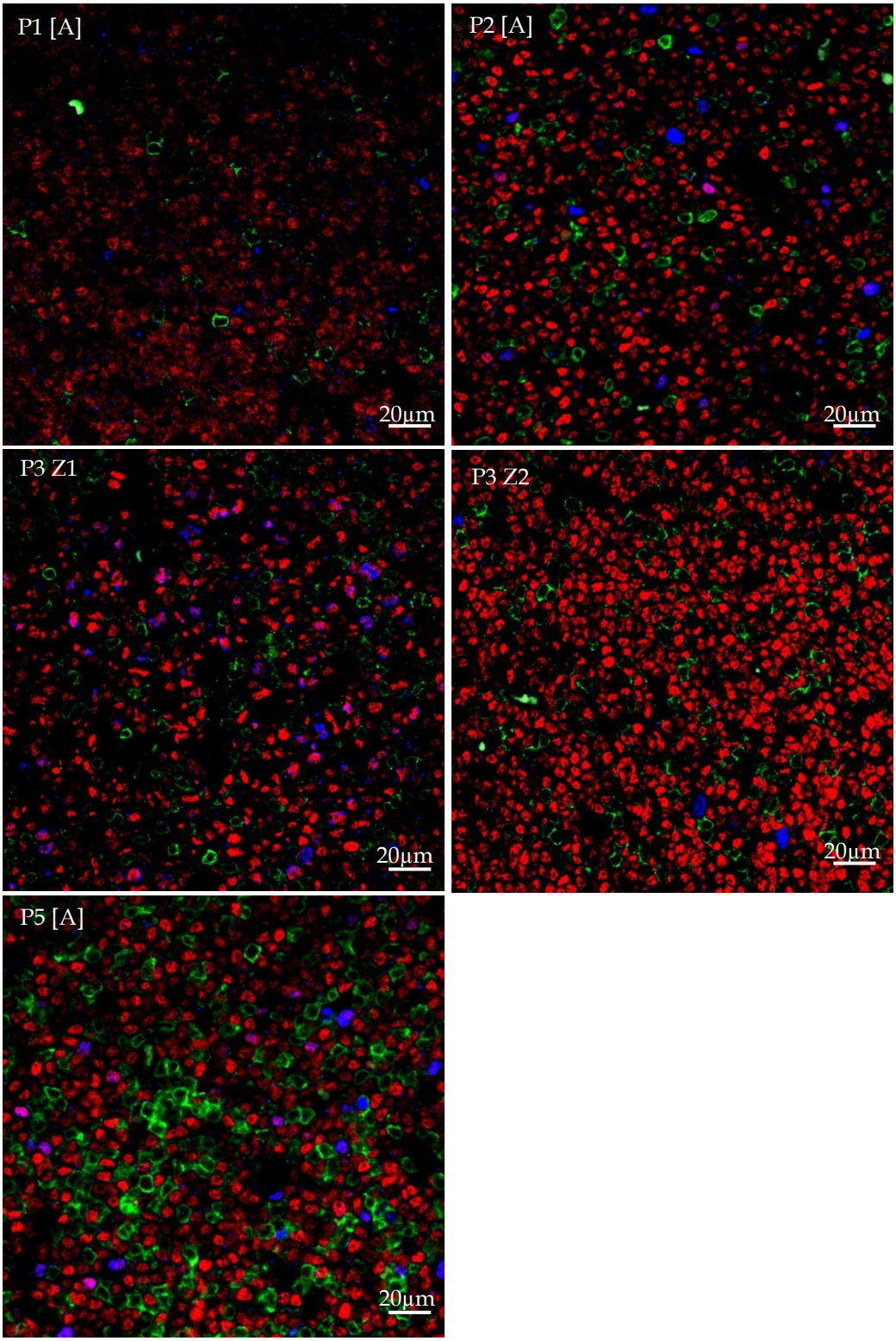

Figure 15A. T cell presence in CLL LN and healthy spleen tissue shows close proximity to proliferative CLL cells.

CLL LN and healthy spleen tissue sections were stained for the expression of CD3 (green), PAX5 (red) and Ki-67 (blue). Representative images (x40 objective) are shown for stage A patient samples (n=4). Samples labelled with patient code and [stage of disease]. Further images for later stage disease and healthy spleen tissue shown below.

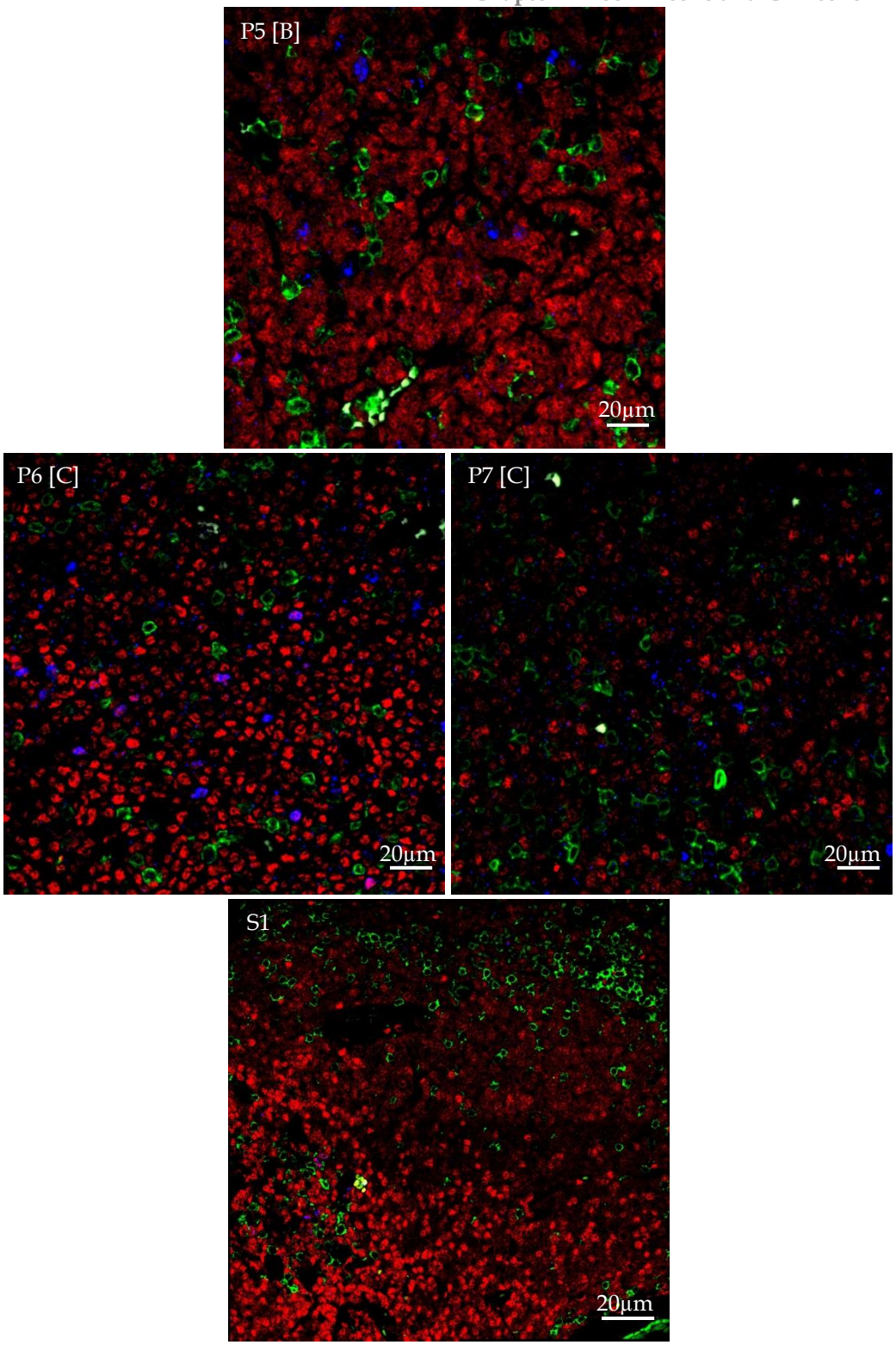

Figure 15B. T cell presence in CLL LN and healthy spleen tissue shows close proximity to proliferative CLL cells.

CLL LN and healthy spleen tissue sections were stained for the expression of CD3 (green) PAX5 (red) and Ki-67 (blue). Continued from figure 15A; Representative images (x40 objective) are shown for immunofluorescent staining of stage B (n=1) & C (n=2) patient samples and healthy spleen tissue (n=1). Samples labelled with patient code and [stage of disease].

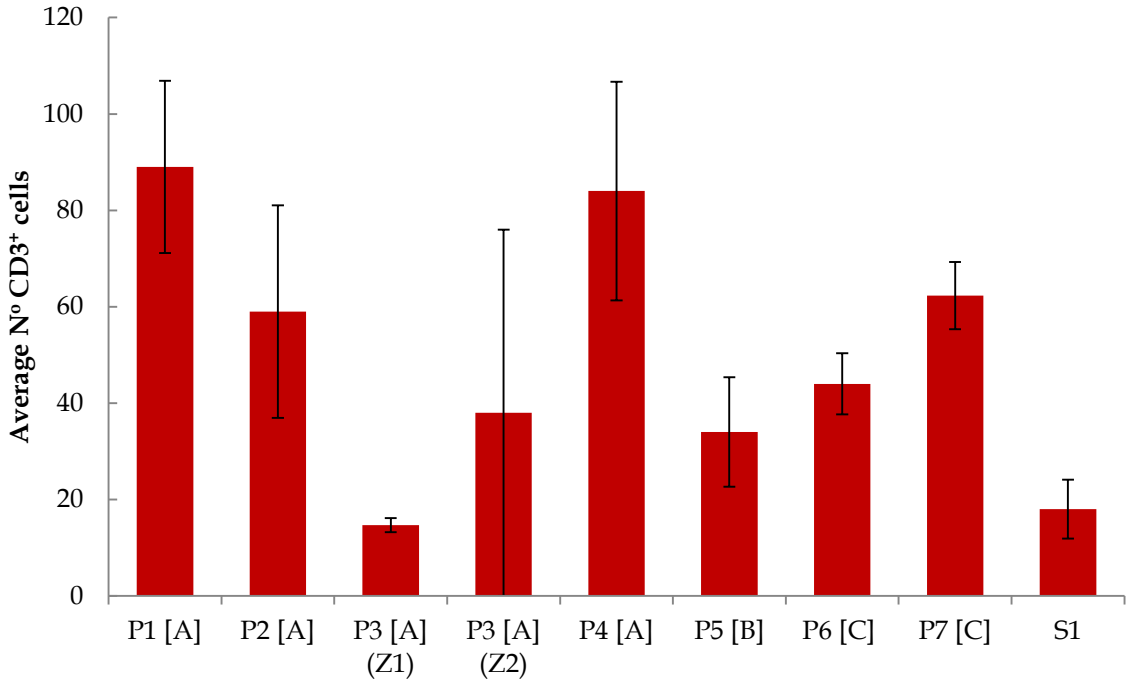

Figure 16. Average numbers of CD3⁺ T cells vary across all stages of CLL disease and variability of expression is also seen within samples.

Sections of seven CLL LN tissue samples and one healthy spleen sample were immunofluorescently stained for the expression of CD3. Three areas from each tissue were imaged (with the exception of sample P3, which had 3 areas images from each of Z1 and Z2) and these images were quantitatively analysed for CD3 positivity using Fiji Image J analysis software. Numbers of positive cells were averaged across the three images collected for each sample and mean data is plotted with S.E.M. Samples are labelled with [stage of disease] along the x-axis.

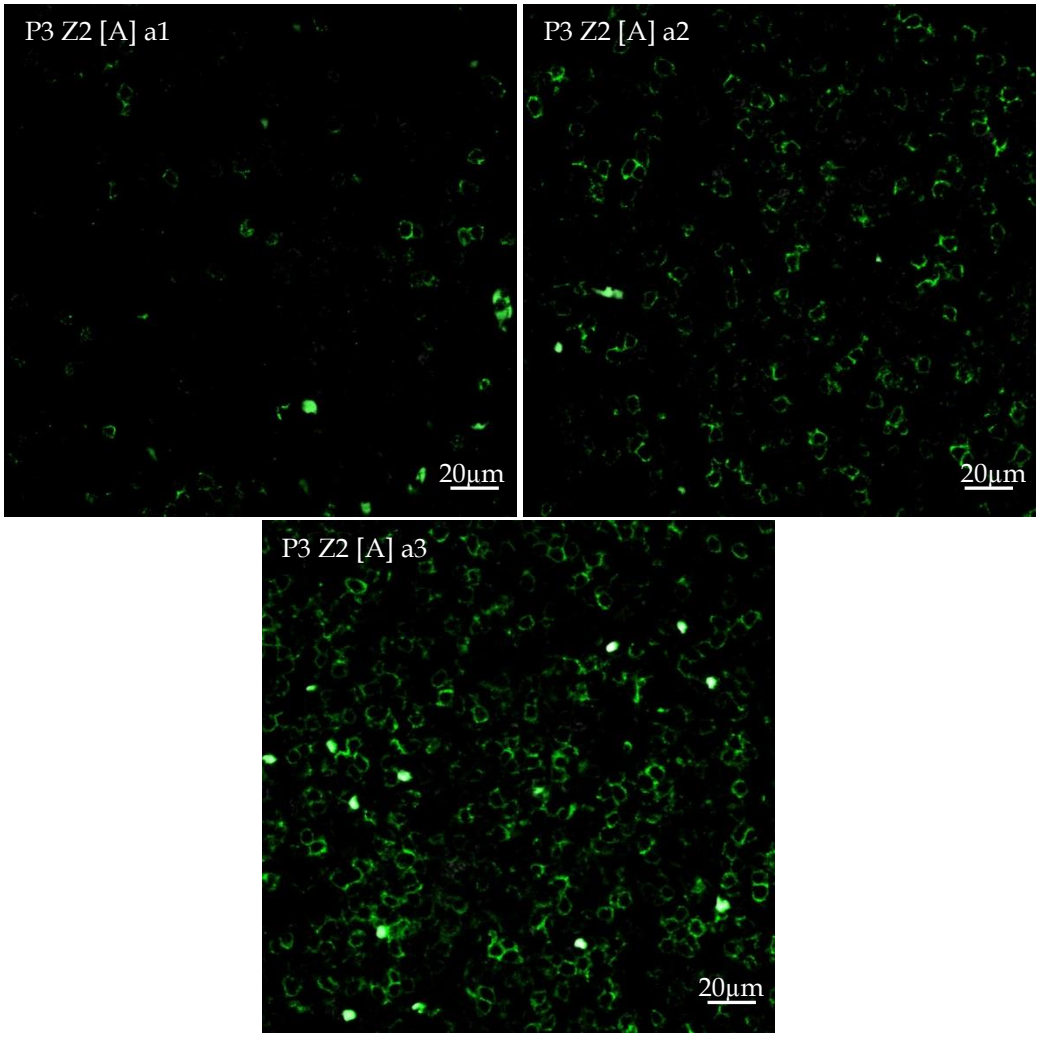

Figure 17. CD3 positive cells vary greatly in numbers within a single CLL LN sample.

CLL LN and healthy spleen tissue sections were stained for the expression of CD3 (green) and showed variability in expression between the three images from each sample. The three immunofluorescent staining images (x40 objective) are shown for sample P3 Z2 and demonstrate the variability in the presence of T cells within the same tissue. Samples labelled with patient code, [stage of disease] and area number.

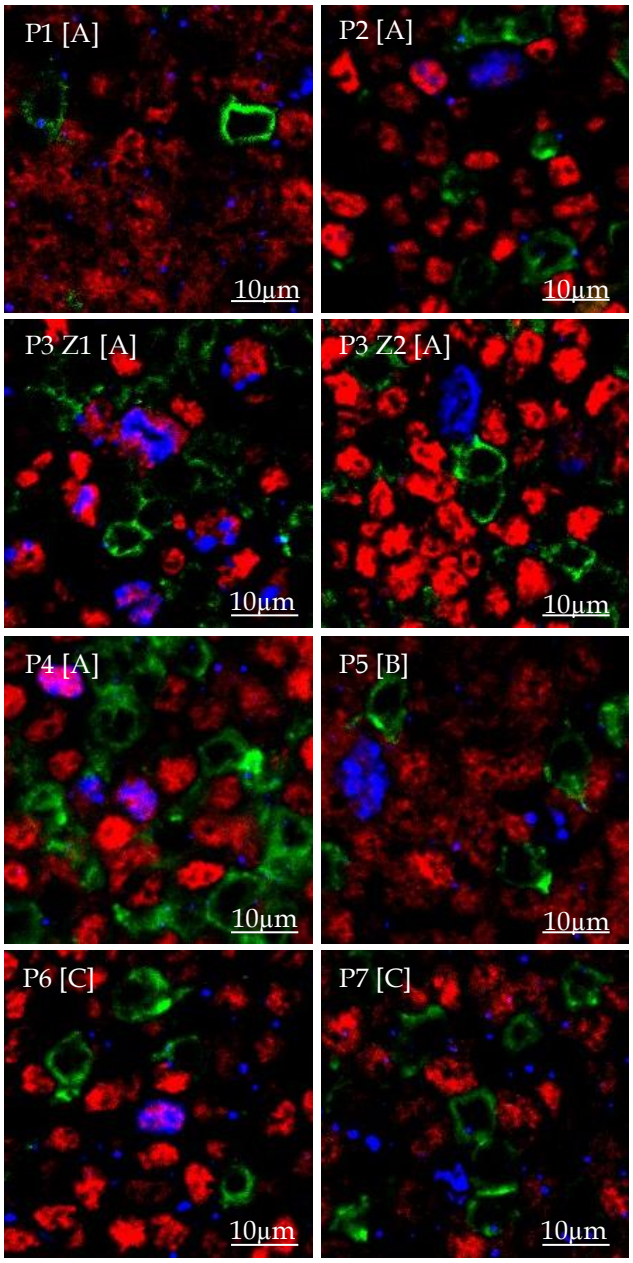

Figure 18. Localisation of Ki-67⁺ CLL cells in the CLL LN in relation to T cells.

Seven CLL LN tissue sections were stained for the expression of CD3 (green), PAX5 (red) and Ki-67 (blue). Representative images (x40 objective) are shown for stage A (n=4), stage B (n=1) and stage C (n=2) patient samples. Samples labelled with patient code and [stage of disease]. These images demonstrate the close proximity of $CD3^+$ cells (green) to $Ki67^+PAX5^+$ cells (pink/purple).

3.4 T cell subsets in the CLL LN

Following the observations in chapter 3.3 and considering the current literature regarding the impact of CLL on the T cell compartment (Chapter 1.4.1) the tissues were stained to determine the subtypes of T cells seen within the CLL LN.

CLL and healthy spleen sections were stained for the presence of T cell subtypes using a combination of CD3, CD4 and CD8 antibodies (figure 19A & B). The dual positivity of the pan-T cell marker CD3 with the subtype marker CD4 denoted the presence of T helper cells (T_h), whilst dual positivity of CD3 with CD8 denoted the presence of cytotoxic T cells (T_{cyt}). As noted previously when considering the total T cell presence in the CLL LN, there was variability seen in the expression of T cell subtype markers CD4 and CD8, particularly during early stage disease (figure 20).

Whilst expression in these tissues does not appear to link to stage of disease, the spatial patterns of the global $CD3^+$ and $CD3^+CD8^+$ T cells in the CLL LN intimate that stage A CLL LNs retain some of the architecture of the healthy node (figure 21) although this would need to be confirmed on further tissue samples.

Overall these data indicated that both T_{cyt} and T_h cells are present in the CLL LN at all stages of disease and the relative prevalence of these subtypes varies from patient to patient irrespective of disease stage. In addition, the architecture of the LN is progressively altered as disease advances which is reflected by the spatial distribution of T cell subtypes within the tissue and may suggest a significant change in the roles played by these cell types within the disease.

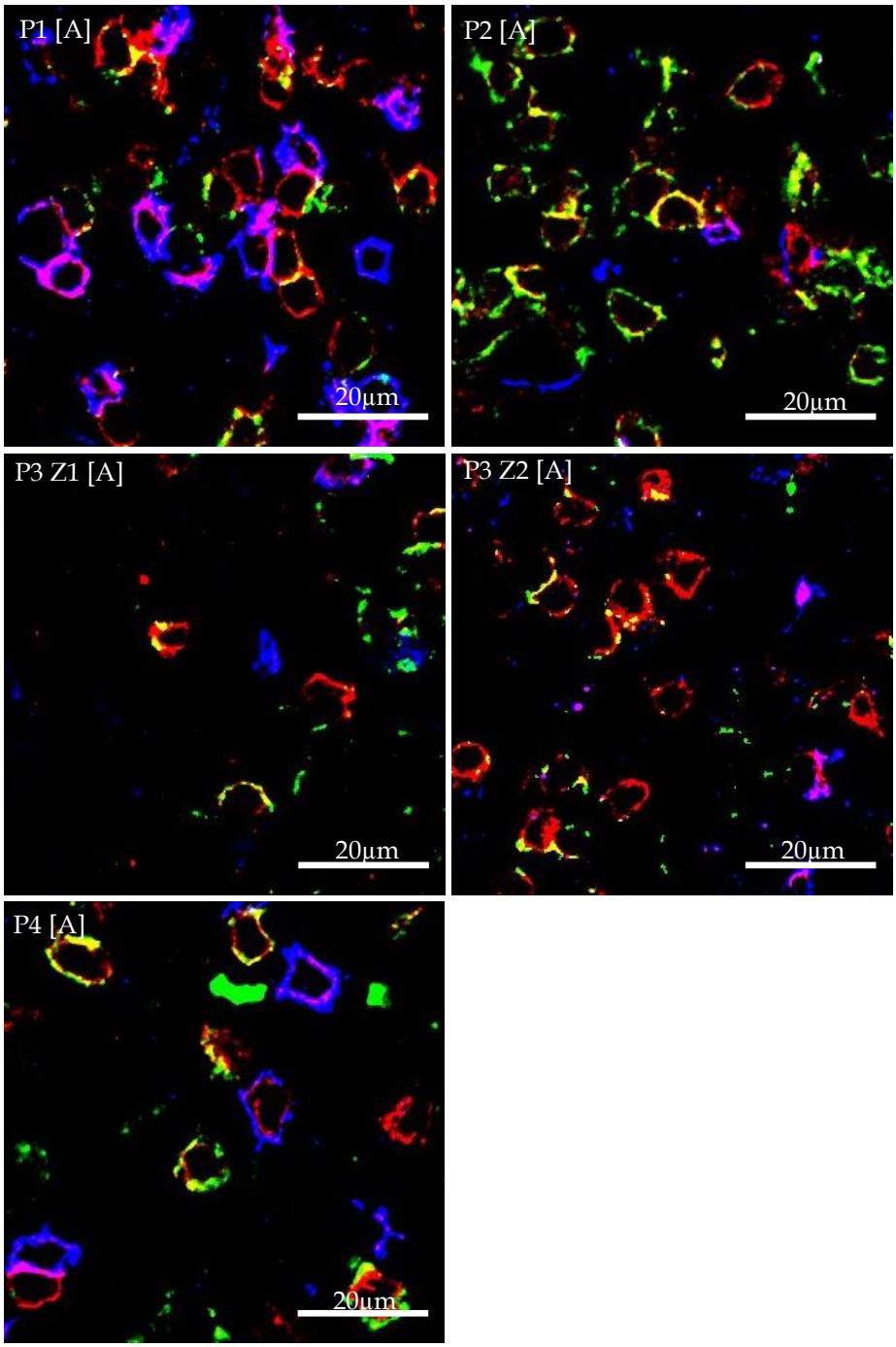

Figure 19A. The balance of CD4⁺ and CD8⁺ T cell subsets within CLL LN and healthy spleen tissue is variable and does not correlate to stage of disease.

CLL LN and healthy spleen tissue sections were stained for the expression of CD3 (red), CD4 (green) and CD8 (blue). Representative images (x40 objective) are shown for stage A patient samples (n=4). Samples labelled with patient code and [stage of disease]. CD3 (red) co-localises with either CD4 (yellow) denoting T_h cells or CD8 (pink) denoting T_{cyt} cells. Further images for later stage disease and healthy spleen tissue shown below.

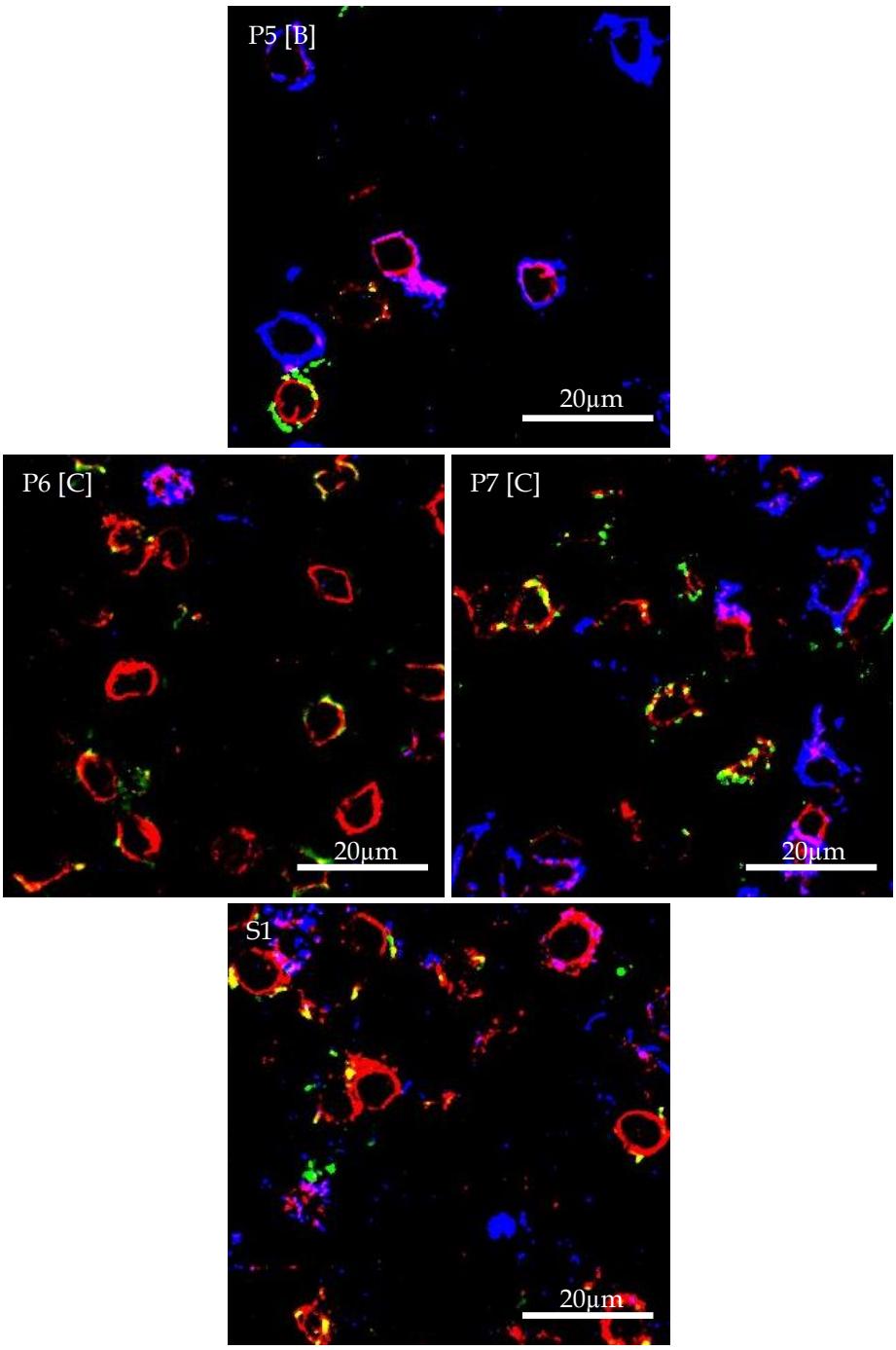

Figure 19B. The balance of CD4⁺ and CD8⁺ T cell subsets within CLL LN and healthy spleen tissue is variable and does not correlate to stage of disease.

CLL LN and healthy spleen tissue sections were stained for the expression of CD3 (red), CD4 (green) and CD8 (blue). Continued from figure 18A; Representative images (x40 objective) are shown for immunofluorescent staining of stage B (n=1) & C (n=2) patient samples and healthy spleen tissue (n=1). Samples labelled with patient code and [stage of disease]. CD3 (red) co-localises with either CD4 (yellow) denoting T_h cells or CD8 (pink) denoting T_{cyt} cells.

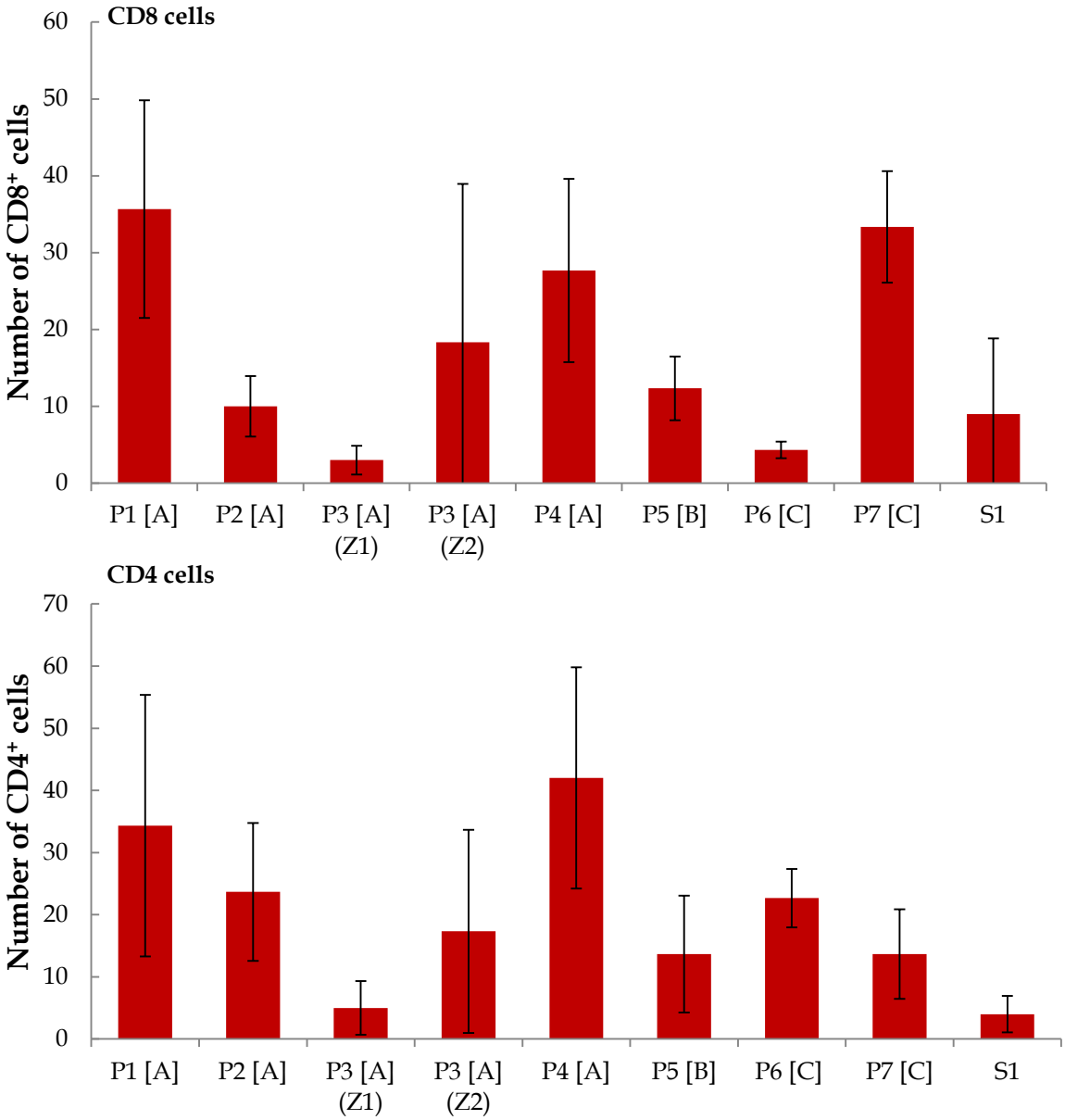

Figure 20. Presence of T cell subtypes is variable across CLL LN samples unrelated to stage of disease, with high variability of expression within samples also seen in early stage disease.

Sections of seven CLL LN tissue samples and one healthy spleen sample were immunofluorescently stained for the expression of CD3, CD4 and CD8. Three areas from each tissue were imaged (with the exception of sample P3, which had 3 areas images from each of Z1 and Z2) and these images were quantitatively analysed for $CD3^+CD4^+$ or $CD3^+CD8^+$ dual positivity using Fiji Image J analysis software. Numbers of positive cells were averaged across the three images collected for each sample and mean data is plotted with S.E.M. Samples are labelled with [stage of disease] along the x-axis.

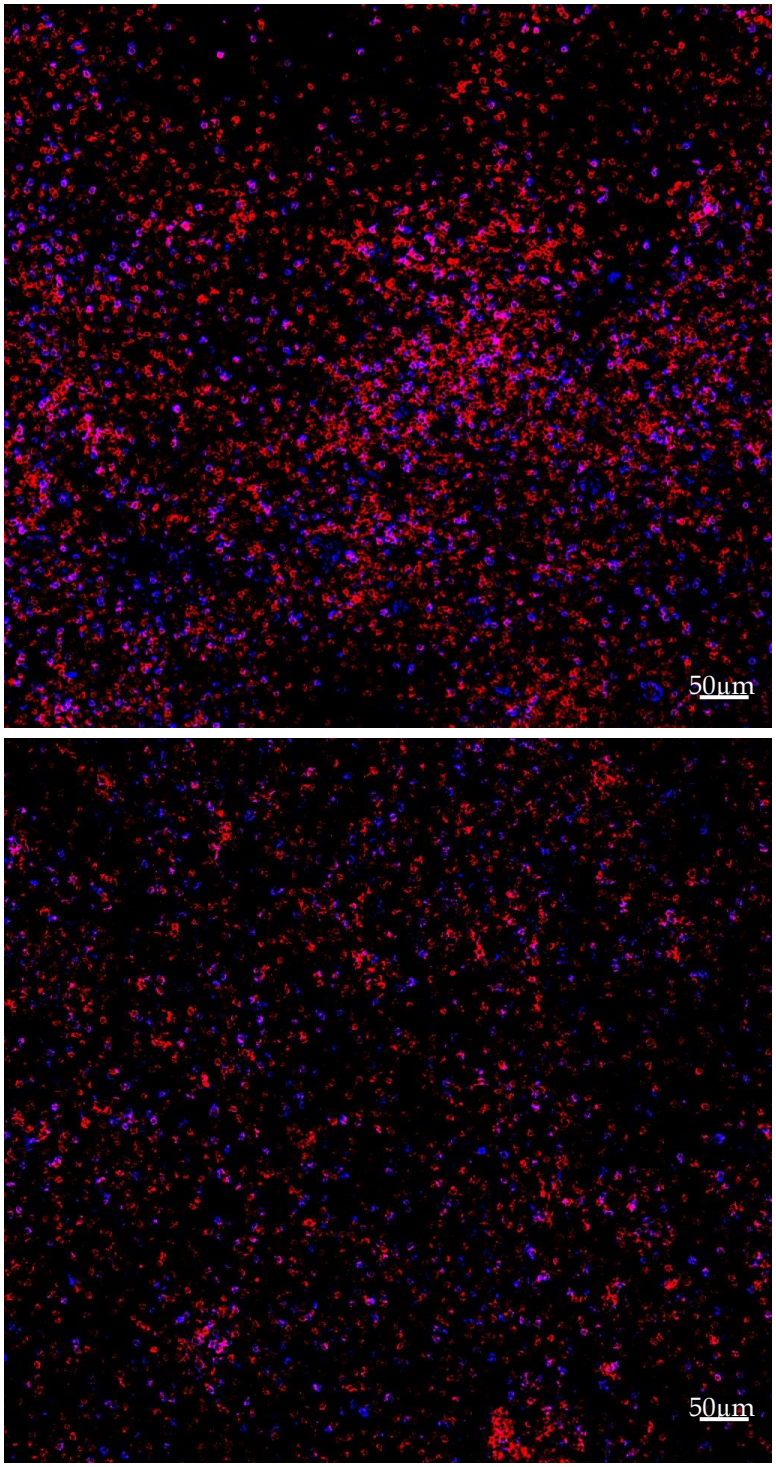

Figure 21. Spatial distribution of T_{cyt} in the CLL LN may relate to stage of disease and account for variability during quantification.

CLL LN tissue sections were stained for the expression of CD3 (red) and CD8 (blue). Representative images (x10 objective) are shown for a single stage A patient (n=1) and a single stage C patient (n=1). Samples labelled with patient code and [stage of disease]. Images display the difference in spatial distribution of T_{cyt} cells (pink/purple) in early v.s. late CLL LN tissues. Late stage disease appears to lose organised structure of T cell zones.

3.5 The balance of proliferation and apoptosis in the CLL LN

It is commonly reported that the balance of proliferation and apoptosis is skewed to favour disease progression in many cancers (Hanahan & Weinberg 2000; Evan & Vousden 2001). By studying a combination of the cell cycle activation marker Ki-67 and cleaved caspase 3, a marker for early apoptosis, this study sought to determine whether there was a difference in the balance of proliferation and apoptosis in this cohort of patient samples.

CLL LN samples and healthy spleen control tissue were stained for their expression of Ki-67 and cleaved caspase 3 in combination with PAX5 (figure 22A & B). Strikingly, the levels of expression of cleaved caspase 3 across all CLL LN tissues was markedly lower than that seen within healthy spleen, and within the proliferative zone of sample P3 (figure 23). It should be noted from the literature that healthy lymph node tissues are reported to have relatively high expression levels of cleaved caspase 3 when compared to healthy spleen tissue; between 25-75% of germinal centre cells and up to 25% of non-germinal centre cells in lymph node tissues express caspase 3 compared to up to 25% of cells in the red pulp and rare in the white pulp within spleen tissue (Ponten et al. 2008). When the data herein is considered in context of this literature, it is even more striking to note that the CLL lymph node tissue (with the exception of P3) have such a reduced expression of cleaved caspase 3 compared to the healthy spleen control.

Whilst expression of cleaved caspase 3 alone was informative, this staining was further interrogated by comparing relative levels of cleaved caspase 3 and Ki-67 expression within each tissue (figure 24, top graph). When comparing this ratio of proliferation to apoptosis in healthy spleen tissue and CLL LN tissue, it was apparent that the balance in CLL LN tissue at all stages greatly deviates from this study's example of normal homeostasis (healthy spleen). When the lymph node tissue values were normalised to healthy spleen (figure 24,

bottom graph where spleen ratio value= 1.0) it became clear that within different stages of CLL disease, this proliferation and apoptosis ratio is very variable. The ratio within sample P3 (Z1 & Z2) were the lowest seen across the different CLL tissues and closest to the healthy spleen control (i.e. indicating that levels of proliferation are only slightly higher than levels of apoptosis). Once again this supports the concept that sample P3 may represent very early stage A disease. Despite this similarity, there is still a greater than 10 fold difference in the ratio between P3 Z2 and the healthy spleen sample (13.5 v.s. 1.0). Overall, these results suggest that the global balance of apoptosis within the CLL LN is significantly disrupted compared to healthy tissue and that this disruption occurs even from a relatively early stage of disease.

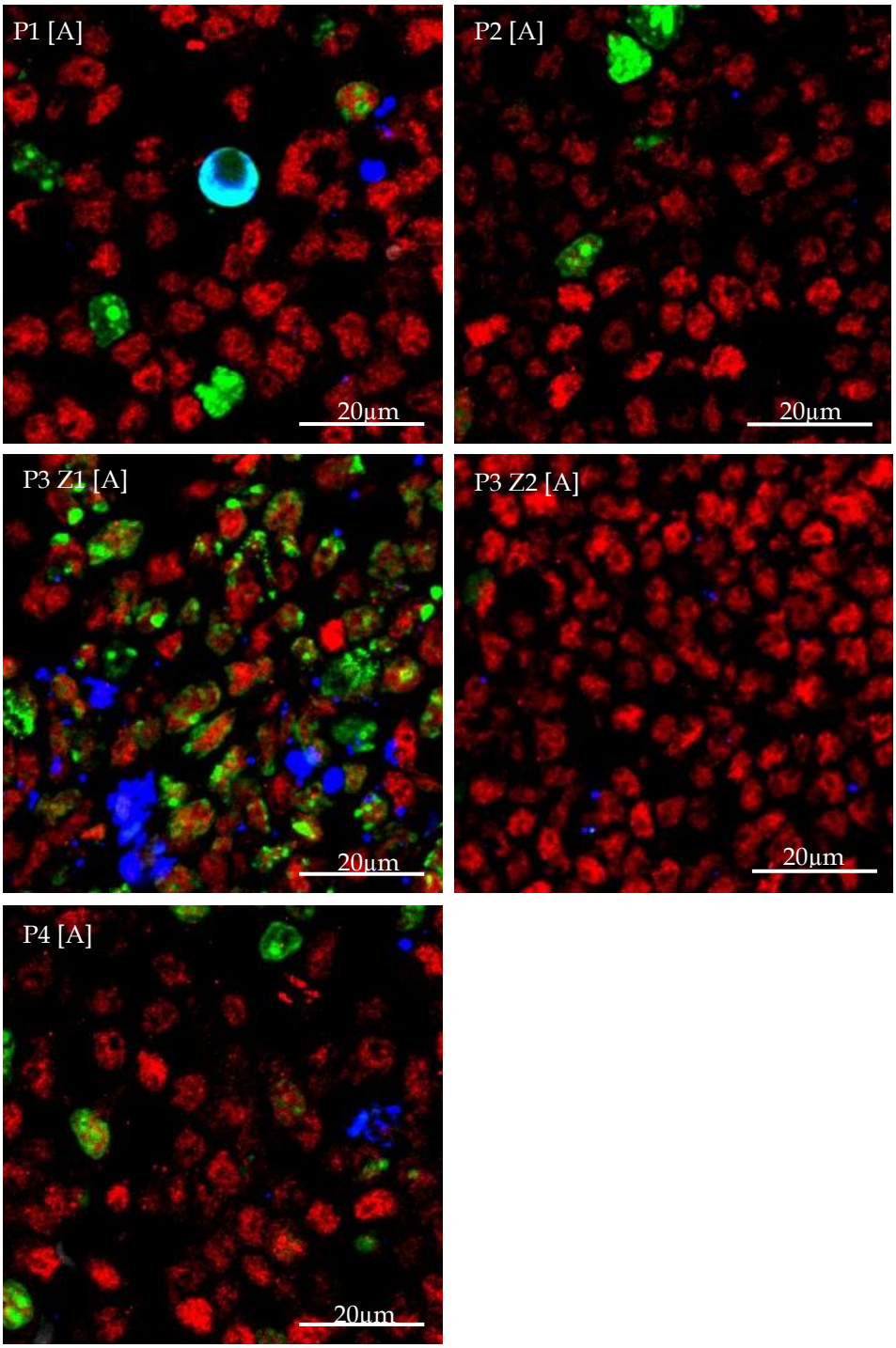

Figure 22A. CLL samples have variable levels of cleaved caspase 3 and Ki-67 seemingly unrelated to disease stage.

CLL LN and healthy spleen tissue sections were stained for the expression of Ki-67 (green) PAX5 (red) and cleaved caspase 3 (blue). Representative images (x40 objective) are shown for stage A patient samples (n=4). Samples labelled with patient code and [stage of disease]. Further images for later stage disease and healthy spleen tissue shown below.

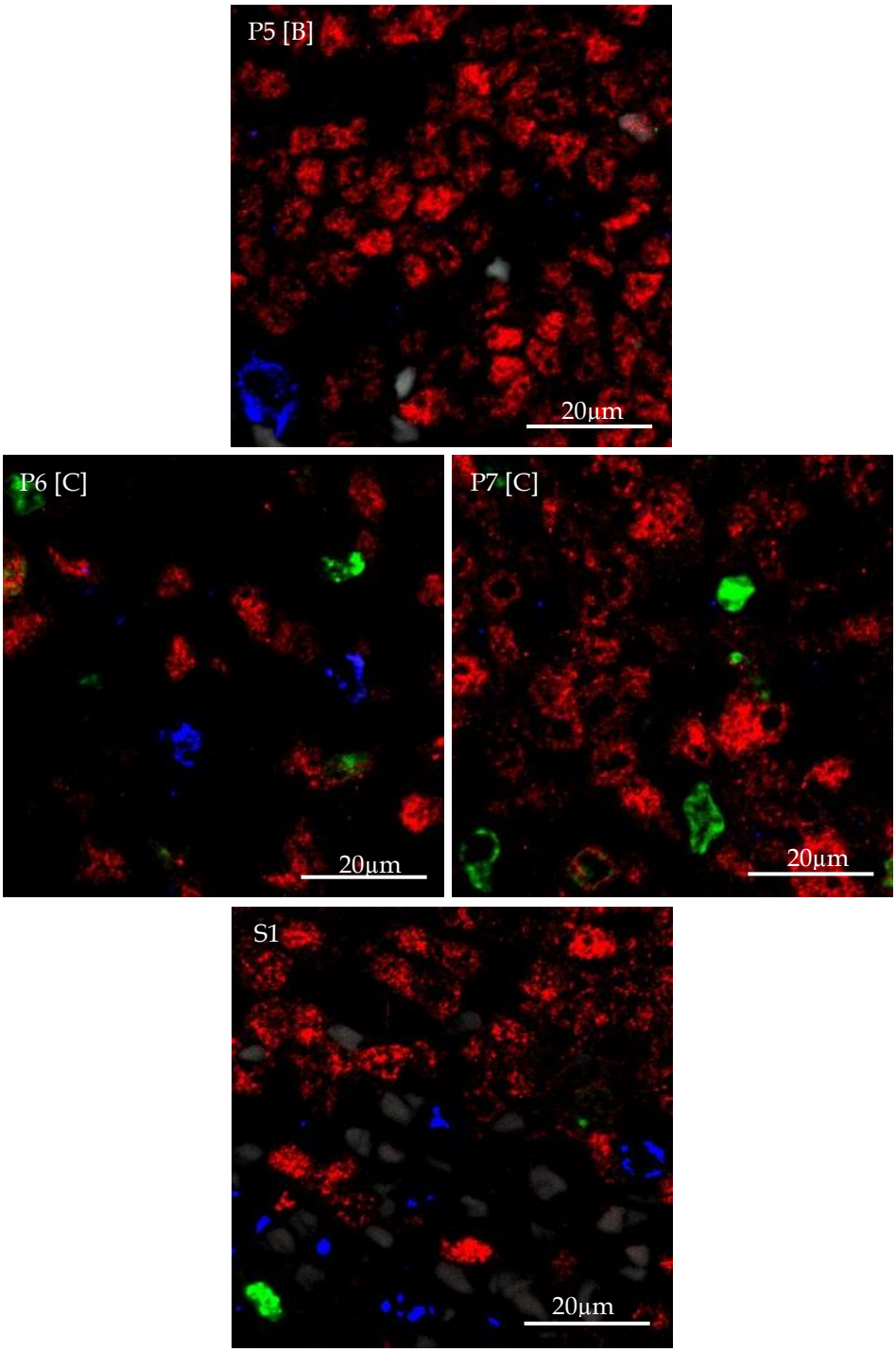

Figure 22B; CLL samples have variable levels of cleaved caspase 3 and Ki-67 seemingly unrelated to disease stage.

CLL LN and healthy spleen tissue sections were stained for the expression of Ki-67 (green) PAX5 (red) and cleaved caspase 3 (blue). Continued from figure 22A; Representative images (x40 objective) are shown for immunofluorescent staining of stage B (n=1) & C (n=2) patient samples and healthy spleen tissue (n=1). Samples labelled with patient code and [stage of disease].

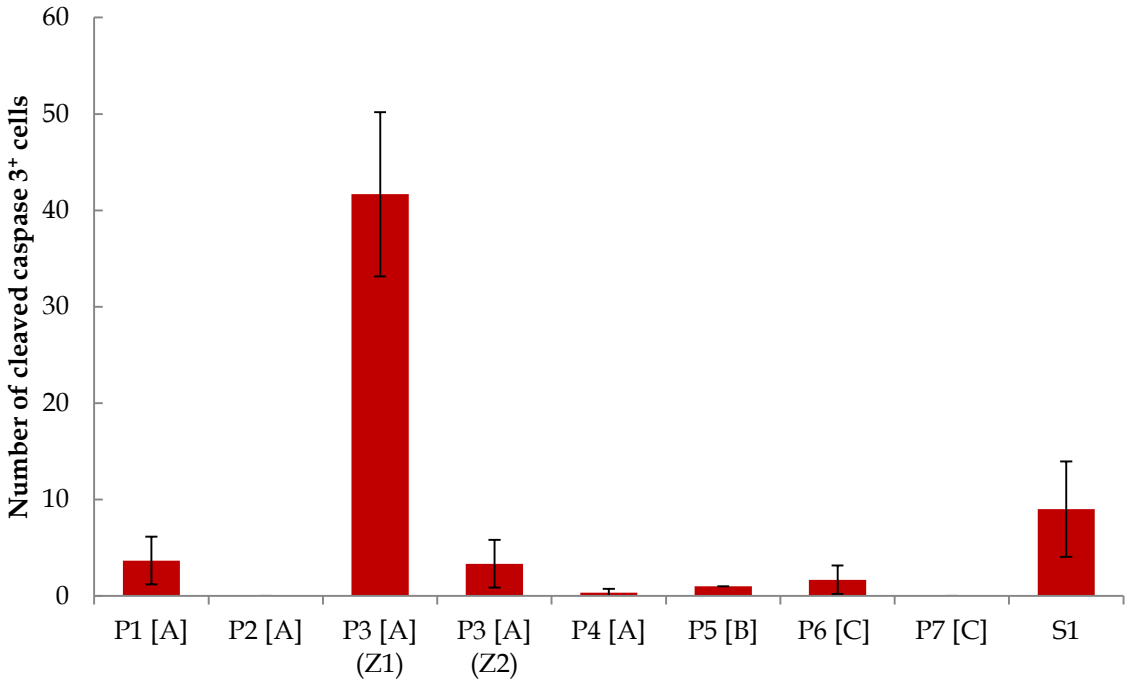

Figure 23. Typically low level average expression of cleaved caspase 3 in CLL LN tissues compared to healthy spleen.

Sections of seven CLL LN tissue samples and one healthy spleen sample were immunofluorescently stained for the expression of cleaved caspase 3. Three areas from each tissue were imaged (with the exception of sample P3, which had 3 areas images from each of Z1 and Z2) and these images were quantitatively analysed for cleaved caspase 3 positivity using Fiji Image J analysis software. Numbers of positive cells were averaged across the three images collected for each sample and mean data is plotted with S.E.M. Samples are labelled with [stage of disease] along the x-axis.

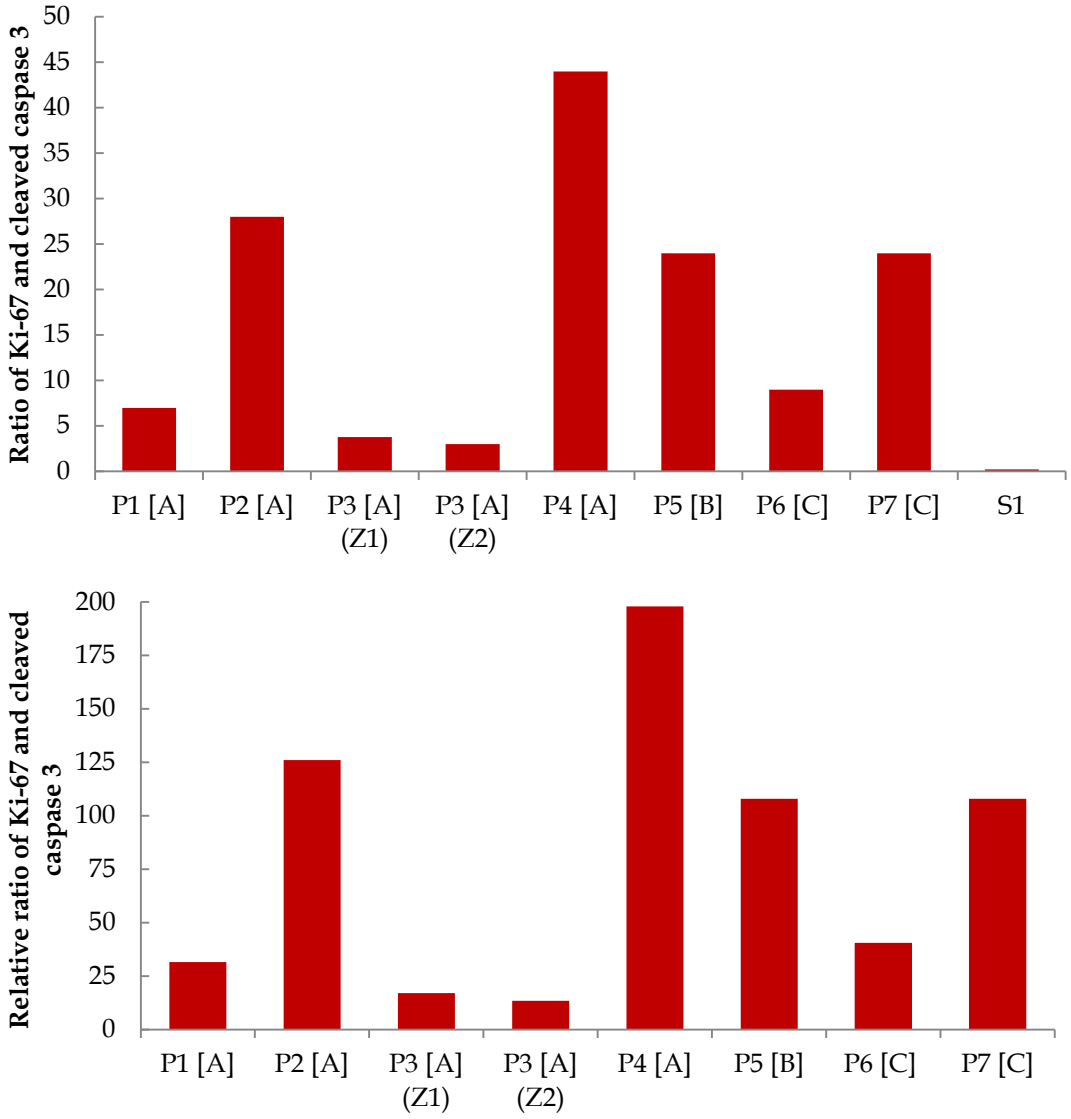

Figure 24. The ratio of proliferation to apoptosis reveals a broad but variable aberration in CLL compared to healthy tissue.

Sections of seven CLL LN tissue samples and one healthy spleen sample were immunofluorescently stained for expression of cleaved caspase 3 and Ki-67. Three areas from each tissue were imaged (with the exception of sample P3 which had 3 areas images from each of Z1 and Z2) and these images quantitatively analysed for positivity using Fiji Image J analysis software. Average numbers of positive cells from the three images collected for each sample and mean data used to determine a ratio of proliferative to apoptotic cells. **Upper graph**: Ratio for each tissue (mean Ki-67/mean cleaved caspase 3) **Lower graph**: Ratio for each CLL patient normalised to healthy spleen tissue (healthy spleen = 1.0). Samples are labelled with [stage of disease] along the x-axis.

3.6 Discussion

The data collated herein have demonstrated that archived FFPE CLL LN samples can be used to produce robust data via multicolour immunofluorescent staining and quantitative analysis and promotes the ongoing development of these techniques for future studies. The use of these samples has allowed insight into CLL disease biology which cannot be recapitulated by *in vitro* or *in vivo* animal studies and as such advocates the use of these methods in combination with other techniques to allow a fuller understanding of the disease to be developed.

In addition to the development of these methods, this work has produced several key findings. Firstly, the Ki-67 profiles of these CLL LN tissues have raised queries over the structure and composition of proliferation centres in these tissues. Whilst H&E staining data collected in this study confirm the presence of traditional proliferation centres, it appears that Ki-67 positive cells in the CLL LN are typically diffusely spread and their prevalence is unrelated to disease stage. These data indicate that traditional PC presence in the LN may not represent areas of intense proliferation. As reports of PC in LN continue to be referenced in the literature and their size has been correlated to aggressiveness of disease (Ciccone et al. 2012) these data may suggest that PC represent areas of localised interactions between CLL cells and microenvironmental cells, rather than areas of intense proliferation. In this scenario, PC in the LN would indicate pro-survival areas, rather than pro-proliferative areas.

Secondly it was shown that there is a decrease in the expression of PAX5 as stage of disease progresses, likely a reflection of a reduced expression of PAX5 within tumour cells. This appears particularly prevalent within the proliferative CLL cell population and this hypothesis is more likely than the premise that disease progression leads to a reduction in

tumour cell presence in the LN. Reduced PAX5 expression has been reported within other B cell tumours and is linked to more aggressive disease (Teo et al. 2015).

In addition, these data demonstrated the prevalence of T cells within the CLL LN regardless of stage of disease and showed infiltration of these cells throughout the tissues. Furthermore it was shown that in all patient samples, Ki-67$^+$ CLL cells were commonly found adjacent to T cells indicating a likely interaction occurring *in vivo*. Finally, whilst the total numbers of T cell subsets did not link to stage of disease in this study, it was noted that the spatial distribution of T cells in these tissues appears to alter as disease progresses and likely reflects the changing global architecture of the node and the cells within.

The ratio of proliferation to apoptosis in these tissues is also relatively variable but suggests that the balance of these processes in CLL is skewed compared to healthy tissue (Ponten et al. 2008). In context of proliferation data collected by (Messmer et al. 2005) utilising heavy water, these data also suggest that the LN microenvironment is highly protective towards CLL cells and that significant levels of tumour cell death must be occurring in the periphery.

Subsequent work focused upon the role of the T cell in the LN microenvironment, with an *in vitro* assay being constructed to observe the impact of CLL cells on T cells and vice versa. These data are described in the following chapter.

4 T CELLS AND CLL CELLS *IN VITRO*

4.1 Introduction

As described in Chapter 1, T cell interactions with CLL cells in the LN are thought to produce important pro-survival and pro-proliferative signals within CLL cells. The data presented in Chapter 3 further support this concept showing that T cells and CLL cells within the LN niche reside in close proximity and Ki-67$^+$ CLL cells are typically adjacent to T cells (also shown here in figure 25).

As also outlined in Chapter 1.7.1 several studies have attempted to address the biology of CLL cell-T cell interactions using either autologous or allogeneic T cell and CLL co-cultures. This chapter presents new observations obtained using CLL cell-allogeneic T cell co-cultures and has implications for the interpretation of these types of studies in the future.

In the outset the response of CD4$^+$ T cells to antigenic stimulation by CLL cells was investigated. The experiments set out to determine whether CLL cells induce a proliferative response in allogeneic T cells.

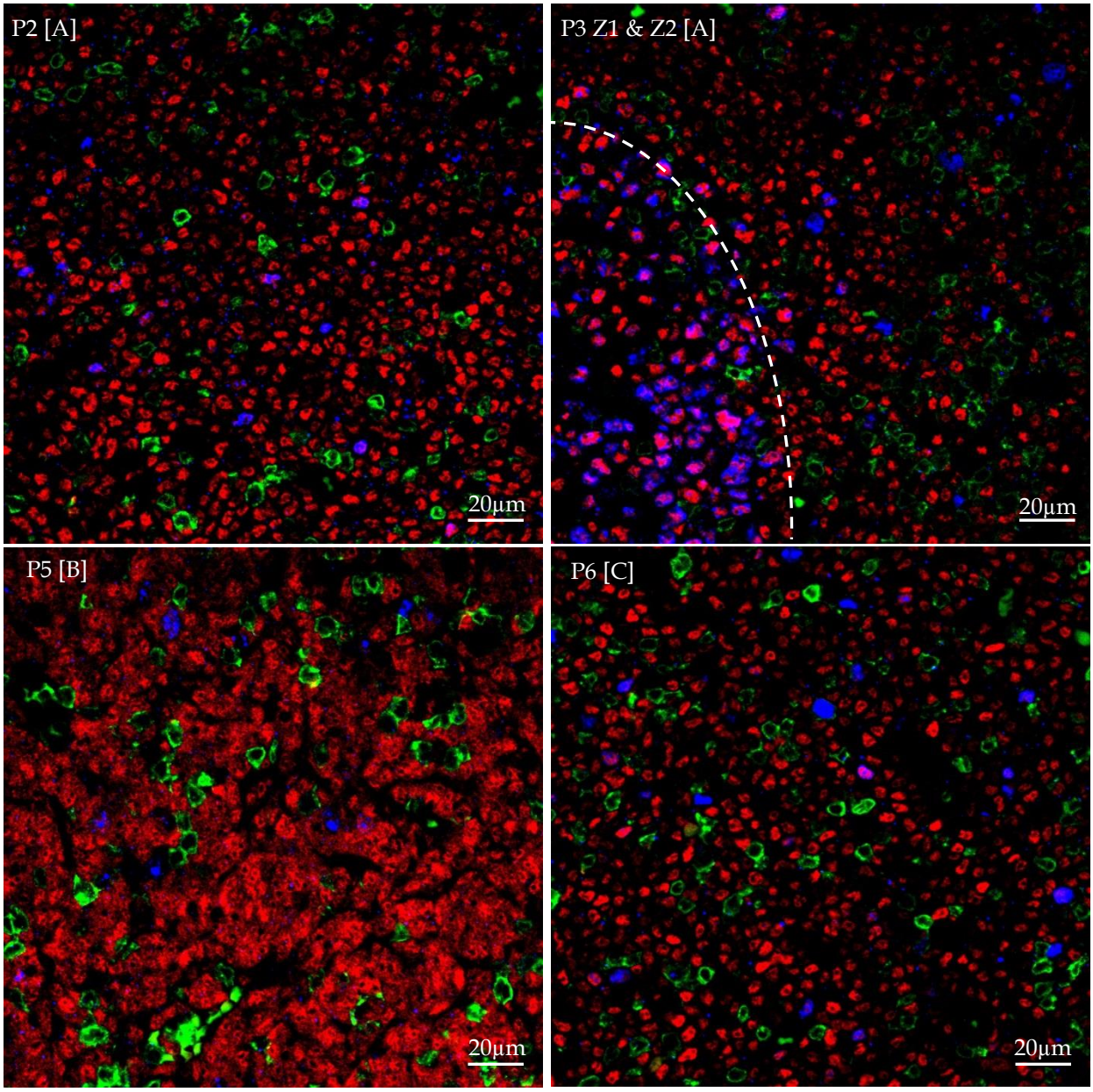

Figure 25. Proliferative CLL cells in the CLL LN commonly reside in close proximity to T cells at all stages of disease.

CLL LN tissue sections were stained for the expression of CD3 (green), PAX5 (red) and Ki-67 (blue). Representative images (x40 objective) are shown for stage A (n=2) stage B (n=1) and stage C (n=1) patient samples. Samples labelled with patient code and [stage of disease]. Images highlight the prevalence of proliferative CLL cells (pink/purple) being in close proximity to T cells (green) across a range of disease stages. The white dashed line denotes the different zones within sample P3.

4.2 Irradiated CLL cells induce healthy donor allogeneic CD4+ T to incorporate ^{3}H-thymidine

An established method for measuring cell proliferation *in-vitro* is the incorporation of ^{3}H-thymidine into newly synthesised DNA (Taylor et al., 1957). In this assay a given pulse of ^{3}H-thymidine allows the determination of the relative populations of cells in S-phase of the cell cycle across different experimental groups within a given experiment. ^{3}H-thymidine incorporation was therefore used to assess the impact of CLL cells on allogeneic T cell proliferation in a co-culture system.

CLL cells were first irradiated to render them mitotically incompetent (Noorizadeh et al. 2004) and subsequently mixed at a 1:1 ratio with magnetically purified healthy donor allogeneic CD4+ T cells (hdaCD4+ T cells) and co-cultured. ^{3}H-thymidine was pulsed into relevant wells 24 hours prior to harvest on 7 consecutive days and its incorporation analysed (figure 26). Despite the heterogeneity of ^{3}H-thymidine incorporation, co-cultured wells (red) showed a significantly larger incorporation of ^{3}H-thymidine at day 7 when compared to irradiated CLL cells alone (green) or hdaCD4+ T cells alone (blue). Statistical significance was shown across all 4 co-cultures when compared to hdaCD4+ T cell alone at day 7 (p=0.011, 0.038, 0.017 and 0.013 respectively using a students paired t-test). Mean data from n=18 samples and n=9, at days 5 and 7 respectively (figure 27) showed a similar trend and were also highly significant (p=0.0027 and 0.00018 using Wilcoxon signed rank test). Subsequent assays were predominantly measured at day 5 alone. Initial interpretation of these data indicated that the co-culture of hdaCD4+T cells with division incompetent CLL cells induced marked T cell proliferation as measured by uptake of ^{3}H-thymidine.

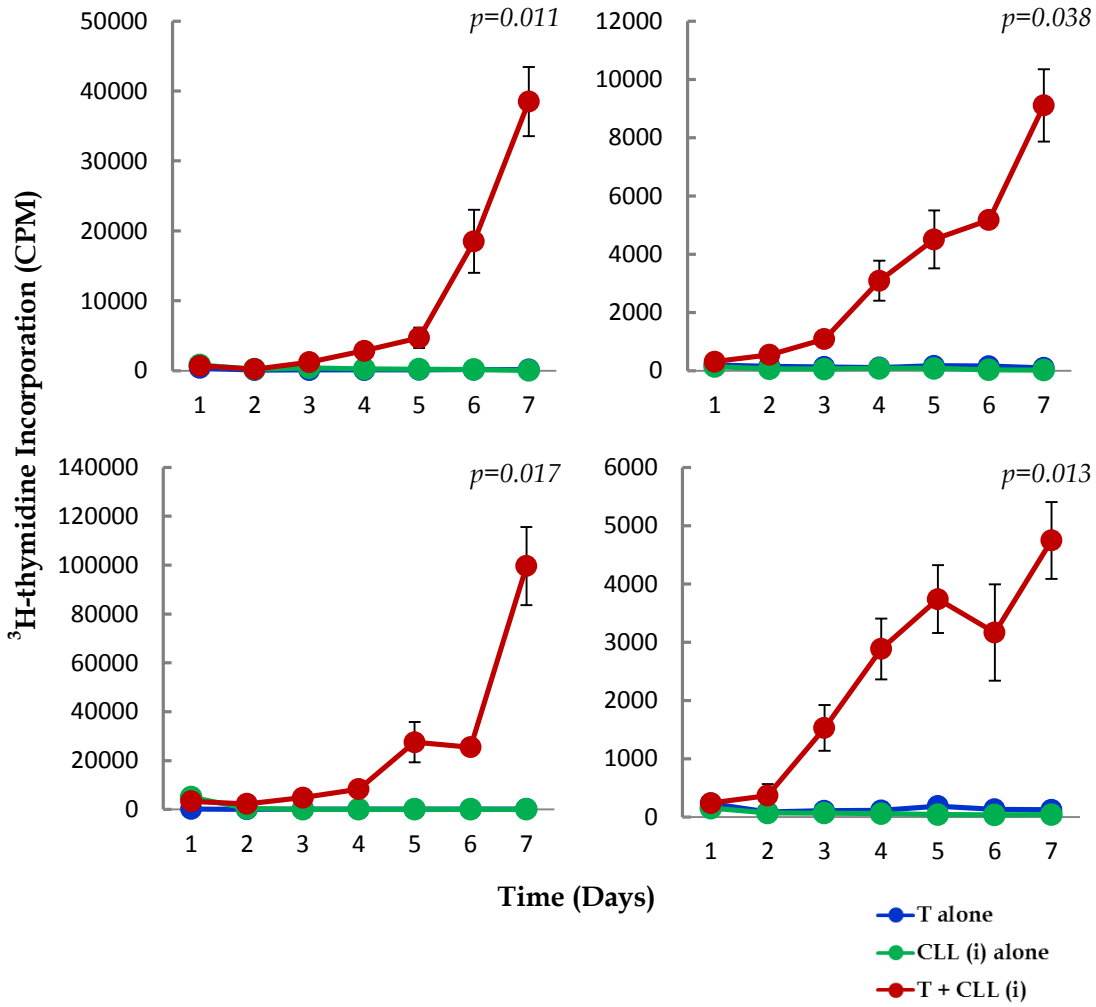

Figure 26. HdaCD4⁺T cells incorporated ^{3}H-thymidine when cultured with irradiated CLL cells.

HdaCD4⁺ T cells and irradiated CLL cells were each seeded at 2.5x10^{5}cells/well either in combination or alone. Wells were pulsed with ^{3}H-thymidine 24 hours prior to harvest and harvested every 24 hours for 7 days. Data is the mean of triplicate wells ±S.E.M. Experiments were set using four different CLL samples and 2 different hdaCD4⁺Tcell samples. Note that different scales are used on each "y" axis which reflects the variation in ^{3}H-thymidine incorporation between different CLL and hdaCD4⁺ T cell co-cultures. The difference in ^{3}H-thymidine incorporation between co-culture and hdaCD4⁺ T cell alone wells showed statistical significance at day 7 in all cases (student's t-test, *p* values shown on each graph).

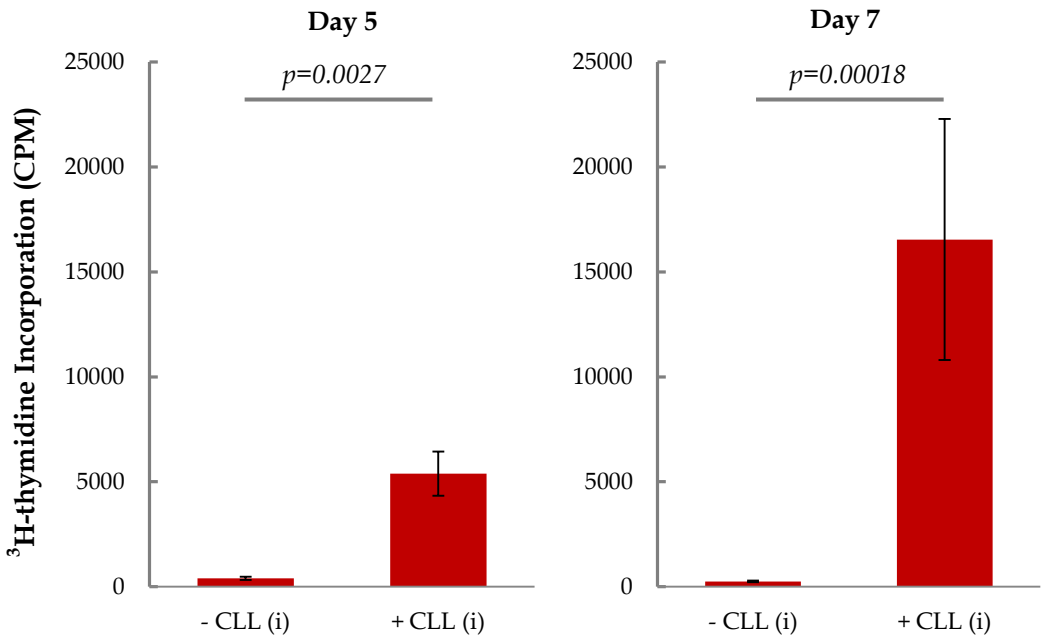

Figure 27. ^{3}H-thymidine assay showed significant difference in incorporation at day 5 and day 7 of co-culture.

HdaCD4$^+$ T cells were cultured with irradiated CLL cells, each seeded at 2.5x10^{5}cells/well in triplicate. Wells were pulsed with ^{3}H-thymidine 24 hours prior to harvest and incorporation was assessed at day 5 (left) and day 7 (right). Average ^{3}H-thymidine incorporation is plotted ±S.E.M. for hdaCD4$^+$ T cells alone (-CLL (i)) vs. co-culture wells (+CLL (i)). Data represents n=18 & 9 samples at day 5 and 7 respectively and differences in incorporation were highly significant at both time points ($p<0.005$).

4.3 Purification of the CLL samples prior to irradiation and culture significantly affects the incorporation of ^{3}H-thymidine by co-cultured cells

The above experiments utilised unpurified mononuclear cell (MNC) CLL preparations. Whilst the CLL samples used in all co-culture experiments had a minimum $CD19^{+}$ purity of 75% (as routinely tested by flow cytometry) the impact of the non-CLL MNC fraction within the co-culture was investigated. ^{3}H-thymidine was again employed to determine whether the incorporation response in co-culture wells was altered by purification of the CLL MNC. Prior to their irradiation CLL samples were positively or negatively purified (as described in Chapter 2.2.3). Samples were tested for $CD19^{+}$ purity by flow cytometry pre- and post-purification (figure 28). Purified or non-purified irradiated CLL cells from the same samples were subsequently mixed with hda$CD4^{+}$ T cells and cultured. ^{3}H-thymidine incorporation was measured at day 5 (figure 29). Co-cultures containing purified CLL cells had a significantly lower level of ^{3}H-thymidine incorporation compared to non-purified CLL MNC samples. These data suggested that the hda$CD4^{+}$ T cells proliferate more in the presence of non-purified CLL samples, and whilst purified CLL cells were also able to induce significant ^{3}H-thymidine incorporation during co-culture, this indicates a significant role for non-CLL MNC in the activation of T cells with potential implications for the CLL LN microenvironment.

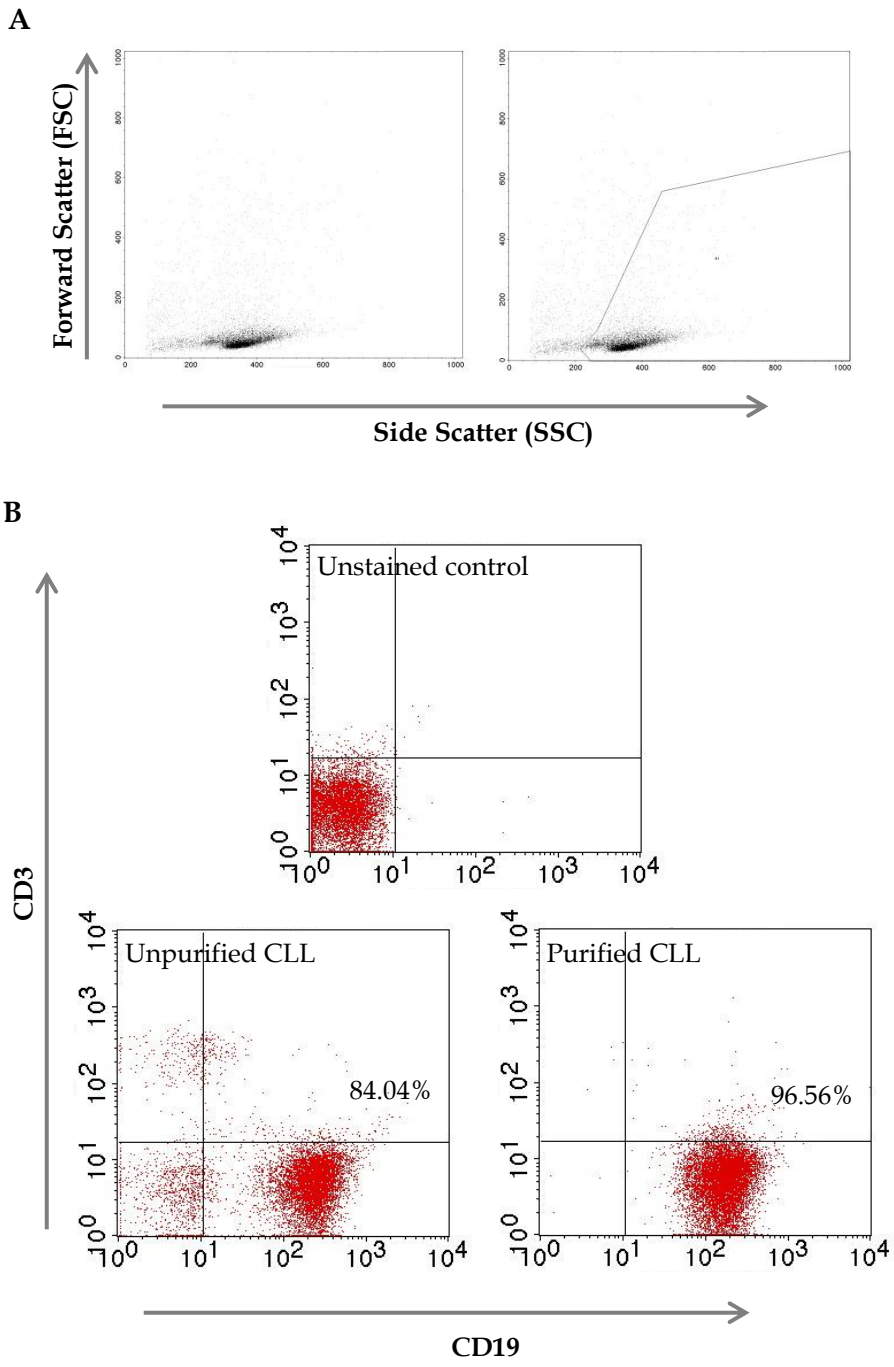

Figure 28 Flow cytometry analysis of CLL sample CD19 purity.

CLL samples were routinely tested for their CD19 purity before and after purification steps. Representative images show a single CLL sample tested for purity pre- and post- positive selection purification. (A) Samples were viably gated using the FSC/SSC profile and (B) viable cells were subsequently tested for their CD19/CD3 positivity. Representative images for negative selection can be found in Appendix I.

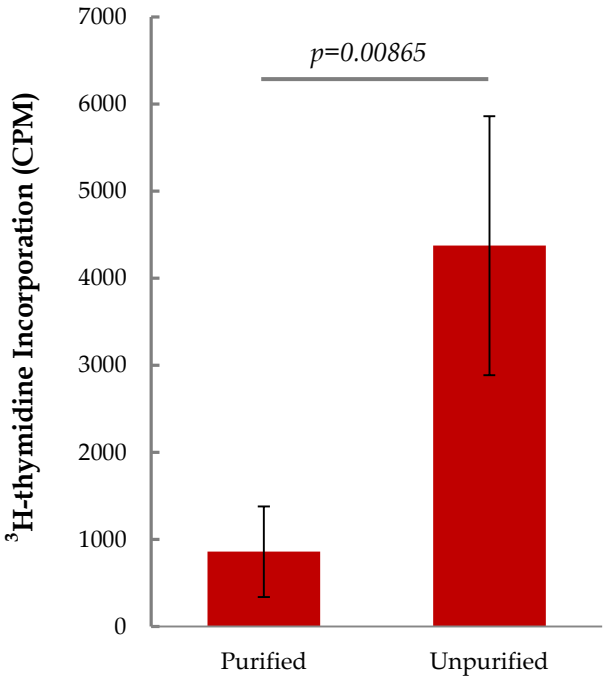

Figure 29. Purification of CLL samples significantly affected co-culture ^{3}H-thymidine incorporation.

HdaCD4^{+} T cells were cultured with either unpurified irradiated CLL samples or purified irradiated CLL cells, each seeded at 2.5x10^{5}cells/well in triplicate. Wells were pulsed with ^{3}H-thymidine 24 hours prior to harvest and incorporation was assessed at day 5. Data shown here represents the average ^{3}H-thymidine incorporation of co-culture wells plotted ±S.E.M. for n= 8 samples (CLL samples were either positively or negatively purified as described in Chapter 2.2.3).

4.4 Purification of CLL samples also significantly affects their incorporation of ^{3}H-thymidine in response to CD40L stimulation

The data above showed that CLL cell enrichment had an impact on co-culture incorporation of ^{3}H-thymidine which was deemed to be an indicator of reduced hdaCD4^{+} T cell proliferation. These data showed that the presence of non-CLL MNC from CLL MNC preparations induced a greater incorporation of ^{3}H-thymidine in co-culture wells than purified CLL cells alone induced. These data do not clearly demonstrate whether the non-CLL MNC have a direct impact upon the T cell population or whether they impact the CLL cells and augment a CLL cell-induced T cell proliferation. It should be noted that following purification, CLL samples still contained a small proportion of contaminant cells (~3.5%, figure 28) and this cannot be ruled out as the source of the induced ^{3}H-thymidine incorporation in purified co-culture wells. To better determine whether the non-CLL MNC might interact with CLL cells in co-culture, non-CLL MNC were tested for their ability to affect CLL cell proliferation. CLL cells were cultured using a stromal T cell mimetic assay to induce proliferation. CD40L is an important T cell derived stimulatory signal and has been routinely used in previous studies by this group and others to stimulate CLL cell proliferation *in-vitro* (Hayden et al. 2009; Pascutti et al. 2013).

Purified or whole CLL MNC samples were cultured on CD40L expressing stromal cells (L-40 stroma, described in Chapter 2.3). In these experiments CLL cells were left un-irradiated to allow their proliferation. ^{3}H-thymidine incorporation was measured at day 5 (figure 30) and demonstrated that purified CLL cells showed a significantly reduced incorporation of ^{3}H-thymidine compared to unpurified samples (p=0.025). It should be noted that a stroma alone control was always included in these experiments to ensure that Mitomycin C treatment of

the stroma (to prevent their proliferation and subsequent uptake of ^{3}H-thymidine as described in chapter 2.3.3) was successful.

This data shows that CLL cell proliferation following CD40L stimulation is enhanced by the presence of non-CLL MNC indicating a significant role for other cell types in the LN microenvironment and supporting the data seen in co-cultures above. This observation resonates with recent reports of Nurse-like Cells (NLC) in the CLL LN (as discussed in Chapter 1.5.3) and were the reason behind the studies described later in Chapter 5.

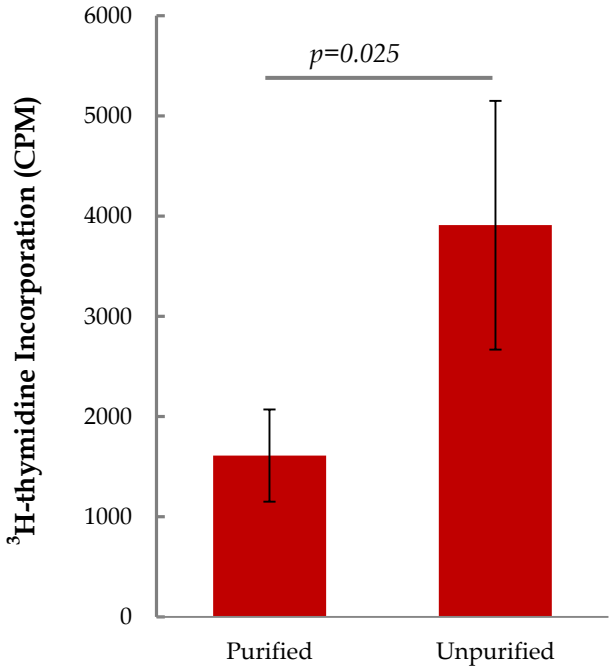

Figure 30. Purification of CLL samples significantly affected ^{3}H-thymidine incorporation during T cell signal derived stimulation.

CD19$^+$ purified and untouched cells from the same CLL samples were seeded at 2.5x10^{5}cells/well in triplicate onto L-40 stroma. Wells were pulsed with ^{3}H-thymidine 24hrs prior to harvest and incorporation was assessed at day 5. Data is the average ^{3}H-thymidine incorporation of n=3 samples and is plotted ±S.E.M.

4.5 Co-cultured cells have improved viability however ^{3}H-thymidine incorporation seen in co-cultures does not relate to cell proliferation

The above experiments appeared to indicate a proliferative response by hdaCD4^{+} T cells in response to CLL MNC, albeit enhanced by the presence of non-CLL cell MNC in the irradiated samples. Whilst T cell-driven proliferation of CLL cells is widely accepted to occur in the CLL LN and appears to be supported by the staining of CLL LN shown in Chapter 3 and here in figure 4.1, to what extent CLL cells and T cells induce reciprocal proliferation in the same interaction is uncertain. The relatively small number of Ki-67^{+} T cells in CLL LN in Chapter 3 (figure 15) questioned the apparent proliferation of hdaCD4^{+} T cells in response to CLL MNC seen in these *in vitro* co-cultures.

The above experiments employed irradiated CLL MNC in order to restrict ^{3}H-thymidine incorporation to the T cells. However, use of non-irradiated CLL MNC permitting the mutual responses of both cell types to be observed would better reflect the *in vivo* situation. An assay was therefore developed to allow simultaneous measurement of T cell and CLL MNC proliferation.

4.5.1 Viability

As the LN microenvironment has a pro-survival effect upon CLL cells in addition to the pro-proliferative effect, viability within the co-culture was also tested. Furthermore since T_{fh} cells, which reside in the LN, have been shown to support CLL cell proliferation *in vitro* through the secretion of IL-21 recombinant human IL-21 was added to co-cultures. This was deemed relevant because culture volumes used in the experiments would greatly dilute any endogenous IL-21 produced *in vitro*.

HdaCD4$^+$ T cells and CLL MNC were cultured alone and together for five days in the presence of IL-21. Cells were harvested and propidium iodide incorporation (PI) was measured in combination with CD4 and CD19 expression using flow cytometry (figure 31). PI is excluded from viable cells by an efficient efflux mechanism and therefore an increase in PI positivity denotes reduced viability. The data indicates that co-culture of hdaCD4$^+$ T cells and CLL MNC significantly reduced the incorporation of PI by CD19$^+$ CLL cells and CD4$^+$ T cells (figure 32). As such, co-culture sustained the viability of both CLL cells and T cells compared to their culture alone thereby supporting the concept of reciprocal interactions between CLL cells, the CLL MNC and T cells in the CLL LN.

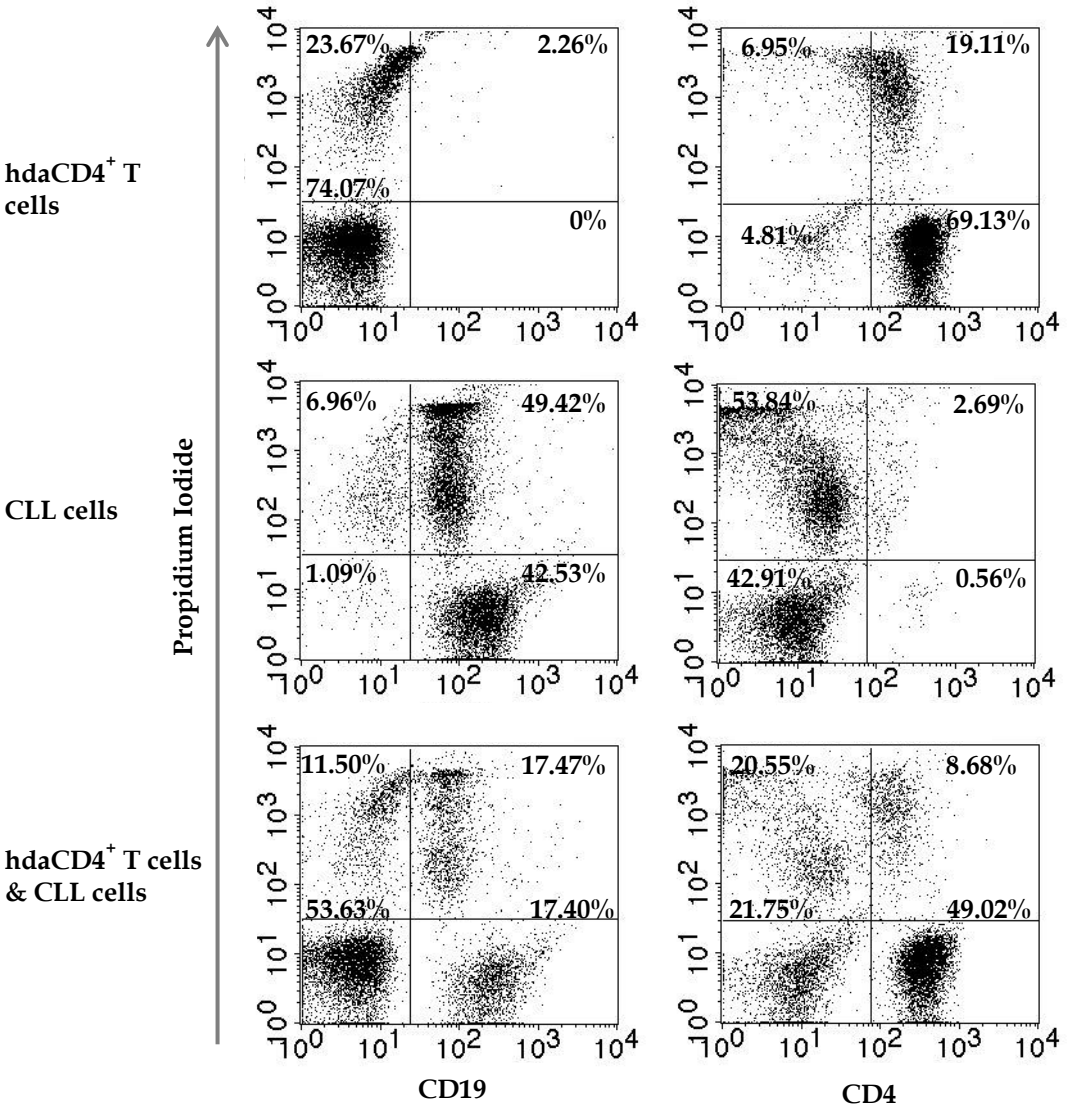

Figure 31. HdaCD4+T cell and CLL cell co-culture viability is improved compared to either cell type cultured alone.

HdaCD4+ T cells were cultured alone or in combination with CLL MNC, each seeded at $2.5x10^5$ cells/well in triplicate in the presence of IL-21. All wells were harvested at day 5 and pooled triplicate wells were analysed via flow cytometry for their expression of CD19, CD4 and incorporation of propidium iodide. Representative flow cytometry data shown (n=1).

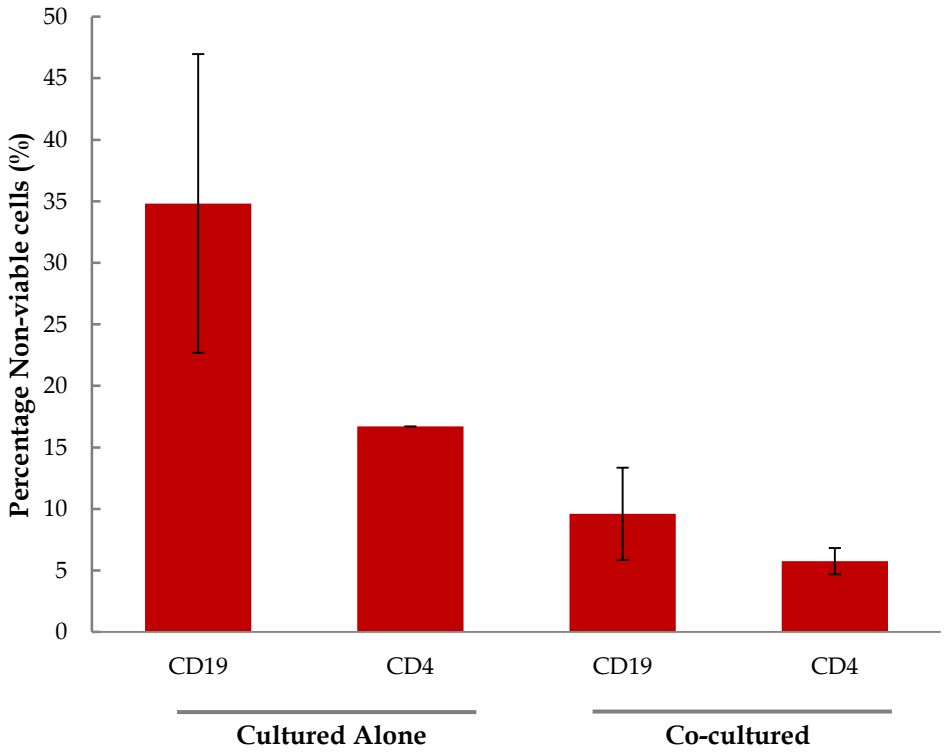

Figure 32. Reduction in Propidium Iodide incorporation by co-cultured CLL cells and hdaCD4⁺ T cells in comparison to culturing alone indicates improved viability.

HdaCD4⁺ T cells were cultured alone or in combination with CLL cells, each seeded at $2.5x10^5$ cells/well in triplicate in the presence of IL-21. All wells were harvested at day 5 and pooled triplicate wells were analysed via flow cytometry for their expression of CD19, CD4 and incorporation of propidium iodide. Data represents the average propidium iodide incorporation of CD19⁺ and CD4⁺ cells during co-culture compared to their culture alone. Data represents n=3 samples ±S.E.M.

4.5.2 Proliferation

To monitor cellular proliferation, the viable cell fluorescent labels CellTrace™ CFSE and CellTrace™ Far Red were utilised (Lyons, 1999). In this approach each cellular division reduces the fluorescence intensity of the labelled cells, which can be measured by flow cytometry. Parallel staining CLL MNC with one label and T cells with the other rendered it possible to observe cell division in each population following co-culture.

HdaCD4$^+$ T cells and CLL MNC were CellTrace™ labelled prior to their culture and a base line fluorescence intensity reading taken at day zero (figure 33). Following five days of culture cellular proliferation was measured (figures 34 & 35) against the baseline values. In addition, cultures were monitored to determine what proportions of the cells were in active cell cycle (figure 36).

Unexpectedly, these data demonstrated that co-culture of hdaCD4$^+$ T cells and CLL MNC does not induce strong proliferation of either cell type. This was supported by cell cycle analysis that demonstrated co-cultures had a quiescent cell cycle profile, as revealed by a dominant G_o/G_1 population and lack of cells in S and G_2/M phases of the cell cycle. The lack of detection of cycling cells was not technical since cell proliferation by CellTrace™ detection and cell cycle activity was readily observed in CLL MNC that had been cultured on L-40 stroma (figures 34, 35 & 36). It should be noted that there does appear to be a very small number of hdaCD4$^+$ T cells that have a reduced CellTrace™ Far Red signal (figure 34) although this is only slightly above that seen in T cell alone wells (figure 35) and was difficult to align with previously reported ^{3}H-thymidine incorporation data.

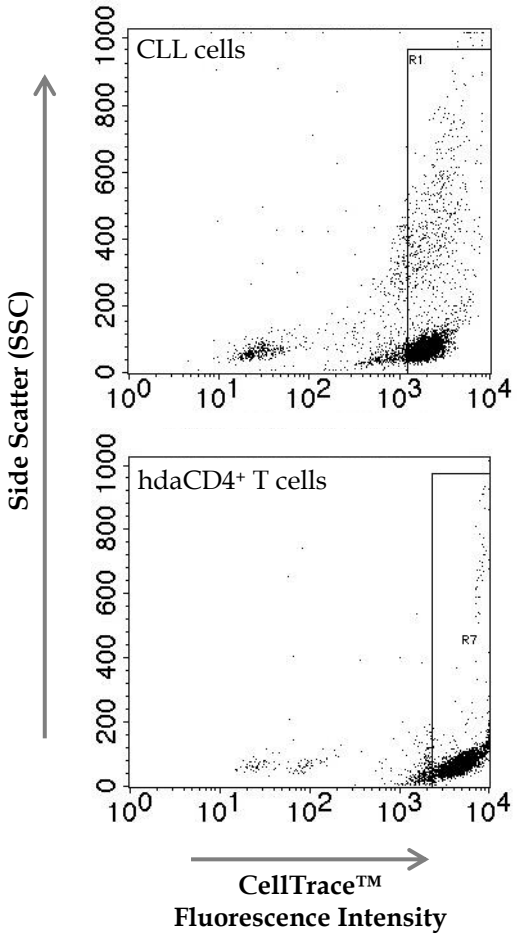

Figure 33. Optimisation of CellTrace™ labelling to monitor proliferation.

Prior to culture hdaCD4$^+$ T cells and CLL MNC were labelled with different CellTrace™ dyes. Cells were analysed by flow cytometry at Day 0 to allow a base line fluorescent signal to be determined. This baseline was gated (R1/R7) and used in subsequent analyses to determine the proliferation status of hdaCD4$^+$T cells and CLL MNC during culture. Representative data shown; CLL MNC labelled with CellTrace™ CFSE and hdaCD4$^+$ T cells labelled with CellTrace™ Far Red fluorescent dyes.

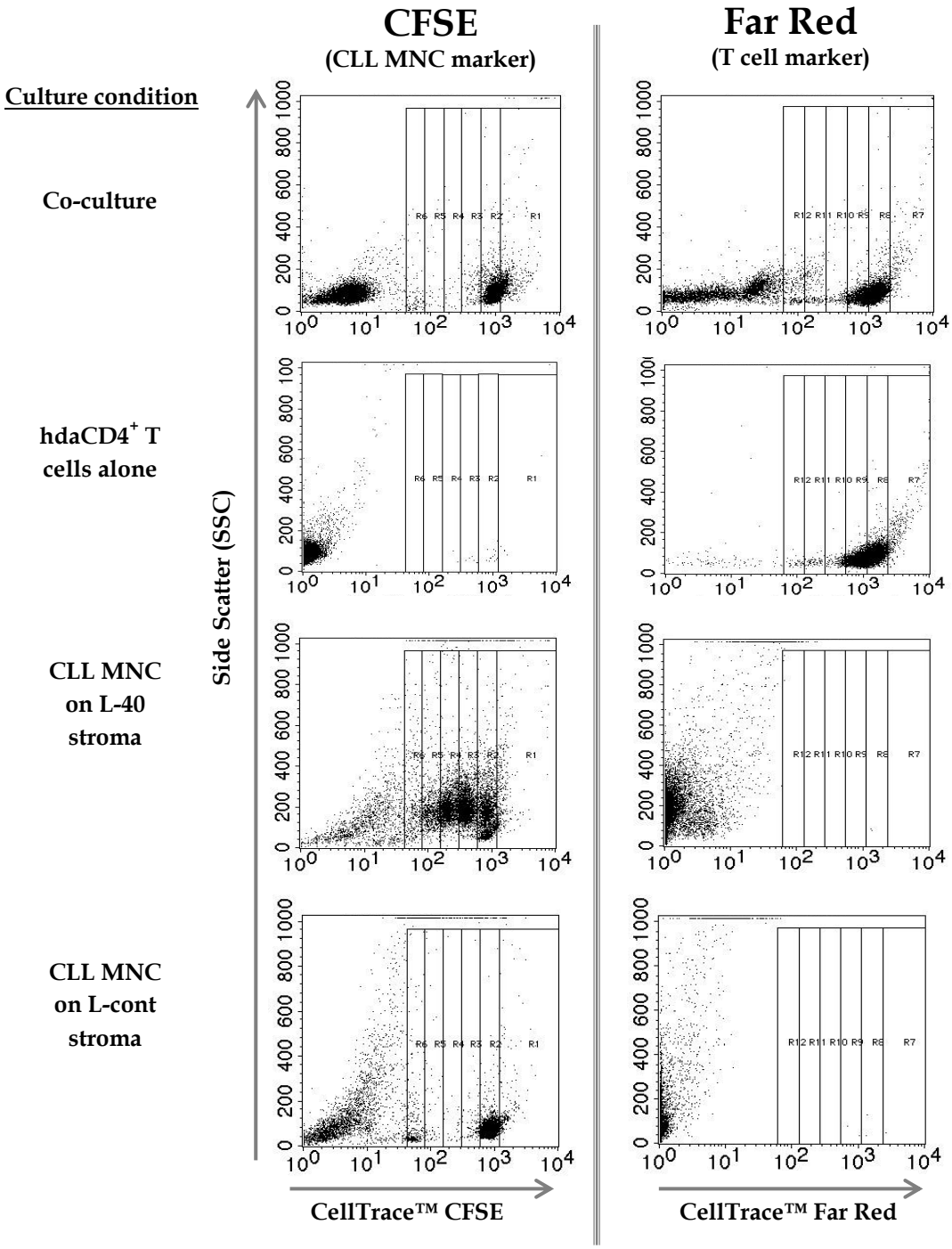

Figure 34. Flow cytometry analysis of CellTrace™ fluorescence intensity.

Prior to culture hdaCD4+ T cells were labelled with CellTrace™ Far Red and CLL MNC with CellTrace™ CFSE to monitor cellular proliferation. Representative data shown for both dyes of; co-culture of hdaCD4+ T cells and CLL MNC, hdaCD4+ T cells alone, CLL MNC alone on L-40 stroma and L-cont stroma. Cells were each seeded at 2.5x10^{5}cells/well in triplicate in the presence of IL-21 and harvested at day 5. R1 and R7 gates were determined as previously described. Proliferation rates were calculated using gates R2-R6 (CLL MNC) and R8-R12 (hdaCD4+ T cells).

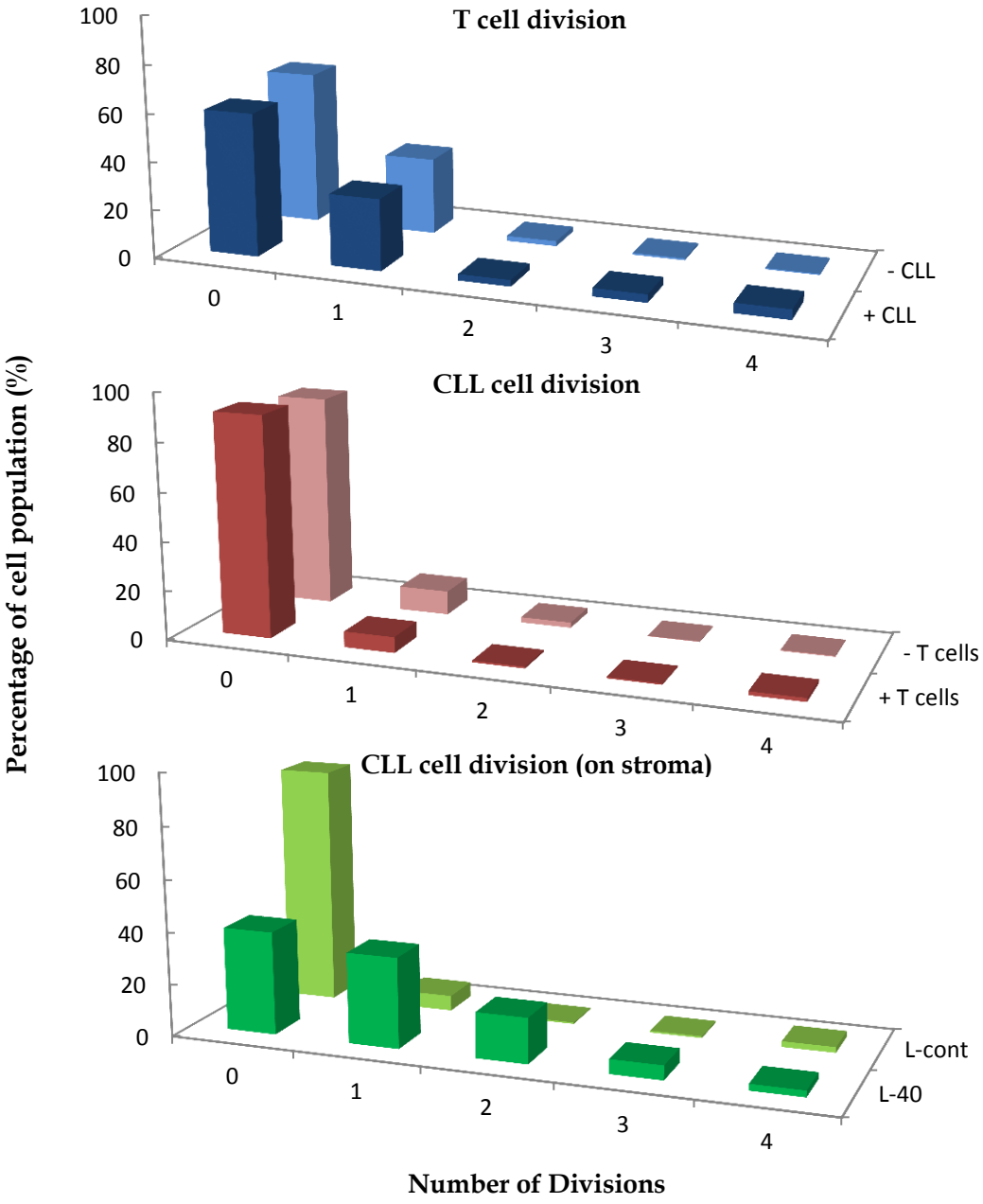

Figure 35. Analysis of cellular proliferation using CellTrace™ fluorescent dyes indicates an absence of strong proliferation in co-culture wells.

Prior to culture hdaCD4⁺ T cells were labelled with CellTrace™ Far Red and CLL MNC with CellTrace™ CFSE to monitor cellular proliferation. Cells were cultured in the following conditions; co-culture of hdaCD4⁺ T cells and CLL MNC, hdaCD4⁺ T cells alone, CLL MNC alone on L-40 stroma and L-cont stroma. Cells were each seeded at $2.5x10^5$cells/well in triplicate in the presence of IL-21 and harvested at day 5. Data shown are the analysis of events in gates R1-R12 as shown in figure 33.

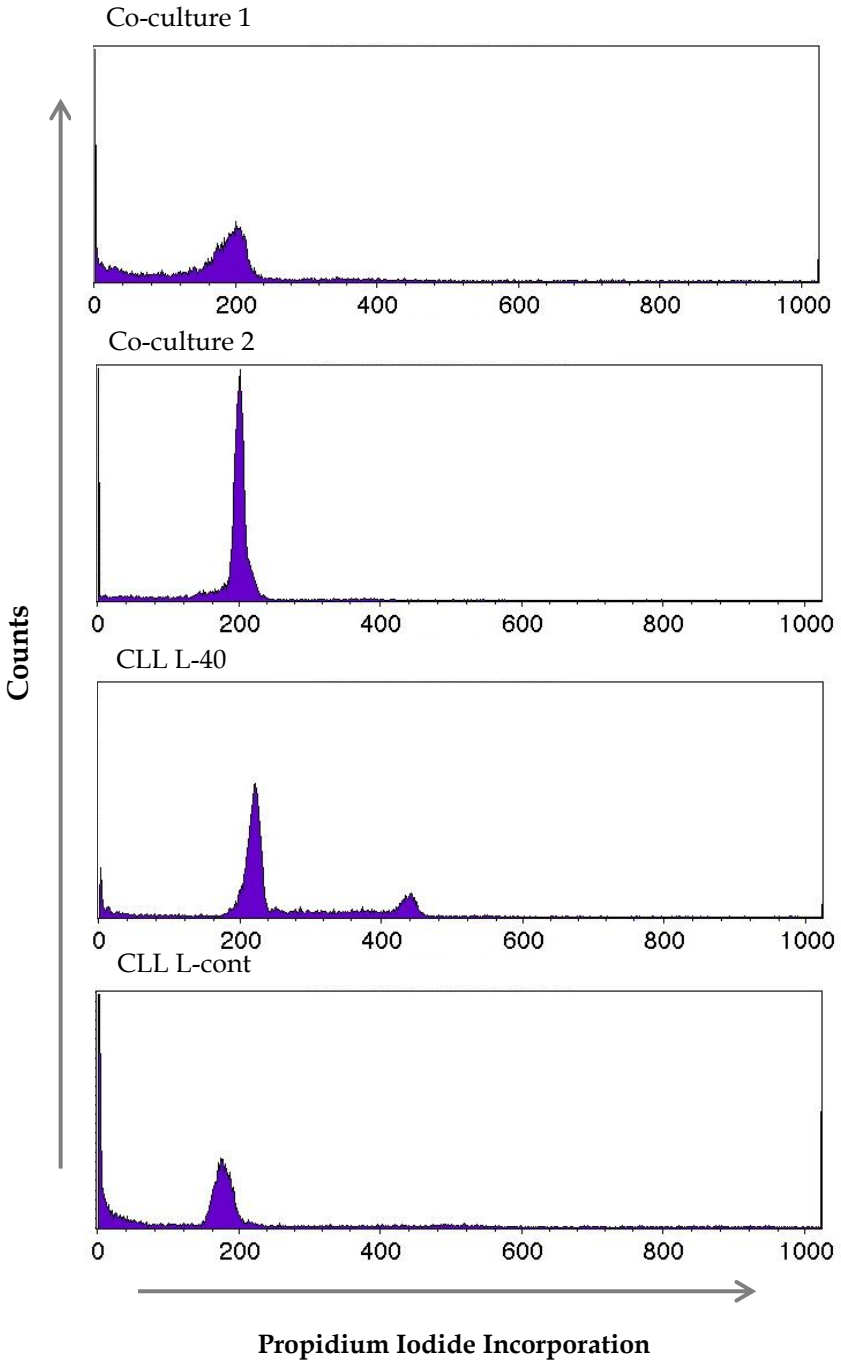

Figure 36. Cell cycle analysis indicates a quiescent profile in co-cultures.

HdaCD4$^+$ T cells and CLL MNC were cultured alone or in combination each seeded at 2.5x10^5 cells/well in triplicate in the presence of IL-21. All wells were harvested at day 5 and pooled triplicate wells were incubated with cell cycle buffer containing PI to monitor cell cycle activity. Representative data shown from pooled triplicate wells; hdaCD4$^+$ T cells donor 1 with CLL MNC sample, hdaCD4$^+$ T cells donor 2 with CLL MNC sample, CLL MNC sample on L-40 stroma, CLL MNC sample on L-cont stroma.

These data from the flow-cytometric analyses of proliferation indicated that the apparent hdaCD4$^+$ T cell expansion in response to CLL MNC seen by ^{3}H-thymidine (figures 26-29) was not a response to CLL and accessory cells *per se* but rather a response to CLL and accessory cells that had been irradiated. To address this, co-cultures were established to look at the CellTrace™ profiles of T cells when they were co-cultured with irradiated CLL MNC (figure 37 & 38) and in parallel co-cultures of T cells with irradiated and non-irradiated CLL MNC were monitored for their incorporation of ^{3}H-thymidine (figure 39 and 40).

As seen previously, the use of CellTrace™ indicated no strong or significant proliferation of hdaCD4$^+$ T cells when co-cultured with either irradiated CLL MNC or non-irradiated controls. However, both irradiated and non-irradiated CLL MNC induced the uptake of ^{3}H-thymidine in co-cultures, although this was seen to a lesser extent in non-irradiated co-cultures. Overall these data now indicated that the ^{3}H-thymidine incorporation seen in the earlier experiments may not relate solely to proliferation in these co-cultures.

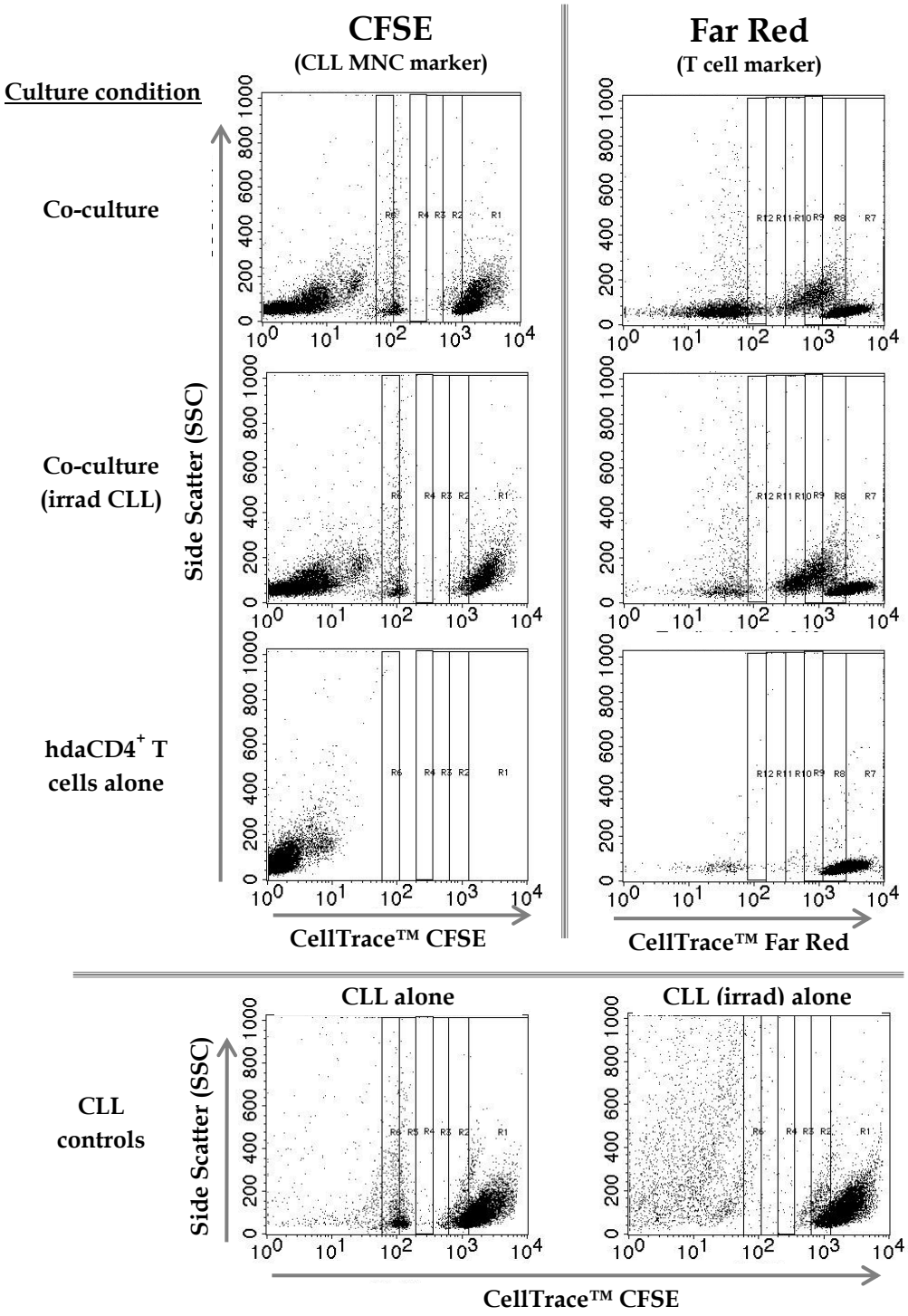

Figure 37. Flow cytometry analysis of CellTrace™ fluorescence intensity.

Prior to culture hdsCD4+ T cells were labelled with CellTrace™ Far Red and CLL MNC with CellTrace™ CFSE to monitor cellular proliferation. CLL MNC were separated into 2 fractions, one irradiated and the other left un-irradiated. Irradiated and non-irradiated fractions of CLL MNC were co-cultured with the same hdaCD4+ T cell sample, or alone as control. Cells were each seeded at 2.5x10^5cells/well in triplicate in the presence of IL-21 and harvested at day 5. Proliferation rates were calculated using gates R1-R12 as previously described.

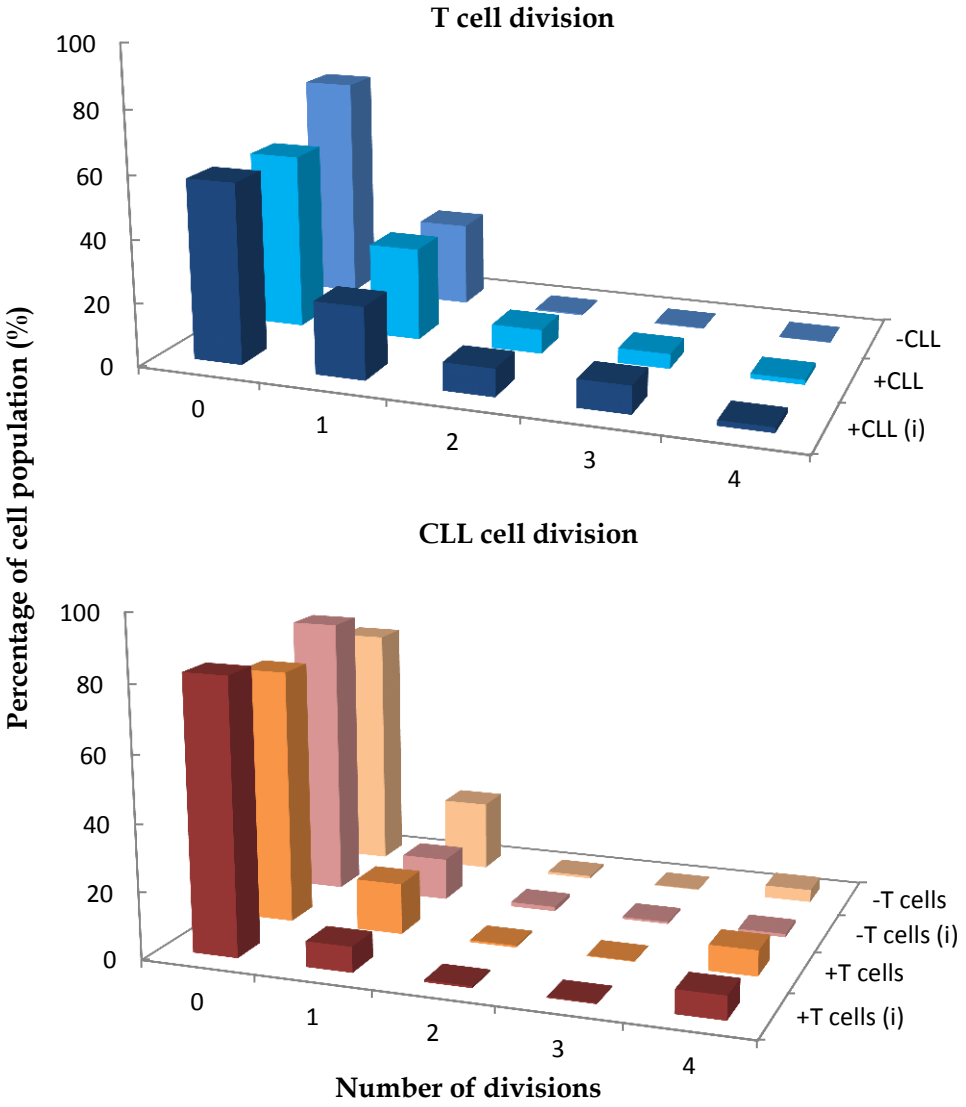

Figure 38. CellTrace™ analysis of irradiated CLL MNC co-culture with hdaCD4⁺ T cells demonstrated a lack of strong proliferation.

Prior to culture hdaCD4⁺ T cells were labelled with CellTrace™ Far Red and CLL MNC with CellTrace™ CFSE to monitor cellular proliferation. CLL MNC were separated into 2 fractions, one was irradiated and the other left un-irradiated. Irradiated and non-irradiated fractions of the CLL MNC samples were co-cultured with the same hdaCD4⁺ T cell sample, or alone as control. Representative data shown for both dyes of; co-culture of hdaCD4⁺ T cells and CLL MNC (irradiated and non-irradiated fraction), hdaCD4⁺ T cells alone and CLL MNC alone (irradiated and non-irradiated fraction). Cells were each seeded at $2.5x10^5$cells/well in triplicate in the presence of IL-21 and harvested at day 5. Data shown are the analysis of events in gates R1-R12 as shown in figure 36.

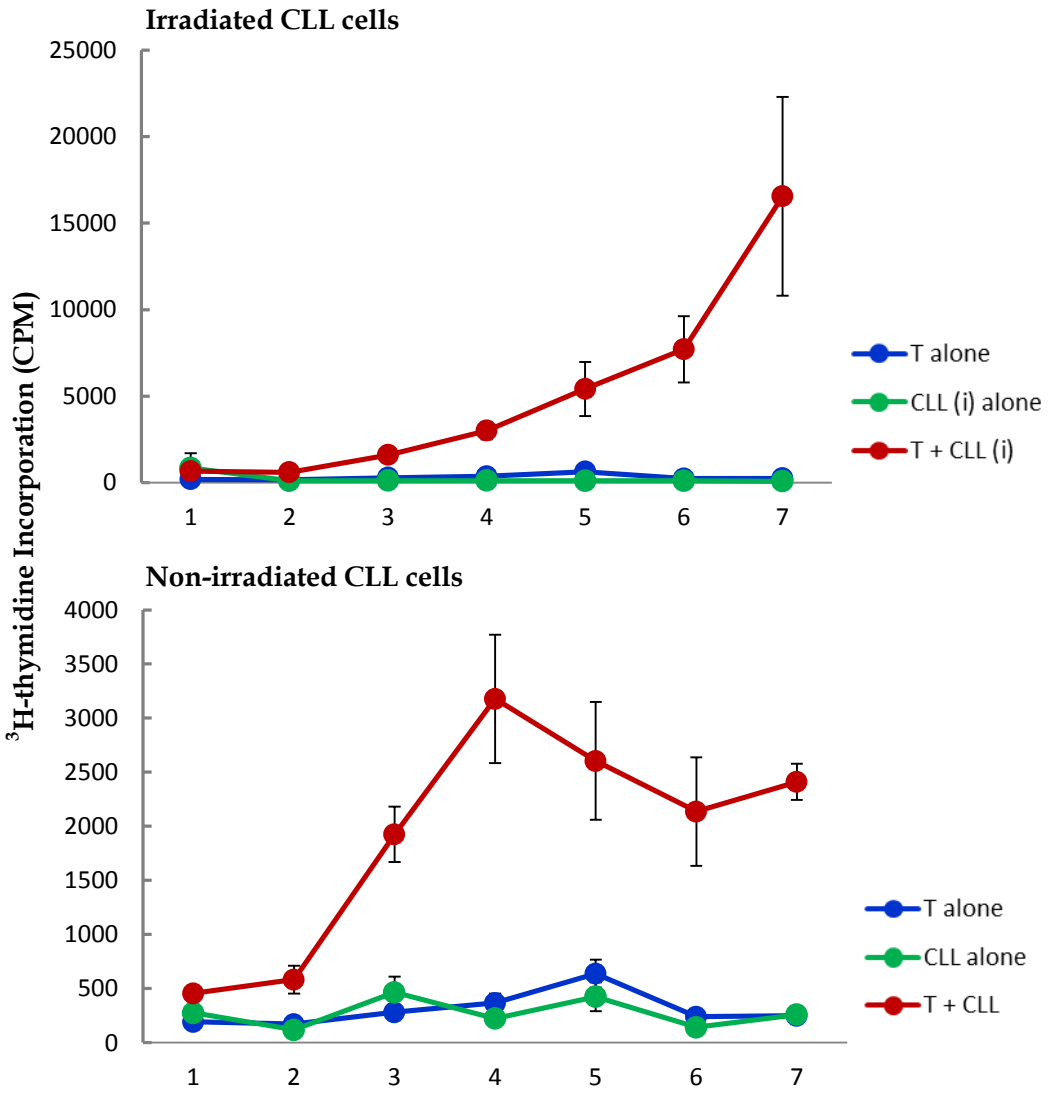

Figure 39. ^{3}H-thymidine incorporation occurred in co-cultures of hdaCD4$^+$ T cells with both irradiated and non-irradiated CLL MNC.

HdaCD4$^+$ T cells were cultured with irradiated CLL MNC (top panel) or non-irradiated CLL MNC (bottom panel) each seeded at 2.5x10^{5}cells/well in triplicate. Wells were pulsed with ^{3}H-thymidine 24 hours prior to harvest and harvested every 24 hours for 7 days. Average ^{3}H-thymidine incorporation is plotted ±S.E.M. for n=9 (top) & n=5 (bottom) samples. It should be noted that different scales are used on each "y" axis which reflects the reduced ^{3}H-thymidine incorporation in non-irradiated CLL MNC and hdaCD4$^+$ T cell co-cultures.

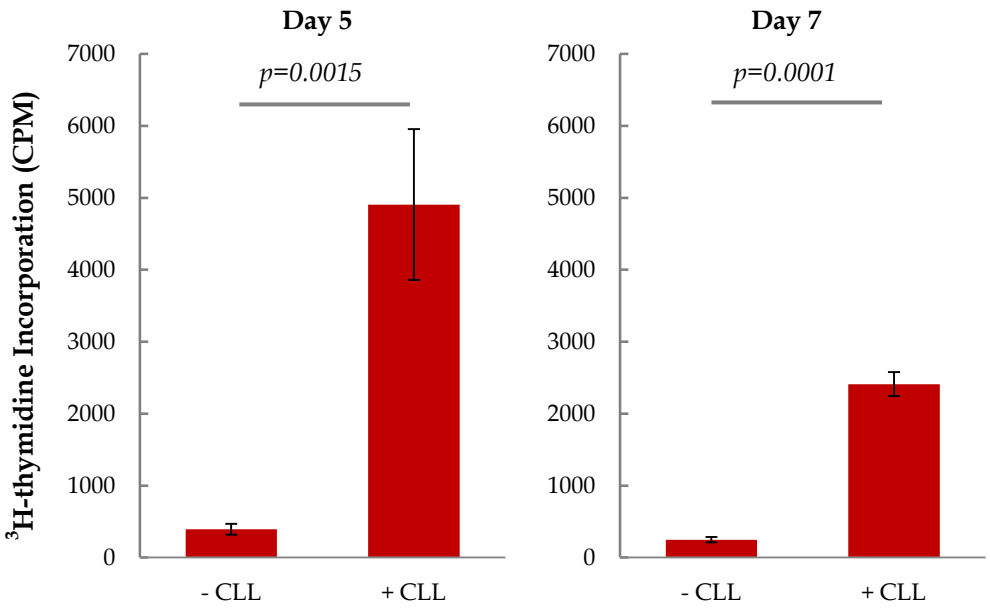

Figure 40. ^{3}H-thymidine incorporation in co-cultures of hdaCD4$^+$ T cells and CLL MNC showed significant difference at day 5 and day 7.

HdaCD4$^+$ T cells were cultured with or without non-irradiated CLL MNC, each seeded at 2.5x10^{5}cells/well in triplicate. Wells were pulsed with ^{3}H-thymidine 24 hours prior to harvest and incorporation was assessed at day 5 (left) and day 7 (right). Average ^{3}H-thymidine incorporation is plotted ±S.E.M. for hdaCD4$^+$ T cells alone vs. co-culture wells. Data represents n=14 & 5 samples at day 5 and 7 respectively.

In combination, the collective data confirmed that there was significant uptake of ^{3}H-thymidine by cells within the co-cultures which appeared to represent a small proportion of T cell proliferation which was not limited to cultures with irradiated cells (although irradiation of CLL MNC did exacerbate uptake). Whilst there appeared to be a small proportion of T cells which were proliferating by CellTrace™ analysis, these data were unsupported by cell cycle analysis, although viability data (figures 31 & 32) confirmed that there was a reciprocal pro-survival effect of co-culturing compared to either cell type cultured alone indicating cell-cell interaction.

One explanation for the increase in ^{3}H-thymidine uptake with apparent lack of strong proliferation (as seen by CellTrace™ labelling and cell cycle analysis) was that this may represent a very tiny percentage of T cells which continually proliferate over the course of 5-7 days and show an increase the ^{3}H-thymidine counts whilst making only a small impact on CellTrace™ readings. However, the high levels of ^{3}H-thymidine uptake over 7 days does not easily reconcile with the small changes in CellTrace™ assays and lack of active cell cycle data. As such, other contributing causes for this apparent disconnect were further interrogated. After consideration of the literature it was noted that ^{3}H-thymidine incorporation has also been reported as an indicator of DNA repair (Herman 2002, Cleaver 2014). This raised the possibility that a portion of the ^{3}H-thymidine incorporation in co-cultures could reflect DNA damage repair and that the greater incorporation seen when irradiated CLL MNC were used may reflect greater levels of DNA repair by these cells (figure 40).

4.6 BrdU incorporation of irradiated cultures shows a perinuclear subcellular localisation consistent with DNA repair

To further investigate alternative causes of ^{3}H-Thymidine incorporation by co-cultured cells the thymidine analogue bromodeoxyuridine (BrdU) was employed. This label has the advantage that it can be detected immunoflouresently and therefore visualised (Calkins & Reddy 2011; Lentz et al. 2010; Campana et al. 1988). Co-cultures of hdaCD4^{+} T cells and irradiated CLL MNC were pulsed with BrdU containing media in triplicate and harvested at days 3, 5 and 7. Cytospins were created from pooled wells and were subsequently immunofluorescently stained for the incorporation of BrdU and observed using confocal microscopy. The main objectives of these experiments were (i) to determine whether the incorporation of ^{3}H-thymidine as seen above could be recapitulated by a thymidine analogue and (ii) if so, whether the incorporation was localised to a specific cellular compartment which could aid in elucidating the mechanism for such uptake.

Representative data from these experiments is shown (figure 41). Firstly, these data support previous experiments by confirming that uptake of a thymidine analogue occurs in co-cultures even when using BrdU in place of ^{3}H-thymidine. Secondly, these data also support the theory that DNA repair may be occurring in these co-cultures, as uptake appears to localise to a specific subcellular region.

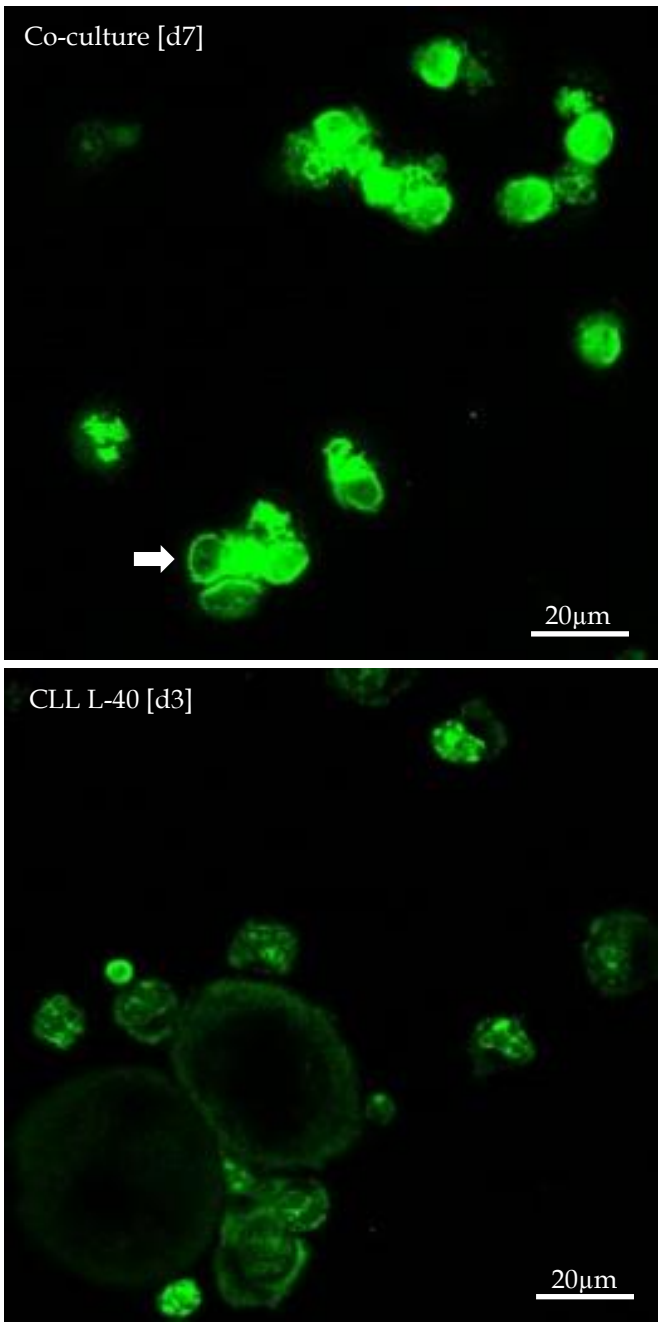

Figure 41. Subcellular localisation of BrdU incorporation differs between actively proliferating cells and those in co-culture conditions.

HdaCD4^{+} T cells were cultured with irradiated CLL MNC each seeded at 2.5x10^{5}cells/well in triplicate. As a control for proliferating cells, CLL MNC (non-irradiated) were cultured on L-40 stroma with IL-21. Wells were pulsed with BrdU at day 0 and harvested at day 3 (CLL L-40) & day 7 (co-culture). Cytospins from pooled triplicate wells were immunofluorescently stained for BrdU incorporation. Representative images (x40 objective) are shown. Arrow highlights potential perinuclear staining, samples labelled with culture condition and [day of culture].

As expected CLL MNC cultured on L-40 stroma in the presence of IL-21 showed strong nuclear staining in a sub-population of cells that was consistent with some cells being in S-phase during the period of pulsing with BrdU. However, the distribution of BrdU staining and level of staining observed within the co-culture was strikingly different. $BrdU^+$ co-cultured cells showed a staining pattern reminiscent of a perinuclear rather than intra-nuclear distribution. This distribution was visualised dependent upon the focal plane when observing the samples and examples of these suspected perinuclear ring structures can be seen in figure 41, highlighted by the white arrow.

Perinuclear location of incorporated BrdU in this preliminary work is consistent with DNA repair since it has been reported that damaged DNA is shuttled to the pores in the nuclear membrane to allow access to necessary scaffold and repair proteins found in the perinuclear region (Nagai et al. 2008). For confirmation of this suspected perinuclear subcellular localisation, future work would look to repeat this experiment in combination with the presence of a nuclear stain such as DAPI or Hoescht 33343.

Attempts were made to combine staining for BrdU with B cell and T cell markers to determine whether incorporation was restricted to either CLL MNC or $hdaCD4^+$ T cells. However the processing required to render incorporated BrdU accessible for staining destroyed the antigenicity of both B and T cell markers.

Despite these limitations, these new observations in combination with earlier data would be consistent with the hypothesis that co-culture of CLL MNC with $hdaCD4^+$ T cells can induce T cell-driven CLL MNC DNA repair. However, it is not possible to rule out a reciprocal induction of DNA repair in T cells by co-culture with CLL MNC. Mutual protection in this way could underlie the common improvements in sustained viability *in vitro* when CLL

MNC and hdaCD4$^+$ T cells were co-cultured. It should also be noted that proliferation of a small proportion of the T cell population in these co-cultures may also be occurring and account for the ^{3}H-thymidine incorporation observed.

4.7 Discussion

Overall the data presented in this chapter have produced several significant findings which will impact future interpretations of data and has given a new insight in to the role that T cells may play in the CLL LN.

Firstly, this work has shown that monitoring ^{3}H-thymidine incorporation as a measure of proliferation should always be performed in conjunction with other assays for confirmation.

Although co-culture of CLL MNC with hdaCD4^{+} T cells induced the incorporation of ^{3}H-thymidine, these co-cultures showed only a small amount of proliferation by CellTrace™ analysis and this was not confirmed by cell cycle profile analysis. Further investigations using BrdU as an alternative thymidine analogue indicated that a proportion of this incorporation may be due to the activation of a DNA repair response, although it should be noted that these data were early preliminary findings and would need confirmation in future work. Nevertheless, the response is specific to co-culture wells and is seen to a higher level where CLL MNC have been irradiated prior to culture. These data may also be consistent with the presence of a small population of actively proliferating T cells within the co-cultures, at a level too low to be clearly observed in cell cycle analysis and only seen in small numbers when observing the CellTrace™ data.

Furthermore these data have indicated that non-CLL-non-T cells have an impact on this ^{3}H-thymidine uptake response either through direct or indirect means. These data support the understanding that multiple cell types within the CLL LN are likely to contribute to CLL survival and disease progression.

An alternative explanation for the suspected perinuclear distribution of BrdU incorporation in co-cultures is the induction of mitochondrial replication which can also be focused

perinuclearly (Calkins & Reddy 2011; Lentz et al. 2010). However mitochondrial replication also localises to other additional subcellular areas which are not observed in these experiments (Calkins & Reddy 2011). Future experiments should seek to confirm and further clarify the subcellular distribution of BrdU incorporation in co-cultures.

Subsequent work within this project concentrated upon the interaction of CLL cells with other cell types in the LN microenvironment, focusing on monocyte-derived cells which have been previously indicated as a significant contributor to disease (as discussed in Chapter 1.5.3).

5 MACROPHAGES & NURSE-LIKE CELLS IN THE CLL LN

5.1 Introduction

Data shown here in combination with findings from other groups highlight the significant role that non-T cells have upon CLL cells. In recent studies the supportive role of Nurse-like cells (NLC) in the LN has been extensively investigated *in-vitro* using PB as the source (Burger et al. 2000; Ysebaert & Fournié 2011; Tsukada et al. 2002). As discussed in Chapter 1.4.3, the presence of these cell types within the LN has recently been suggested however little work to confirm this has been performed. As such this project sought to investigate the presence of macrophages and NLC within the CLL LN, primarily to confirm their presence in the node and further to consider this presence in the context of stage of disease.

In addition, the balance of CLL cells with T cells and NLC in the CLL LN were considered in concert and collated data indicated a potential new method for categorising CLL patients based upon the proportions of these three cell types within the LN.

5.2 Nurse-like Cells have a variable presence in CLL LN unrelated to disease stage

As described in Chapter 1.4.3, NLC are cells derived from the monocyte lineage and gene expression profiling (GEP) experiments identified close similarities between NLC and the immunosuppressive macrophage subtype M2 (Ysebaert & Fournié 2011). NLC have been described as the tumour associated macrophage (TAM) of CLL (Ysebaert & Fournié 2011; Filip, Ciseł, Koczkodaj, et al. 2013; Lewis & Pollard 2006) and many *in vitro* studies have shown improved survival and drug resistance of CLL cells during their co-culture with autologous NLC (Nishio et al. 2005; Filip, Ciseł & Wasik-Szczepanek 2013; Burger et al. 2000; Tsukada et al. 2002).

Despite these relatively extensive investigations into the role of NLC *in vitro*, little has been shown regarding the presence of NLC in the LN microenvironment and as such this distinctive cell type has yet to be considered in context. In particular it has yet to be definitively confirmed that NLC are a significant component of the CLL LN and not a by-product of the long term *ex vivo* culture of CLL PB.

CLL LN tissue sections were stained for the presence of NLC utilising the surface expression of CD163. It should be noted that CD163 is also expressed by the M2 macrophage and as such future work would look to determine an independent marker of these cells for confirmation. The presence of $CD163^+$ cells was common across most CLL LN tissues but the total numbers varied greatly and in this cohort of samples did not associate with stage of disease (figure 42). It should be noted that sample P3 had no apparent $CD163^+$ in either Z1 or Z2 areas of the tissue and the cause of this is unclear. This striking absence may be important as $CD163^+$ were seen in both healthy and disease tissues and lack of these cells may represent a significant change in the biology of this sample.

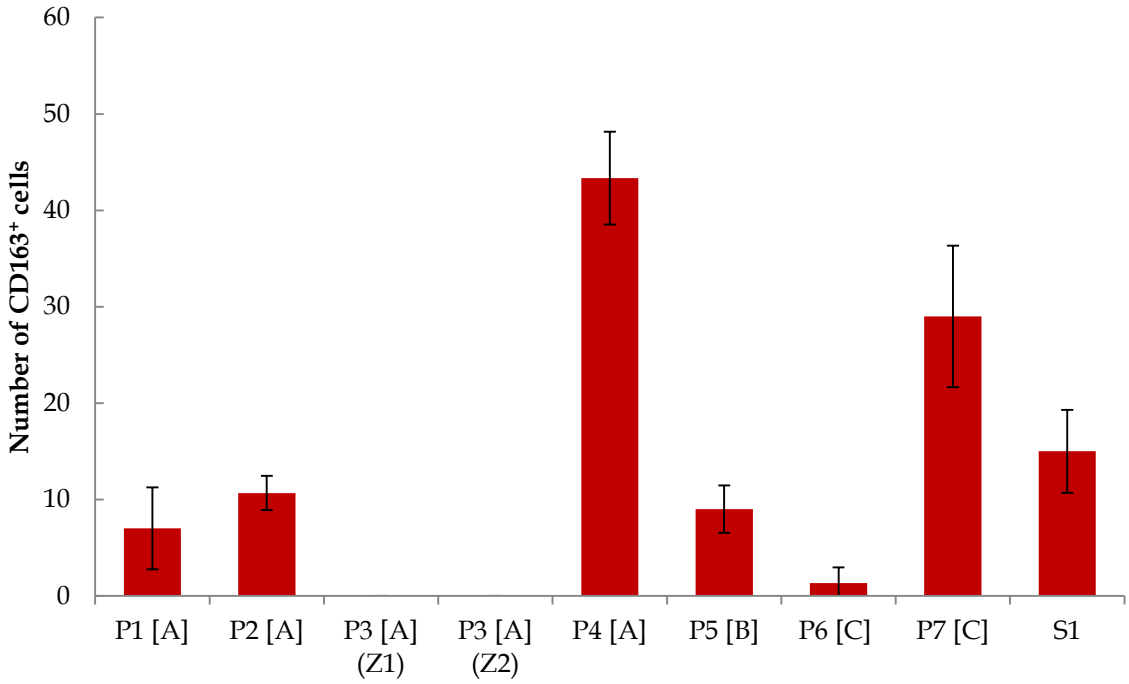

Figure 42. Average CD163⁺ cell presence is highly variable and does not correlate to disease stage.

Sections of seven CLL LN tissue samples and one healthy spleen sample were immunofluorescently stained for the expression of CD163. Three areas from each tissue were imaged (with the exception of sample P3, which had 3 areas images from each of Z1 and Z2) and these images were quantitatively analysed for CD68⁺ positivity using Fiji Image J analysis software. Numbers of positive cells were averaged across the three images collected for each sample and mean data is plotted ±S.E.M. Samples are labelled with [stage of disease] along the x-axis.

Figure 43 shows representative images of stage A and C disease tissues stained for the presence of $CD163^+$ cells as well as healthy spleen tissue for comparison. $CD163^+$ cells were not isolated to disease tissue alone but were seen in significant numbers in healthy spleen tissue. Despite the presence of these cells in both healthy and disease tissues, there were clear differences in their distribution within spleen tissue v.s. CLL LN tissues (figures 43 and 44) suggesting that despite a common cell surface marker, the cell types within healthy tissue differ in phenotype to those in the CLL LN. In healthy tissue, the $CD163^+$ cell population appear to be adjacent to $PAX5^+$ cells, whilst in CLL LN tissue, when present, $CD163^+$ cells appear dispersed within the $PAX5^+$ cell population (figure 44). This would support the current belief that whilst $CD163^+$ in the spleen may relate to normal M2 macrophages, $CD163^+$ in the CLL LN relates to NLC presence (figure 45). Future work is needed to address this possibility, although to date an independent marker for NLC has yet to be identified and so an alternative approach such as laser capture dissection and GEP of cells from these tissues may be better employed to confirm this theory.

Furthermore, despite close localisation of $CD163^+$ cells to $Ki\text{-}67^+PAX5^+$ cells (figures 44 and 45) no correlation was seen between proliferative activity and $CD163^+$ presence in these tissues.

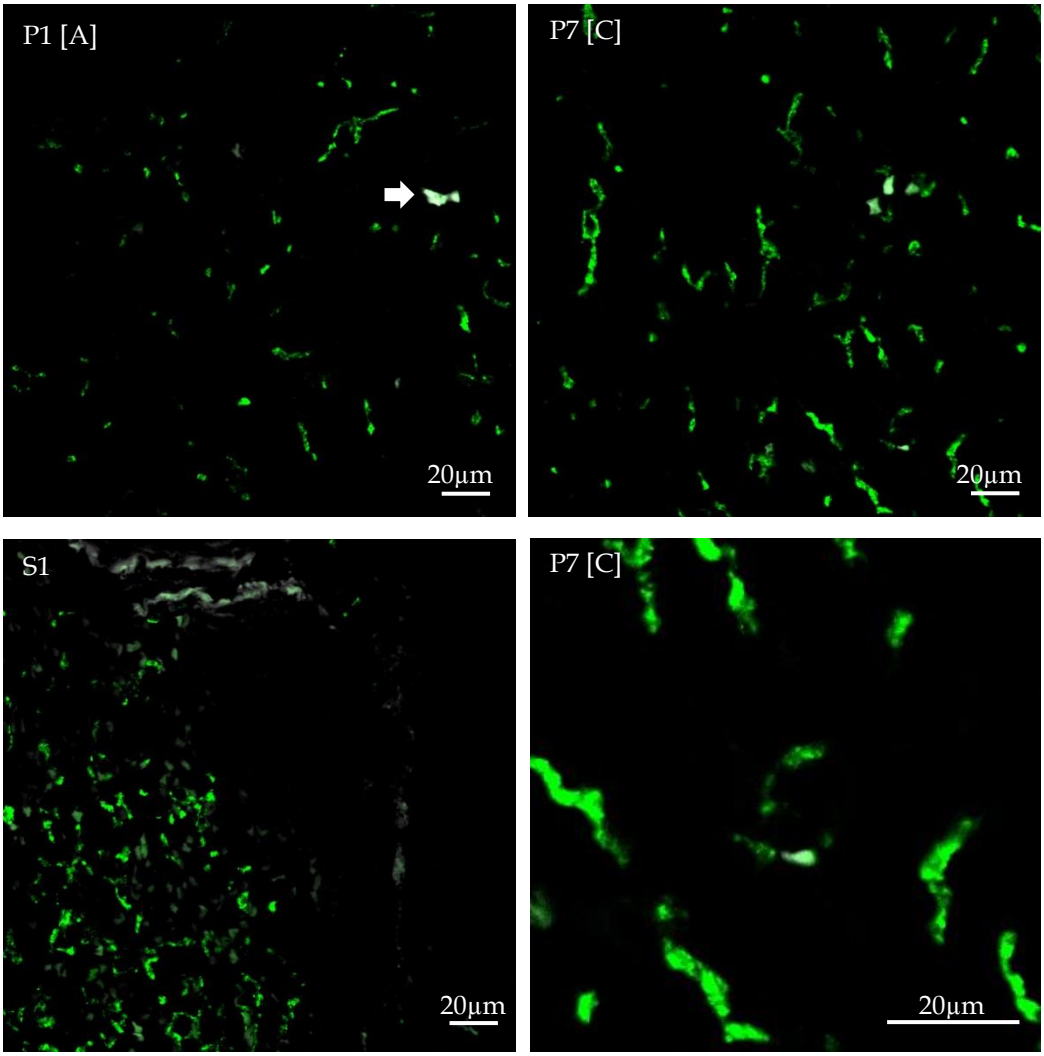

Figure 43. CD163⁺ cells may be present in both early and late stage CLL cases and appear monocytic based on their morphology.

CLL LN and healthy spleen tissue sections were stained for the expression of CD163 (green). Representative images (x40 objective) are shown for stage A (n=1) and stage C (n=1) patient samples as well as healthy spleen tissue (n=1). The lower right image is a larger, cropped version of the upper right image to show morphology in greater detail. An example of false positive staining from a red blood cell is highlighted (white arrow). Samples labelled with patient code and [stage of disease].

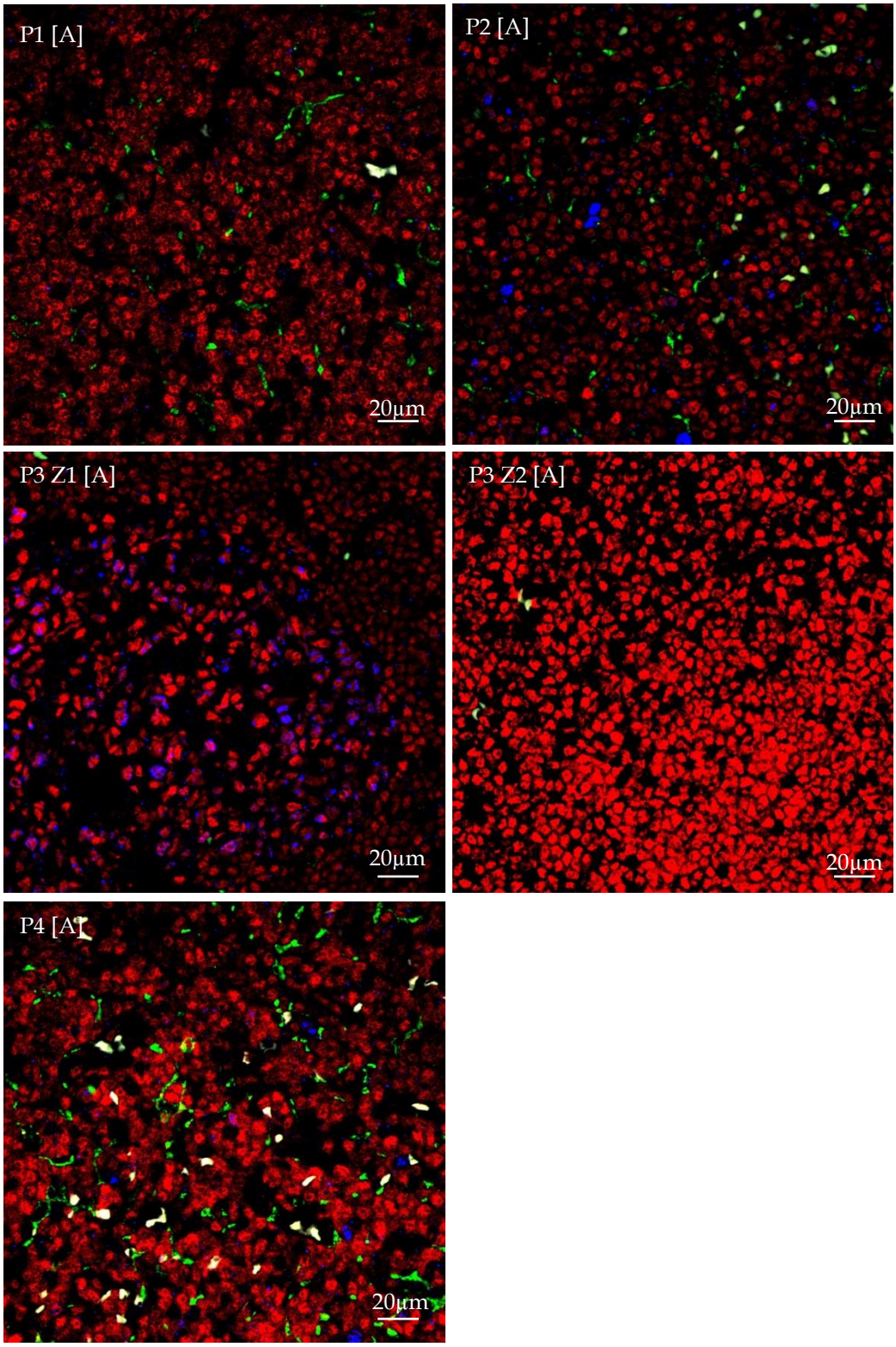

Figure 44A. The presence of CD163⁺ cells varies across CLL tissues irrespective of disease stage & their distribution is markedly different in healthy spleen.

CLL LN and healthy spleen tissue sections were stained for the expression of CD163 (green) PAX5 (red) and Ki-67 (blue). Representative images (x40 objective) are shown for stage A patient samples (n=4). Samples labelled with patient code and [stage of disease]. Further images for later stage disease and healthy spleen tissue shown below.

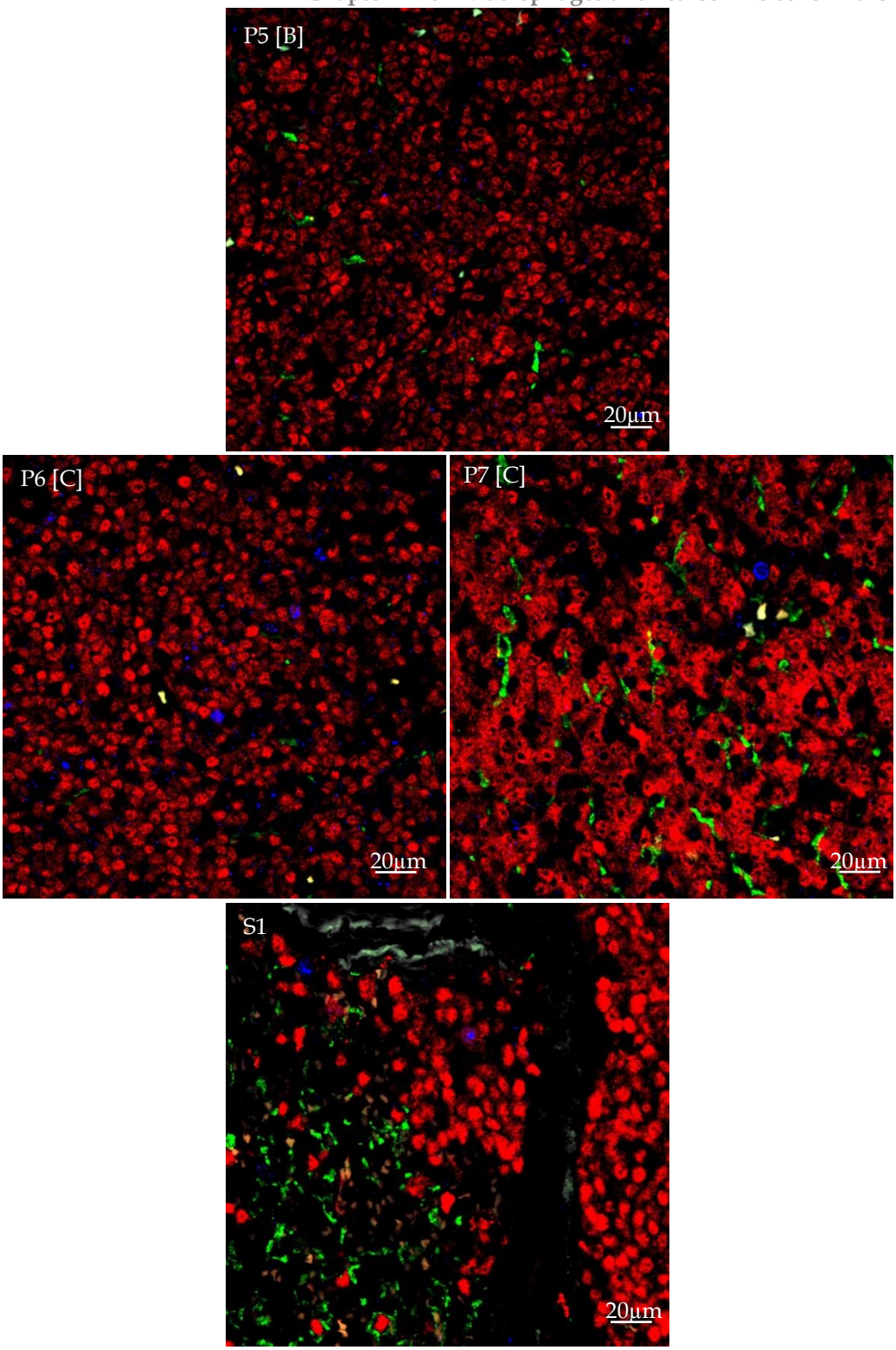

Figure 44B. The presence of CD163⁺ cells varies across CLL tissues irrespective of disease stage & their distribution is markedly different in healthy spleen.

CLL LN and healthy spleen tissue sections were stained for the expression of CD163 (green) PAX5 (red) and Ki-67 (blue). Continued from figure 44A; Representative images (x40 objective) are shown for immunofluorescent staining of stage B (n=1) & C (n=2) patient samples and healthy spleen tissue (n=1). Samples labelled with patient code and [stage of disease].

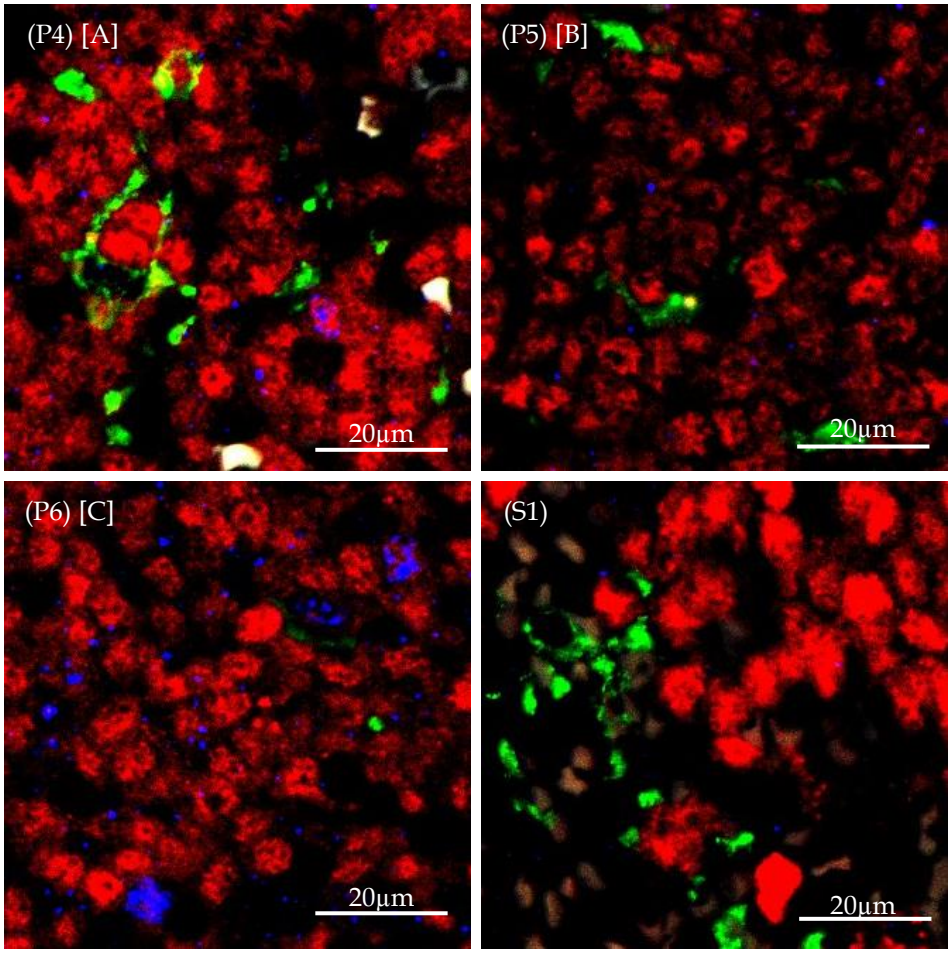

Figure 45. Differences in the distribution of CD163⁺ cells in CLL LN (at all stages of disease) compared to healthy spleen suggest an alternative phenotype in disease which may represent NLC.

CLL LN and healthy spleen tissue sections were stained for the expression of CD163 (green) PAX5 (red) and Ki-67 (blue). Representative images (x40 objective) are shown for stage A (n=1) stage B (n=1) and stage C (n=1) patient samples and healthy spleen tissue (n=1). Samples labelled with patient code and [stage of disease].

5.3 Macrophage presence diminishes correlated to stage of disease with no apparent relative increase in NLC

Macrophages have been reported to be present within the CLL LN (Bürkle & Niedermeier 2007; Maffei et al. 2013) and their presence in these tissue samples was investigated by targeting the expression of CD68. The total number of $CD68^+$ cells in these tissues varied (figure 46), and their distribution in CLL LN was different to that seen in healthy spleen (figure 47A & B). Overall, the data indicated a general reduction in the frequency of macrophages per field of observation in CLL LN correlated to the advancement of disease (figure 48). Interestingly, as shown in chapter 5.2, this relative decrease in $CD68^+$ macrophages did not correlate to changes in $CD163^+$ cell presence in these tissues, despite previous reports that NLC are also $CD68^+$. These data may suggest that CD68 expression by NLC alters as disease advances but this is as yet inconclusive. Confirmation of NLC expression of CD68 across different disease stages requires further investigation, including dual staining of these tissues with CD68 and CD163.

Despite these contrasting findings concerning NLC CD68 positivity, the general reduction in $CD68^+$ cells (figure 48) does support the current understanding of growing immunosuppression within the niche as disease progresses, as lower "healthy" CD68+ macrophages would provide less opportunity for functional immune responses against CLL cells.

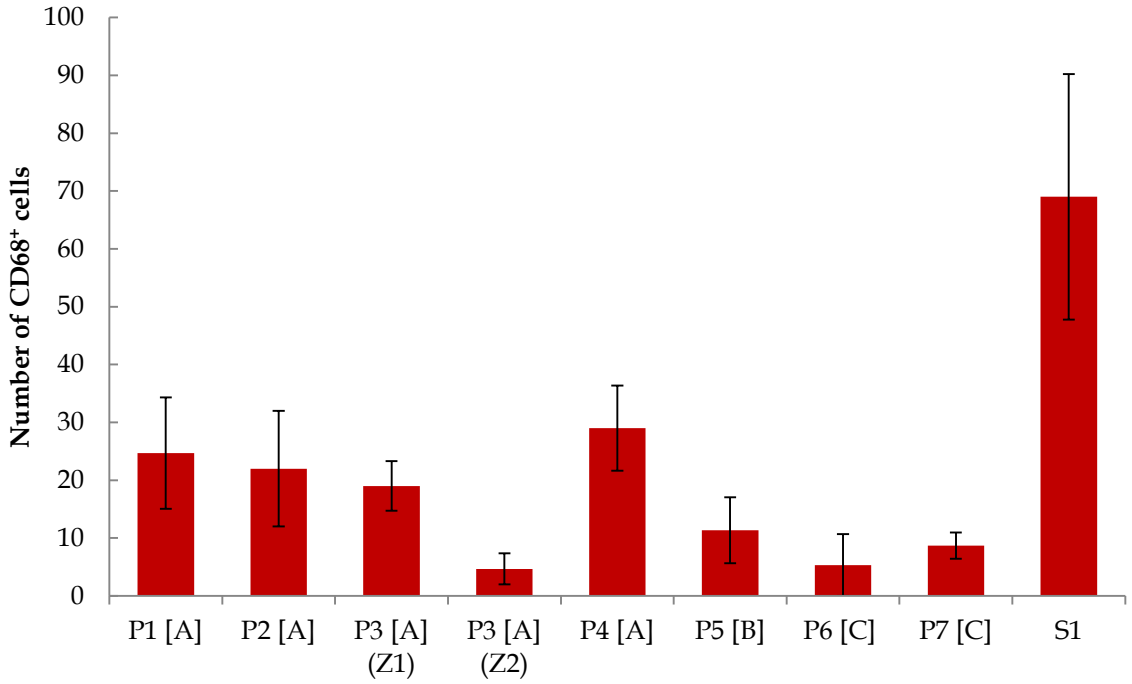

Figure 46. The frequency of CD68⁺ cells in CLL LN tissue varies between samples and is typically lower than healthy spleen tissue.

Sections of seven CLL LN tissue samples and one healthy spleen sample were immunofluorescently stained for the expression of CD68⁺. Three areas from each tissue were imaged (with the exception of sample P3, which had 3 areas images from each of Z1 and Z2) and these images were quantitatively analysed for CD68 positivity using Fiji Image J analysis software. Numbers of positive cells were averaged across the three images collected for each sample and mean data is plotted ±S.E.M. Samples are labelled with [stage of disease] along the x-axis.

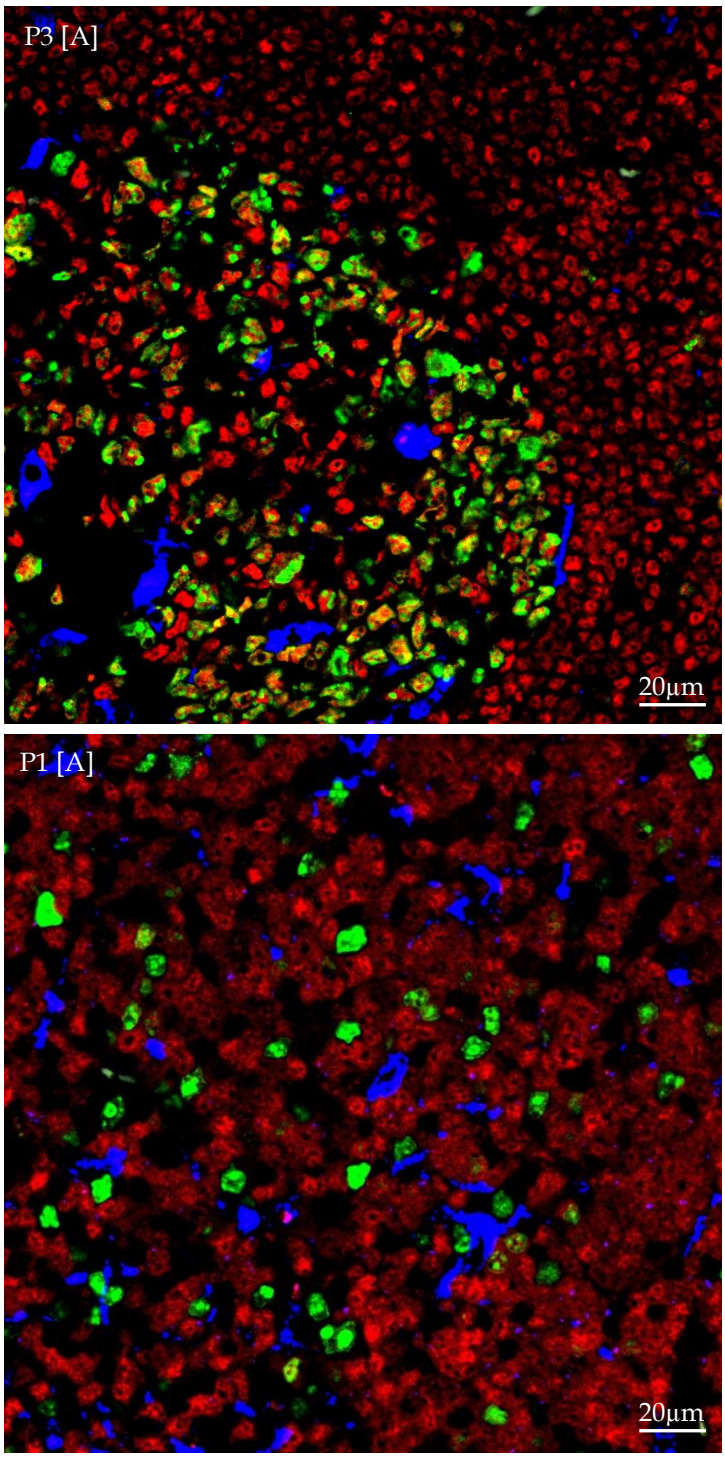

Figure 47A. Frequency of CD68⁺ cells varied across CLL LN samples and their distribution differs markedly from that seen in healthy spleen tissue.

CLL LN and healthy spleen tissue sections were stained for the expression of Ki-67 (green) PAX5 (red) and CD68 (blue). Representative images (x40 objective) are shown for stage A patient samples (n=2). Samples labelled with patient code and [stage of disease]. Further images for later stage disease and healthy spleen tissue shown below.

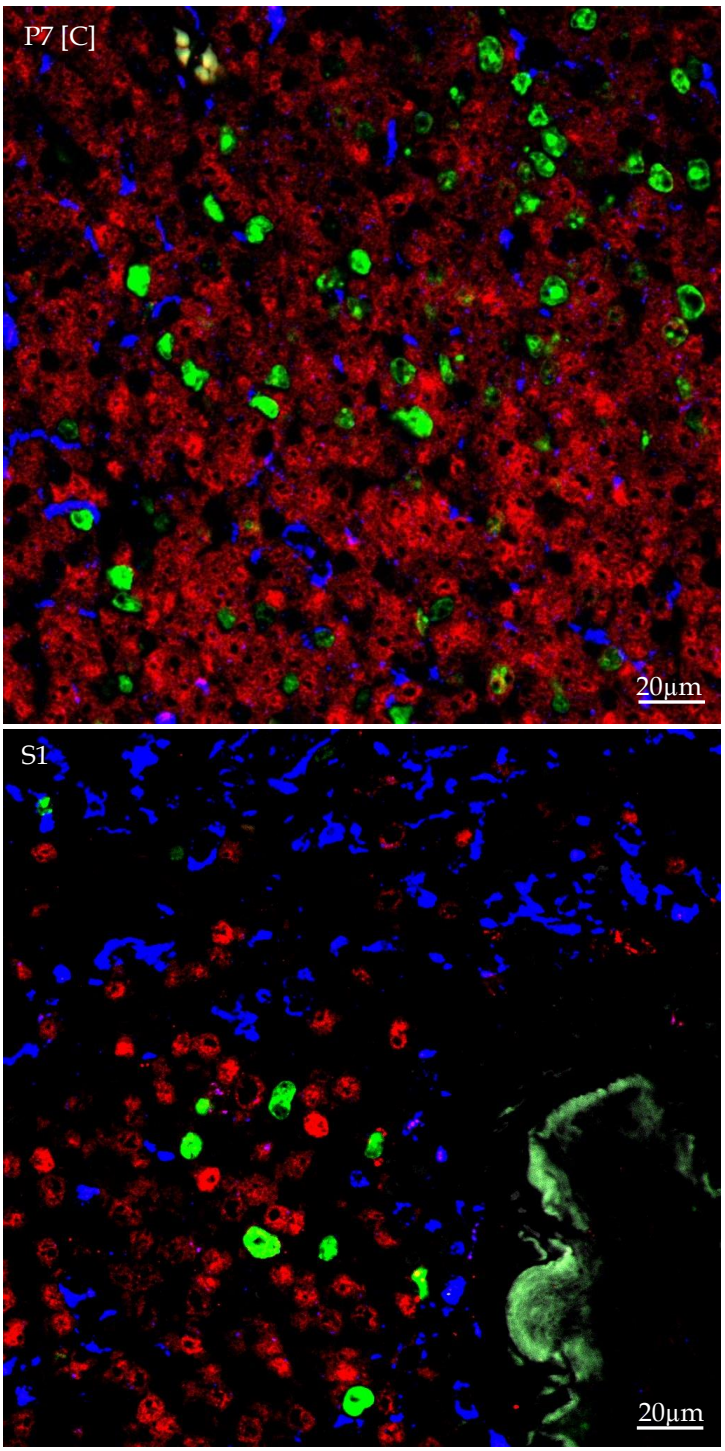

Figure 47B. Frequency of CD68⁺ cells varied across CLL LN samples and their distribution differs markedly from that seen in healthy spleen tissue.

CLL LN and healthy spleen tissue sections were stained for the expression of Ki-67 (green) PAX5 (red) and CD68 (blue). Continued from figure 47A; Representative images (x40 objective) are shown for immunofluorescent staining of a stage C (n=1) patient sample and healthy spleen tissue (n=1). Samples labelled with patient code and [stage of disease].

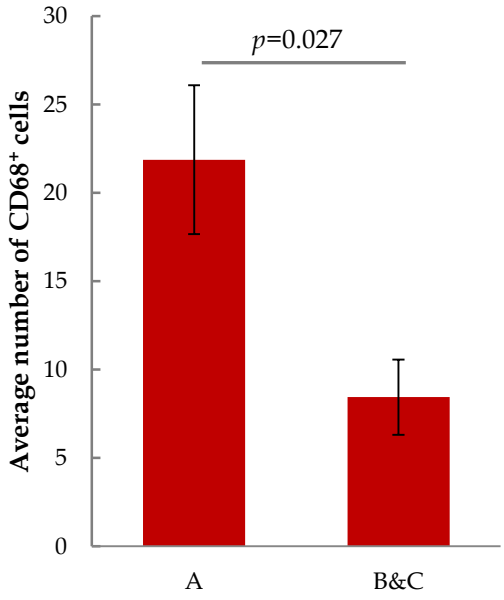

Figure 48. Comparison of early and late stage CLL tissue shows a decrease in CD68⁺ cells as disease progresses.

Sections of seven CLL LN tissue samples were immunofluorescently stained for expression of CD68⁺. Three areas from each tissue or zone were imaged and quantitatively analysed for CD68⁺ positivity using Fiji Image J analysis software. Numbers of positive cells were averaged across the three images and mean data collected for early (stage A (n=4)) and late (stage B & C (n=3)) samples to compare the presence of CD68⁺ cells. Average data are plotted ± S.E.M. and differences were statistically significant (students t-test).

5.4 Nicotinamide phosphoribosyltransferase (NAMPT) expression decreases suggesting a reduced recruitment of M2 cells in later stage disease

As discussed in Chapter 1.4.7, NAMPT is an enzyme and signalling molecule whose expression has been linked to the polarisation of macrophages to the M2 subtype in CLL, other diseases and in healthy tissues (Audrito et al. 2015). NAMPT has also been implicated as having a role in the recruitment of these cells to specific tissues. Whilst the levels of NAMPT have been studied in PB CLL samples and *in vitro* culture, little has been studied in the LN microenvironment. This project investigated the expression of NAMPT alone and in the context of PAX5 expression in these tissues. Representative images are shown of seven CLL LN tissue sections stained for the presence of NAMPT and PAX5 (figure 49A & B). Whilst $NAMPT^+$ cells often appear adjacent to $PAX5^+$ cells there is little to no cellular co-localisation indicating that CLL cells are not directly expressing this recruitment signal nor instructing the polarisation of macrophages to the M2 subtype. This supports previous demonstrations by other groups that NAMPT expression co-localises with CD163 expression, suggesting NAMPT is a monocyte derived signal and that recruited M2 or NLC present in the tissues are the source. In light of the data presented here, this expression by NLC/M2 cells in the LN may be induced by their close proximity to CLL cells.

These data showed variable expression of NAMPT across individual tissues (figure 50) and no direct correlation was seen between $NAMPT^+$ cells and either $CD163^+$ or $CD68^+$ cells within in each tissue. Nevertheless, average expression of NAMPT in early vs. late stage disease showed a reduction in expression as disease progresses (figure 51), reflecting the trend seen in $CD68^+$ cell presence. These data suggest that any M2 or NLC recruitment to the LN during later stage disease is at least partially NAMPT-independent, or that following their recruitment, NAMPT expression is switched off. Future work would look to stain

tissue samples with PAX5, NAMPT and CD163 markers simultaneously, to further clarify the cell types which may be expressing NAMPT in the CLL LN. This was not possible within the current project due to limitations on the combination of available NAMPT and CD163 primary antibodies (both were mouse monoclonal antibodies).

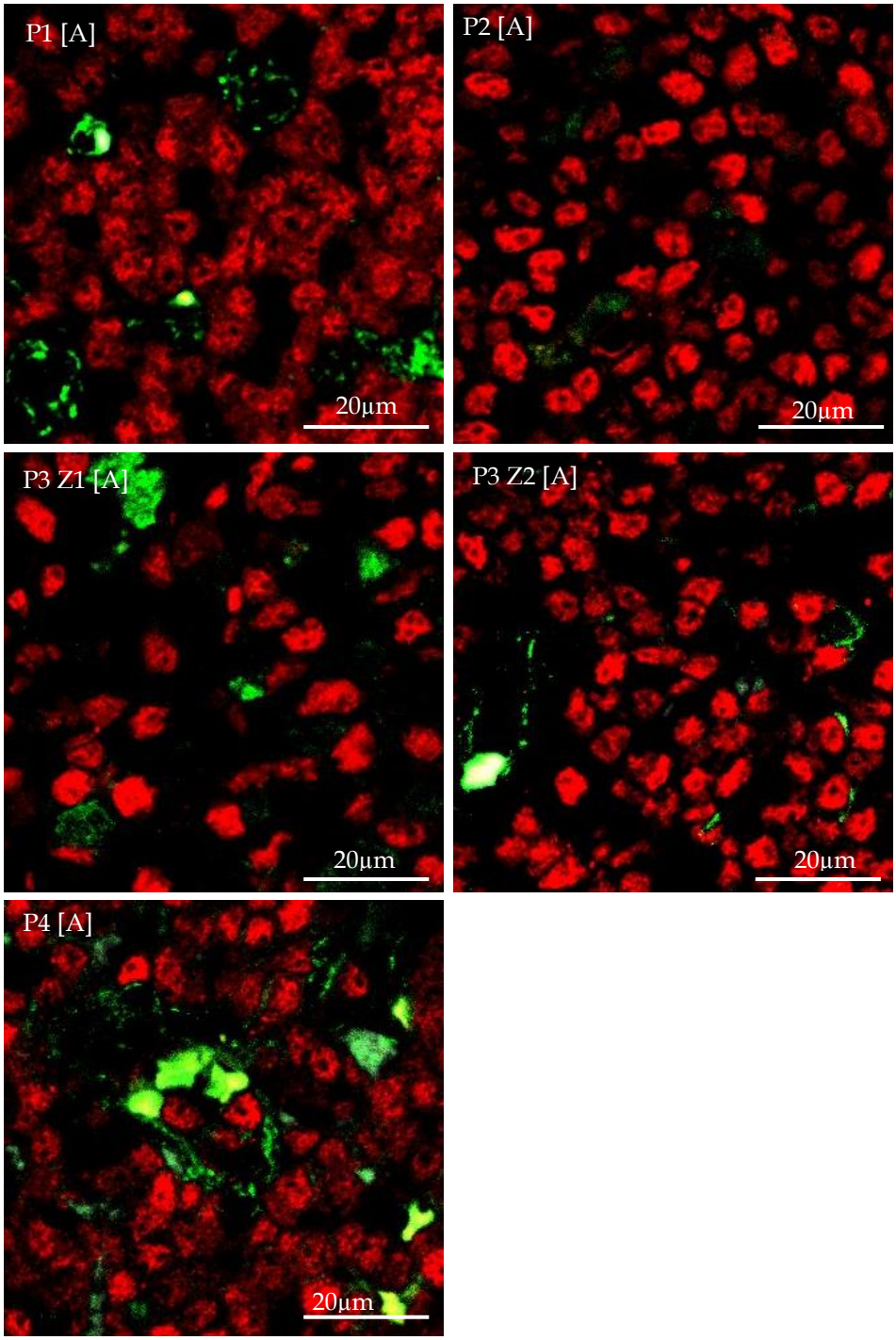

Figure 49A. NAMPT positivity in CLL is variable and localises adjacent to PAX5 staining indicating non-CLL cell expression in the LN.

CLL LN and healthy spleen tissue sections were stained for the expression of NAMPT (green) and PAX5 (red). Representative images (x40 objective) are shown for stage A patient samples (n=4). Samples labelled with patient code and [stage of disease]. Further images for later stage disease and healthy spleen tissue shown below.

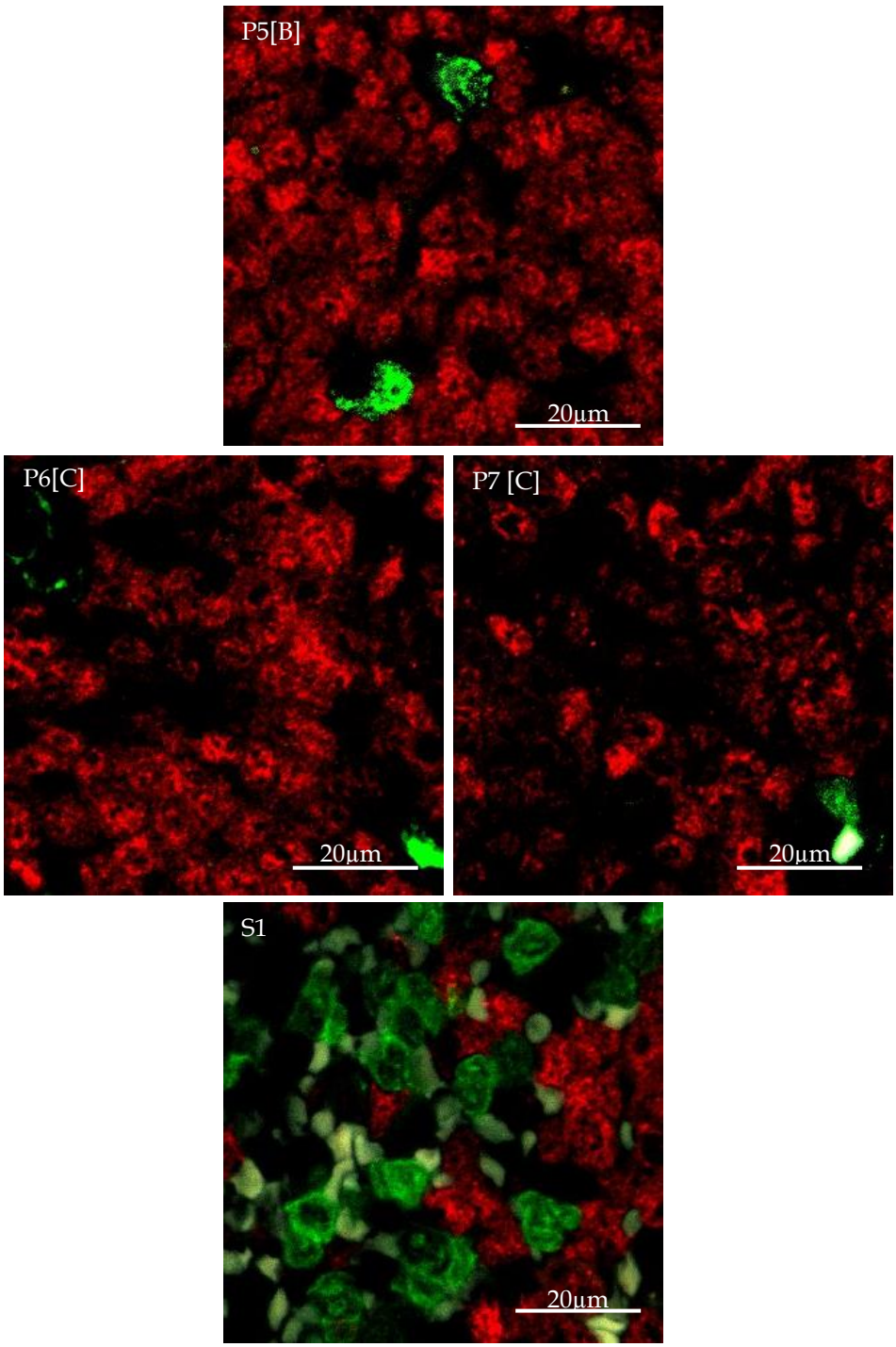

Figure 49B. NAMPT positivity in CLL is variable and localises adjacent to PAX5 staining indicating non-CLL cell expression in the LN.

CLL LN and healthy spleen tissue sections were stained for the expression of NAMPT (green) and PAX5 (red). Continued from figure 49A; Representative images (x40 objective) are shown for immunofluorescent staining of stage B (n=1) & C (n=2) patient samples and healthy spleen tissue (n=1). Samples labelled with patient code and [stage of disease].

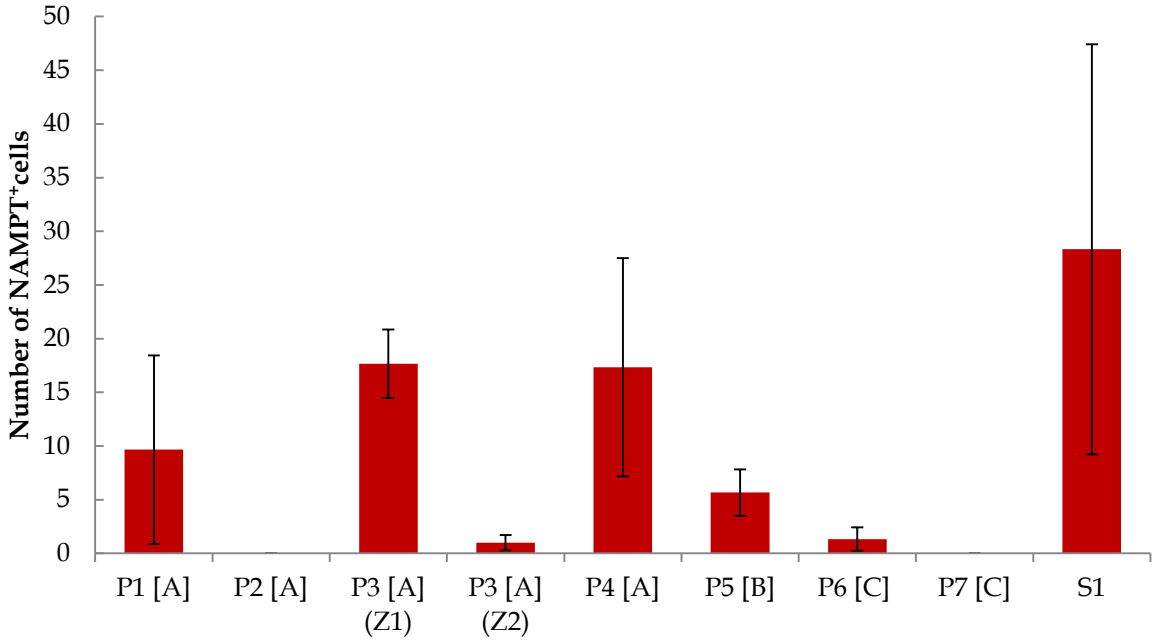

Figure 50. Expression of NAMPT is variable between CLL LN tissue samples.

Sections of seven CLL LN tissue samples and one healthy spleen sample were immunofluorescently stained for the expression of NAMPT. Three areas from each tissue were imaged (with the exception of sample P3, which had 3 areas images from each of Z1 and Z2) and these images were quantitatively analysed for NAMPT positivity using Fiji Image J analysis software. Numbers of positive cells were averaged across the three images collected for each sample and mean data is plotted ± S.E.M. Samples are labelled with [stage of disease] along the x-axis.

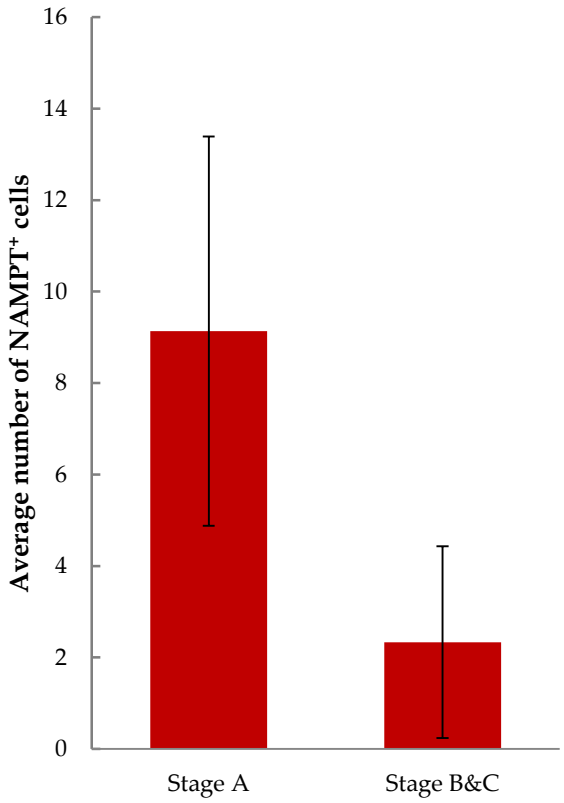

Figure 51. The comparative frequency of NAMPT expression in early and late stage CLL samples suggests a reduction in expression as disease progresses.

Sections of seven CLL LN tissue samples were immunofluorescently stained for expression of NAMPT. Three areas from each tissue or zone were imaged and quantitatively analysed for NAMPT positivity using Fiji Image J analysis software. Numbers of positive cells were averaged across the three images and mean data collected for early (stage A (n=4)) and late (stage B & C (n=3)) samples to compare the presence of NAMPT$^+$ cells. Average data are plotted ± S.E.M.

5.5 The balance of T cells and NLC in the CLL LN varies between patient samples and may reflect different subtypes of CLL

The interaction of CLL cells with T cells and NLC have been the focus of many studies within the CLL field. Whilst these cell types have been considered in isolation, the study of all three cell types in combination was deemed important to visualise potential interactions in the niche. Immunofluorescent staining of CLL LN and normal spleen for the presence of CD163, CD3 and PAX5 allowed consideration of the spatial distribution of these cell types (figure 52A & B) and quantitative analysis allowed insight as to whether proportions of these cell types correlated to stage of disease.

The CLL LN samples could be subdivided into samples with low, medium or high frequencies of $CD163^+$ cells, deemed NLC for this analysis. Based upon these groupings the proportions of all three cell types showed distinct differences.

Whilst "medium" NLC-containing LN had an average ratio of 35 CLL cells and 7 T cells for each NLC, "high" NLC–containing LN had an average ratio of 4 CLL cells and 2 T cells for each NLC. These represent comparatively different cellular balances within this important microenvironment. If these differences are representative of the general patient population, this would allow the construction of more representative *in vitro* models of CLL and aid in the development of new targeted therapies.

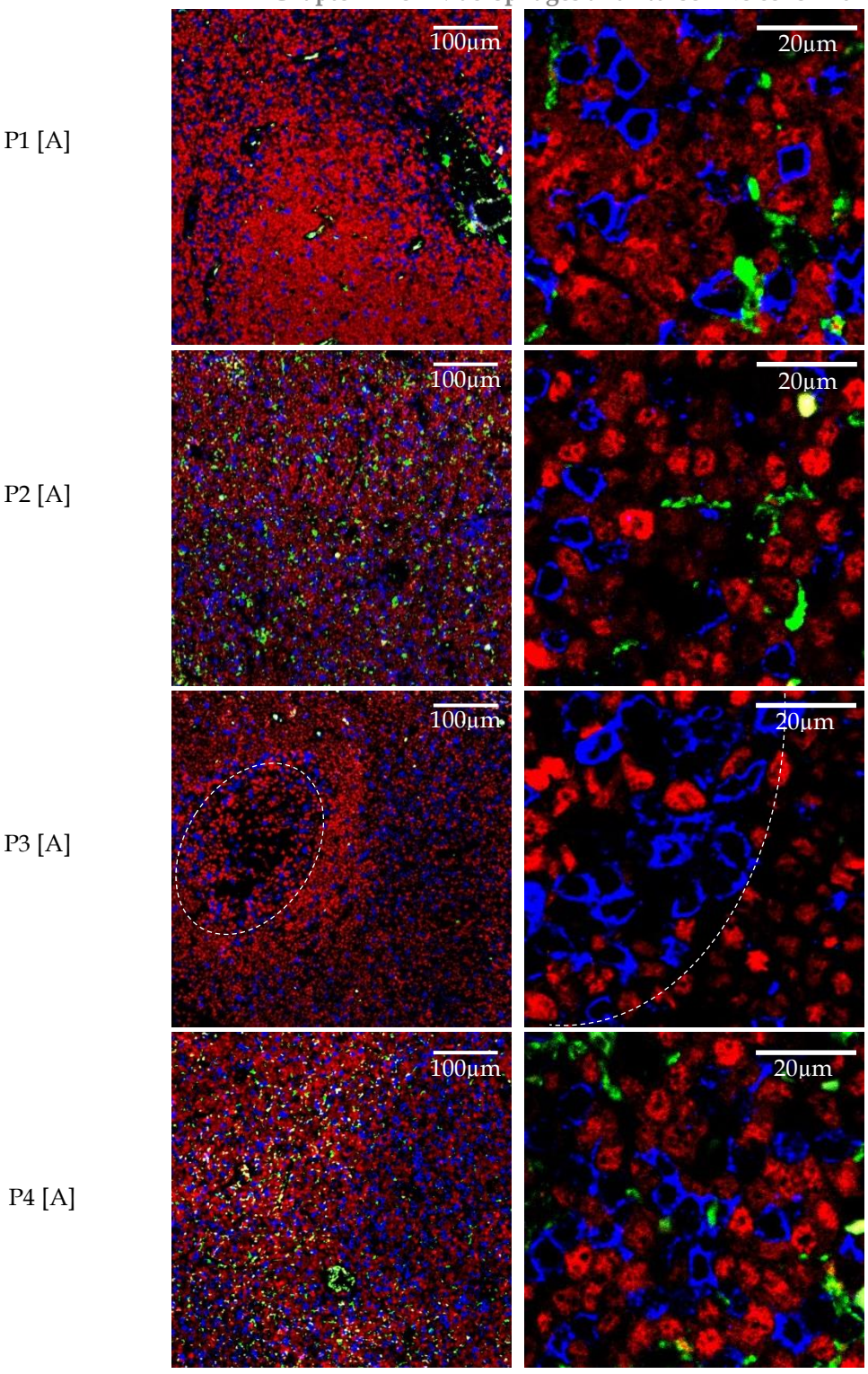

Figure 52A. Variable proportions and distribution of T cells & NLC in CLL LN tissue may highlight differences that could be exploited therapeutically.

CLL LN and healthy spleen tissue sections were stained for the expression of CD163 (green) PAX5 (red) and CD3 (blue). Representative images (x10 and x40 objective (left and right respectively)) are shown for stage A patient samples (n=4). Samples labelled with patient code and [stage of disease], further images for later stage disease and healthy spleen tissue shown below.

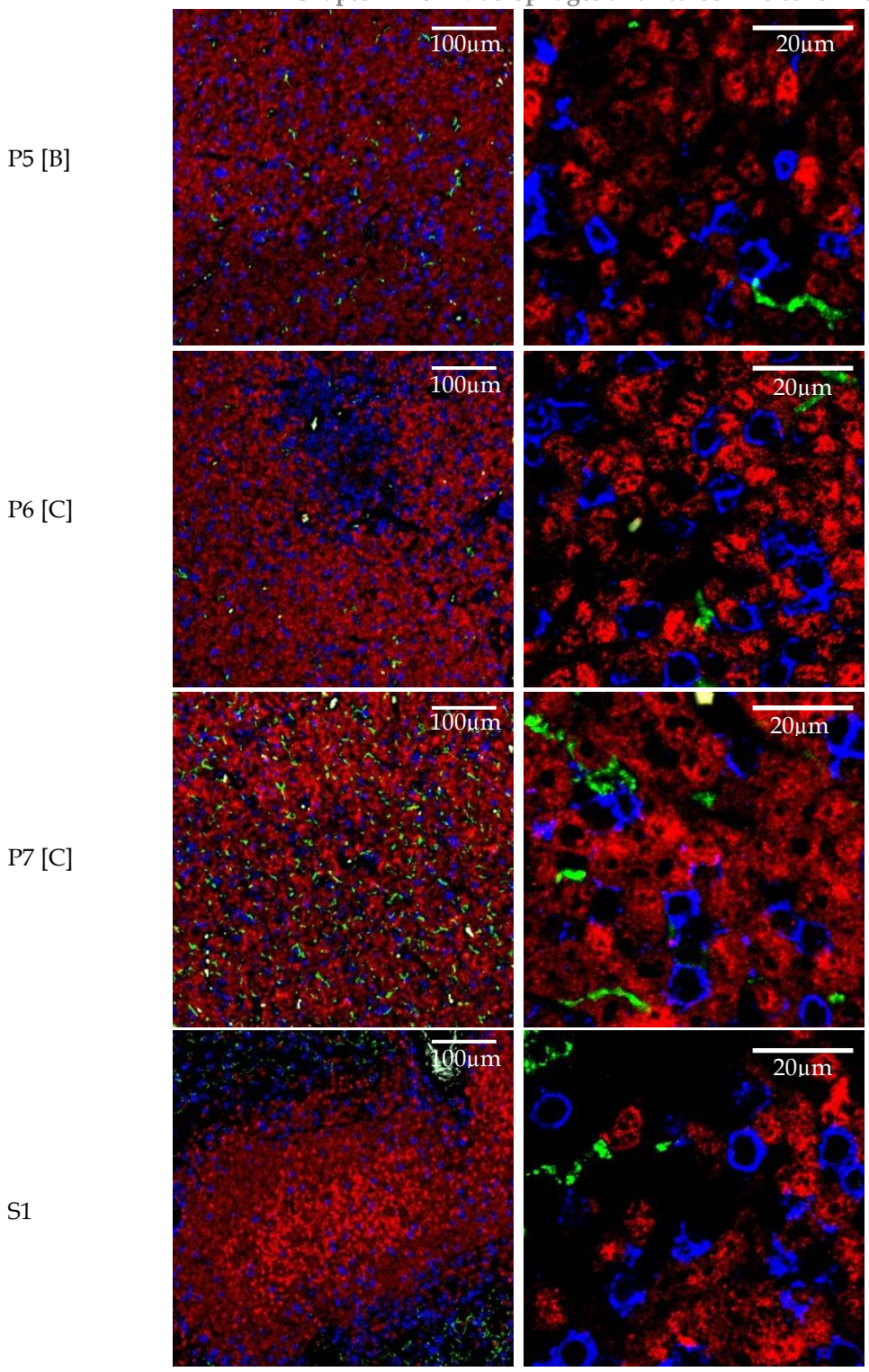

Figure 52B. Variable proportions and distribution of T cells & NLC in CLL LN tissue may highlight differences that could be exploited therapeutically.

CLL LN and healthy spleen tissue sections were stained for the expression of CD163 (green) PAX5 (red) and CD3 (blue). Continued from figure 52A; Representative images (x10 and x40 objective (left and right respectively)) are shown for stage B (n=1) & C (n=2) patient samples and healthy spleen tissue (n=1). Samples labelled with patient code and [stage of disease].

5.6 Discussion

These data have supported the concept that NLC are present within the CLL LN microenvironments although $CD163^+$ appears highly variable, unrelated to disease stage and unconnected to the reduced presence of $CD68^+$ cells in these nodes. Whilst NLC have been previously compared to the immunosuppressive M2 phenotype and share a common extracellular marker, the data collected also fails to show a connection between CD163 and NAMPT expression in the tissues. These data do serve to highlight the complexity of the involvement of monocyte/macrophage subtypes within the CLL LN and highlights that teasing apart this component of the niche will require further in-depth interrogation of tissues with more specific panels of markers.

Furthermore, the data collected from immunofluorescent staining within this project have also highlighted the close spatial relationship of T cells and NLC ($CD163^+$ cells) to CLL cells *in vivo*. Analysis of the ratios of these supportive cell types have revealed that consideration should be given to their proportions within individual patient samples as this may reflect different subtypes of disease. These data warrant future investigation to determine their significance.

6 GENERAL DISCUSSION

6.1 Discussion

This study sought to investigate the cellular contents and interactions within the CLL LN, through a combination of *in vitro* co-cultures and *ex vivo* interrogations of FFPE CLL LN tissues. Ultimately, this project aimed to inform a real-world view of this complex microenvironment and highlight the potential benefits of harnessing archived tissues to better understand this important niche.

The CLL LN was investigated for its proliferative signature using Ki-67 expression and comparative H&E staining. The Ki-67 data indicated a lack of the traditionally envisaged CLL proliferation centres in all but one CLL sample, a finding contrary to most current literature discussions (Ciccone et al. 2012; Soma et al. 2006; Ponzoni et al. 2011). Reports of proliferation centres within CLL LN tissue discuss distinct "pale" areas of tissue (H&E staining) containing a concentration of Ki-67$^+$ cells (Schmid & Isaacson 1994; Bonato et al. 1998). However, when this study considered the Ki-67 expression of CLL LN tissues, in combination with many other markers across serial sections of samples, distinct centres of proliferation were absent in all but sample P3 - despite the appearance of these structures in the H&E staining data. These data suggest that proliferation centre may be a misnomer, where these pale areas seen in H&E staining relate more to the interaction of CLL cells with different supportive cell types rather than areas of intense proliferation. Indeed this work is supported by observations of such architecture by other groups (Vandewoestyne et al. 2011) and may indicate that the use of the alternative name for these areas – pseudofollicles – would be more appropriate. This concept requires further investigation.

Initial studies also revealed that as disease progresses, tumour cells appear to lose some of the normal features of B cells, as evidenced by the decreased expression of the important pan-B cell marker PAX5. Tissue sections were analysed for their mean fluorescence intensity

of PAX5 signal (instead of numbers of cells expressing PAX5) due to a limitation in the sensitivity of the analysis software in distinguishing adjacent $PAX5^+$ cells from one another. As such, the observation that PAX5 expression decreases as stage of disease progresses will need further investigation to determine whether it represents a reduction in the total number of cells expressing PAX5, a reduction in the amount of PAX5 expression within individual cells or a combination of these scenarios. Regardless of the mechanism of $PAX5^+$ reduction, this is a key finding. PAX5 is an important transcription factor which directs the development of CLP along the B cell lineage, expressed from the pre-B cell stage of development until B cell differentiation into plasma cells (Cobaleda et al. 2007). Mutations in this transcription factor have been indicated to predispose individuals to B cell Acute Lymphoblastic Leukaemia (B-ALL) (Hyde & Liu 2013) and it has been recently shown that $PAX5^-$ Mantle Cell Lymphoma cells have higher levels of proliferation, are more invasive *in vivo* and display a higher resistance to current therapy (Teo et al. 2015), confirming a role for this transcription factor in tumour progression. Even more indicative of a change in biology is the reduction seen in $Ki67^+$ tumour cells; whilst the average drop in PAX5 expression in stage B&C samples compared to stage A samples was ~33%, the drop in $Ki\text{-}67^+PAX5^+$ cells between these stages was ~66%, indicating that proliferative tumour cells are more likely to have reduced PAX5 expression. When considered in this context, the reduction in PAX5 expression seems telling of a gradual underlying change in the tumour cell biology of CLL. This hypothesis could only be confirmed by the staining of serial tissue samples from the same patients to follow disease progression over time.

Proliferative $Ki67^+$ CLL cells were shown to be often adjacent to T cells, which were dispersed throughout the tissues. Whilst the presence of T cells, even when considering subtypes, appeared unrelated to stage of disease it was apparent that the structural layout of

the CLL LN varied from sample to sample and this structural degradation may be linked to disease stage.

The balance of apoptosis and proliferation was interrogated using Ki-67 and cleaved caspase 3 expression in each of the samples, demonstrating that even from early stage disease the balance between these fundamental cellular processes are skewed. This finding fits well with the current understanding that the CLL LN is a pro-survival environment for CLL cells and in combination with data from other groups indicates that the relatively significant amount of CLL cell death per day (estimated up to ~$1x10^{12}$ CLL cells die per day (Messmer et al. 2005; Chiorazzi 2007)) predominantly occurs in the periphery. This further supports the notion that prolonged exclusion from the supportive LN microenvironment alone may well be sufficient to induce cell death in CLL cells and is supported by the efficacy seen of the BCR inhibitor therapies which exclude cells from the node. It was intriguing to note the variability between different patient samples in their ratios of proliferation to apoptosis; for example both samples P2 and P4 were classed as stage A CLL disease but had a distinctly higher balance of proliferation to apoptosis compared to other stage A samples in this study. It would be interesting to determine whether this reflected the type of disease these patient samples represent (e.g. early v.s. late stage A or perhaps M-CLL v.s. U-CLL samples) and future work will look to determine whether these samples do differ in their biology. Future work will also look to investigate other markers of apoptosis which could be used to confirm these intriguing preliminary findings.

Based on these initial data and the visually intriguing intimacy of T cells to the proliferative components of the tumour clone in CLL, an *in vitro* study was initiated to look into T cell-CLL cell interactions. In healthy individuals, $CD4^+$ T_h cell activation, through engagement of the MHC II on B cells induces proliferation of the T cell, up regulation of CD40L on its cell

surface and subsequent reciprocal activation of the B cell; ultimately leading to both cell types proliferating (Klaus et al. 1999).

Here a co-culture assay was used to investigate the interactions between T cells and CLL cells. The experiments used allogeneic T cells, isolated from healthy volunteer donors (hdaCD4$^+$ T cells). As CLL cells have been shown to dysregulate the T cell compartment in CLL, using autologous T cells in these cultures would have required artificial stimulation prior to co-culture, for example the addition of anti-CD3 and anti-CD28 activating antibodies. This stimulation could have potentially masked any observation of cognate CLL:T cell activation. Unlike autologous T cell interactions, allogeneic T cells co-cultured with CLL cells should induce a non-self-immune response. As inducers of a non-self-immune response it was predicted that interactions of allogeneic T cells and CLL cells would drive the up-regulation of CD40L expression by CD4$^+$ T_h cells and induce the release of activating cytokines, such as IL-2 and IL-4 (Saudemont & Madrigal 2014; Ramsay et al. 2008). The presence of such signals would reciprocally activate the CLL cells to proliferate. In this way the use of allogeneic T cells would promote CLL cell proliferation and survival, via many of the cognate and paracrine signals hypothesised to be important during CLL:T cell interactions in the malignant LN. However, despite this expectation, the data presented here indicates that the majority of hdaCD4$^+$ T cells do not proliferate in response to co-culture with CLL samples and nor do they induce proliferation of CLL cells.

The lack of CLL cell proliferation in this co-culture is informative, indicating that there were insufficient stimulatory signals present to induce CLL proliferation. As such, the co-culture does not recapitulate the proliferative qualities of the LN microenvironment (as can be seen from data presented in Chapter 4). Despite a lack of CLL cell proliferation, the co-cultures did replicate the protective aspects of the LN microenvironment. Co-cultures cells had

higher viability compared to each cell type cultured alone indicating the induction of a pro-survival signature for both cell types.

As discussed in Chapter 4.7 the staining of BrdU incorporation seen from cells in co-culture wells appeared strikingly different in its localisation and quantity when compared to actively proliferating cells. The distribution of this staining, which appeared reminiscent of perinuclear localisation, is unlikely to be a consequence of mitochondrial replication as the subcellular localisation of this is understood to be both perinuclear and dispersed within the cytoplasm (Calkins & Reddy 2011; Lentz et al. 2010), which was not apparent in these images. If confirmed by future work - by combining this staining with a nuclear stain - this would suggest that cells within the co-culture are undergoing DNA repair processes, where perinuclear localisation is due to the transport of damaged DNA to nuclear pores for repair (Lee 2001, Nagai 2008). Confirmation of these data is required and should also include an assay that can determine levels of DNA damage and repair, such as the comet assay (Collins 2004).

The data also show that the irradiation of CLL samples prior to their co-culture produced a higher incorporation of ^{3}H-thymidine than non-irradiated samples. Irradiation has been shown to cause DNA damage and cell cycle arrest as part of the cellular stress response (Bluwstein et al., 2013). In light of this, it could be proposed that "additional" DNA damage present in the CLL samples caused by irradiation prior to co-culture is reflected in a higher amount of DNA repair during culture.

It has been previously described that CLL samples are capable of DNA repair within 2 hours of treatment with DNA damaging agents, although this ability varies greatly between samples (Muller 1997) and is at relatively low levels (Barret et al. 1996). As CLL cells appear

predisposed to DNA repair, the data presented here suggest that it is the CLL cells within the co-culture, rather than the hdaCD4$^+$ T cells, that are undergoing DNA repair and that these high levels of repair are only possible in the presence of T cells. In addition, it could be postulated that the non-CLL MNC fraction (which would include autologous T cells) could be responsible for previously reported low-level DNA repair. As such, future work for this study should consider the role of autologous T cells present within the co-culture assay. These collective data insinuate that CLL cells initiate DNA repair in the presence of allogeneic T cells and that this response may reflect a process that also occurs with autologous T cells.

Overall these findings have considerable implications when considering the CLL LN microenvironment. It is understood that the LN microenvironment can protect CLL cells from many front-line therapies but the exact mechanisms are as yet unclear. If the responses seen in this study are confirmed in future work and are similar to the effect that autologous T cells have upon CLL cells in the LN microenvironment, this would indicate that T cells in the LN assist CLL cells initiating DNA repair following chemotherapy and/or radiation therapy. When considered in the context of current front line therapies used to treat CLL this information becomes even more intriguing. The gold standard of therapy in CLL treatment for many patients remains the chemoimmunotherapy combination FCR.

These data would suggest that the way in which patients are treated could be improved to minimise the protective effect of the CLL LN and produce more robust remissions. The use of a T cell targeting therapy in combination with current front-line DNA damaging agents may help reduce the ability of CLL cells to recover from this treatment. Alternatively, it could be recommended that future combinations of therapies should exclude DNA

damaging agents entirely, or include inhibitors of DNA repair in order to minimise the induction of support from the CLL LN following treatments.

Whilst this theory of T cell driven CLL cell DNA repair is intriguing, an alternative explanation for the current data can be proposed. This is that a small population of T cells within the co-culture have consistently and exponentially proliferated over the course of 5-7 days. In doing so, they account, at least in part, for the large amount of ^{3}H-thymidine incorporation seen by the end of the co-culture experiments. This expanded cell population is likely to be of hdaCD4^{+} T cell origin as it is present within both irradiated and non-irradiated co-cultures. Despite the observation of a variable and small presence of proliferating T cells via CellTrace™, the lack of detection of this population via cell cycle analysis remains discouraging. However, it should be noted that these co-cultures were analysed for cell cycle activity and CellTrace™ analysis at day 5 whilst the peak incorporation of ^{3}H-thymidine was seen at day 7 and this may account for the discrepancies seen between these forms of analysis. Future work should look to measure CellTrace™ and cell cycle activity every 24 hours for 7 days of co-culture to determine if there are any changes in either parameter that can be observed. This would need careful planning as the amount of available primary material to initiate these experiments was a continuing limitation within this project. Nevertheless, if a small population of hdaCD4^{+} T cells are proliferating in these co-cultures, future work should look to determine whether they represent a specific subset of T cells. Based on current data which demonstrated an increase in the viability of CLL cells and T cells within these cultures, it could be postulated that these cells are unlikely to be Th1 effector cells, which have a role in Fas-mediated cell killing. Alternatively, if this population of expanding cells are Th1 cells, their ability to induce CLL cell death may have already been perturbed by the presence of CLL cells within the cultures,

similar to the reported effects CLL cells have upon autologous T cells as discussed in Chapter 1.5.3.

This work highlights the potential for misinterpretation of ^{3}H-thymidine incorporation, which is still routinely used as a marker of proliferation and of DNA damage repair. This study suggests caution in its future use and recommends that it be used as a tool in combination with several other markers of cellular proliferation or DNA repair to elucidate the true meaning.

The data also indicated that a proportion of ^{3}H-thymidine incorporation within co-culture wells was driven by the presence of accessory cells, from the non-CLL MNC fraction of CLL PB. The additive responses seen by unpurified CLL samples in these co-cultures advocates the use of unpurified CLL samples during *in vitro* culture to better represent the cellular presence in the LN. Additionally these data suggest a significant role for other cell types in supporting CLL DNA repair processes and/or the expansion of T cells.

Finally, it should be noted that these data need to be compared with the co-culture of hdaCD4^{+} T cells and healthy B cell or healthy MNC counterparts to determine if the responses seen are truly CLL specific.

In addition to T cells, macrophages and NLC are of significant interest within the CLL LN microenvironment due to studies showing their ability to promote CLL cell survival and drug resistance (Burger et al. 2013; Burger et al. 2000). As mentioned in Chapter 1, NLC are thought to derive from the monocyte/macrophage lineage and represent the tumour associated macrophage population within CLL (Filip et al. 2013). These NLC have been shown to express CD163 in addition to CD68 *in vitro* and as such are difficult to distinguish from the M2 polarised macrophage population (Giannoni et al. 2014; Tsukada et al. 2002;

Burger et al. 2000; Ysebaert & Fournié 2011). Nevertheless, the role of tumour-associated macrophages in solid cancers has been well documented (Lewis & Pollard 2006) and CD163 is used as a marker of tumour associated macrophages (TAM) in classical Hodgkins lymphoma (Harris et al. 2012), with its presence being shown to predict outcome in these patients (Klein et al. 2014).

As the presence of NLC in the CLL LN had not been widely investigated, this project examined the presence of $CD163^+$ cells in these tissues to provide a putative insight into NLC presence in this niche.

Whilst initial studies herein confirmed the presence of $CD163^+$ cells in the CLL LN microenvironment it also highlighted the large variability of this presence. Although a reduction in both $CD68^+$ cell presence and NAMPT expression correlated to stage of disease this did not appear to relate to $CD163^+$ presence.

Notably, whilst the majority of samples did show some relationship in their expression of CD68 and CD163, this was completely absent in two patient samples - P4 & P7 (figures 40 and 44). Both P4 (stage A) and P7 (stage C) had relatively high expression of CD163 with a lack of heightened $CD68^+$ cell presence. Overall these data suggest that there may be three distinct subsets of monocyte-lineage cells within these samples; $CD68^+$ $CD163^-$ (currently thought to represent M1 type macrophages), $CD68^+$ $CD163^+$ (currently thought to represent M2 polarised macrophages/TAM/NLCs) and $CD68^-$ $CD163^+$ cells which are previously unreported. This population of $CD68^-CD163^+$ cells may represent a different form of monocyte/macrophage cell and requires further characterisation to determine its possible role in CLL.

Overall, these preliminary data are insufficient to confirm the presence of NLC in the CLL LN and further testing with more cell-specific markers is required. Nevertheless, these data do highlight the presence of several distinct macrophage/monocyte cell types present in varying levels within the CLL LN that warrant further investigation.

As seen in previous work, the use of multicolour staining does highlight the cellular architecture within the CLL niche which would otherwise go unobserved (Patten et al. 2008; Vandewoestyne et al. 2011). This ability to stain for multiple cell types and markers simultaneously in each tissue allows for robust quantification and comparison of the proportions of these cell types, leading to a novel insight into this important microenvironment.

Whilst the absolute numbers of these accessory cells in these tissues had no clear link to the stage of disease of patients and the number of patient samples in this study were small, the data suggested that these samples could be categorised based on CLL cell to accessory cell ratios. Within this cohort there appears to be different types of LN microenvironment; those with high $CD163^+$ NLC who typically had low ratios of T cells to NLC and CLL cells and those with low $CD163^+$ NLC, which have a much higher comparative presence of T cells (representation of this seen in figure 53 below).

These differences may reflect types of CLL disease which have high or low reliance upon the external LN microenvironment and it would be important in future work to correlate the proportions of these cell types to disease progression and response to therapy.

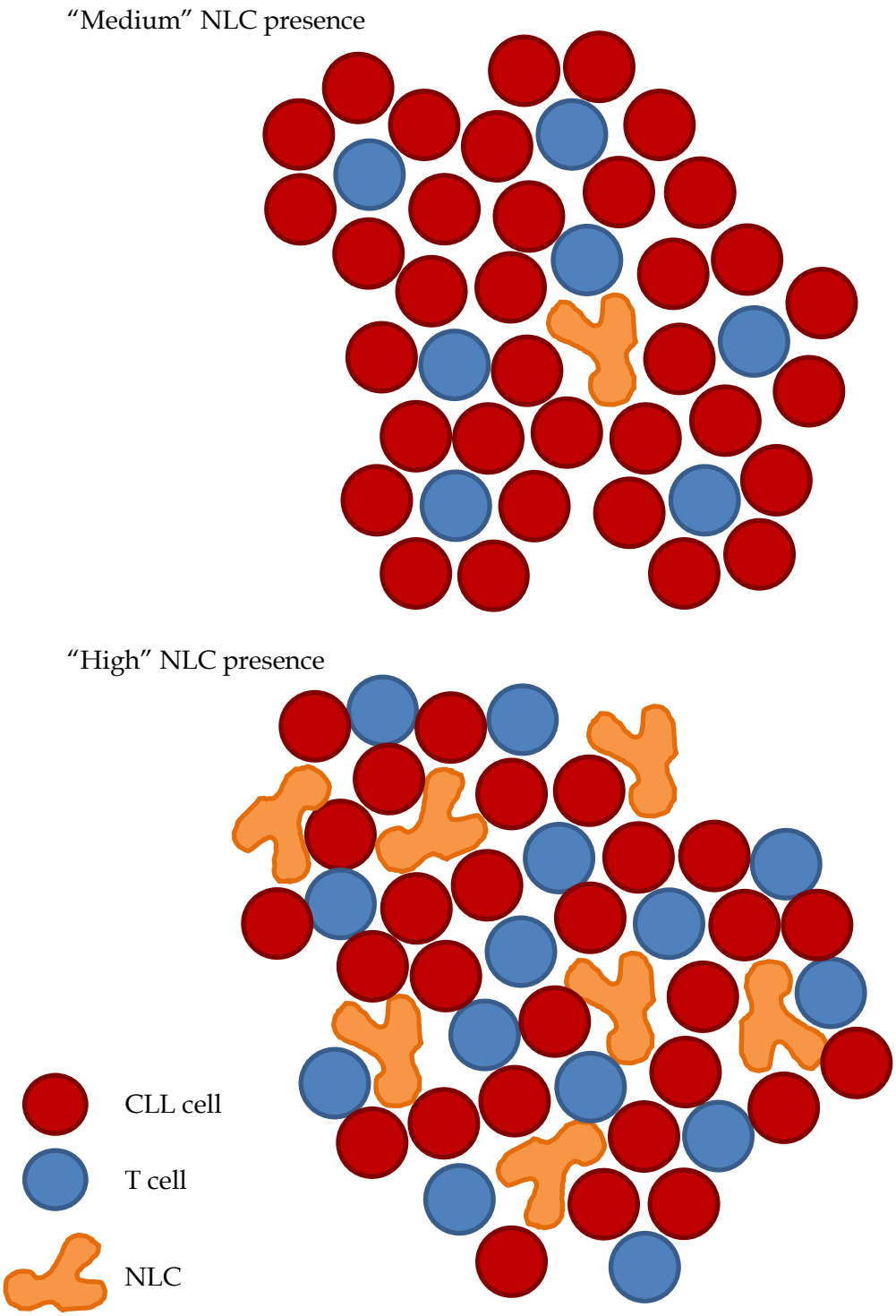

Figure 53. Representation of the differences between "medium" and "high" Nurse-like cell presence in the LN.

Whilst "medium" samples had an average of thirty-five CLL cells (red) and seven T cells (blue) per NLC (orange), "high" samples had an average of four CLL cells and two T cells. These lead to striking differences in the cellular architecture in these LN samples.

This work may prove to be a new method for stratification of patients and help to determine the types of therapy which would be most suitable. A limitation of this study was the lack of healthy LN tissue for direct comparison and future work should look to address this. It could be argued that based on the analysis of these samples, patient sample P3 would be best utilised as a form of control for the patient cohort in lieu of the availability of healthy LN tissue. This suggestion is based on a combination of the tissue architecture (where there appears to be germinal centre structures and T cells zones remaining), the expression levels of the different cell markers seen within this study and the patient notes which appear to indicate that the disease resolved over time. However utilising sample P3 in this manner would need to be approached with caution, as this could greatly impact the way in which the overall sample data were analysed and would likely skew the interpretation of such a small study; healthy lymph node tissue would still be the most beneficial as a reliable control for these samples. Future work should also include multicolour immunofluorescent interrogation of more CLL patients FFPE LN samples to strengthen the initial findings highlighted within this study. In particular, confirming the presence and role of NLC in combination with T cells and CLL cells in the LN is of key importance.

To confirm the findings from the *in vitro* studies, future investigation of the relative levels of DNA damage in CLL samples pre- and post-co-culture with both hdaCD4$^+$ T cells and autologous T cells is needed. In addition, the impact of chemotherapy on these cultures would be important to determine and will be a future aim for the project

7 REFERENCES

ACEBES-HUERTA, A. ET AL., 2014. Lenalidomide Induces Immunomodulation in Chronic Lymphocytic Leukemia and Enhances Antitumor Immune Responses Mediated by NK and CD4 T Cells. *BioMed Research International*, 2014, pp.1–11. Available at: http://www.hindawi.com/journals/bmri/2014/265840/.

AGATHANGELIDIS, A. ET AL., 2012. Stereotyped B-cell receptors in one third of chronic lymphocytic leukemia: towards a molecular classification with implications for targeted therapeutic interventions. *Blood*, 119(19), pp.4467–4476.

AHEARNE, M.J. ET AL., 2013. Enhancement of CD154/IL4 proliferation by the T follicular helper (Tfh) cytokine, IL21 and increased numbers of circulating cells resembling Tfh cells in chronic lymphocytic leukaemia. *British Journal of Haematology*, 162(3), pp.360–370. Available at: http://www.ncbi.nlm.nih.gov/pubmed/23710828 [Accessed January 6, 2015].

APOLLONIO, B. ET AL., 2013. Targeting B cell anergy in chronic lymphocytic leukemia. *Blood*, 121(19), pp.3879–3889.

ASSLABER, D. ET AL., 2012. Mimicking the microenvironment in chronic lymphocytic leukaemia – where does the journey go. *British Journal of Haematology*, (Cll), pp.711–714.

AUDRITO, V. ET AL., 2015. Extracellular nicotinamide phosphoribosyltransferase (NAMPT) promotes M2 macrophage polarization in chronic lymphocytic leukemia. , 125(1), pp.111–124.

AUSTEN, B. ET AL., 2007. Mutation status of the residual ATM allele is an important determinant of the cellular response to chemotherapy and survival in patients with chronic lymphocytic leukemia containing an 11q deletion. *Journal of Clinical Oncology*, 25(34), pp.5448–5457.

BADOUX, X.C. ET AL., 2011. Lenalidomide as initial therapy of elderly patients with chronic lymphocytic leukemia. *Blood*, 118(13), pp.3489–3498.

BAGNARA, D. ET AL., 2011. A novel adoptive transfer model of chronic lymphocytic leukemia suggests a key role for T lymphocytes in the disease. *Blood*, 117(20), pp.5463–72. Available at: http://www.pubmedcentral.nih.gov/articlerender.fcgi?artid=3109718&tool=pmcentrez&rendertype=abstract [Accessed December 21, 2014].

BARRET, J.M. ET AL., 1996. DNA repair activity in protein extracts of fresh human malignant lymphoid cells. *Molecular pharmacology*, 49(5), pp.766–771.

BHATTACHARYA ET AL., 2014. Loss of cooperativity of secreted CD40L and increased dose-response to IL4 on CLL cell viability correlates with enhanced activation of NF-kB and STAT6. *International journal of cancer. Journal international du cancer*, 00, pp.65–73. Available at: http://www.ncbi.nlm.nih.gov/pubmed/24828787.

BHATTACHARYA ET AL., 2011. Non-malignant B cells and chronic lymphocytic leukemia cells induce a pro-survival phenotype in CD14+ cells from peripheral blood. *Leukemia*, 25(4), pp.722–726.

BICHI, R. ET AL., 2002. Human chronic lymphocytic leukemia modeled in mouse by targeted TCL1 expression. *Proceedings of the National Academy of Sciences of the United States of America*, 99(10), pp.6955–6960.

BOLOGNA, L. ET AL., 2012. Ofatumumab Is More Efficient than Rituximab in Lysing B Chronic Lymphocytic Leukemia Cells in Whole Blood and in Combination with Chemotherapy.

The Journal of Immunology, 190(1), pp.231–239. Available at: http://www.jimmunol.org/cgi/doi/10.4049/jimmunol.1202645.

BONATO, M. ET AL., 1998. Lymph node histology in typical and atypical chronic lymphocytic leukemia. *The American journal of surgical pathology*, 22(1), pp.49–56.

BRACHTL, G. ET AL., 2011. Differential bone marrow homing capacity of VLA-4 and CD38 high expressing chronic lymphocytic leukemia cells. *PLoS ONE*, 6(8).

BROWN, J.R. ET AL., 2014. Idelalisib, an inhibitor of phosphatidylinositol 3-kinase p110δ, for relapsed/refractory chronic lymphocytic leukemia. *Blood*, 123(22), pp.3390–3397.

BURGER, J. A ET AL., 2000. Blood-derived nurse-like cells protect chronic lymphocytic leukemia B cells from spontaneous apoptosis through stromal cell-derived factor-1. *Blood*, 96(8), pp.2655–2663.

BURGER, J. A, 2011. Nurture versus nature: the microenvironment in chronic lymphocytic leukemia. *Hematology / the Education Program of the American Society of Hematology. American Society of Hematology. Education Program*, 2011, pp.96–103. Available at: http://www.ncbi.nlm.nih.gov/pubmed/22160019.

BURGER, J. A. ET AL., 2009. High-level expression of the T-cell chemokines CCL3 and CCL4 by chronic lymphocytic leukemia B cells in nurselike cell cocultures and after BCR stimulation. *Leukemia*, 113(13), pp.3050–3059.

BURGER, J. A. & KIPPS, T.J., 2006. CXCR4: A key receptor in the crosstalk between tumor cells and their microenvironment. *Blood*, 107(5), pp.1761–1767.

BURGER, J.A. ET AL., 2013. Blood-dervied nurse-like cells protect chronic lymphocytic leukemia B cells from spontaneous apoptosis through stromal cell − derived factor-1. *Blood*, pp.2655–2663.

BÜRKLE, A. & NIEDERMEIER, M., 2007. Overexpression of the CXCR5 chemokine receptor and its ligand CXCL13 in B-cell chronic lymphocytic leukemia. *Blood*, 110(9), pp.3316–3325. Available at: http://bloodjournal.hematologylibrary.org/content/110/9/3316.full-text.pdf+html.

BUTTON, L. ET AL., 1981. The effects of irradiation on blood components. *Transfusion*, 21(4), pp.419–426. Available at: http://apps.webofknowledge.com/full_record.do?product=UA&search_mode=GeneralSearch&qid=2&SID=Y1ko6ihJgYVh5ZCowtW&page=1&doc=6 [Accessed September 23, 2015].

BYRD, J.C. ET AL., 2013. Targeting BTK with ibrutinib in relapsed chronic lymphocytic leukemia. *The New England journal of medicine*, 369(1), pp.32–42. Available at: http://www.pubmedcentral.nih.gov/articlerender.fcgi?artid=3772525&tool=pmcentrez&rendertype=abstract.

CALISSANO, C. ET AL., 2011. Intraclonal complexity in CLL - fractions enriched in recently born-divided and older-quiescent cells. *Molecular Medicine*, 17(11-12), p.1. Available at: http://www.molmed.org/content/pdfstore/11_360_Calissano.pdf.

CALKINS, M.J. & REDDY, P.H., 2011. Assessment of newly synthesized mitochondrial DNA using BrdU labeling in primary neurons from Alzheimer's disease mice: Implications for impaired mitochondrial biogenesis and synaptic damage. *Biochimica et Biophysica Acta - Molecular Basis of Disease*, 1812(9), pp.1182–1189.

CAMPANA, D., COUSTAN-SMITH, E. & JANOSSY, G., 1988. Double and triple staining methods

for studying the proliferative activity of human B and T lymphoid cells. *Journal of immunological methods*, 107(1), pp.79–88.

CHAVEZ, J.C., SAHAKIAN, E. & PINILLA-IBARZ, J., 2013. Ibrutinib: An evidence-based review of its potential in the treatment of advanced chronic lymphocytic leukemia. *Core Evidence*, 8, pp.37–45.

CHIGRINOVA, E. ET AL., 2014. Two main genetic pathways lead to the transformation of chronic lymphocytic leukemia to Richter syndrome. *Blood*, 122(15), pp.2673–2682.

CHIORAZZI, N., 2007. Cell proliferation and death: forgotten features of chronic lymphocytic leukemia B cells. *Best practice & research. Clinical haematology*, 20(3), pp.399–413. Available at: http://www.sciencedirect.com/science/article/pii/S1521692607000448 [Accessed August 24, 2015].

CHIORAZZI, N., KANTI, R. & FERRARINI, M., 2005. Chronic lymphocytic leukemia. *The New England Journal of Medicine*, 352(1), pp.804–815.

CICCONE, M. ET AL., 2012. Proliferation centers in chronic lymphocytic leukemia: correlation with cytogenetic and clinicobiological features in consecutive patients analyzed on tissue microarrays. *Leukemia*, 26(3), pp.499–508. Available at: http://dx.doi.org/10.1038/leu.2011.247.

COBALEDA, C. ET AL., 2007. Pax5: the guardian of B cell identity and function. *Nature immunology*, 8(5), pp.463–470.

COIFFIER, B. ET AL., 2008. Guidelines for the management of pediatric and adult tumor lysis syndrome: an evidence-based review. *Journal of Clinical Oncology*, 26(16), pp.2767–2778.

COLLINS, A R., 2004. The comet assay for DNA damage and repair: principles, applications, and limitations. *Molecular Biotechnology*, 26(3), pp.249–261. Available at: http://www.ncbi.nlm.nih.gov/pubmed/15004294.

COLVIN, E.K., 2014. Tumor-associated macrophages contribute to tumor progression in ovarian cancer. *Frontiers in oncology*, 4(June), p.137. Available at: http://www.pubmedcentral.nih.gov/articlerender.fcgi?artid=4047518&tool=pmcentrez&rendertype=abstract.

DAMLE, R.N. ET AL., 1999. Ig V gene mutation status and CD38 expression as novel prognostic indicators in chronic lymphocytic leukemia. *Blood*, 94(6), pp.1840–1847.

DAMLE, R.N., CALISSANO, C. & CHIORAZZI, N., 2011. Chronic lymphocytic leukemia: A disease of activated monoclonal B cells. *Best Pract Res Clin Haematol*, 23(1), pp.33–45. Available at: http://www.pubmedcentral.nih.gov/articlerender.fcgi?artid=2921990&tool=pmcentrez&rendertype=abstract.

DAVIS, J.E. & RITCHIE, D.S., 2014. The passive-aggressive relationship between CLL-B cells and T cell immunity. *Leukemia research*, 38(10), pp.1160–1. Available at: http://www.ncbi.nlm.nih.gov/pubmed/25182688 [Accessed January 6, 2015].

DAVIS, R.E. ET AL., 2010. Chronic active B-cell-receptor signalling in diffuse large B-cell lymphoma. *Nature*, 463(7277), pp.88–92. Available at: http://dx.doi.org/10.1038/nature08638.

DÖHNER, H. ET AL., 2000. Genomic Aberrations and Survival in Chronic Lymphocytic Leukemia. *New England Journal of Medicine*, 343(26), pp.1910–1916.

DUBRAVKA, D. & SCOTT, D.W., 2000. Activation-induced cell death in B lymphocytes. *Cell research*, 10(3), pp.179–192.

EICHHORST, B.F. ET AL., 2013. First-line therapy with fludarabine compared with chlorambucil does not result in a major benefit for elderly patients with advanced chronic lymphocytic leukemia. *Blood*, 114(16), pp.3382–3391.

EVAN, G.I. & VOUSDEN, K.H., 2001. Proliferation, cell cycle and apoptosis in cancer. *Nature*, 411(May), pp.342–348.

FARINHA, P. ET AL., 2005. Analysis of multiple biomarkers shows that lymphoma-associated macrophage (LAM) content is an independent predictor of survival in follicular lymphoma (FL). *Blood*, 106(6), pp.2169–2174.

FAROOQUI, M.Z.H. ET AL., 2015. Ibrutinib for previously untreated and relapsed or refractory chronic lymphocytic leukaemia with TP53 aberrations: a phase 2, single-arm trial. *The Lancet. Oncology*, 16(2), pp.169–76. Available at: http://www.sciencedirect.com/science/article/pii/S1470204514711829 [Accessed August 28, 2015].

FECTEAU, J.-F. ET AL., 2014. Lenalidomide inhibits the proliferation of chronic lymphocytic leukemia cells via a cereblon/p21WAF1/Cip1-dependent mechanism independent of functional p53. *Blood*, 124(10), pp.1637–1645. Available at: http://www.ncbi.nlm.nih.gov/pubmed/24990888.

FECTEAU, J.-F. & KIPPS, T.J., 2012. Structure and function of the hematopoietic cancer niche: focus on chronic lymphocytic leukemia. *Changes*, 29(6), pp.997–1003.

FERRARI, S. ET AL., 2007. Mutations of the Igbeta gene cause agammaglobulinemia in man. *The Journal of experimental medicine*, 204(9), pp.2047–2051.

FERRER, G. ET AL., 2014. B cell activation through CD40 and IL4R ligation modulates the response of chronic lymphocytic leukaemia cells to BAFF and APRIL. *British journal of haematology*, 164(4), pp.570–8. Available at: http://www.ncbi.nlm.nih.gov/pubmed/24245956 [Accessed January 6, 2015].

FILIP, A., CISEŁ, B., KOCZKODAJ, D., ET AL., 2013. Circulating microenvironment of CLL: Are nurse-like cells related to tumor-associated macrophages? *Blood Cells, Molecules, and Diseases*, 50(4), pp.263–270.

FILIP, A., CISEŁ, B. & WASIK-SZCZEPANEK, E., 2013. Guilty bystanders: nurse-like cells as a model of microenvironmental support for leukemic lymphocytes. *Clinical and Experimental Medicine*, 15, pp.73–83.

FINNEY, R.D. ET AL., 1996. Guidelines on gamma irradiation of blood components for the prevention of transfusion-associated graft-versus-host disease. *Transfusion medicine*, 6(3), pp.261–271.

FIORCARI, S. ET AL., 2014. Lenalidomide interferes with tumor-promoting properties of nurse-like cells in chronic lymphocytic leukemia. *Haematologica*, 100(2), pp.253–262. Available at: http://www.haematologica.org/cgi/doi/10.3324/haematol.2014.113217 [Accessed January 6, 2015].

FOLLOWS, G.A. ET AL., 2015. Interim statement from the BCSH CLL Guidelines Panel.

FUXA, M. ET AL., 2004. Pax5 induces V- to- DJ rearrangements and locus contraction of the immunoglobulin heavy-chain gene. *Genes & Development*, (D), pp.411–422.

GHIA, P. ET AL., 2002. Chronic lymphocytic leukemia B cells are endowed with the capacity to attract CD4+, CD40L+ T cells by producing CCL22. *European journal of immunology*, 32(5), pp.1403–1413.

GHIA, P., CALIGARIS-CAPPIO, F. & DC, W., 2012. Monoclonal B-cell lymphocytosis right track or red herring? *Blood*, 119(19), pp.4358–4362.

GIANNONI, P. ET AL., 2014. Chronic lymphocytic leukemia nurse-like cells express hepatocyte growth factor receptor (c-MET) and indoleamine 2,3-dioxygenase and display features of immunosuppressive type 2 skewed macrophages. *Haematologica*.

GIRBL, T. ET AL., 2013. CD40-mediated activation of chronic lymphocytic leukemia cells promotes their CD44-dependent adhesion to hyaluronan and restricts CCL21-induced motility. *Cancer Research*, 73(2), pp.561–570.

GOEDE, V., FISCHER, K., ET AL., 2015. Obinutuzumab as frontline treatment of chronic lymphocytic leukemia: updated results of the CLL11 study. *Leukemia*, (February), pp.1602–1604. Available at: http://www.nature.com/doifinder/10.1038/leu.2015.14.

GOEDE, V. & HALLEK, M., 2015. Towards improved frontline treatment of CLL in the elderly. *The Lancet*, 385(9980), pp.1814–1815. Available at: http://linkinghub.elsevier.com/retrieve/pii/S0140673615602938.

GOEDE, V., KLEIN, C. & STILGENBAUER, S., 2015. Obinutuzumab (GA101) for the Treatment of Chronic Lymphocytic Leukemia and Other B-Cell Non-Hodgkin's Lymphomas: A Glycoengineered Type II CD20 Antibody. *Oncology Research and Treatment*, 38(4), pp.185–192. Available at: http://www.karger.com/?doi=10.1159/000381524.

GONZALEZ-RODRIGUEZ, A.P. ET AL., 2010. Prognostic significance of CD8 and CD4 T cells in chronic lymphocytic leukemia. *Leukemia & lymphoma*, 51(10), pp.1829–36. Available at: http://apps.webofknowledge.com/full_record.do?product=UA&search_mode=GeneralSearch&qid=3&SID=R1W4LGsPZY4FqZqKoxl&page=1&doc=1 [Accessed September 20, 2015].

GOODNOW, C.C. ET AL., 1988. Altered immunoglobulin expression and functional silencing of self-reactive B lymphocytes in transgenic mice. *Nature*, 334(6184), pp.676–682.

GOODNOW, C.C., ADELSTEIN, S. & BASTEN, A, 1990. The need for central and peripheral tolerance in the B cell repertoire. *Science (New York, N.Y.)*, 248(4961), pp.1373–1379.

GOODNOW, C.C., BRINK, R. & ADAMS, E., 1991. Breakdown of self-tolerance in anergic B lymphocytes. *Nature*, 352(6335), pp.532–536.

GÖRGÜN, G. ET AL., 2005. Chronic lymphocytic leukemia cells induce changes in gene expression of CD4 and CD8 T cells. *The Journal of clinical investigation*, 115(7), pp.1797–1805.

GUO, B. ET AL., 2000. Engagement of the human pre-B cell receptor generates a lipid raft-dependent calcium signaling complex. *Immunity*, 13(2), pp.243–253.

HAIAT, S. ET AL., 2006. Role of BAFF and APRIL in human B-cell chronic lymphocytic leukaemia. *Immunology*, 118(3), pp.281–292.

HALLEK, M. ET AL., 2010. Addition of rituximab to fludarabine and cyclophosphamide in patients with chronic lymphocytic leukaemia: A randomised, open-label, phase 3 trial. *The Lancet*, 376(9747), pp.1164–1174.

HALLEK, M. ET AL., 2008. Guidelines for the diagnosis and treatment of chronic lymphocytic

leukemia: A report from the International Workshop on Chronic Lymphocytic Leukemia updating the National Cancer Institute-Working Group 1996 guidelines. *Blood*, 111(12), pp.5446–5456.

HAMBLIN, T.J. ET AL., 1999. Unmutated Ig VH Genes are associated with a more aggresive form of Chronic Lymphocytic Leukemia. *Blood*, 94(6), pp.1848–1854.

HAMILTON, E. ET AL., 2012. Mimicking the tumour microenvironment: Three different co-culture systems induce a similar phenotype but distinct proliferative signals in primary chronic lymphocytic leukaemia cells. *British Journal of Haematology*, 158(5), pp.589–599.

HANAHAN, D. & WEINBERG, R. A., 2000. The hallmarks of cancer. *Cell*, 100, pp.57–70.

HARRIS, J. A ET AL., 2012. CD163 versus CD68 in tumor associated macrophages of classical hodgkin lymphoma. *Diagnostic Pathology*, 7(1), p.12. Available at: http://www.pubmedcentral.nih.gov/articlerender.fcgi?artid=3281786&tool=pmcentrez&rendertype=abstract [Accessed January 6, 2015].

HARTLEY, S.B. ET AL., 1991. Elimination from peripheral lymphoid tissues of self-reactive B lymphocytes recognizing membrane-bound antigens. *Nature*, 353(6346), pp.765–769.

HAYDEN, R.E. ET AL., 2011. Treatment of Chronic Lymphocytic Leukemia requires targeting of the protective lymph node environment with novel therapeutic approaches. *Leukemia & lymphomaukemia & Lymphoma*, 53(4), pp.537–549.

HAYDEN, R.E. ET AL., 2009. Treatment of primary CLL cells with bezafibrate and medroxyprogesterone acetate induces apoptosis and represses the pro-proliferative signal of CD40-ligand, in part through increased 15dDelta12,14,PGJ2. *Leukemia : official journal of the Leukemia Society of America, Leukemia Research Fund, U.K*, 23(2), pp.292–304.

HELTEMES-HARRIS, L., LIU, X. & MANSER, T., 2004. Progressive surface B cell antigen receptor down-regulation accompanies efficient development of antinuclear antigen B cells to mature, follicular phenotype. *Journal of immunology (Baltimore, Md. : 1950)*, 172(2), pp.823–833.

HERISHANU, Y. ET AL., 2011. The lymph node microenvironment promotes B-cell receptor signaling, NF-κB activation, and tumor proliferation in chronic lymphocytic leukemia. *Blood*, 117(2), pp.563–574. Available at: http://www.pubmedcentral.nih.gov/articlerender.fcgi?artid=3031480&tool=pmcentrez&rendertype=abstract [Accessed December 8, 2014].

HERMAN, S.E.M. ET AL., 2014. Ibrutinib-induced lymphocytosis in patients with chronic lymphocytic leukemia: correlative analyses from a phase II study. *Leukemia*, 28(April), pp.1–9. Available at: http://www.ncbi.nlm.nih.gov/pubmed/24699307 [Accessed December 22, 2014].

HILLMEN, P. ET AL., 2015. Chlorambucil plus ofatumumab versus chlorambucil alone in previously untreated patients with chronic lymphocytic leukaemia (COMPLEMENT 1): a randomised, multicentre, open-label phase 3 trial. *Lancet*, 385(9980), pp.1873–1883. Available at: http://www.sciencedirect.com/science/article/pii/S0140673615600277 [Accessed May 6, 2015].

HILLMEN, P. ET AL., 2014. Rituximab plus chlorambucil as first-line treatment for chronic lymphocytic leukemia: Final analysis of an open-label phase II study. *Journal of Clinical Oncology*, 32(12), pp.1236–1241.

HILLMEN, P., 2011. Using the Biology of Chronic Lymphocytic Leukemia to Choose

Treatment. *Hematology*, 2011(1), pp.104–109.

HIOM, K., MELEK, M. & GELLERT, M., 1998. DNA transposition by the RAG1 and RAG2 proteins: a possible source of oncogenic translocations. *Cell*, 94(4), pp.463–470.

HOCK, B.D. ET AL., 2014. Chronic lymphocytic leukaemia cells become both activated and immunosuppressive following interaction with CD3 and CD28 stimulated PBMC. *Leukemia research*, 38(10), pp.1217–23. Available at: http://www.sciencedirect.com/science/article/pii/S0145212614001830 [Accessed August 29, 2015].

HOELLENRIEGEL, J. ET AL., 2011. The phosphoinositide 3′-kinase delta inhibitor, CAL-101, inhibits B-cell receptor signaling and chemokine networks in chronic lymphocytic leukemia. *Blood*, 118(13), pp.3603–3612.

HUERGO-ZAPICO, L. ET AL., 2014. Expansion of NK Cells and Reduction of NKG2D Expression in Chronic Lymphocytic Leukemia. Correlation with Progressive Disease. *PLoS ONE*, 9(10), p.e108326. Available at: http://dx.plos.org/10.1371/journal.pone.0108326.

HUTCHINSON, C. V. & DYER, M.J.S., 2014. Breaking good: The inexorable rise of BTK inhibitors in the treatment of chronic lymphocytic leukaemia. *British Journal of Haematology*, 166(1), pp.12–22.

HWANG, K.K. ET AL., 2014. IGHV1-69 B cell chronic lymphocytic leukemia antibodies cross-react with HIV-1 and hepatitis C virus antigens as well as intestinal commensal bacteria. *PLoS ONE*, 9(3).

HYDE, R.K. & LIU, P.P., 2013. Germline PAX5 mutations and B cell leukemia. *Nature genetics*, 45(10), pp.1104–5. Available at: http://www.ncbi.nlm.nih.gov/pubmed/24071841.

JAIN, N., O'BRIEN, S. & BRIEN, S.O., 2015. Initial treatment of CLL : integrating biology and functional status. *Blood*, 126(4), pp.463–471. Available at: http://www.bloodjournal.org/cgi/doi/10.1182/blood-2015-04-585067.

JAMES, D.F. & KIPPS, T.J., 2011. Rituximab in chronic lymphocytic leukemia. *Advances in Therapy*, 28(7), pp.534–554.

JANEWAY, C.A.J. ET AL., 2001. Immunobiology. Available at: http://www.ncbi.nlm.nih.gov/books/NBK10757/ [Accessed September 21, 2015].

JOHNSON, A.J. ET AL., 2006. Characterization of the TCL-1 transgenic mouse as a preclinical drug development tool for human chronic lymphocytic leukemia. , 108(4), pp.1334–1338.

KAMDJE, A H.N. ET AL., 2012. Role of stromal cell-mediated Notch signaling in CLL resistance to chemotherapy. *Blood Cancer Journal*, 2(5), p.e73. Available at: http://dx.doi.org/10.1038/bcj.2012.17.

KATSUMATA, M. ET AL., 1992. Differential effects of Bcl-2 on T and B cells in transgenic mice. *Proceedings of the National Academy of Sciences of the United States of America*, 89(23), pp.11376–11380.

KAY, N.E. & ZARLING, J., 1987. Restoration of impaired natural killer cell activity of B-chronic lymphocytic leukemia patients by recombinant interleukin-2. *American journal of hematology*, 24(2), pp.161–167.

KEATING, M.J. ET AL., 2005. Early results of a chemoimmunotherapy regimen of fludarabine,

cyclophosphamide, and rituximab as initial therapy for chronic lymphocytic leukemia. *Journal of Clinical Oncology*, 23(18), pp.4079–4088.

KIKUSHIGE, Y. ET AL., 2011. Self-Renewing Hematopoietic Stem Cell Is the Primary Target in Pathogenesis of Human Chronic Lymphocytic Leukemia. *Cancer Cell*, 20(2), pp.246–259. Available at: http://dx.doi.org/10.1016/j.ccr.2011.06.029.

KLAUS, G.G. ET AL., 1999. Interaction of B cells with activated T cells reduces the threshold for CD40-mediated B cell activation. *International immunology*, 11(1), pp.71–79.

KLEIN, J.L. ET AL., 2014. CD163 immunohistochemistry is superior to CD68 in predicting outcome in classical Hodgkin lymphoma. *American journal of clinical pathology*, 141(3), pp.381–387.

KLEIN, U. ET AL., 2001. Gene expression profiling of B cell chronic lymphocytic leukemia reveals a homogeneous phenotype related to memory B cells. *The Journal of experimental medicine*, 194(11), pp.1625–1638.

KOCZULA, K.M. ET AL., 2015. Metabolic plasticity in CLL: Adaptation to the hypoxic niche. *Leukemia*, (January), pp.1–9. Available at: http://www.nature.com/doifinder/10.1038/leu.2015.187.

KREIG, A. ET AL., 1995. CpG motifs in bacterial DNA trigger direct B-cell activation. , pp.546–549.

KUWAHARA, K. ET AL., 1996. Cross-linking of B cell antigen receptor-related structure of pre-B cell lines induces tyrosine phosphorylation of p85 and p110 subunits and activation of phosphatidylinositol 3-kinase. *International immunology*, 8(8), pp.1273–1285.

LAGNEAUX, L. ET AL., 1998. Chronic lymphocytic leukemic B cells but not normal B cells are rescued from apoptosis by contact with normal bone marrow stromal cells. *Blood*, 91(7), pp.2387–2396.

LAGRUE, K. ET AL., 2015. Lenalidomide augments actin remodeling and lowers NK-cell activation thresholds. *Blood*, 126(1), pp.50–61.

LAMANNA, N., 2012. Treatment of older patients with chronic lymphocytic Leukemia. *Current Hematologic Malignancy Reports*, 7(1), pp.21–25.

LANDAU, D. A ET AL., 2014. Clonal evolution in hematological malignancies and therapeutic implications. *Leukemia*, 28(1), pp.34–43. Available at: http://www.pubmedcentral.nih.gov/articlerender.fcgi?artid=3934006&tool=pmcentrez&rendertype=abstract.

LANDAU, D. A. ET AL., 2013. Evolution and impact of subclonal mutations in chronic lymphocytic leukemia. *Cell*, 152(4), pp.714–726. Available at: http://dx.doi.org/10.1016/j.cell.2013.01.019.

LANGERBEINS, P. ET AL., 2015. The CLL12 trial protocol : a placebo-controlled double-blind Phase III study of ibrutinib in the treatment of early-stage chronic lymphocytic leukemia patients with risk of early disease progression. *Future Oncology*, 13(11), pp.1895–1903.

LANNUTTI, B.J. ET AL., 2011. CAL-101, a p110δ selective phosphatidylinositol-3-kinase inhibitor for the treatment of B-cell malignancies, inhibits PI3K signaling and cellular viability. *Blood*, 117(2), pp.591–594.

LASCANO, V. ET AL., 2013. Chronic lymphocytic leukemia disease progression is accelerated by APRIL-TACI interaction in the TCL1 transgenic mouse model. *Blood*, 122(24),

pp.3960–3. Available at: http://www.ncbi.nlm.nih.gov/pubmed/24100449.

LEBIEN, T.W., 2000. Fates of human B-cell precursors. *Blood*, 96(1), pp.9–23.

LEBIEN, T.W. & TEDDER, T.F., 2008. B lymphocytes: How they develop and function. *Blood*, 112(5), pp.1570–1580.

LEFRANC, M.P., 2014. Immunoglobulin and T cell receptor genes: IMGT and the birth and rise of immunoinformatics. *Frontiers in Immunology*, 5(FEB), pp.1–22.

LENTZ, S.I. ET AL., 2010. Mitochondrial DNA (mtDNA) Biogenesis: Visualization and Duel Incorporation of BrdU and EdU Into Newly Synthesized mtDNA In Vitro. , 58(2), pp.207–218.

LEWIS, C.E. & POLLARD, J.W., 2006. Distinct role of macrophages in different tumor microenvironments. *Cancer research*, 66(2), pp.605–12. Available at: http://www.ncbi.nlm.nih.gov/pubmed/16423985 [Accessed September 26, 2014].

LISSBRANT, I. ET AL., 2000. Tumor associated macrophages in human prostate cancer- relation to clinicalpathological variables and survival. *International Journal of Oncology*, 17, pp.445–451.

MAFFEI, R. ET AL., 2015. Targeting neoplastic B cells and harnessing microenvironment: the "double face" of ibrutinib and idelalisib. *Journal of Hematology & Oncology*, 8(1). Available at: http://www.jhoonline.org/content/8/1/60.

MAFFEI, R. ET AL., 2013. The monocytic population in chronic lymphocytic leukemia shows altered composition and deregulation of genes involved in phagocytosis and inflammation. *Haematologica*, 98(7), pp.1115–1123.

MCCLANAHAN, F. ET AL., 2015. Mechanisms of PD-L1/PD-1 mediated CD8 T-cell dysfunction in the context of aging-related immune defects in the E -TCL1 CLL mouse model. *Blood*, 44(0). Available at: http://www.bloodjournal.org/cgi/doi/10.1182/blood-2015-02-626754.

MCHEYZER-WILLIAMS, L.J. & MCHEYZER-WILLIAMS, M.G., 2005. Antigen-specific memory B cell development. *Annual review of immunology*, 23(9), pp.487–513.

MELAMED, D. & NEMAZEE, D., 1997. Self-antigen does not accelerate immature B cell apoptosis, but stimulates receptor editing as a consequence of developmental arrest. *Proceedings of the National Academy of Sciences of the United States of America*, 94(17), pp.9267–9272.

MESSMER, B.T. ET AL., 2005. In vivo measurements document the dynamic cellular kinetics of chronic lymphocytic leukemia B cells. *Journal of Clinical Investigation*, 115(3), pp.755–764.

MESSMER, B.T. ET AL., 2004. The pattern and distribution of immunoglobulin VH gene mutations in chronic lymphocytic leukemia B cells are consistent with the canonical somatic hypermutation process. *Blood*, 103(9), pp.3490–3495.

MINEGISHI, Y. ET AL., 1999. Mutations in Igα (CD79a) result in a complete block in B-cell development. *Journal of Clinical Investigation*, 104(8), pp.1115–1121.

MURAMATSU, M. ET AL., 2000. Class switch recombination and hypermutation require activation-induced cytidine deaminase (AID), a potential RNA editing enzyme. *Cell*, 102(5), pp.553–563.

NAGAI, S. ET AL., 2008. Functional targeting of DNA damage to a nuclear pore-associated SUMO-dependent ubiquitin ligase. *Science (New York, N.Y.)*, 322(5901), pp.597–602.

NIMMERJAHN, F. & RAVETCH, J. V, 2008. Fcgamma receptors as regulators of immune responses. *Nature reviews. Immunology*, 8(1), pp.34–47.

NISHIO, M. ET AL., 2005. Nurselike cells express BAFF and APRIL, which can promote survival of chronic lymphocytic leukemia cells via a paracrine pathway distinct from that of SDF-1. *Blood*, 106(3), pp.1012–1020.

DI NOIA, J.M. ET AL., 2007. Dependence of antibody gene diversification on uracil excision. *The Journal of experimental medicine*, 204(13), pp.3209–3219.

DI NOIA, J.M. & NEUBERGER, M.S., 2007. Molecular mechanisms of antibody somatic hypermutation. *Annual review of biochemistry*, 76, pp.1–22.

NOORIZADEH, M. ET AL., 2004. Effects of Gamma Irradiation on Proliferation and IL-5 Production of Peripheral Blood Lymphocytes. , 8(October), pp.211–214.

NUNES, C. ET AL., 2012. Expansion of a CD8 PD-1 replicative senescence phenotype in early stage CLL patients is associated with inverted CD4:CD8 ratios and disease progression. *Clinical Cancer Research*, 18(3), pp.678–687.

OETTINGER, M.A. ET AL., 1990. RAG-1 and RAG-2, Adjacent Genes That Synergistically Activate V(D)J Recombination. , (D).

OSCIER, D. ET AL., 2012. Guidelines on the diagnosis, investigation and management of chronic lymphocytic leukaemia. *British Journal of Haematology*, 159, pp.541–564.

PANAYIOTIDIS, P. ET AL., 1996. Human bone marrow stromal cells prevent apoptosis and support the survival of chronic lymphocytic leukaemia cells in vitro. *British journal of haematology*, 92(1), pp.97–103.

PARIKH, S. A. & SHANAFELT, T.D., 2014. Risk Factors for Richter Syndrome in Chronic Lymphocytic Leukemia. *Current Hematologic Malignancy Reports*, 9(3), pp.294–299. Available at: http://link.springer.com/10.1007/s11899-014-0223-4.

PASCUTTI, M.F. ET AL., 2013. IL-21 and CD40L signals from autologous T cells can induce antigen-independent proliferation of CLL cells. *Blood*, 122(17), pp.3010–9. Available at: http://www.ncbi.nlm.nih.gov/pubmed/24014238 [Accessed December 15, 2014].

PATTEN, P.E.M. ET AL., 2008. CD38 expression in chronic lymphocytic leukemia is regulated by the tumor microenvironment. *Blood*, 111(10), pp.5173–5181. Available at: http://www.ncbi.nlm.nih.gov/pubmed/18326821 [Accessed November 14, 2014].

PIEPER, K., GRIMBACHER, B. & EIBEL, H., 2013. B-cell biology and development. *Journal of Allergy and Clinical Immunology*, 131(4), pp.959–971. Available at: http://dx.doi.org/10.1016/j.jaci.2013.01.046.

PLANDER, M. ET AL., 2009. Different proliferative and survival capacity of CLL-cells in a newly established in vitro model for pseudofollicles. *Leukemia : official journal of the Leukemia Society of America, Leukemia Research Fund, U.K*, 23(11), pp.2118–2128. Available at: http://www.ncbi.nlm.nih.gov/pubmed/19657365 [Accessed January 6, 2015].

PLANELLES, L. ET AL., 2004. APRIL promotes B-1 cell-associated neoplasm. *Cancer Cell*, 6(4), pp.399–408.

PONTEN, F., JIRSTROM, K. & UHLEN, M., 2008. The Human Protein Atlas - a tool for pathology. *Journal of Pathology*, 216, pp.387–393.

PONZONI, M., DOGLIONI, C. & CALIGARIS-CAPPIO, F., 2011. Chronic Lymphocytic Leukemia: the pathologist's view of lymph node microenvironment. *Seminars in Diagnostic*

Pathology.

PUENTE, X.S. ET AL., 2011. Whole-genome sequencing identifies recurrent mutations in chronic lymphocytic leukaemia. *Nature*, 475(7354), pp.101–105.

PURROY, N. ET AL., 2014. Co-culture of primary CLL cells with bone marrow mesenchymal cells, CD40 ligand and CpG ODN promotes proliferation of chemoresistant CLL cells phenotypically comparable to those proliferating in vivo. *Oncotarget*.

QIAN, B.Z. & POLLARD, J.W., 2010. Macrophage Diversity Enhances Tumor Progression and Metastasis. *Cell*, 141(1), pp.39–51.

TE RAA, G.D. ET AL., 2014. The impact of SF3B1 mutations in CLL on the DNA-damage response. *Leukemia*, (August 2014), pp.1133–1142. Available at: http://www.nature.com/doifinder/10.1038/leu.2014.318.

RAFF, M.C., 1973. T and B lymphocytes and immune responses. *Nature*, 242(5392), pp.19–23.

RAMIRO, A.R. ET AL., 2006. Role of genomic instability and p53 in AID-induced c-myc-Igh translocations. *Nature*, 440(7080), pp.105–109.

RAMSAY, A.G. ET AL., 2008. Chronic lymphocytic leukemia T cells show impaired immunological synapse formation that can be reversed with an immunomodulating drug. *Journal of Clinical Investigation*, 118(7), pp.2427–2437.

RAMSAY, A.G. ET AL., 2012. Multiple inhibitory ligands induce impaired T-cell immunologic synapse function in chronic lymphocytic leukemia that can be blocked with lenalidomide : establishing a reversible immune evasion mechanism in human cancer. , 120(7), pp.1412–1421.

REDDY, S.T. & GEORGIOU, G., 2011. Systems analysis of adaptive immunity by utilization of high-throughput technologies. *Current Opinion in Biotechnology*, 22(4), pp.584–589. Available at: http://dx.doi.org/10.1016/j.copbio.2011.04.015.

REINERS, K.S. ET AL., 2013. Soluble ligands for NK cell receptors promote evasion of chronic lymphocytic leukemia cells from NK cell anti-tumor activity. *Blood*, 121(18), pp.3658–3665.

REVY, P. ET AL., 2000. Activation-induced cytidine deaminase (AID) deficiency causes the autosomal recessive form of the Hyper-IgM syndrome (HIGM2). *Cell*, 102(5), pp.565–575.

RICHES, J.C. ET AL., 2013. T cells from CLL patients exhibit features of T-cell exhaustion but retain capacity for cytokine production. *Blood*, 121(9), pp.1612–1621.

RICHES, J.C., RAMSAY, A.G. & GRIBBEN, J.G., 2010. T-cell function in chronic lymphocytic leukaemia. *Seminars in Cancer Biology*, 20(6), pp.431–438. Available at: http://dx.doi.org/10.1016/j.semcancer.2010.09.006.

ROSATI, E. ET AL., 2009. Constitutively activated Notch signaling is involved in survival and apoptosis resistance of B-CLL cells. *Blood*, 113(4), pp.856–865.

ROSENWALD, A ET AL., 2001. Relation of gene expression phenotype to immunoglobulin mutation genotype in B cell chronic lymphocytic leukemia. *The Journal of experimental medicine*, 194(11), pp.1639–1647.

ROSE-ZERILLI, M.J.J. ET AL., 2014. ATM mutation rather than BIRC3 deletion and/or mutation predicts reduced survival in 11q-deleted chronic lymphocytic leukemia: Data from the UK LRF CLL4 trial. *Haematologica*, 99(4), pp.736–742.

ROSS, J. & AUGER, M., 1993. *The Biology of the Macrophage*, Oxford University Press.

SAGAERT, X., SPRANGERS, B. & DE WOLF-PEETERS, C., 2007. The dynamics of the B follicle: understanding the normal counterpart of B-cell-derived malignancies. *Leukemia : official journal of the Leukemia Society of America, Leukemia Research Fund, U.K*, 21(7), pp.1378–1386.

SAUDEMONT, A. & MADRIGAL, J.A., 2014. Allogeneic T cells: Maestro in the co-ordination of the immune response after hematopoietic stem cell transplantation. *Haematologica*, 99(2), pp.203–205.

SAULEP-EASTON, D. ET AL., 2015. The BAFF receptor TACI controls IL-10 production by regulatory B cells and CLL B cells. *Leukemia*, (October 2014), pp.1–10. Available at: http://www.nature.com/doifinder/10.1038/leu.2015.174.

SCHATZ, D.G., OETTINGER, M.A. & SCHLISSEL, M.S., 1992. V (D) J RECOMBINATION : Molecular Biology and Regulation. *Annual review of immunology*, 10(D), pp.359–383.

SCHINDELIN, J. ET AL., 2012. Fiji: an open-source platform for biological-image analysis. *Nature Methods*, 9(7), pp.676–682.

SCHMID, C. & ISAACSON, P.G., 1994. Proliferation centres in B-cell malignant lymphoma, lymphocytic (B-CLL): an immunophenotypic study. *Histopathology*, 24(5), pp.445–451. Available at: http://apps.webofknowledge.com/full_record.do?product=UA&search_mode=GeneralSearch&qid=9&SID=V1QkeHEAarj1RomNnfe&page=1&doc=1 [Accessed September 22, 2015].

SCHUH, A. ET AL., 2012. Monitoring chronic lymphocytic leukemia progression by whole genome sequencing reveals heterogeneous clonal evolution patterns. *Blood*, 120(20), pp.4191–4196.

SCHULZ, A. ET AL., 2013. Lenalidomide reduces survival of chronic lymphocytic leukemia cells in primary cocultures by altering the myeloid microenvironment. *Blood*, 121(13), pp.2503–11. Available at: http://www.ncbi.nlm.nih.gov/pubmed/23349394 [Accessed January 6, 2015].

SHANAFELT, T.D. ET AL., 2015. Impact of ibrutinib and idelalisib on the pharmaceutical cost of treating chronic lymphocytic leukemia at the individual and societal levels. *Journal of oncology practice / American Society of Clinical Oncology*, 11(3), pp.252–8. Available at: http://jop.ascopubs.org/content/11/3/252.abstract [Accessed August 28, 2015].

SHERRINGTON, P.D. ET AL., 1992. HumanRAG2, likeRAGI, is on chromosome II band p13 and therefore not linked to ataxia telangiectasia complementation groups. *Genes, Chromosomes and Cancer*, 5(4), pp.404–406. Available at: http://apps.webofknowledge.com/full_record.do?product=UA&search_mode=GeneralSearch&qid=13&SID=R1TUrFVzEGeTPfb14mU&page=1&doc=1 [Accessed August 30, 2015].

SOMA, L. A., CRAIG, F.E. & SWERDLOW, S.H., 2006. The proliferation center microenvironment and prognostic markers in chronic lymphocytic leukemia/small lymphocytic lymphoma. *Human Pathology*, 37(2), pp.152–159.

STAMATOPOULOS, B. ET AL., 2012. AMD3100 disrupts the cross-talk between chronic lymphocytic leukemia cells and a mesenchymal stromal or nurse-like cell-based microenvironment: Pre-clinical evidence for its association with chronic lymphocytic

leukemia treatments. *Haematologica*, 97(4), pp.608–615.

STANKOVIC, T. ET AL., 1999. Inactivation of ataxia telangiectasia mutated gene in B-cell chronic lymphocytic leukaemia. *Lancet (London, England)*, 353(9146), pp.26–9. Available at: http://www.sciencedirect.com/science/article/pii/S0140673698101174 [Accessed September 18, 2015].

STAVNEZER, J., 2008. Mechanism and regulation of class switch recombination. *Annual review of immunology*, pp.1–31. Available at: http://www.ncbi.nlm.nih.gov/pmc/articles/PMC2707252/.

STEVENSON, F.K. & CALIGARIS-CAPPIO, F., 2004. Chronic lymphocytic leukemia: Revelations from the B-cell receptor. *Blood*, 103(12), pp.4389–4395.

STEVENSON, F.K.F. ET AL., 2011. B-cell receptor signaling in chronic lymphocytic leukemia. *Blood*, 118(16), pp.4313–4320. Available at: http://bloodjournal.hematologylibrary.org/content/118/16/4313.short\nhttp://www.ncbi.nlm.nih.gov/pubmed/21816833.

STILGENBAUER, S. & ZENZ, T., 2010. Understanding and managing ultra high-risk chronic lymphocytic leukemia. *Hematology / the Education Program of the American Society of Hematology. American Society of Hematology. Education Program*, 2010, pp.481–488.

STRATI, P. ET AL., 2015. Second Cancers and Richter Transformation Are the Leading Causes of Death in Patients With Trisomy 12 Chronic Lymphocytic Leukemia. *Clinical lymphoma, myeloma & leukemia*, 15(7), pp.420–7. Available at: http://www.sciencedirect.com/science/article/pii/S2152265015000300 [Accessed August 28, 2015].

STRATI, P. & SHANAFELT, T., 2015. Monoclonal B-cell lymphocytosis and early stage CLL: diagnosis, natural history, and risk stratification. *Blood*, (507). Available at: http://www.bloodjournal.org/cgi/doi/10.1182/blood-2015-02-585059.

STREFFORD, J.C., 2014. The genomic landscape of chronic lymphocytic leukaemia: biological and clinical implications. *British Journal of Haematology*, (December 2014), p.n/a–n/a. Available at: http://doi.wiley.com/10.1111/bjh.13254.

SUTTON, L.-A. & ROSENQUIST, R., 2015. The complex interplay between cell-intrinsic and cell-extrinsic factors driving the evolution of chronic lymphocytic leukemia. *Seminars in Cancer Biology*. Available at: http://linkinghub.elsevier.com/retrieve/pii/S1044579X15000346.

SYLVAN, S.E. ET AL., 2012. Phase I study of lenalidomide and alemtuzumab in refractory chronic lymphocytic leukaemia: Maintaining immune functions during therapy-induced immunosuppression. *British Journal of Haematology*, 159(5), pp.608–612.

TADMOR, T. & POLLIACK, A., 2012. Optimal management of older patients with chronic lymphocytic leukemia: Some facts and principles guiding therapeutic choices. *Blood Reviews*, 26(1), pp.15–23. Available at: http://dx.doi.org/10.1016/j.blre.2011.09.002.

TAM, C.S. ET AL., 2008. Long-term results of the fludarabine, cyclophosphamide, and rituximab regimen as initial therapy of chronic lymphocytic leukemia. *Blood*, 112(4), pp.975–980.

TEO, A E. ET AL., 2015. Differential PAX5 levels promote malignant B-cell infiltration, progression and drug resistance, and predict a poor prognosis in MCL patients independent of CCND1. *Leukemia*, (May), pp.1–14. Available at:

http://www.nature.com/doifinder/10.1038/leu.2015.140.

TORLAKOVIC, E. ET AL., 2002. The value of anti-pax-5 immunostaining in routinely fixed and paraffin-embedded sections: a novel pan pre-B and B-cell marker. *The American journal of surgical pathology*, 26(10), pp.1343–1350.

TORRES, M. ET AL., 2007. The immunoglobulin heavy chain constant region affects kinetic and thermodynamic parameters of antibody variable region interactions with antigen. *Journal of Biological Chemistry*, 282(18), pp.13917–13927.

TSANG, M. ET AL., 2015. The efficacy of ibrutinib in the treatment of Richter syndrome. *Blood*, 125(10), pp.1676–1678. Available at: http://apps.webofknowledge.com/full_record.do?product=UA&search_mode=GeneralSearch&qid=4&SID=P2Xa3Ok74KEY9P5AlqC&page=1&doc=1 [Accessed August 30, 2015].

TSIMBERIDOU, A.M. & KEATING, M.J., 2005. Richter syndrome: Biology, incidence, and therapeutic strategies. *Cancer*, 103(2), pp.216–228.

TSUKADA, N. ET AL., 2002. Distinctive features of "nurselike" cells that differentiate in the context of chronic lymphocytic leukemia. *Blood*, 99(3), pp.1030–1037. Available at: http://www.bloodjournal.org/cgi/doi/10.1182/blood.V99.3.1030 [Accessed December 21, 2014].

UNDERHILL, G.H. ET AL., 2012. IgG plasma cells display a unique spectrum of leukocyte adhesion and homing molecules IgG plasma cells display a unique spectrum of leukocyte adhesion and homing molecules. *In Vivo*, 99(8), pp.2905–2912.

VANDEWOESTYNE, M.L. ET AL., 2011. Laser microdissection for the assessment of the clonal relationship between chronic lymphocytic leukemia/small lymphocytic lymphoma and proliferating B cells within lymph node pseudofollicles. *Leukemia : official journal of the Leukemia Society of America, Leukemia Research Fund, U.K*, 25(5), pp.883–888.

WIESTNER, A. ET AL., 2003. ZAP-70 expression identifies a chronic lymphocytic leukemia subtype with unmutated immunoglobulin genes, inferior clinical outcome, and distinct gene expression profile. *Blood*, 101(12), pp.4944–4951.

WOOF, J.M. & KEN, M. A., 2006. The function of immunoglobulin A in immunity. *Journal of Pathology*, 208(2), pp.270–282.

WOYACH, J. A. & JOHNSON, A. J., 2015. Targeted therapies in CLL: mechanisms of resistance and strategies for management. *Blood*. Available at: http://www.bloodjournal.org/cgi/doi/10.1182/blood-2015-03-585075.

WU, L.C. & ZARRIN, A. A, 2014. The production and regulation of IgE by the immune system. *Nature reviews. Immunology*, 14(4), pp.247–59. Available at: http://www.ncbi.nlm.nih.gov/pubmed/24625841.

YSEBAERT, L., FEUGIER, P. & MICHALLET, A.-S., 2015. Management of elderly patients with chronic lymphocytic leukemia in the era of targeted therapies. *Current Opinion in Oncology*, 27(5), pp.365–370. Available at: http://content.wkhealth.com/linkback/openurl?sid=WKPTLP:landingpage&an=00001622-201509000-00002.

YSEBAERT, L. & FOURNIÉ, J.-J., 2011. Genomic and phenotypic characterization of nurse-like cells that promote drug resistance in chronic lymphocytic leukemia. *Leukemia & lymphoma*, 52(7), pp.1404–6. Available at:

http://www.ncbi.nlm.nih.gov/pubmed/21699388 [Accessed December 21, 2014].

ZENZ, T. ET AL., 2010. TP53 mutation and survival in chronic lymphocytic leukemia. *Journal of Clinical Oncology*, 28(29), pp.4473–4479.

ZHANG, Z. ET AL., 2006. Transcription factor Pax5 (BSAP) transactivates the RAG-mediated V(H)-to-DJ(H) rearrangement of immunoglobulin genes. *Nature immunology*, 7(6), pp.616–624.

8 APPENDIX I

Buffers and Recipes

2.2.3 MACS Buffer

500mL DPBS with the addition of 2mM sterile filtered EDTA and 1% (v/v) FBS. Store at 4°C.

2.5.3 FACS Fix (Flow Cytometry)

500mL DPBS with addition of 1% (v/v) formaldehyde and 2% (v\v) FBS. Store at 4°C

2.5.4 Cell Cycle Buffer (Flow Cytometry)

500mL ddH_2O with the addition of 30µg PI, 0.1mM $NaCl_2$, 1% (w/v) sodium citrate, 0.1% TritonX100. Store at 4°C protected from light.

Quantitative Analysis of Immunofluorescent staining

3.3 Use of Fiji Image J for quantitative analysis.

For analysis of the expression of a particular marker, multicolour immunofluorescent images were analysed by using Fiji Image J Open Source Software and custom built macros which allowed automation of the analysis stages to ensure consistency across all samples. Each stage of analysis briefly described herein.

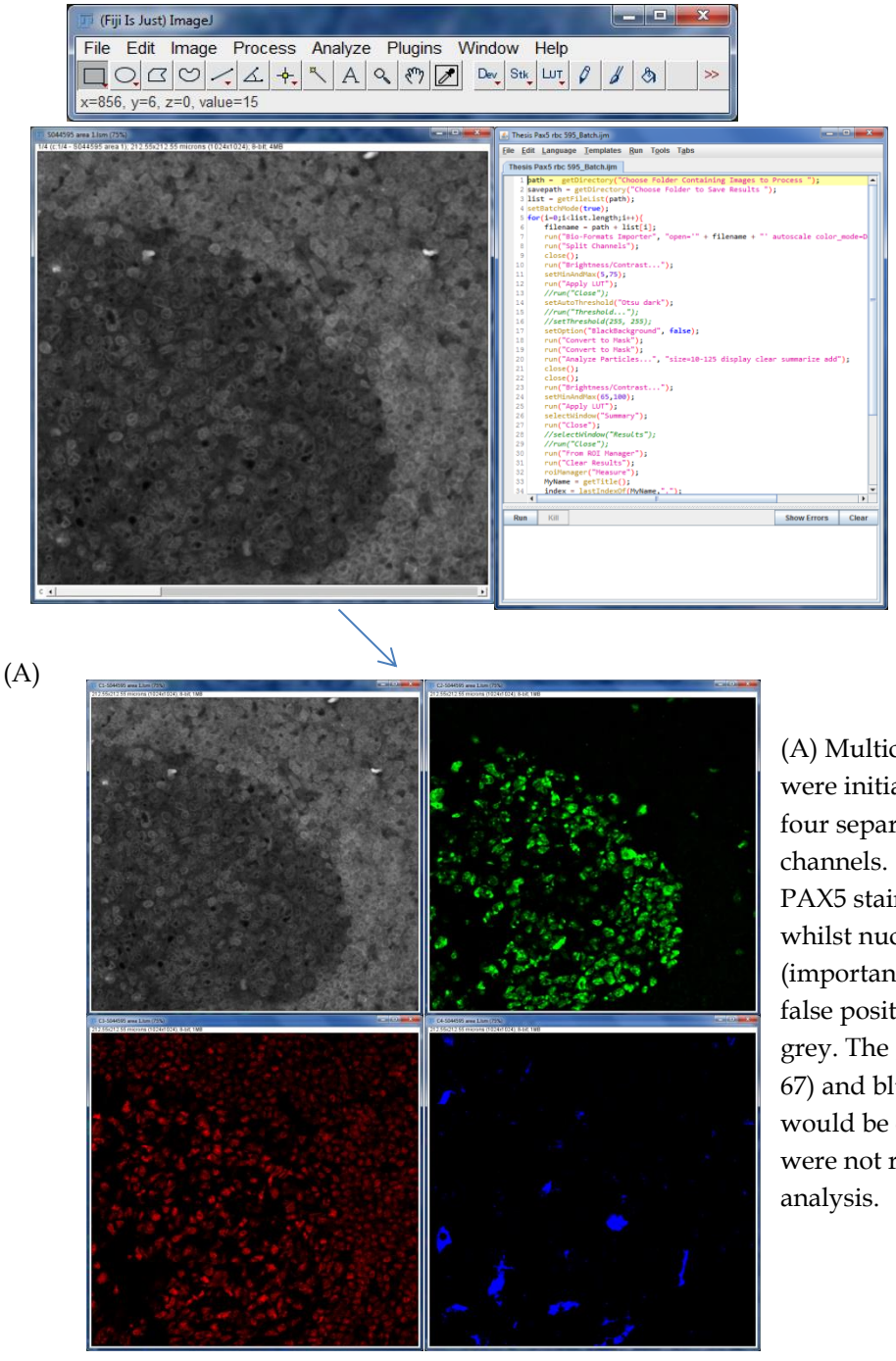

(A)

(A) Multicolour images were initially split into their four separate colour channels. In this example, PAX5 staining is in red, whilst nuclear staining (important for removing false positive events) is in grey. The green channel (Ki-67) and blue channel (Cd68) would be closed as these were not required for this analysis.

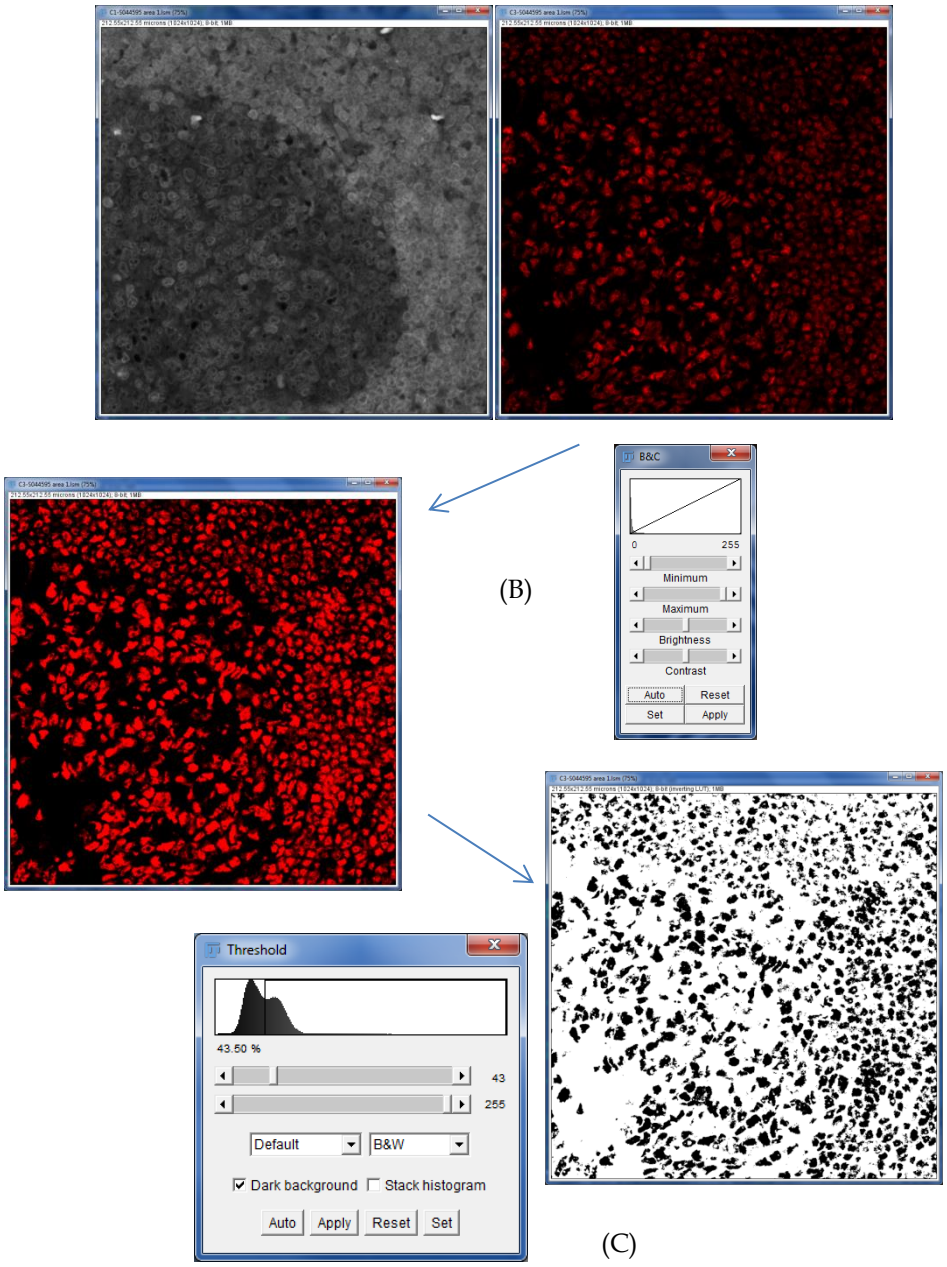

(B)

(C)

The marker of interest (PAX5) was initially analysed. First, the brightness/contrast levels were altered to ensure good definition of stained v.s. non stained cells (B). This was calculated through use of the isotype control staining images to ensure false positivity was not introduced. Subsequently, the image was converted using a threshold function to a binary image (C), where black = on/yes and white = off/no. The binary image allowed the software to determine the edge of the staining area for each event or cell.

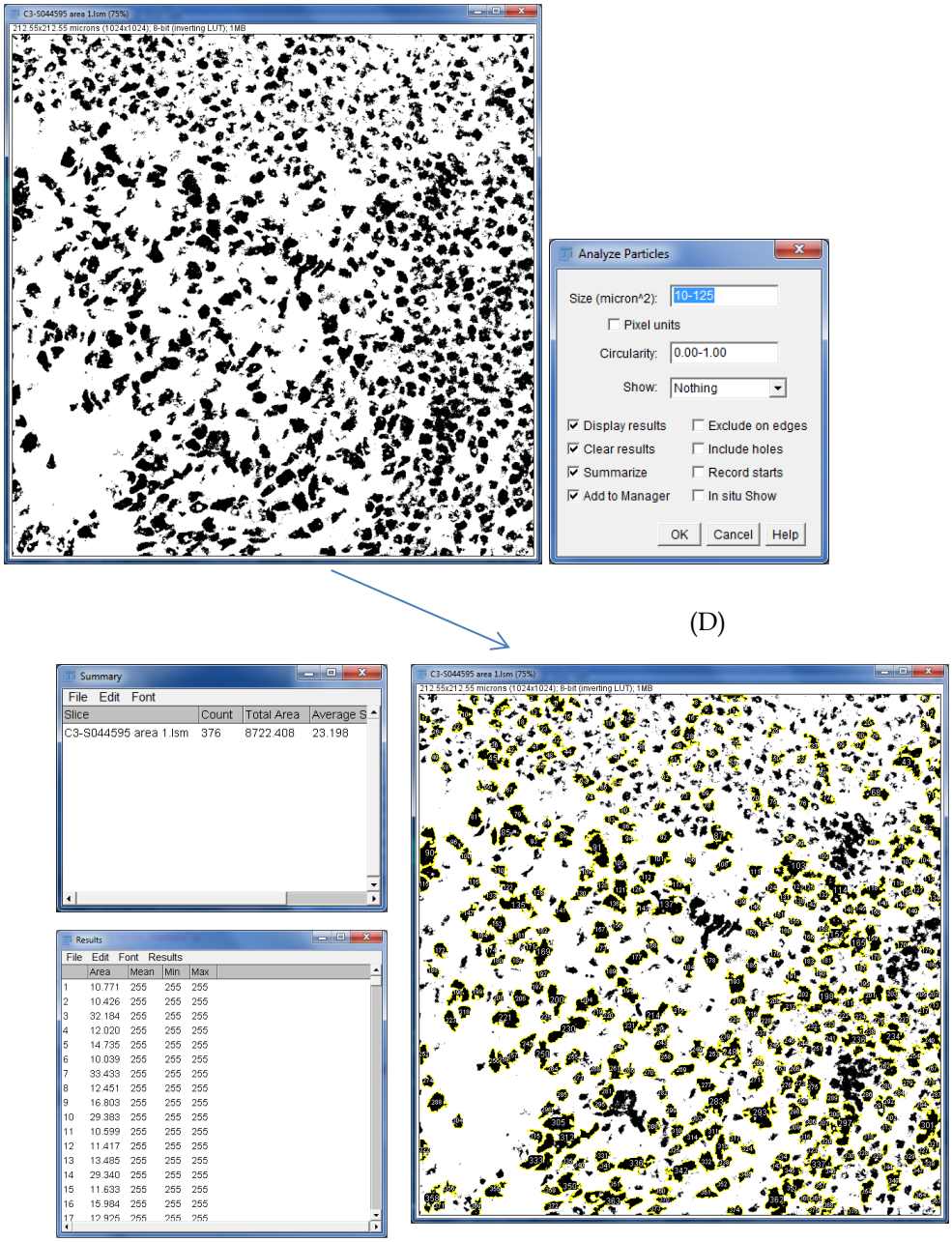

Once in binary form, the Analyse Particles function could be employed, which allowed number of events (or particles/cells) to be counted based upon sizing parameters (D). The size parameters for each staining target were determined individually based upon the isotype control staining to ensure accuracy. Small events were excluded (typically 10micron^2) to remove any debris or non-cellular staining and very large events were typically excluded to prevent large vessels or clumps of cells being included in the analysis. Numbers of events for each analysis were stored and analysed in Microsoft Excel.

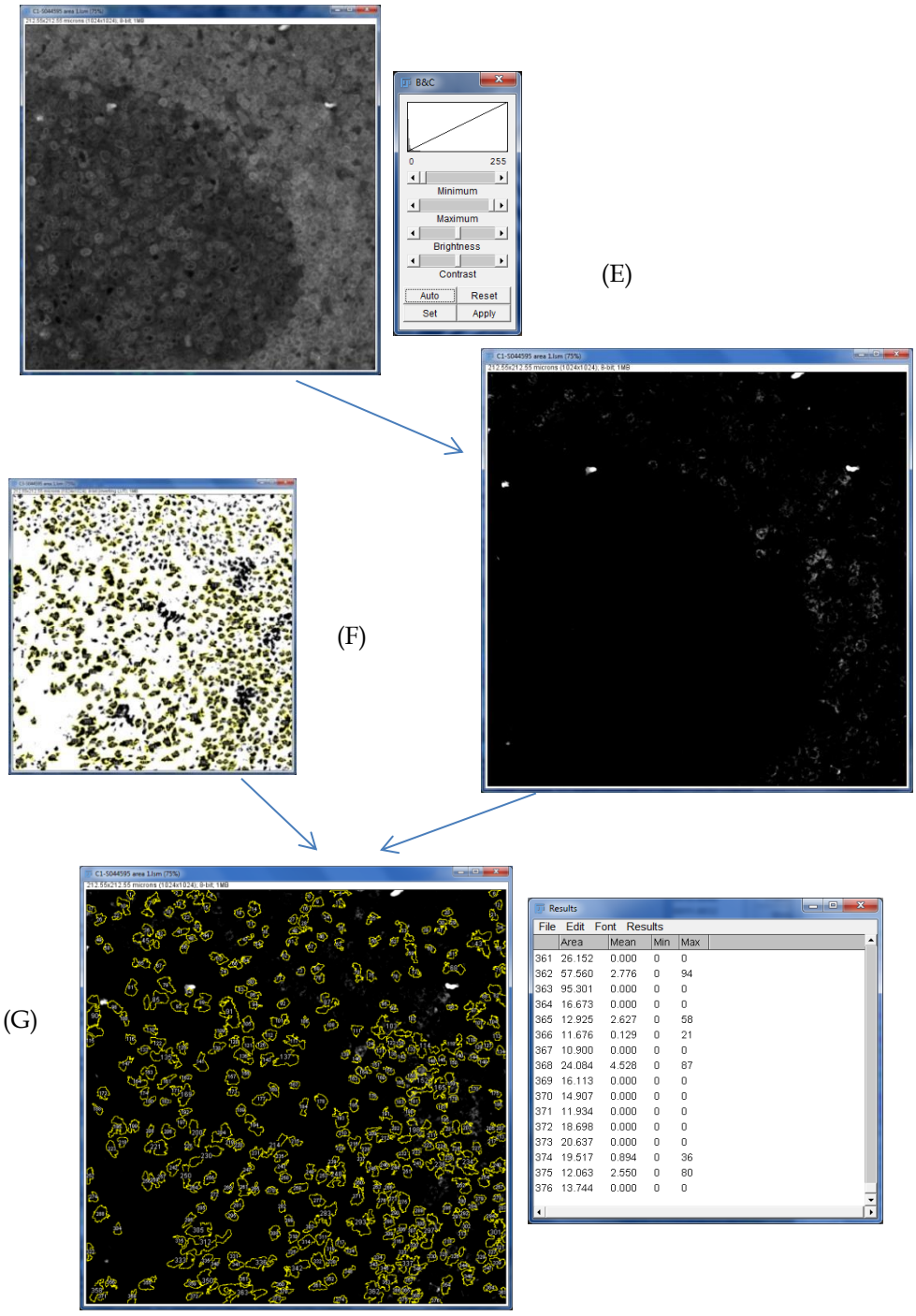

Once the staining of interest was recorded (D), the nuclear staining channel (DAPI) could be employed to remove any false-positive staining due to red blood cell autofluorescence. The DAPI channel brightness/contrast settings were adjusted to leave only the extremely bright events (autofluorescence) (E) and then the previously analysed marker of interest (for example PAX5 staining) (F) was overlayed onto the DAPI channel (G). The overlay could then be reanalysed for positivity and anything which had high positivity in the DAPI

channel was excluded from subsequent analysis. Numbers of events for each analysis were stored and analysed in Microsoft Excel.

Supplementary Data

4.4 Flow Cytometry analysis of CLL sample CD19 purity

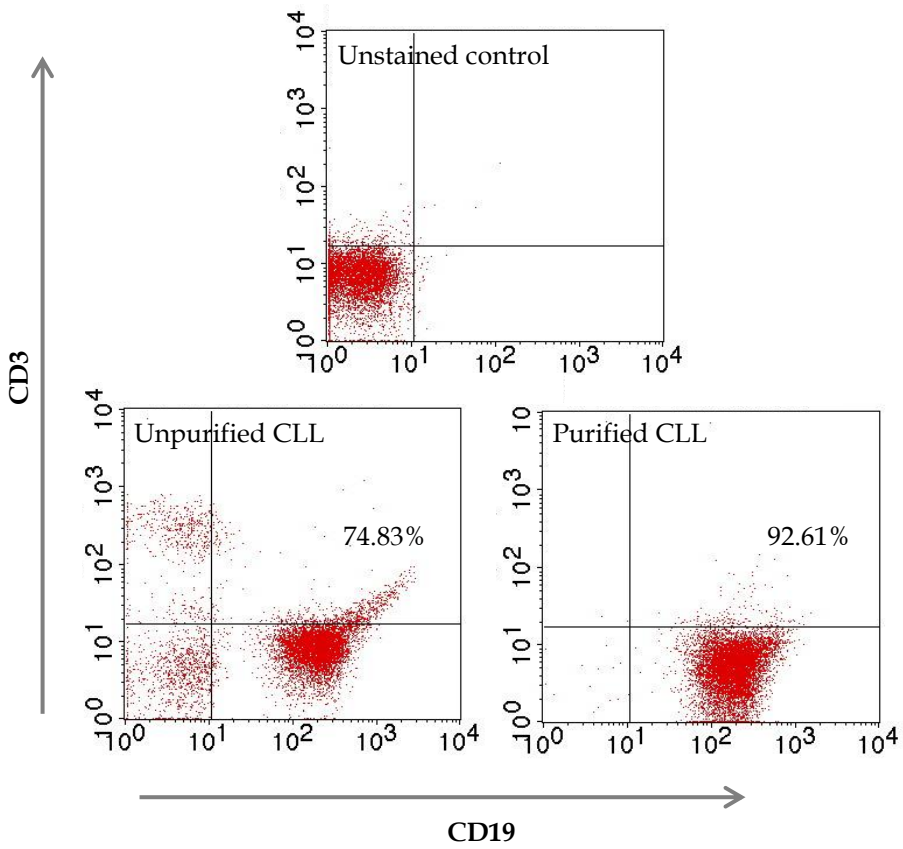

Representative images show a single CLL sample tested for purity pre- and post-negative selection purification.